

## **General Disclaimer**

### **One or more of the Following Statements may affect this Document**

- This document has been reproduced from the best copy furnished by the organizational source. It is being released in the interest of making available as much information as possible.
- This document may contain data, which exceeds the sheet parameters. It was furnished in this condition by the organizational source and is the best copy available.
- This document may contain tone-on-tone or color graphs, charts and/or pictures, which have been reproduced in black and white.
- This document is paginated as submitted by the original source.
- Portions of this document are not fully legible due to the historical nature of some of the material. However, it is the best reproduction available from the original submission.

# Evaluation of Stress-Corrosion Cracking Susceptibility Using Fracture Mechanics Techniques

D. O. Sprowls  
M. B. Slumaker  
J. D. Walsh  
Chemical Metallurgy Division  
Alcoa Laboratories

J. W. Coursen  
Engineering Properties and Testing Division  
Alcoa Laboratories

Prepared for:  
George C. Marshall Space Flight Center  
Contract No. NAS 8-21487

Final Report - Part I  
May 31, 1973

N74-10935

Unclas  
15326

G3/32

CSCI 20K

NASA-CR-124469) EVALUATION OF STRESS  
CORROSION CRACKING SUSCEPTIBILITY USING  
FRACTURE MECHANICS TECHNIQUES, PART 1  
Final Report, 1 Jul. 1968 (Aluminum Co.  
of America) 303 p HC \$17.25



EVALUATION OF STRESS-CORROSION CRACKING SUSCEPTIBILITY  
USING FRACTURE MECHANICS TECHNIQUES

FINAL REPORT - PART I  
(For The Period July 1, 1968 to August 31, 1972)  
Issued May 31, 1973

Prepared for GEORGE C. MARSHALL SPACE FLIGHT CENTER  
Contract No. NAS 8-21487

Reported by: *D. O. Sprowls*  
D. O. Sprowls  
*M. B. Shumaker*  
M. B. Shumaker  
*JWC J. W. Coursen*  
J. W. Coursen  
*J. D. Walsh*  
J. D. Walsh

Approved by: *J. L. Brandt*  
J. L. Brandt, Division Manager  
Chemical Metallurgy Division  
*J. G. Kaufman*  
J. G. Kaufman, Division Manager  
Engineering Properties & Testing Div.  
*C. J. Walton*  
C. J. Walton  
Assistant Director for  
Surface Technology

## Foreword

This report was prepared by the Aluminum Company of America under Contract NAS 8-21487 for the George C. Marshall Space Flight Center of the National Aeronautics and Space Administration. The work described herein was performed in the period from July 1, 1968 to August 31, 1972. The project was administered under the technical direction of the Propulsion and Vehicle Engineering Laboratory, Materials Division of the George C. Marshall Space Flight Center with Mr. T. S. Humphries serving as Project Manager.

A number of Alcoa Research Laboratories personnel in addition to the authors of this report made significant contributions to the work. Mr. B. W. Lifka supervised the environmental screening tests and other exploratory work to determine the optimum test conditions to use for precracked specimens of the aluminum alloys. Dr. W. G. Fricke, Jr. and Mr. John Ptasienski supervised and performed the fractographic examinations with the scanning electron microscope. Mr. R. H. Stevens supervised the metallographic examinations with the light microscope.

Acknowledgements are also made to Mr. E. E. Denhard, Jr. of the Armco Steel Corporation and to Mr. W. C. Beck of the Allegheny-Ludlum Steel Corporation for their assistance with the heat treatment and metallographic examination of the steel samples and for their helpful review of this final report.

This report may not be reproduced or published in any form, in whole or in part, without prior approval of the U.S. Government.

Part II of this contract titled, "Investigation of Smooth Specimen SCC Test Procedures - Variations in Environment, Specimen Size, Stressing Frame and Stress State" was reported separately.

## Abstract

Stress-corrosion cracking (SCC) tests were performed on 13 aluminum alloys, 13 precipitation hardening stainless steels, and two titanium 6Al-4V alloy forgings to compare fracture mechanics techniques with the conventional smooth specimen procedures. Commercially fabricated plate and rolled or forged bars 2 to 2.5-in. thick were tested.

Exposures were conducted outdoors in a seacoast atmosphere and in an inland industrial atmosphere to relate the accelerated tests with service type environments. With the fracture mechanics technique tests were made chiefly on bolt loaded fatigue precracked compact tension specimens of the type used for plane-strain fracture toughness tests. Additional tests of the aluminum alloys were performed on ring loaded compact tension specimens and on bolt loaded double cantilever beams. For the smooth specimen procedure 0.125-in. dia. tensile specimens were loaded axially in "constant deformation" type frames.

Comparative ranking of the relative resistance to SCC of materials tested with precracked and smooth specimens varied with the alloy and temper. Aluminum and steel alloys with a low threshold stress,  $\sigma_{th}$ , for initiating SCC in a smooth surface also showed a low threshold stress intensity factor,  $K_{Isc}$ , for initiating SCC in a pre-existing mechanical crack, and a relatively high SCC growth rate under plane-strain conditions. Conversely, aluminum alloys and tempers with a high  $\sigma_{th}$  also showed a high  $K_{Isc}$  and a relatively low SCC growth rate. However, most of the precipitation hardening steel alloys and the titanium materials exhibited a low  $K_{Isc}$  and high SCC growth rate even though the  $\sigma_{th}$  was high. Thus, while tests of precracked specimens are not required for the evaluation of the resistance of aluminum alloys to SCC, tests of both precracked and smooth specimens are essential for materials such as the precipitation hardening stainless steels and titanium alloys.

For both aluminum and steel alloys comparative SCC growth rates obtained from tests of precracked specimens provide an additional useful characterization of the SCC behavior of an alloy. It is emphasized, however, that SCC growth rates and  $K_{Isc}$  data, like  $\sigma_{th}$  data, depend upon the test environment and other conditions.

Consideration is given to a number of formidable experimental difficulties with tests of precracked specimens that must be overcome if meaningful  $K_{Isc}$  and accurate K-Rate curves are to be obtained for all types of alloys and product forms. Discriminating between highly resistant alloys and tempers still poses a problem because of difficulties associated with identification of extremely slow crack growth rates.

Because of the experimental difficulties associated with the determination of precise SCC thresholds ( $\sigma_{th}$  and  $K_{Isc}$ ) and SCC growth rates, a method of classifying the SCC ranking of materials into broad groups based on accelerated tests of both smooth and precracked specimens merits consideration. An example of this approach is presented for aluminum alloys.

## TABLE OF CONTENTS

	<u>Page</u>
I. INTRODUCTION	1
II. MATERIALS	2
A. Aluminum Alloys	2
B. Stainless Steel Alloys	4
C. Titanium 6Al-4V Alloy	6
III. EXPERIMENTAL PROCEDURES	7
A. Tensile Properties	7
B. Plane-Strain Fracture Toughness	8
C. Stress Corrosion Tests With Smooth Specimens	9
D. Stress Corrosion Tests With Fracture Mechanics Techniques	10
E. Stress Corrosion Test Environments	16
F. Evaluation and Interpretation	18
IV. RESULTS OF TENSILE PROPERTY TESTS	19
A. Aluminum Alloys	19
B. Stainless Steel Alloys	20
C. Titanium 6Al-4V Alloy	21
V. RESULTS OF PLANE-STRAIN FRACTURE TOUGHNESS TESTS	21
A. Aluminum Alloys	21
B. Stainless Steel Alloys	22
C. Titanium 6Al-4V Alloy	24
VI. RESULTS OF STRESS CORROSION TESTS OF ALUMINUM ALLOYS	25
A. Tests With Smooth Specimens	25
B. Tests With Bolt Loaded Precracked Specimens	30
1. Exploratory Tests	30
2. Performance of Compact Tension Specimens	37
3. Performance of Boeing DCB Specimens	47

	<u>Page</u>
C. Tests With Ring Loaded Compact Tension Specimens	52
D. Fractographic Examination	50
VII. RESULTS OF STRESS CORROSION TESTS OF STAINLESS STEEL ALLOYS	61
A. Tests With Smooth Specimens	61
B. Tests With Bolt Loaded Precracked Specimens	66
C. Fractographic Examination	74
D. Comparison of Alloys	75
VIII. RESULTS OF STRESS CORROSION TESTS OF TITANIUM 6Al-4V ALLOY	79
A. Tests With Smooth Specimens	79
B. Tests With Bolt Loaded Precracked Specimens	80
IX. GENERAL DISCUSSION	86
A. Comparison of Alloy Ratings By Precracked and Smooth Specimen Tests	86
B. Design Implications of Stress Corrosion Test Data	93
C. Problems in Interpretation of SCC Test Data	98
X. SUMMARY AND CONCLUSIONS	106

TABLES I - XXX

FIGURES 1-112

APPENDIX A - GLOSSARY OF TERMS

APPENDIX B - REFERENCES

APPENDIX C - BIBLIOGRAPHY

APPENDIX D - DETAILED DATA FOR SCC TESTS OF PRECRACKED SPECIMENS

APPENDIX E - DISTRIBUTION LIST

## I. INTRODUCTION

The application of linear-elastic fracture mechanics analyses to the study of stress-corrosion cracking (SCC) and other subcritical-crack growth problems has undergone considerable development in recent years<sup>(1,2,3,4)</sup>. The use of precracked specimens for stress corrosion testing has been given widespread consideration and trial since Brown promoted the  $K_{I_{SCC}}$  threshold concept by using precracked cantilever beam specimens in testing high strength steel alloys<sup>(3,4)</sup>. Justification for the use of the crack-tip stress-intensity factor for opening mode,  $K_I$ , to characterize the mechanical driving force in SCC has been reviewed by Johnson and Paris<sup>(5)</sup> and by Wei<sup>(6)</sup>. Further experimental verification with studies of titanium and steel alloys has been provided by the investigations of Smith, et. al.<sup>(7)</sup> and Novak and Rolfe<sup>(8)</sup>. However, the earliest tests of high strength aluminum alloys by the fracture mechanics approach<sup>(9,10)</sup> indicated that test results obtained by this new method might not rate aluminum alloys in the same order as the tests by conventional smooth specimen methods. The present investigation was initiated because it was evident that there was need for more information about this new method of SCC testing.

An experimental program was developed to evaluate with both precracked and smooth test specimens the resistance to SCC of a variety of high strength alloys of aluminum, titanium and precipitation hardening stainless steel; all these alloys are of interest to the aerospace industry. The objectives are to:

(1) compare the relative ratings for resistance to SCC by the two methods, (2) determine the applicability of the test data obtained by the two methods for alloy selection and engineering design, and (3) investigate some of the variable test conditions associated with the fracture mechanics method of SCC testing these alloys.

A review was made of the published literature to aid in planning and performing the work in this program. Attention is called to the most significant published articles and reports in the numerous references and the attached bibliography.

## II. MATERIALS

A list of all of the materials and the sources of supply is given in Table I. Specific information regarding the various alloys is presented in more detail below.

### A. Aluminum Alloys

#### 1. Composition

The aluminum alloy product selected for evaluation was commercially rolled and heat treated plate, 2.00 to 2.50 inches thick. Thirteen items were selected to provide a variety of alloy types with different strengths, fracture toughnesses and degrees of resistance to stress-corrosion cracking. The chemical compositions of the plates are given in Table II and all are within the composition limits published<sup>(11)</sup> by the Aluminum Association for the alloys.

#### 2. Heat Treatment and Microstructure

All aluminum alloys included in this investigation except

5456 are strengthened by solution heat treatment followed by quenching and a precipitation heat treatment. Typical thermal treatments for the alloys and tempers are given in Table III. Alloy 5456 is strengthened by strain-hardening during hot rolling.

The aluminum alloy plates were examined metallographically to verify that the microstructures were typical of the alloys and tempers. Representative photomicrographs, illustrating the grain structure in all three directions, were given in a previous report<sup>(12)</sup>. Examples of two representative alloy-temper combinations are shown in Figure 1. The highly directional grain structure illustrated for 7075-T651 alloy is representative of that for most of the other alloys including 2014-T651, 2024-T351 and T851, 5456-H117, 6061-T651, 7039-T6351, 7079-T651 and 7075-T7351. Certain of the plates recrystallize during hot rolling and solution heat treatment and have a somewhat less directional grain structure, as exemplified by alloy 2219-T37 in Figure 1; alloys in this group include 2219-T87 and 2021-T81.

The microstructure of 5456-H117 alloy plate is required to be free from "continuous" precipitation in the grain boundaries (Interim Federal Specification QQ-A-00250/20). The microstructure of the 2.5" plate of 5456-H117 used in this investigation is satisfactory as shown by Figure 2. With this type of microstructure 5456 alloy plate is expected to be immune to SCC. To obtain a sample of a 5XXX type alloy in a condition susceptible to SCC a portion of the H117 temper plate was heated for three days at 300°F. The high degree of continuity of grain boundary precipitation for this sample shown in Figure 2 indicates that a

relatively low resistance to SCC can be expected when the plate is tested in the short-transverse direction.

### 3. Tensile Properties

The tensile properties of the aluminum alloy plates determined by ASTM Methods E8<sup>(13)</sup> and B557<sup>(14)</sup> are summarized in Table IV, and described in more detail in Section IV. The properties of the several alloys and tempers conform to the various applicable standards.

### 4. Special Properties

The resistance to SCC of alloys 2219-T87 and 7075-T7351 must comply with certain military and federal specifications (Specification MIL-A-8920A (ASG) for 2219-T87, and Specification QQ-A-250/12 for 7075-T7351). The specifications require that short-transverse specimens, stressed at 75 per cent of the guaranteed long-transverse yield strength shall be capable of passing a 30-day alternate immersion test (3.5% NaCl solution) without stress-corrosion cracking. The plate samples employed in this investigation complied with these requirements.

Lot acceptance criteria of the specified resistance to SCC of 7075-T7351 alloy plate also contain a requirement (QQ-A-250/12) based upon an electrical conductivity-tensile yield strength relationship. The conductivity of the contract plates exceeded the 40% IACS requirement and the tensile properties were in the required range.

### B. Stainless Steel Alloys

The steel alloys were commercially fabricated in the form of rolled bar and plate 1.25 to 2.25 inches thick (Table I). Six

high strength stainless steels, including one chromium type martensite hardenable alloy (431) and five chromium-nickel type precipitation hardening alloys were selected to provide a variety of compositions and tempers with differing strength, toughness and degrees of resistance to SCC. All but one of the items were received in mill condition A or R100, intermediate tempers with good machinability because these alloys are not easily machined in the fully hardened tempers. The 15-5 PH steel in the H1150M condition was in the final temper when received from the mill.

#### 1. Composition

The composition of each steel is given in Table V, and the compositions were within manufacturers' specifications. Analyses of the finished products were in good agreement with the cast analyses furnished by the manufacturers.

#### 2. Heat Treatment and Microstructure

Visual examination of macroetched slices and metallographic examination, with metallurgical assistance by the research laboratories of the Armco and Allegheny Ludlum steel companies<sup>(15,16)</sup>, showed that each of the steel products was free of gross defects and had grain structures typical of the product alloys and tempers. Representative micrographs illustrating the grain structures in each of the products were shown in previous reports<sup>(12,17)</sup>. Examples illustrating the grain structures in two of the steels are shown in Figure 3. The directional grain structure illustrated for the 17-7 PH alloy is also representative of the PH15-7Mo alloy, while the relatively non-directional structure shown for the 431 alloy is representative of the

remaining samples. The directional characteristics of the grain structure were not appreciably altered by the thermal treatments employed.

The procedures employed in preparing and heat treating the various steels are outlined in Table VI. With the exception of the 15-5 PH steel received in the H1150M finish condition, all materials were thermally treated as specimens in a partially or fully machined condition.

### 3. Tensile Properties

The tensile properties of the stainless steel products determined by ASTM Methods E8 and A370<sup>(18)</sup> and summarized in Table VII are representative of the various alloys and tempers. Although the H1150 temper of 15-5 PH alloy was ordered from Armco, its tensile properties more closely matched those of the double overaged temper H1150M. Armco was not able to verify that the bar had been double overaged but agreed that it should be listed as H1150M rather than H1150.

### C. Titanium 6Al-4V Alloy

Titanium 6Al-4V alloy was included in this investigation because of its wide commercial use, and because early investigations<sup>(19)</sup> with precracked stress corrosion specimens had shown that its performance is affected by microstructural variations resulting from thermomechanical processing.

#### 1. Composition

The ingot composition of the titanium alloy, determined by Titanium Metals Corporation, is given in Table VIII. The hydrogen content determined at the Alcoa Research Laboratories

for the final forged bars is also listed.

## 2. Forging Procedures and Microstructure

Forged bars, 2-1/4" x 6", were fabricated at the Alcoa Forging Plant, Cleveland, Ohio, from 16" diameter billet purchased from the Titanium Metals Corporation. The forging sequence consisted of a two stage draw to 6" square bar from temperatures of 1950°F and 1850°F, separating this bar into two lengths and then drawing to the finish size by two processing methods:

- (1) Beta Forging - Drawn from a reheat temperature of 1950°F, above the alpha-beta transus temperature (1825°F).
- (2) Alpha-beta Forging - Drawn from a subtransus reheat temperature of 1770°F.

The two forgings were then annealed 2 hr. at 1300°F.

Microstructures of the finish forgings shown in Figure 4 are representative of beta forged and alpha-beta forged materials.

## 3. Tensile Properties

The tensile properties of the two forged bars given in Table VIII are representative of the products described.

### III. EXPERIMENTAL PROCEDURES

#### A. Tensile Properties

The tensile property tests were performed in accordance with ASTM Standard Methods of Tension Testing of Metallic Materials, Designation E8-69<sup>(13)</sup>. Choices of test specimens and test directions were dictated by the material specifications to demonstrate that the materials under study conformed to the applicable specifications. Additional tests were made in many instances to identify the properties with the location and orientation of the stress corrosion

test specimens. A general diagram of the specimen locations and orientations is shown in Figure 5.

B. Plane-Strain Fracture Toughness

Ambient fracture toughness tests were performed on duplicate test specimens for the given test directions with compact tension specimens (Figure 6) in accordance with ASTM Standard Method of Test for Plane-Strain Fracture Toughness of Metallic Materials, Designation E399-70T<sup>(20)</sup>. The loads at 5% secant offset were determined from load-deformation diagrams, and candidate values of the plane-strain fracture toughness were calculated with the equation:

$$K_{Q^*} = \frac{P\sqrt{a}}{BW} \left[ 29.6 - 185.5 \left(\frac{a}{W}\right) + 655.7 \left(\frac{a}{W}\right)^2 - 1017 \left(\frac{a}{W}\right)^3 + 638.9 \left(\frac{a}{W}\right)^4 \right] \dots (1)$$

Where. P = load, lb.  
a = crack length, in.  
B = specimen thickness, in.  
W = specimen width (depth), in.

The  $K_Q$  values were evaluated in accordance with requirements in ASTM Method E399 to determine their validity as  $K_{Ic}$  values.

Ambient fracture-toughness tests were also conducted with ARL type double cantilever beam specimens of alloys 2024-T351 and 7075-T651. This is not a standard fracture toughness test method, but the applicable features of ASTM Method E399 were employed. In these tests, the load for  $K_Q$  calculation was determined at the first visible evidence of crack growth on the load-deformation diagram. Candidate values of the plane-strain fracture toughness

---

\* Fracture toughness terms are defined in the Glossary in Appendix A.

were calculated with the equation<sup>(21)</sup>:

$$K_Q = \frac{2P}{B} \left[ \frac{3(a + 0.6h)^2 + h^2}{h^3} \right]^{1/2} \dots\dots\dots (2)$$

Where 2h = specimen height, in.

C. Stress Corrosion Tests with Smooth Specimens

Conventional stress corrosion tests were performed on smooth 0.125-in. diameter x 2-in. long threaded end tension specimens loaded in the Alcoa Research Laboratory stressing frames shown in Figure 7. This specimen and the loading system has been used extensively with aluminum alloys by ARL and has been described in previous publications<sup>(22,23)</sup>. An investigation of the compliance of this specimen - frame assembly was made as another phase of this contract, and the results were reported separately<sup>(24)</sup>. Although this stressing frame appears to be a "constant deformation" method, the increase in average net section stress that occurs as an isolated crack grows is almost equal to that occurring in a dead load situation, as illustrated by the schematic diagram in Figure 8. Thus, for isolated cracking the time to fracture, which is related to the per cent reduction in area of net section to achieve fracture stress, would be nearly the same with the two stressing systems. Although other patterns of attack ranging to numerous small cracks or uniform corrosion have very little effect on the rate of increase of the average stress on the net section with dead loading, the effect can be pronounced with the ARL stressing frame. For other patterns of attack, particularly in alloys that have relatively high resistance to SCC, the time to fracture can

be quite variable and specimens that undergo uniform attack will not fracture.

A similar specimen stressed with a relatively elastic loading ring also has been used extensively with steel alloys by Loginow<sup>(25)</sup>.

#### D. Stress Corrosion Tests with Fracture Mechanics Techniques

##### 1. Specimen Configuration

The compact tension specimen with a bolt loading system<sup>(8)</sup> was selected for the majority of the tests with the fracture mechanics method. These specimens are compact, self-contained and easy to handle and thus are well suited for the large volume of testing conducted under this contract. However, two designs of double cantilever beam (DCB) specimens were also tested with the aluminum alloys, one similar to the type used by Hyatt<sup>(26)</sup> and one somewhat larger (an elongated compact tension specimen as shown in Figure 6 with  $W_1 = 8.0$  in.) to allow loading with a testing machine. Dimensional details of the modified Boeing DCB are shown in Figure 9. The effect of specimen thickness was also studied with the compact tension specimen. Other testing variables studied include the type of precrack (tension vs. fatigue) and type of loading (ring loading vs. bolt loading and single vs. double-bolt loading).

##### 2. Compliance Data for Stress-Corrosion Testing

Load-deflection compliance data were obtained so that crack opening displacement (COD) could be used to determine the applied load in bolt loaded tests and to monitor crack growth in ring loaded tests. This was done by making successive saw cuts in compact tension specimens over an  $\frac{a}{W}$  range of 0.45 to 0.80 and

in ARL-type double cantilever beam specimens over a crack length range of 0.95 to 5.50 in. The specimens were loaded with a testing machine and the crack opening displacement was measured with a clip gage. Using a least squares analysis, a series of polynomial equations were fitted to the data. The equations providing the best fit and used in subsequent calculations were as follows:

Compact Tension Specimen

$$\text{COD} = v = \frac{P}{EB} \left[ 643.44 - 2306.9 \left(\frac{a}{W}\right) + 226.62 \left(\frac{a}{W}\right)^2 - 1122.6 \left(\frac{a}{W}\right)^3 + 53930 \left(\frac{a}{W}\right)^4 - 85568 \left(\frac{a}{W}\right)^5 + 44989 \left(\frac{a}{W}\right)^6 \right] \dots\dots (3)$$

$$a = W \left[ 0.18728 + 8.0737 \times 10^{-3} \left(\frac{VEB}{P}\right) - 4.8716 \times 10^{-5} \left(\frac{VEB}{P}\right)^2 + 1.410 \times 10^{-7} \left(\frac{VEB}{P}\right)^3 - 1.5267 \times 10^{-10} \left(\frac{VEB}{P}\right)^4 \right] \dots\dots (4)$$

ARL-Type-Double Cantilever Beam Specimens

$$\text{COD} = v = \frac{P}{EB} \left[ 513.53 - 1451.1a + 1633.7a^2 - 871.72a^3 + 245.14a^4 - 33.974a^5 + 1.848a^6 \right] \dots\dots\dots (5)$$

$$a = 0.42884 + 1.6778 \times 10^{-2} \left(\frac{VEB}{P}\right) - 3.8737 \times 10^{-5} \left(\frac{VEB}{P}\right)^2 + 5.1343 \times 10^{-8} \left(\frac{VEB}{P}\right)^3 - 3.2880 \times 10^{-11} \left(\frac{VEB}{P}\right)^4 + 9.0418 \times 10^{-15} \left(\frac{VEB}{P}\right)^5 \dots\dots\dots (6)$$

For double cantilever beam specimens of the Boeing type the crack length is measured and the stress intensity is calculated using the equation:

$$K_{I_r} = \frac{VEh \left[ 3h (a_f + 0.6h)^2 + h^3 \right]^{1/2}}{4 \left[ (a_f + 0.6h)^3 + h^2 a_f \right]} \dots\dots\dots (7)$$

Where V = deflection at the load line (COD), in.

A nomograph developed by Hyatt<sup>(26)</sup> relating the stress intensity to crack length for various magnitudes of V is given in Figure 10.

### 3. Bolt-Load Method

Bolt loading provides a constant deflection type test in which the specimen is "self-loaded". The applied load is not measured directly, but is obtained indirectly by measuring crack opening displacement as the bolt is turned. When crack growth occurs during exposure of either the compact tension specimen or the double cantilever beam specimens, the load and stress intensity level will decrease, and theoretically, the crack will arrest when the stress intensity level reaches a threshold value.

Stainless steel bolts with a 2-in. radius machined on the ends were used to apply load, and stainless steel "back up" pins were inserted in the pin hole opposite the bolt to prevent excessive deformation under load. The majority of the specimens were loaded with one bolt as illustrated in Figure 11. However, two bolts, as recommended by Smith and Piper<sup>(27)</sup>, were used in a special test of a few specimens. To accommodate the second bolt a tapped hole was placed in the other branch of the specimen directly in line with the bolt hole in the opposite branch. To load the specimen the opposing bolts were turned equal amounts to make contact in the crack-line and then tightened slowly in alternating small increments until "pop-in" occurred or until the desired

reading was obtained on the clip gauge.

Some of the specimens scheduled for exposure in each environment were precracked in tension with a bolt (particularly the Boeing DCB specimens) which remained in the specimen during exposure. The initial applied stress intensity in that case was assumed to be equal to about 95-100% of the  $K_{Ic}$  or  $K_Q$  value determined in ambient tests.

The majority of the specimens, however, were precracked in fatigue by axial-stress loading ( $R = \pm 0.1$ ) in accordance with ASTM Method E399-70T. A few cycles of relatively high reversed load were used to precondition the notch and initiate the crack; the load was then reduced so that the last 0.05 to 0.10-in. of the fatigue crack was developed at a stress intensity level  $\ll 50\%$  of the ambient  $K_{Ic}$  value (or  $K_Q$ ). The crack length was measured on each side of the specimen and assumed to be uniform through the thickness. Using this crack length, the load required to produce the desired stress intensity (nominal 95, 75, 50, or 25% of  $K_{Ic}$  or  $K_Q$ ) was calculated with either equation (1) or (2) as appropriate, and the corresponding crack opening displacement was calculated with equations (3) or (5). A clip gauge was placed in the crack opening and the specimen was loaded in a vise with a torque wrench to turn the bolt until the desired COD, and thus the inferred initial stress intensity ( $K_{I_i}$ ), was obtained.

For specimens that were to be exposed to one of the aqueous test media, a few drops of the corrodent were placed in the tip of the precrack as the bolt was given the final turns. The bolt and loading pin were then coated with wax to eliminate general or galvanic corrosion, and the specimens exposed to the environ-

ment. During exposure periodic measurements of the crack length to the nearest 0.01 in. were made on both sides of the specimen. After it appeared that crack growth had definitely come to an arrest, or after arbitrarily chosen exposure periods, specimens were unloaded with the torque wrench, measuring the final crack opening displacement with the displacement gage. The final load on the specimen was measured by reloading the specimen in a testing machine to the same final COD, and the final crack length determined by breaking the specimen and measuring the fracture surface. Crack lengths were measured at the center, quarter points and edges of the specimens, and an average value determined by giving one-half weight to the edge measurements and full weight to the other three measurements. Knowing the residual load and the final crack length and assuming the COD to be constant, the residual stress intensity was calculated with a combination of equations (1) and (3) or (2) and (5) or (7), as appropriate.

#### 4. Ring Load Method

Short-transverse compact tension specimens from each aluminum alloy and ARL type DCB specimens from alloys 2024-T351 and 7075-T651 were tested in a salt-dichromate-acetate solution with ring loading as shown in Figure 12. The aluminum alloy loading ring was designed so that for compact tension specimens, the deflection of the ring is large (at least 4 to 1) compared with the deflection of the specimen. When crack growth occurs, the load decreases slightly, but the stress intensity increases, thus accelerating crack growth and resulting in complete failure of the specimen. For DCB specimens, the stress intensity also increases,

but at a slower rate, and the test is not necessarily terminated by failure of the specimen. The rings were instrumented so that in these tests, both load and crack opening displacement, and thus stress intensity levels, could be monitored throughout the test. The crack lengths were measured on the sides of the specimens and the loads required to produce the desired stress intensity were calculated with equations (1) or (2). The specimens were immersed in containers of salt-dichromate-acetate solution, clip gages were placed in the crack openings and the loads were applied. Since the fatigue crack front is seldom straight through the thickness of the specimen, the crack opening displacements and actual initial stress intensities were usually slightly different than the estimates based on side measurements of the crack lengths.

Usually 5 to 8 tests were conducted simultaneously. Load and crack opening displacement readings were taken automatically every 8 hours with a B & F multi channel digital strain indicator. These readings were printed on a teletype and also punched on paper tape in a form suitable for computer analysis. The data logging unit and a bank of rings are illustrated in Figure 13.

Computer programs were developed to sort the data by test, plot raw load and crack opening displacement data, and fit polynomial equations to these data. A typical plot of the raw data and the best fit curves is shown in Figure 14. Using these best fit equations and equations 1, 2, 4 and 6, loads, crack lengths and stress intensities were evaluated at given time intervals throughout the life of the test. The crack growth rate was also

determined by differentiating the equation for crack length vs. time. A typical computer print-out is shown in Figure 15.

#### E. Stress Corrosion Test Environments

##### 1. Outdoor Atmosphere

In the evaluation of aluminum and high strength steel alloys of interest to the aerospace industry, it is important that realistic test media be used that will relate to the serviceability in aerospace applications. Exposures to both seacoast and inland industrial atmospheres have been used by ARL for many years<sup>(22)</sup> to evaluate aluminum alloys and to calibrate accelerated SCC tests. Thus, for the present investigation these same environments were chosen as reference exposures for both precracked and smooth specimens. The seacoast location is at Point Judith, Rhode Island, where specimens located about 100 yards from the surf are exposed to prevailing off-shore breezes. The inland industrial location is on the roof of the Alcoa Research Laboratories in New Kensington, Penna. A photograph showing the manner of exposure of the test specimens at both test sites is shown in Figure 16.

##### 2. Accelerated Test Media

a. Aluminum Alloys - The smooth specimens were exposed to 3.5% NaCl solution by alternate immersion. The solution was made with sodium chloride of 99 minimum per cent NaCl, 0.1 maximum per cent NaI plus city of New Kensington tapwater containing <200 ppm total solids with the solution pH ranging between 6.4 and 7.2. Evaporation losses were made up regularly by the addition of

tapwater, and a change of solution was made each month. The alternate immersion cycle consisted of total immersion of the specimens for 10 minutes each hour; for the remaining 50 minutes the specimens dried in the room atmosphere at ambient temperature and humidity.

Exploratory tests were conducted on selected alloys to determine the optimum corrodent for the precracked specimens. Although the 3.5% NaCl alternate immersion test is suitable for conventional SCC tests of most high strength aluminum alloys<sup>(22,28)</sup> it is not well suited for the precracked specimens. In the first tests of precracked compact tension specimens of high strength aluminum alloys exposed by this method<sup>(29)</sup>, cracks grew slowly and were accompanied by considerable general corrosion of the specimen. As a result of the various tests described in Section VI-B the following corrodent, referred to frequently in this report as the salt-dichromate-acetate solution, was chosen for evaluation of the aluminum alloys: 0.6M (3.5%) NaCl + 0.02M Na<sub>2</sub>Cr<sub>2</sub>O<sub>7</sub> + 0.07M NaC<sub>2</sub>H<sub>3</sub>O<sub>2</sub> + HC<sub>2</sub>H<sub>3</sub>O<sub>2</sub> to a pH of 4. This is a chromate-inhibited, acetate-buffered acidic 3.5% sodium chloride solution that causes rapid SCC growth in precracked specimens of susceptible alloys without causing appreciable corrosion of the metal surface. A set of short-transverse smooth specimens was also exposed by continuous immersion in this solution.

Because of the extensive work done at the Boeing Company under the ARPA program<sup>(26)</sup> with 3.5% NaCl solution added dropwise three times a day to their DCB specimen, a series of Boeing DCB specimens exposed to 3.5% NaCl by the Boeing method, to the salt-

dichromate-acetate solution and to the outdoor atmospheres was added to the original program for this investigation.

b. Stainless Steels and Titanium - The smooth specimens were exposed to the 3.5% NaCl alternate immersion test, the same as the aluminum alloys. They were, however, exposed to solution in a separate container so that heavy metal ions from the steel specimens would not contaminate the solution to which the aluminum alloys were exposed.

The rather limited literature indicated that 3.5% NaCl solution would probably be suitable for the precracked specimens<sup>(30,31)</sup> but in view of Freedman's preference<sup>(32)</sup> for a 20% NaCl solution it was decided to conduct a pilot test with those two solutions and synthetic sea water. On the basis of these tests it was decided to use the 20% NaCl solution for the steel alloys and 3.5% NaCl solution for the titanium 6Al-4V alloy.

#### F. Evaluation and Interpretation

Because of the extremely high stress intensities developed in many of the precracked test specimens, and a desire to separate mechanical deformation effects from environmental crack growth and SCC, the test specimens were examined in detail. All fractured test specimens, smooth or precracked, were visually examined, and extensive use was made of photographs and scanning electron microscope (SEM) fractographs to record the different types of fracture characteristics observed. Many of the precracked specimens were cut into two pieces at mid-thickness so that a metallographic cross section of the crack in one half could be correlated with the examination of the fracture surface of the other half.

The results of the smooth specimen tests were evaluated in terms of the stress levels at which the alloys were susceptible to SCC. Although it is necessary to select significant exposure periods for each environment for practical purposes, the use of the time to failure is not regarded as an adequate measure of the resistance of a material to SCC except in certain contexts.

The results of the tests of the precracked specimens were evaluated in terms of (a) the extent and rate of environmental crack growth or SCC and (b) the threshold stress intensity. Many graphical presentations of these parameters were made and will be described in more detail in later sections.

For the purpose of this investigation the term "stress-corrosion cracking" (SCC) is reserved for the mode of crack propagation traditionally associated with this phenomenon in the alloys tested -- intergranular for the aluminum and steel alloys and transgranular for the titanium alloy included in this investigation. The term "environmental crack growth" is used in a broader sense requiring no particular mode of propagation. The definition of SCC recently published<sup>(33)</sup> by the ASTM is: "A cracking process requiring the simultaneous action of a corrodent and sustained tensile stress. This excludes corrosion-reduced sections which fail by fast fracture. It also excludes intercrystalline or transcrystalline corrosion which can disintegrate an alloy without either applied or residual stress".

#### IV. RESULTS OF TENSILE PROPERTY TESTS

##### A. Aluminum Alloys

The tensile properties of the aluminum alloy plates were determined in the three principal orientations, and are summarized

in Table IV.

The properties were representative of the particular alloy, temper and section thickness. The directional tendencies vary with the different alloys and tempers, but the general trend for the per cent elongations in the short-transverse direction to be lower than in the other two directions is evident.

#### B. Stainless Steel Alloys

Tensile properties were determined in the long-transverse direction for all alloys and additionally in the longitudinal and short-transverse direction for selected alloys. The test data are summarized in Table VII.

The tensile properties are representative of published values of the various alloys and tempers except for the yield strength of the SCT 850 temper of the AM355 alloy plate. Although the yield strength is 12.5 ksi below the minimum yield strength of 165 specified for this product, both the ultimate tensile of 219 ksi and the per cent elongation of 16.0 are representative. The yield strength value appears anomalous, but there was good agreement in the yield determinations of duplicate specimens, and therefore the values obtained were used as the basis for stressing the smooth stress corrosion test specimens.

Longitudinal and short-transverse tests were made of both tempers of the rolled bars of PH13-8MO, 431 and AM355 alloys. The properties were uniform in all three directions for the PH13-8MO alloy, but there was a marked reduction in the per cent elongation in the short-transverse direction of the 431 and AM355 alloy bars.

### C. Titanium 6Al-4V Alloy

Tensile properties determined in the three principal orientations with 0.160" diameter specimens machined from the center of the forged bars are presented in Table VIII. Directional effects are small although, unlike the aluminum and the stainless steel alloys, there is an indication that the tensile and yield strengths tend to be highest in the long-transverse direction. Also the per cent elongations tend to decrease slightly in going from the longitudinal, to long-transverse, to the short-transverse directions. These indications are the same in both forgings, with both the strengths and elongations being slightly higher for the alpha-beta forging.

## V. RESULTS OF PLANE-STRAIN FRACTURE TOUGHNESS TESTS

### A. Aluminum Alloys

The plane-strain fracture toughness of each of the plates in the longitudinal (L-T) and short-transverse (S-L) orientations was determined with 1" thick (or in two cases, 0.75" thick) compact tension specimens of the design shown in Figure 6. The results of the tests are presented in Table IX.

Valid or meaningful values of  $K_{Ic}$  were obtained for most of the plate samples. However, the values for the longitudinal (L-T) specimens of 2219-T37, 5456-H117, 5456-Sens. and 6061-T651; and short-transverse (S-L) specimens of 2219-T37, 5456-H117 and 5456-Sens. did not meet the ASTM criteria for valid  $K_{Ic}$  values, primarily because the specimen thickness was insufficient to assure plane-strain conditions for these relatively tough alloys.

Because the  $K_Q$  values undoubtedly were less than the true  $K_{Ic}$  values for these alloys, and they can be expected to reflect the behavior of the specimens used in the stress corrosion tests, they were used as a basis for calculating the initial stress intensities,  $K_{Ii}$ , applied to the stress corrosion specimens. For the alloys and tempers for which valid  $K_{Ic}$  values were obtained, the longitudinal (L-T) values ranged from 23.3 ksi  $\sqrt{\text{in.}}$  for 2024-T851 to 31.1 ksi  $\sqrt{\text{in.}}$  for 2021-T81, and the short-transverse (S-L) values ranged from 16.7 ksi  $\sqrt{\text{in.}}$  for 2024-T851 to 21.4 ksi  $\sqrt{\text{in.}}$  for 6061-T651.

The results of additional tests with various sizes of longitudinal (L-T) specimens of 2219-T37 and T87 are shown in Table X. The  $K_{Ic}$  values for 2219-T87 were valid and did not vary greatly when determined with specimens of various sizes; the higher values for the larger specimens are the result of the longer crack lengths. However, even with the larger specimens, valid  $K_{Ic}$  values could not be obtained for 2219-T37 because excessive yielding occurred in the specimens during the test (indicative of high toughness). These results, however, confirmed that the invalid results from the 0.75 and 1" specimens may be considered to be lower bound values.

#### B. Stainless Steel Alloys

The plane-strain fracture toughness of each of the alloys and tempers in the long-transverse (T-L) orientation was determined with 1" thick compact tension specimens. If the size of the stock permitted, tests were also conducted with thicker, 1.93-2.00" long-transverse (T-L) specimens. Fracture toughness in the

longitudinal (L-T) and short-transverse (S-L) orientations was also determined for certain materials with 0.75 or 1" thick specimens. The results of the tests are summarized in Table XI.

Valid  $K_{Ic}$  values were obtained with at least one of the long-transverse (T-L) specimens of all but the 15-5 PH alloy in the H1150M temper and the 431 alloy in the HT125 temper. A comparison of the data for 1.0 and 2.0" thick long-transverse (T-L) specimens showed that the results obtained with the two specimen sizes were in good agreement in three instances, but were in poor agreement in five instances. The fact that the  $K_{Ic}$  values were invalid for specimens of both thicknesses of 15-5 PH - H1150M alloy, and for the 1.0" thick specimens of the 431-HT125 alloy probably accounts for the lack of agreement in those two cases, but there is no apparent reason for the differences noted in tests of PH13-8Mo-H1050, 431-HT200 and AM355-SCT 1000 steels. In seven of the eight available comparisons,  $K_Q$  values for the 2.0" thick specimens were higher than those for the 1.0" thick specimens as would be expected because of the longer crack lengths in the larger specimens. Because the smaller specimens are in the range where specimen geometry can influence the test results, the higher values probably are more reasonable. However, it is also possible that variations in structure through the thickness may have accounted for some of the differences.

Considerable scatter was noted between the values of replicate specimens from certain of the alloys for which valid  $K_{Ic}$  values were obtained, particularly alloys 15-5PH-H900 and H1150M, 431-HT125 and AM355-SCT 1000.

Comparison of results for specimens of the three orientations (L-T, T-L and S-L) shows that  $K_{Ic}$  was generally highest in the longitudinal (L-T) direction and lowest in the long-transverse (T-L) direction. One exception to this was the 431-HT125 steel for which the short-transverse (S-L) value was definitely lower than the long-transverse (T-L) value.

C. Titanium 6Al-4V Alloy

The results of tests in the long-transverse (T-L) orientation determined for each of the forged bars with 0.5, 1.0 and 1.5" thick compact tension specimens are summarized in Table XII. All of the tests with 1" thick specimens yielded valid  $K_{Ic}$  values, but the values were below those sometimes achieved with other forgings of this alloy (60 to 80 ksi  $\sqrt{\text{in.}}$ ). Values obtained with the 0.5 and 1.5" thick specimens showed that for the alpha-beta forging, the  $K_{Ic}$  values were nearly independent of thickness, with the value for the 1" thick specimens being on the high side of the range. For the beta forging, the value for the 0.5" thick specimens clearly underestimated  $K_{Ic}$ ; the value of the 1" thick specimens may have overestimated  $K_{Ic}$  as the result for the 1-1/2" thick specimen, the largest which could be obtained from the material, indicated a lower  $K_{Ic}$ .

These data are in line with general experience in that beta forged material characteristically develops a higher  $K_{Ic}$  than alpha-beta forged material, but as indicated above the value for this beta forged sample is below that usually obtained (60-80 ksi  $\sqrt{\text{in.}}$ ).

Because the stress corrosion tests utilized 1" thick specimens,

the  $K_{Ic}$  values from tests of that size of specimen were used in the analysis of test data.

## VI. RESULTS OF STRESS CORROSION TESTS OF ALUMINUM ALLOYS

### A. Tests with Smooth Specimens

The purpose of these tests was twofold: (1) to compare the performance of the particular lots of plate procured for the contract with that previously established for the respective alloys and tempers, and (2) to provide a base-line for comparison with the data obtained with precracked specimens.

#### 1. Atmospheric Exposures

Seacoast and inland industrial atmospheric exposures have completed about three years at this writing, and the exposures will be continued for at least a 4 year period. Lists of the specimens and the failures to date are given in Tables XIII and XIV. These data are consistent with other outdoor tests of products of these alloys<sup>(22,34)</sup>, and will be used for reference in interpreting the accelerated test results.

It is evident from a comparison of the number of days to failure of the short-transverse specimens stressed at 27, 20 and 10 ksi that the seacoast environment is more aggressive in causing SCC than the inland industrial atmosphere. As anticipated, there have been no SCC failures of the short-transverse specimens from the group of highly resistant alloys. Likewise, there have been no SCC failures of the longitudinal specimens of any of the alloys. However, longitudinal specimens of certain of the low resistance alloys were removed from the seacoast exposure because of severe exfoliation, as noted in Table XIII.

2. Alternate Immersion in 3.5% NaCl Solution

a. Longitudinal Specimens

None of the longitudinal specimens failed during the 84-day exposure, again verifying the high resistance to SCC that is characteristic of aluminum alloy products when stressed parallel to the longitudinal direction of the grain structure.

Tensile tests were made on the exposed specimens, and the per cent decrease in tensile strength calculated in comparison with unexposed specimens. These data are given in Table XV. Inasmuch as the applied stress did not appreciably increase the corrosion damage to specimens of any of the alloys, the data for unstressed and stressed specimens were combined to make a comparison of the general resistance to corrosion of the alloys. When the alloys are listed in order of increasing per cent loss in tensile strength caused by corrosion, they fall into five groups that can be related to the increasing copper content of the alloys. The grouping shown below is a typical representation of the inherent resistance to corrosion of the alloys in relatively corrosive marine environments.

<u>Alloy</u>	<u>% Cu</u>	<u>% Loss in T.S.</u>
5456-H117, 6061-T651 and 7039-T651	0-0.3	0
7079-T651	0.8	5-7
7075-T651, T7351	1.8	8-15
2014-T651, 2021-T81, 2024-T851, 2219-T87	4.2-6.4	15-24
2024-T351, 2219-T37	4.2-6.4	26-53

However, such ratings are influenced by the temper and the environment and should be used with caution. For example, in the seacoast

atmosphere the relative resistance of 7075-T651 was similar to that of 2024-T351 and 2219-T37 and was very poor because of exfoliation corrosion (Table XIII) performance of those alloys.

b. Short-Transverse Specimens

A listing of the short-transverse specimen failures and the times to failure is given in Table XVI. The performance of the alloys with low resistance to SCC generally was in line with the performances in the atmospheric exposures. The slightly better performance of alloy 7039-T6351 was not unexpected because it has been observed previously that the alternate immersion test may not be as critical for copper-free 7XXX type alloys as an industrial atmosphere<sup>(23,34)</sup>.

A number of short-transverse specimens from the group of alloys with high resistance to SCC fractured when stressed at 75% of the yield strength. These failures were of alloys that have relatively low resistance to pitting corrosion in this test environment, and thus, there is a possibility that some of the fractures may have resulted from reduction of the cross-section of the specimens by corrosion (Refer to Fig. 8). Therefore, all of the ten failures from this group of alloys were examined metallographically to determine the cause of failure. Intergranular stress-corrosion cracking, illustrated in Figure 17, occurred only in the three 2024-T851 specimens stressed at 75% Y.S. The single 2024-T851 failure at 25 ksi and the three 2021-T81 specimens at 75% Y.S. revealed only deep directional pitting with no secondary cracking. In the case of alloy 2219-T87 deep directional pitting was observed with short transgranular cracks emanating from occasional sites

of pitting (Figure 18). The single 7075-T7351 failure (Figure 19) showed deep, rounded pitting with mixed mode (predominantly transgranular) cracks emanating from many of the pits. Fractographs of these transgranular cracks are shown in Figure 20. The crack surfaces were similar in the two alloys except that there was a greater tendency for branching in the 7075-T7351 alloy. On the 2219-T87 fracture there are a few beachmarks near the crack tip and sites of corrosive attack adjacent to rounded particles of constituent. These transgranular cracks, which are not typical stress-corrosion cracks in aluminum alloys have a striking resemblance to fatigue and corrosion fatigue cracks; see references 35, 36 and 37. Additional studies are being made to try to reproduce these cracks with other types of loading. No cracks of this type occurred in the precracked specimens (See Section VI-D).

### 3. Continuous Immersion in Salt-Dichromate-Acetate Solution

Exploratory tests of less corrosive solutions than 3.5% sodium chloride to use with precracked specimens (Section VI-B1) led to the choice of an inhibited solution containing 0.6M (3.5%) NaCl + 0.02M Na<sub>2</sub>Cr<sub>2</sub>O<sub>7</sub> + 0.07M NaC<sub>2</sub>H<sub>3</sub>O<sub>2</sub> + HC<sub>2</sub>H<sub>3</sub>O<sub>2</sub> to pH 4. In this solution SCC propagated rapidly in all of the alloys in the low resistance group. Therefore, a set of the smooth tension specimens was exposed to this solution to determine whether SCC would initiate readily. Specimens were continuously immersed for 90 days (2160 hr.); the same as the precracked specimens. No appreciable corrosion occurred with any of the alloys, with the surfaces of the

specimens remaining bright and shiny. A summary of the stress corrosion failures is presented in Table XVII.

Only one short-transverse specimen fractured in the group of high resistance alloys, and that was a 7075-T7351 specimen stressed at 75% Y.S. However, metallographic examination (footnote 3, Table XVII) indicated it most likely resulted from reduction of the cross-section at a single pit, rather than by stress-corrosion cracking.

In the group of low resistance alloys, specimens of sensitized 5456 failed rapidly (within 1-2 days) at all stress levels including 10 ksi. Specimens of the Al-Zn-Mg alloys 7039-T6351, 7075-T651 and 7079-T651 failed at 75% Y.S. and at 27 ksi but not at 10 ksi; the most rapid failures (4 days) in this group were of 7039-T6351 stressed at 75% Y.S. During the 90-day exposure stress-corrosion cracking initiated in only one specimen of the three low-resistance Al-Cu alloys (2014-T651, 2024-T351 and 2219-T37), and that was a specimen of 2219-T37 stressed at 27 ksi that cracked on one shoulder in the crevice under the protective coating; none failed at 10 ksi or at the highest stresses of 75% Y.S.

Under the test conditions employed the salt-dichromate-acetate solution does not appear to be suitable for testing smooth specimens of a variety of aluminum alloys. However, in view of the rapid SCC velocity observed with precracked specimens of all of these alloys in this solution it appears that some modification of the procedure could be found that would enhance the initiation stage and make this solution useful for smooth specimens. For example, Helfrich (38) found that a somewhat similar solution

was effective for smooth specimens of a variety of alloys provided the solution was at an elevated temperature and the specimen surface was given a caustic etch. Comparison of the performance of these smooth specimens with that of the precracked specimens presented in Section VI-B indicated a similarity in the relative performance of the various alloys.

These test results illustrate the ultimate need of accelerated tests that realistically relate to intended service conditions. For service in atmospheric environments an 84-day exposure to 3.5% NaCl by alternate immersion relates better than an 84-day period of continuous immersion in the salt-dichromate-acetate solution (other tests at ARL have shown that the results are not improved when specimens are exposed to this solution by alternate immersion). On the other hand a high resistance to SCC in the atmosphere is not a reliable criterion of serviceability in special chemical environments such as inhibited red fuming nitric acid (IRFNA)<sup>(39)</sup>.

## B. Tests with Bolt Loaded Precracked Specimens

### 1. Exploratory Tests

Because of the relatively limited amount of available information on the optimum techniques for testing the materials in this program with precracked specimens, exploratory tests were performed to determine certain of the procedures to be used.

#### a. Accelerated Test Media

Previous tests at Alcoa Research Laboratories with bolt-loaded compact tension specimens immersed in 3.5% NaCl solution<sup>(27)</sup> have revealed two problems: (a) relatively slow SCC growth rates, with uncertainty in detecting arrest, and (b) difficulty in measuring crack lengths because of corrosion on the sides of the

specimens.

Although there are several variables that should be investigated in order to develop an optimum accelerated test procedure, most of these involving such things as specimen configuration, loading system, etc., can best be evaluated after a suitable corrodent is chosen. Therefore, a preliminary program of tests was undertaken to evaluate a number of test media based on a search of stress corrosion literature.

Because it is known that the effectiveness of an environment can vary markedly with alloy type, two susceptible alloys, 2024-T351 and 7075-T651, with different electrochemical characteristics were selected for comparing three control solutions and nine experimental solutions. The nine experimental solutions are types that have been reported in the literature for use with smooth specimens. Basically they represent 3.5 per cent sodium chloride solutions with the addition of chromate, nitrate or sulfate.

Duplicate S-L compact specimens were bolt loaded to develop a precrack in tension and an initial stress-intensity ( $K_{I_1}$ ) at or near  $K_{Ic}$  ("pop-in") and exposed by continuous immersion. A few drops of the test solution were added just prior to the final stage of the precracking. Crack lengths were then measured on the specimen surface and the specimens partially immersed in the solution without delay. The specimens were placed on end with the precrack extending downward and the water-line at the tip of the chevron. Frequent measurements of the pH of the solution and inspections of the specimens were made. The specimens were periodically removed from the solution for measurement of the crack

length at 20X magnification. Plots of crack growth versus exposure time are shown in Figure 21 for each of the solutions.

(1) Control Solutions

The crack growth noted on the 7075-T651 specimens continuously immersed in 0.6M (3.5%) NaCl was similar to that noted previously in this solution<sup>(29)</sup>. Use of synthetic seawater did not affect the rate of crack growth appreciably though it did reduce somewhat the amount of general corrosion of both alloys. In distilled water, very slow crack growth occurred in 7075-T651 after a two week incubation, but no growth occurred in 2024-T351 during the entire 140 day period of exposure. None of the specimens that developed cracks in the control solutions showed definite arrest.

(2) Experimental Solutions

The objective of these tests was to find a solution which would cause faster crack growth, with less general corrosion than the sodium chloride solutions in order to:

1. obtain a rapid test with convenience for measuring crack growth, and
2. minimize extraneous effects from entrapped corrosion products, thereby increasing the possibility of obtaining an arrest.

In the four solutions containing chromates or dichromates there was negligible surface corrosion and the crack was always readily visible on specimens of both alloys. Considerable corrosion, including some exfoliation, occurred in the solution containing nitrate, and plating of copper on the specimen occurred in the solution with sulfate. Consequently the latter two solutions were objectionable from the standpoint of general corrosion.

As can be seen in Figure 21, the most rapid crack growth consistently occurred in the two acidified chloride-dichromate solutions and in the acidified chloride-nitrate solution. Although the more strongly acidic (pH 1.3) chloride-dichromate solution (included to provide an extreme condition) caused the fastest cracking, it was ruled out as a corrodent for general use because of the tendency for severe crevice corrosion and previous experience (with smooth specimens) has shown that it does not realistically reproduce service performance and atmospheric test data on certain alloys<sup>(21)</sup>. In the neutral sodium-chromate solutions crack growth was erratic and not reproducible with duplicate specimens of 2024-T351 alloy. The acidified chloride-nitrate solution caused excessive general corrosion.

The solution that appeared most favorable from all aspects was the chloride-dichromate-acetate solution at pH 4. This solution appears to be well suited for use with both 7075-T651 and 2024-T351 alloys. A final pilot test was performed in this solution on seven additional alloys and tempers, further demonstrating the suitability of this corrodent. A more complete description of the results of these exploratory test results is given in the one year summary report<sup>(12)</sup>.

Two noteworthy observations were made as a result of these experimental tests in the various corrodents. The first is that with high initial stress-intensities near  $K_{Ic}$  very long cracks propagated through almost the entire width of the specimen. Such long crack lengths invalidate the calculation of a residual stress-intensity. Consequently, either lower initial stress-intensities or some other specimen configuration will have to be used in order

to obtain a value of  $K_{I_{SCC}}$  by the arrest method.

The second observation is that the cracking did not always develop simply as an extension of the mechanical precrack, but often initiated at other sites (Figure 22). Cracks tended to develop at the edge of the crack tip plastic zone; i.e., the plastically deformed metal around the tip of the crack, particularly for alloy 2024-T351. This multiplicity of cracking probably accounts for the slower and somewhat more erratic crack growth that was noted on 2024-T351 compared with 7075-T651 and also invalidates calculation of a final stress-intensity.

#### b. Specimen Configuration

The three types of specimens used in these tests are shown in Figure 11. Several S-L specimens of each of the three types were precracked in tension by loading with a single bolt up to the point of initial cracking (pop-in). The actual load applied to the specimen is not known, but it was assumed that the resultant  $K_{I_i}$  was slightly less (i.e., about 95-100%) than  $K_{I_C}$ . Specimens were partially immersed as described previously in the salt-dichromate-acetate solution and in 3.5% NaCl solution. In addition, some tests were conducted by introducing several drops of 3.5% NaCl solution into the cracks in the Boeing DCB specimens three times a day by the Boeing test procedure.

A comparison of the crack growth for the three specimen types in the salt-dichromate-acetate solution is illustrated with 7075-T651 alloy in Figure 23. A similar comparison was obtained for alloy 2024-T351. For both alloys, the initial crack growth rate was about the same for all three specimens, but for the DCB

specimens there was a distinct leveling off or deceleration in crack growth in the range of 400 to 1000 hours followed by an acceleration to almost the original crack growth rate. This behavior suggests that an arrest was being approached but that this tendency was over-riden by an artificial increase in the stress intensity resulting from corrosion product building up in the crack after prolonged exposure. Thus, the longer crack growth possible in the DCB specimens does not clearly represent an advantage for the use of this specimen in determining  $K_{I_{sc}}$ .

A comparison of the crack growth in Boeing DCB specimens in three environmental conditions (Figure 24) shows for both 2024-T351 and 7075-T651 alloys that the rate of crack growth increased in the order: (1) immersion in 3.5% NaCl, (2) immersion in salt-dichromate-acetate solution, and (3) 3.5% NaCl added drop-wise to the precrack three times a day (Boeing procedure).

Tests were made of S-L compact tension specimens of various thicknesses of 2024-T351 and 7075-T651 alloys to determine the effect of deviating from plane strain into mixed-mode stress states. Duplicate specimens bolt loaded to pop-in were exposed to the salt-dichromate-acetate solution. Graphs of the environmental crack growth are shown in Figure 25. There did not appear to be any appreciable effect of the specimen thickness on the crack growth rate for either alloy. It is clear that stress-corrosion cracking in these aluminum alloys is not a "plane-strain" phenomenon and that meaningful indications of crack growth rate at given K-levels can be obtained on relatively thin specimens.

Hyatt<sup>(40)</sup> likewise found no effect of specimen thickness on  $K_{Ic}$ -rate behavior of S-L specimens machined from 7079-T651 plate. DCB specimens ranging in thickness from 1 in. to 0.050 in. were bolt loaded to pop-in and exposed by wetting the precrack three times a day with 3.5% NaCl solution.

c. Tension vs. Fatigue Precrack

The surface of a fatigue crack is readily distinguished visually from that of a tension fracture. Also, with a properly controlled fatigue precrack the crack front through the thickness of the test specimen is straighter and the plastic zone is smaller than for the tension precrack. Hence, the fatigue precrack is preferred for fracture toughness testing, and this type of precrack was chosen for the general program of stress corrosion testing by the fracture mechanics approach.

Tension precracking was used for the exploratory tests described above as an expediency to save time. Previous exploratory tests reported in the one year summary report<sup>(12)</sup> showed that for an alloy with low resistance to SCC (7075-T651) the environmental crack growth tended to be slightly faster for S-L compact tension specimens precracked by tension than when precracked by fatigue. The average crack growth rates sustained over the first 1000 hours of immersion in 3.5% NaCl was  $4 \times 10^{-4}$  in./hr. for specimens bolt loaded to pop-in and  $2 \times 10^{-4}$  in./hr. for fatigue precracked specimens bolt loaded to 90% of  $K_{Ic}$ . Although the initial stress intensities may not have been identical, the growth rates were constant after the first 100 hours of exposure and

independent of the decreasing stress intensity. Additional comparisons of the effect of type of precrack on the environmental crack growth in alloys with high resistance were obtained in subsequent tests in the general program (Section VI-B2-b(2)).

d. Method of Loading

The use of two loading bolts bearing against each other, instead of one bolt bearing against an aluminum surface, requires less effort to start a tension crack (pop-in), especially with the compact tension specimen which has a chevron notch. Because the operator has a better "feel" of the pop-in there is less likely to be a jump when the first evidence of mechanical crack growth is noted, and  $K_{I_1}$  probably will approach more closely the limiting stress intensity factor for the particular test specimen than when one-bolt is used.

To check the environmental crack growth with 2-bolt loading, two DCB specimens of 7079-T651 and one compact specimen each of 2219-T87 and 7075-T7351 were tested. The results shown in Figures 26 and 27 indicate a higher rate of initial crack growth with the 2-bolt specimens.

2. Performance of Compact Tension Specimens

Replicate specimens loaded to several nominal stress intensity levels were exposed to the salt-dichromate-acetate solution and to the atmosphere at the seacoast and at an inland industrial location to determine comparative threshold stress intensities ( $K_{I_{SCC}}$ ) for the various alloys. Most emphasis was placed on short-transverse (S-L) specimens although longitudinal (L-T) specimens also were included. A complete listing of all of the specimens and the

detailed data are given in Tables D-1, D-2 and D-3 in the Appendix.

a. Longitudinal (L-T) Tests

(1) Atmospheric Exposures

No crack growth was visible on any of the high resistance alloy specimens loaded to 95%  $K_{Ic}$  after 19 months at the seacoast and 18 months at the inland industrial location. On certain of the low resistance alloys, however, slight crack growth was observed after relatively short times. Crack extension of about 0.01 in. was noted (after 8 months in the industrial atmosphere) on one of the two specimens loaded to 95%  $K_{Ic}$  of alloys 7039-T6351 and 7079-T651. These and all of the other L-T specimens are continuing in the industrial atmosphere with no crack growth indicated in any other specimens to date (18 months). After 5 months in the seacoast atmosphere, crack growth was noted in one specimen of 2014-T651 and in all three specimens of 2219-T37. The specimen of 2219-T37 with the most growth (0.12 in.) was removed for metallographic examination. The SCC was shown to be branching because of the recrystallized grain structure (Figure 28; refer also to Figure 1) and did not remain in the plane of the precrack. All the other L-T specimens are continuing in the seacoast atmosphere with no crack growth indicated in any other specimens to date (18 months).

(2) Immersion in Salt-Dichromate-Acetate Solution

No crack growth was visible on the exterior surfaces of the specimens of any of the high resistance alloys, and only a slight amount indicated for those of the low resistance alloys. After about 90 days the exposures were discontinued and the residual

stress intensities ( $K_{I_p}$ ) determined. Also, single fatigue precracked specimens exposed without any applied load were tension tested to determine the effect of the exposure on the stress intensity at fracture in air ( $K_{I_x}$ ). All of these  $K_I$  values, expressed as per cent of  $K_{I_c}$ , are summarized in Table XVIII.

The  $K_{I_x}$  data were erratic and of questionable significance. When valid tests were obtained the  $K_{I_x}$  values were fairly close to  $K_{I_c}$ , indicating that the 90 day exposure under no load apparently had no appreciable effect on the intrinsic fracture toughness of the alloys.

The residual stress intensities in all cases were lower than the applied values, as would be expected if crack growth had occurred. However, the data in Table XVIII show that the amount of reduction of  $K_{I_1}$  was not governed by the amount of crack growth. Three types of performance were noted with the various alloys: (a) no crack growth for alloys 5456-H117, 6061-T651 and 7075-T7351, (b) small amount of in-plane crack growth at the interior of specimens of 2219-T87, 2021-T81 and 2024-T851; this extension of the precrack was corroded and resembled ductile tension fracture rather than SCC, and (c) small to large amounts of SCC in planes perpendicular to the precrack for specimens of the low resistance alloys. A photograph of a representative group of fractured specimens is shown in Figure 29. It is evident from these data that the degradation of the applied stress intensities was of about the same order regardless of whether SCC had occurred. In fact, it appears that corrosion was not even involved for alloys 5456-H117 and 6061-T651, and that the reduction in  $K_{I_1}$  probably was the result of

relaxation or creep.

(3) Evaluation and Interpretation of Longitudinal Tests

The L-T compact tension specimens showed a high resistance to SCC even though a reduction of the applied stress intensity was noted at the end of a 90-day exposure to the salt-dichromate-acetate solution. Meaningful estimates of  $K_{I_{SCC}}$  for the various alloys cannot be made because of the wide variation in the  $K_{I_p}$  values irrespective of the presence of corrosion or SCC. The average rate of environmental crack growth for all alloys in the accelerated test was very low (approx.  $10^{-5}$  in./hr.) and of doubtful significance because of mechanical extension of the precrack in some cases, and when SCC occurred, it was usually perpendicular to the plane of the precrack. Wacker and Chu<sup>(41)</sup> noted a similar behavior of L-T cantilever beam specimens machined from rolled plate of alloys 7039-T64, 7002-T6 and X7106-T63. In the specimens from the recrystallized 2219-T37 alloy plate with a less directional grain structure branching SCC progressed more or less in the plane of the precrack (Figure 28) and the average rate of crack growth was about  $10^{-4}$  in./hr. in the salt-dichromate-acetate solution and  $10^{-5}$  in./hr. in the seacoast atmosphere.

b. Short-Transverse (S-L) Tests

(1) Atmospheric Exposures

Five specimens of each alloy, four loaded to 95%  $K_{I_C}$  and one with no load, were exposed at the two atmospheric test sites. In addition, for the low resistance alloys subsequent exposures were made of two specimens loaded to 75%  $K_{I_C}$ , two at 50%  $K_{I_C}$  and one more with no applied load.

(a) Seacoast Atmosphere

SCC started quickly in specimens of the low resistance alloys at all applied  $K_I$  levels. The cracking propagated 0.2 to 0.9 in. within three months, with an average velocity of about 1 to  $4 \times 10^{-4}$  in./hr. depending upon the alloy and, to a lesser extent upon  $K_{I1}$ . Exposure of all of the S-L specimens of the low resistance alloys was discontinued at the end of 8.3 months. Details regarding crack lengths, final  $K_I$  values, etc. are given in Table D-1 of the Appendix.

$K_{I_{SCC}}$  values for these alloys in the seacoast atmosphere obviously is less than 50%  $K_{Ic}$  and undoubtedly is very low, if they do, in fact, exist. Evidence of this for certain of the alloys was indicated by the initiation of small stress corrosion cracks in specimens with no applied load, as shown in Figure 30. The stress responsible for initiating these cracks presumably was developed by wedging action of small amounts of corrosion product formed on the faces of the fatigue precrack. (Residual stresses in mechanically stress-relieved plates normally are very low and would not be expected to be a factor in these tests).

The performance of the high resistance alloys was markedly superior to that of the low resistance alloys. No crack growth was discernible on specimens of 5456-H117 and 6061-T651 after 24 mo. exposure although the stress intensities determined on specimens removed after 8.3 mo. showed a slight reduction; this reduction probably was due to plastic deformation during application of the bolt load. The other four alloys showed small amounts (0.04 - 0.08 in.) of environmental crack growth that initiated after 3 to 8 mo. and was accompanied by an appreciable drop from

the applied stress intensity as shown by the  $K_{I_r}$  values in Table D-1. The average crack growth rate ranged from 5 to  $30 \times 10^{-6}$  in./hr.; however, metallographic examination of single specimens removed at 15 mo. revealed the cracking to be intergranular SCC only in the case of 7075-T7351 (Figures 31, 32) and transgranular tensile fracture in the case of 2021-T81, 2024-T851 and 2219-T87. Extending beyond the transgranular crack tips were discontinuous steps or jogs where small voids had nucleated in stringers of brittle intermetallic compounds (Figure 33). All of the crack surfaces were covered with corrosion products, indicating that the environmental cracking was tension fracture caused by corrosion product wedging. Fractographic examination was impracticable because of the corrosion of the fractures.

(b) Industrial Atmosphere

SCC started quickly in specimens of 7075-T651, 7079-T651, and 7039-T6351 at all applied  $K_I$  levels and propagated at about the same rate as in the seacoast atmosphere. SCC also initiated rapidly in the 5456-Sens. specimens but the propagation rate was about 1/10 of that in the seacoast atmosphere. SCC growth in specimens of 2219-T37, 2024-T351 and 2014-T651 was not evident until after 3 to 12 mo. and cracking then propagated at about  $10^{-5}$  in./hr., which was about 1/10 of the velocity in the seacoast atmosphere.

$K_{I_{SCC}}$  for S-L specimens of the low resistance alloys in the industrial atmosphere also is less than 50%  $K_{I_c}$  and may not be very different from values in a seacoast atmosphere, particularly for the 7XXX-T6 alloys. Small stress corrosion cracks were present at the tip of the precrack in a specimen of 7039-T6351 that was

fractured after exposure at no load for 12 mo.

None of the four S-L specimens of each of the high resistance alloys loaded to 95%  $K_{Ic}$  showed any surface crack extension at the end of 12 mo. when duplicate specimens were removed for tests of  $K_{Ic}$ . Although slight crack extension was evident on the fracture surfaces of the 2219-T87, 2021-T81 and 2024-T851 specimens, the fractures were corroded and the crack growth again was probably caused by corrosion product wedging. Metallographic examination of a third specimen of each alloy removed after 18 mo. exposure revealed transgranular cracking similar to that shown in Figure 33. The average rate of extension at the interior of the specimen was about  $8 \times 10^{-6}$  in./hr., similar to that at the seacoast. The fourth specimen of each alloy still showed no visible crack growth at the surface after 28 mo.

#### (2) Immersion in Salt-Dichromate-Acetate Solution

Specimens of the high resistance alloys were loaded to pop-in, and to 95 and 75% of  $K_{Ic}$ ; specimens of the low resistance alloys were loaded to 75, 50 and 25%  $K_{Ic}$ . Exposure periods in this accelerated test medium were intentionally extended for longer periods than thought necessary for two reasons: (1) to observe slow-start cracking and (2) to observe anticipated corrosion-wedging effects. The occurrence of corrosion-wedging effects, of course, complicates the interpretation of the test results, but this was considered necessary in order to decide upon an optimum period of exposure for future testing. Identification of the specimens and the detailed information regarding their exposure is given in Table D-3 of the Appendix.

Graphs of environmental crack growth for each alloy are presented in Figures 34-38. Additional graphs with crack growth rate ( $da/dt$ ) plotted as a function of stress intensity are presented in Figures 39-43. The latter graphs were derived from the first set by determining the slope of constant regions of the crack growth curves and calculating the stress intensity factor (assuming a constant COD) for the crack length at each end of the region of the constant slope. The K-Rate graphs when read from right to left illustrate how the crack velocity varied with the decreasing stress intensity. Theoretically, for constant deformation loaded specimens such as these, increases in crack length will result in decreases in both stress intensity and in crack growth rate. When the crack growth rate drops to zero, the threshold stress intensity for environmental cracking under the conditions of test will be realized. This theoretical relationship is illustrated by graphs such as those in Figure 41. The normal type of graph was not obtained in some cases because of corrosion of walls of the crack. The salt-dichromate-acetate solution causes aggressive crevice corrosion in copper containing 2XXX and 7XXX alloys, resulting in exfoliation of susceptible alloys such as 2219-T37, 2024-T351 and 7075-T651. The formation of insoluble aluminum oxide corrosion products in the crack causes an increase in the wedge-force crack opening load, and from that point on the behavior does not follow the theoretical trend. The evidence of such effects can be seen especially in Figures 39 and 40, and because of this effect it was necessary to construct "estimated true curves", excluding corrosion-wedging effects.

Several types of characteristic graphs were exhibited by the various alloys and tempers, as shown in Figure 43. It is apparent that specimens of the low resistance alloys developed much higher SCC growth rates and much lower threshold stress intensities than specimens of the high resistance alloys. A summary of the threshold stress intensities and the highest sustained initial crack velocities derived from these graphs is given in Table XIX along with similar data for specimens exposed to the seacoast and the inland industrial atmospheres.

Environmental crack growth in the high resistance alloys initiated sooner and propagated more rapidly when the precrack was produced by tension and the specimen loaded to just under pop-in than in fatigue precracked specimens loaded to 95%  $K_{Ic}$  as shown in Figure 38. This difference in behavior may be related to the larger plastic zone at the tip of the tension precrack causing fracture of brittle alloy constituents and thereby stimulating crack growth.

### (3) Evaluation and Interpretation of Short-Transverse Tests

Specimens of alloys from both the low resistance and the high resistance groups were photographed to show typical forms of environmental crack growth in all three of the test environments (Figures 44 and 45). The fatigue precracks generally were fairly straight or slightly convex for the harder alloys (see also Figure 30); they were irregular or slightly concave for the tougher lower strength alloys such as 5456-H117, 6061-T651, 2024-T351, and 2219-T37. Although the environmental crack growth tended to extend in a front parallel to the front of the precrack, there were exceptions with some alloys and environments. Generally, the

environmental crack front had a convex front, but in some cases the cracks were longer at the surface than at the interior. The most erratic crack growth occurred in alloys such as 2024-T351, 2219-T37 and 5456-Sens.

Painstaking examinations of specimens of the high resistance alloys were required to determine whether the relatively small amounts of environmental crack growth (Figure 38) and the degradations in the applied stress intensities were the result of stress-corrosion cracking. Corrosion was present all along the precrack and had progressed to the tips of the crack extensions with considerable corrosion product being formed on all of the alloys (less on the specimens of 5456-H117 and 6061-T651). Thus, there was ample opportunity for corrosion product wedging to cause a gradual increase in the stress intensity at the crack tip. Mechanical extension of the precrack appeared to be advanced by the brittle cracking of alloy constituents strung out in the plastic zone ahead of the crack tip, as shown in Figures 33 and 46. For alloys with a high resistance to SCC, crack propagation could be entirely by this mechanism, as was observed for 2021-T81 and 2219-T87, or by a combination of this mechanism and intergranular SCC, as was observed for 7075-T7351 and 2024-T851 (salt-dichromate-acetate solution).

A comparison of the performance of the various alloys in the salt-dichromate-acetate accelerated test and in the atmospheric exposures is shown by the data summarized in Table XIX. Comparison of the average initial SCC velocities at an applied  $K_I$  of 95%  $K_{Ic}$  shows that the velocity differs with the environment. Also the

relative ranking of the low resistance alloys differs with the environment. For example, while the SCC velocity of 7079-T651 was four times that of 2014-T651 in the seacoast atmosphere, it was 100 times faster in the industrial atmosphere. The velocity of SCC in 7079-T651 (and other 7XXX-T6 alloys) was about the same in both environments but the SCC growth rate of 2XXX alloys was markedly less in the industrial atmosphere. In the accelerated test, where the rates are about ten times those in the seacoast atmosphere, SCC propagated about ten times faster in 7079-T6 than in 2014-T651.

The accelerated tests in the salt-dichromate-acetate solution provided a good distinction between the high resistance and the low resistance alloys, and ranked the various low resistance alloys in approximately the same order as the seacoast exposure. The length of exposure of bolt loaded specimens in this solution should not exceed about 500 hr. to avoid the occurrence of excessive corrosion in the precrack.

### 3. Performance of Boeing DCB Specimens

A set of Boeing DCB specimens was exposed to each of the test environments used for the compact tension specimens and to 3.5% sodium chloride dripped into the precrack in the manner used by Hyatt<sup>(26)</sup>. Although most of the tests were made with short-transverse (S-L) specimens oriented as shown in Figure 9, limited tests were performed also on longitudinal (L-T) specimens. All specimens were loaded to pop-in, with a single bolt. A complete listing of all of the specimens and the detailed data is given in Tables D-4, D-5 and D-6 in the Appendix.

a. Longitudinal (L-T) Tests

L-T specimens of 2219-T37 and 7079-T6 alloys were exposed in each test environment. These tests were unsatisfactory because SCC generally tended to proceed out of the plane of the precrack and go to one side of the specimen, or cracks would initiate in the bolt hole as shown in Figure 47.

b. Short-Transverse (S-L) Tests

(1) Atmospheric Exposures

The performance of DCB specimens of the various alloys in the outdoor tests is illustrated by the environmental crack growth curves in Figures 48 and 49. A summary of the average initial crack velocities are given in Table XX, and these results may be compared with the test results given in Table XIX for fatigue precracked compact tension specimens. The average initial environmental crack growth rates for the DCB specimens precracked in tension and loaded almost to pop-in were as high or higher than for compact tension specimens precracked by fatigue and loaded to 95% of  $K_{Ic}$ . Small amounts of crack growth in specimens of the high resistance alloys occurred in the atmospheric exposures, and metallographic examinations were performed to determine the type of cracking; these results will be discussed in the next section.

(2) Accelerated Test Exposures

The performances of the various alloys in the two accelerated test media are shown by environmental crack growth curves partially smoothed and plotted without data points in Figures 50 and 51. Considerable variation in crack length occurred from side to side and from specimen to specimen and this is shown by sample graphs

of the individual measurements for 2014-T651 and 7075-T651 alloys in Figure 52.

In order to obtain K-Rate graphs, auxiliary crack growth curves were further smoothed so that slopes ( $da/dt$ ) and  $K_{I}$  values could be determined at points along the curves selected in the manner described previously for the compact specimens.  $K_{I}$  values were calculated with Equation(7) given in Section III-D2.

Unfortunately when the DCB specimens were loaded the crack opening displacements ( $V$ ) were not measured, so substitute values of  $V$  were determined on other replicate specimens. Pop-in experiments were performed on two replicates of each alloy with measurements of the specimen height being made before loading, after loading and after unloading. With one set of specimens India ink was introduced into the notch during pop-in to provide a marker of the crack tip. Crack lengths were measured on the surfaces of all specimens and they were then broken open. Crack lengths were measured on the fractures of those with the ink markers, but the pop-in crack length could not be distinguished on the specimens that had no markers. These data together with the  $V$  values and the calculated  $K_{Ii}$  values are given in Table XXI.

A certain amount of plastic deformation occurred during the pop-in of all alloys; it was very slight with some, but was considerable with the tougher alloys. More realistic values of  $K_{Ii}$  (although still higher than  $K_{Ic}$  in most cases) were obtained when only the elastic portion of the total  $V$  was used, as may be seen in Table XXI, and therefore, the average values of  $V$  (elastic)

were used for all calculations of  $K_{I1}$  used for the K-Rate curves. The K-Rate curves were developed for only the portion of the crack growth curves up to the point when crack growth appeared to have ceased (less than 0.01 in. advance over a period of about 200 hr. in the salt-dichromate-acetate solution or about 500 hr. in the 3.5% NaCl test), or if there did not seem to be an arrest, to the point where it appeared that the influence of corrosion wedging had become dominant. The curves for all of the alloys are grouped in Figures 53 and 54.

Comparing these data for DCB's (Figure 53) with that for compacts (Figure 43), the maximum crack growth rates agreed very well for the low resistance alloys, but for the high resistance 2XXX-T8 alloys the rates were about twice as high with the DCB's. However, it was not possible to compare estimated threshold stress intensities because corrosion wedging prevented crack arrest in the DCB specimens loaded to pop-in. Because compacts were loaded to several lower initial stress intensities, there was a chance to observe whether crack growth initiated at the lower  $K_{I1}$  values before corrosion wedging became dominant. Therefore, the data from the compact specimens provided better estimates of threshold stress intensity factors. This problem with the DCB's in the salt-dichromate-acetate solution was not so troublesome with DCB's exposed to the 3.5% NaCl added dropwise to the crack. The initial environmental crack velocities were similar to those in the salt-dichromate-acetate solution but the crevice corrosion did not proceed as rapidly with the plain salt solution and more complete K-rate curves could be obtained before corrosion wedging became

dominant; compare Figure 53 and Figure 54. Threshold stress intensities indicated in Figure 54 and Figure 43 agreed fairly well. The curves shown in Figure 54 also agree fairly well with those obtained by Hyatt<sup>(26)</sup>.

c. Evaluation and Interpretation of the DCB Tests

With the low resistance alloys both accelerated test media ranked the alloys similarly and about the same as the seacoast atmosphere, and there was no problem interpreting the test results. With the high resistance alloys, however, there was environmental crack growth in small degrees differing with the environment and the general resistance to corrosion of the alloy. Just as with the compact tension specimens discussed previously, there was more crack growth than would be expected for alloys such as 7075-T7351 and the 2XXX-T8 alloys (Figure 55). Metallographic and fractographic examinations were performed to determine the mode of the crack growth. Typical intergranular SCC, as shown in Figure 56, was found only in specimens of 7075-T7351 exposed to the accelerated tests and the seacoast atmosphere, and in specimens of 2024-T851 and 2021-T81 exposed to the salt-dichromate-acetate solution. No SCC was detected in the latter two alloys in the 3.5% NaCl test or in the atmospheric tests. No SCC was found in specimens of 2219-T87, 6061-T651 and 5456-H117 exposed to any of the test environments. In the stressed specimens of these alloys corrosion penetrated to the tip of the precrack and mechanical fracture or tearing advanced through alloy constituents that cracked ahead of the crack tip, as shown in Figure 57 (also Figures 33 and 46). This mechanical fracture advanced slowly as indicated by the severe corrosion of the fracture surfaces.

The measurement of the small amounts of crack growth on the sides of the specimens was difficult and may not be representative of the growth at the interior of the specimen. In cases such as the 2XXX-T8 alloys in the salt-dichromate-solution surface measurements gave an exaggerated indication of the true crack growth (Figure 44); whereas in most cases especially with tension precracks, the crack growth at the interior was greater than at the surface (Figure 55).

The occurrence of the mechanical crack extension as a result of crevice corrosion and corrosion-product wedging is an undesirable feature of tests with bolt loaded precracked specimens. Terminating exposures at about 500 to 600 hours apparently would prevent corrosion wedging effects in the salt-dichromate-acetate test. However, the situation is more complex with the 3.5% NaCl test. Wedging appeared to become dominant at about 200-300 hours for the high resistance alloys, but definite signs were not evident until about 1400 hours for the low resistance alloys (Figure 51). It nevertheless is likely that wedging also was influencing crack growth in the latter after about 200 hr.

### C. Tests With Ring Loaded Compact Tension Specimens

The results of tests of short-transverse (S-L) compact tension specimens under ring loading are summarized in Tables XXII and XXIII. A bank of rings and the data logging unit are shown in Figure 13. Both load and crack opening displacement were monitored at 8 hour intervals throughout the life of each test and a sample of these data is shown in Figures 14\* and 15\*. These

-----  
\*Individual print-cuts for each specimen are appended to the Master copy of this report.

data were analyzed with the equations and procedure described in Section III-D4.

1. General Observations

Before discussing the data for individual alloys it seems appropriate to make some observations concerning the data in general. The calculated initial or applied stress intensity factors ( $K_{I_i}$ ) are usually not exactly equal to the target values because of the difference in the method used to determine the initial crack length. The calculated crack lengths based on measurement of load and COD provide an integrated average crack length, as opposed to an estimated value based on side measurements, and are considered more accurate. General corrosion of the crack faces usually destroys the definition of the end of the fatigue crack, but in the few instances that the end of the fatigue crack could be discerned, the initial crack lengths were found to be very close to the calculated values.

The crack length at fracture (which would normally be the end of the environmental crack growth) was usually clearly defined, and, in general, the crack length measured on the fracture surface was close to the calculated value. Differences larger than about 0.04 in. can be attributed to error in the calculated lengths due to long term drift in the clip gage readings. As expected, the stress intensity level at fracture ( $K_{I_f}$ ) is usually equal to or somewhat greater than the ambient  $K_{I_c}$  value, which provides another check on the data. It is not too surprising that the stress intensity at fracture may be greater than  $K_{I_c}$  because if plane strain conditions are not maintained, the specimen may be loaded

to a stress intensity level greater than  $K_{Ic}$ . This occurred toward the end of many of the ring load tests.

Insight into the behavior of each specimen during the test can be obtained from the load and COD vs. time plots as shown in Figure 14. The load readings were quite stable and a decrease in load of even 2 or 3% is indicative of an event. Therefore, load readings can be used as an indirect indication of crack growth. Sometimes, as shown in Figure 58, there was considerable scatter in the COD data even though no crack growth occurred; this is probably due to thermal effects on the clip gage and long term creep.

The time plots for certain specimens of 2021 and 2219 alloys show a temporary arrest in the crack growth as shown in Figure 59. The cause of this is believed to be a delay in the forward progress of the crack due to crack branching. Metallographic examination of the fractured specimens showed that such branching had occurred (Figure 60; see also Figure 28).

Many of the specimens experienced an incubation period, during which no crack growth occurred at the beginning of test; the duration of this period increased with decreasing applied stress intensity. This was encountered in most of the tests of 2000 series alloys and some of the long term (low applied stress intensity) tests of the 7000 series alloys. The long term tests of alloy 7039-T651 shown in Figure 61 illustrate that relatively long exposures may be necessary, even in an accelerated test environment, to determine whether stress corrosion crack growth will occur. Specimen TL-3 incubated about 1100 hours without any appreciable

evidence of crack growth, after which crack growth accelerated rapidly and the specimen failed within 800 hours. This test is also an example of a case in which the contrast in crack growth rates made it difficult for the computer fit curve to follow the data.

## 2. Comparison of Alloys

Tests were performed at various levels of applied stress intensity ( $K_{I1}$ ) to determine the threshold stress intensity for environmental crack growth. Graphs of  $K_{I1}$  vs. time to fail (fracture) for all of the aluminum alloys are presented in Figure 62 and 63. All "run outs" were examined metallographically, and in some cases, fractographically to check the possibility of cracking having initiated and not progressed to the critical crack length to cause fracture. The information thus gained was used along with the time plots to estimate the stress intensity thresholds listed in Table XXIV.

For alloys such as 6061-T651 where no crack growth occurred even at very high applied stress intensities, it is difficult to draw a conclusion about  $K_{Ith}$ . It is possible (in fact, very probable, considering the established SCC-free service record for 6061-T651) that the alloy is not susceptible to SCC in this test environment. If it is susceptible the  $K_{Ith}$  must be greater than the values used in these tests, or else the incubation period is very long. Specimens of 5456-H117 also showed no evidence of environmental crack growth on the fractures and no appreciable decrease in load (Figure 58) during exposure, yet there was an anomalous increase (0.03") of the calculated crack length. In such

cases  $K_{I_{th}}$  was indicated to be greater than the highest value tested.

In the case of alloy 7075-T7351 there was no change in the load curve to indicate crack growth, yet when the specimen was broken apart, environmental crack growth was evident on the fracture. This crack growth was confirmed as typical intergranular SCC by fractographic examination, to be discussed later in Section VI-D. Because the amount of SCC was small and developed apparently very slowly over a long period of time, the specimen was probably loaded above but very close to  $K_{I_{SCC}}$ . The length of the SCC measured on the fracture surface after 2780 hr., incidentally, is just about what would be expected from the SCC growth rate of  $2-3 \times 10^{-5}$  in./hr. determined with bolt loaded specimens (Tables XIX and XX).

The two specimens of 2219-T87 failed during exposure under extremely high applied stress intensities. One specimen was inadvertently overloaded to 104% of the nominal  $K_{I_C}$  and it fractured within 16 hr.; the fracture was clean, with no evidence of environmental crack growth, and no doubt resulted from the overloading. The other, loaded to 94%  $K_{I_C}$ , developed a calculated crack growth of 0.045 in. while the load decreased only about 0.6% during an exposure of 1816 hr. Then the load was increased to 111%  $K_{I_C}$  and failure occurred after an additional exposure of 504 hr. during which the load gradually decreased about 2%. Although both the precrack and the environmental crack extension were corroded it was estimated that the crack growth at the interior of the specimen amounted to about 0.06 in. This crack growth resembled tension fracture rather than SCC or fatigue. In Section VI-D there

is a fractographic examination illustrating similar tension crack growth in a DCB specimen. It was concluded from these tests that this lot of 2219-T87 was not susceptible to SCC in this test environment even under these extreme loading conditions.

Specimens of 2021-T81 and 2024-T851 loaded to 90%  $K_{Ic}$  failed after relatively short exposures (392 and 240 hr., respectively) but did not fail at the next lower  $K_{I1}$  values (72-76%  $K_I$ ). Although there was no appreciable decrease in load, the calculated crack lengths increased about 0.04 - 0.06 in. The run-out specimens were cut in half so that the fracture could be examined on one half and metallographic examination of the crack tip could be made on the other half. There was no environmental crack growth evident on the fractures nor any SCC shown by the microsections. The relatively small crack growth indicated by the instrumentation readings was probably due to long term drift in the clip gage readings, and thus not indicative of real crack growth.

K-rate curves plotted from data recorded on the computer printouts (Figure 15) generally were erratic because of the deviations in the COD data described previously. Nevertheless with some editing of the data to eliminate negative slopes and the like, representative curves could be obtained. An example of one of the better sets of curves is presented in Figure 64 for alloy 7075-T651 in comparison with the curve for bolt loaded compacts taken from Figure 40. The shapes of the curves indicated by data points in Figure 64 for four different levels of  $K_{I1}$  represent the variety of curves obtained in the various ring load tests. A region of constant velocity was not always seen in the

individual curves, but for a given alloy the crack growth rate at the point of fracture was about the same for the individual specimens. From the several individual specimen data a single representative, or limiting, curve could be drawn to indicate both the estimated threshold stress intensity and the maximum sustained, or plateau, crack growth rate as shown in Figure 64. Because K-rate curves could not be obtained for all of the specimens no general comparisons of the alloys were made by this method.

### 3. Ring Loading vs. Bolt Loading

The approach to the determination of a stress corrosion threshold differs for bolt and ring-loaded specimens because of the different dependence of stress intensity upon increases in crack length. As cracking occurs in a bolt-loaded specimen, the applied load and the resultant stress intensity,  $K_I$ , decrease until a point is reached (theoretically) where crack propagation ceases. It should be possible, therefore, to expose a bolt-loaded specimen at an initial  $K_{I_i}$  sufficiently high to cause environmental crack growth and establish the threshold level,  $K_{I_{th}}$ , for cracking by determination of the residual stress intensity at arrest. However, when a specimen is stressed with a relatively flexible ring and cracking occurs, the applied load tends to remain nearly constant and the stress intensity increases until  $K_{I_f}$  is reached and the specimen fractures. The threshold for environmental crack growth,  $K_{I_{th}}$ , is then determined by exposing specimens at various decreasing  $K_{I_i}$  values until the level is reached where no cracking occurs.

Although the ring-loading method theoretically requires a

greater number of specimens to establish  $K_{I_{scc}}$ , this method has several advantages over bolt loading:

(1) Because the applied load is indicated by the strain in the ring, the magnitude of  $K_{I_1}$  can be determined more accurately.

(2) Crack growth (and applied load) can be monitored more readily by instrumentation, with automatic read-out equipment, so that  $K_I$  can be determined at any point in the test.

(3) Because the crack is continually opened by the ring, there is less chance of wedging forces from entrapped corrosion product.

Bolt loading, on the other hand, is more suited to the testing of large numbers of alloys because it is less expensive and the test specimens require less space. These characteristics and particularly advantageous for long-term outdoor atmospheric exposure tests.

Comparisons of data from ring load and bolt load tests can be made in two different interpretations of the data as shown in Figures 64 and 65. The K-Rate curves for alloy 7075-T651 in Figure 64 show reasonably good agreement for the two methods of loading both in the threshold stress intensity and in the maximum sustained cracking velocity. K-Time curves are shown in Figure 65 for alloys 2014-T651 and 7075-T651. For 2014-T651 the curve for 50%  $K_{I_C}$  bolt loaded specimens levelled off at about the same stress intensity as the curve for the ring loaded specimens, and then corrosion product wedging eventually stimulated further crack growth (Refer to Figure 35: it appears that crack growth in the 75%  $K_{I_C}$  specimen was kept at a high rate by corrosion product wedging). For 7075-T651 a

threshold stress intensity of about 25%  $K_{Ic}$  was indicated by both methods of loading, and the bolt load curves for higher  $K_{I1}$  levels did not show arrests because of corrosion product wedging (Figure 35).

A ranking of the threshold stress intensities of all of the aluminum alloys estimated by the two methods of loading is shown with bar graphs in Figure 66. Results from the two loading methods agreed well with the  $K_{Ith}$  values not differing more than 3 ksi  $\sqrt{in.}$ , and there being no consistent indication that one method was more critical than the other. However, thresholds from the ring load test probably are more reliable because of fewer problems with wedging by corrosion products.

#### D. Fractographic Examination

Fractographs were made with the scanning electron microscope (SEM) to document typical fracture characteristics in the precracked specimens. In Figure 67 is shown the typical fracture characteristics of SCC in the low resistance alloys and transition zones from a fatigue precrack and to a tension fracture. A similar group of fractographs is shown in Figure 68 for a specimen of 7075-T7351 to illustrate that the relatively small amount of environmental crack growth was typical of intergranular SCC. Typical SCC also was observed in 2024-T851 specimens exposed to the salt-dichromate-acetate solution (Figure 69). Even though the environmental crack growth in specimens of 2219-T87 was equal to or exceeded that in 7075-T7351 and 2024-T851, no evidence of typical SCC was present in the 2219-T87; rather the fracture had the same appearance as a tension fracture, as shown in Figure 70. There was not observed in any of the precracked specimens transgranular cracks of the

type that initiated at the bottom of corrosion pits in the smooth specimens.

Although there was no visible crack growth on the fracture surfaces of 5456-H117 and 6061-T651 compacts exposed to salt-dichromate-acetate solution for 2184 hr., the residual stress intensities determined on these specimens at the end of the test were appreciably lower than the initially applied  $K_{Ii}$  (Refer to Table D-3). The transition region between the fatigue precrack and the tension fracture was studied with the SEM for some indication of crack growth, but none was found (Figure 71). It therefore was concluded that the reduction in K was the result of plastic deformation during loading or creep and possibly the combination.

TEM fractographs were made of only a few characteristic fractures to provide a comparison with the SEM illustrations. The typical SCC and tension fracture in a 7075-T651 compact tension specimen is shown in Figure 72. And a comparison of SCC, fatigue and tension fractures in 7075-T7351 is shown in Figure 73.

## VII. RESULTS OF STRESS CORROSION TESTS OF STAINLESS STEEL ALLOYS

### A. Tests With Smooth Specimens

#### 1. Atmospheric Exposures

Seacoast and inland industrial atmospheric exposures have completed 28 months at this time and the exposures will be continued for at least a 4 year period. The alloys and tempers expected to have high resistance to stress-corrosion cracking were stressed to 75 and 50% of their yield strength. The combinations expected to have low resistance to stress corrosion were stressed to 75 and 25% of their yield strength and to a common 27 ksi level at which

the aluminum alloys also were stressed. The specimens in test and the failures to date are listed in Tables XXV and XXVI.

a. Seacoast Atmosphere

Failures to date have occurred in only five of the thirteen alloys, chiefly in the semi-austenitic group. Two out of three transverse specimens of 17-7 PH alloy in the RH1050 temper failed at 75% Y.S. (142.9 ksi) within 141 days. Alloy PH15-7Mo, which is a modification of 17-7 PH alloy for higher mechanical properties especially at elevated temperatures, was less resistant; all three specimens at both 75% Y.S. (146.3 ksi) and 50% Y.S. (97.5 ksi) failed within 73 days. The least resistant of the group was the AM355 alloy in the SCT850 temper for which failures were observed within 141-190 days for specimens stressed even at the lowest stress level evaluated (27 ksi). Two additional failures were transverse specimens of 431 HT200 stressed to 75% Y.S. No failures have been observed to date for the martensitic precipitation hardening, 15-5 PH and PH13-8Mo alloys.

Examination of the effect of tempering to lower strengths on the resistance to SCC was possible with five of the six alloys. There was no effect of temper for two of the alloys (15-5 PH, PH13-8Mo) because there was no failure in either temper. Also in the case of alloy AM355 there was no failure in either temper of the plate, but for the bar there was a marked improvement of the lower strength SCT1000 temper over the SCT850 temper. A similar performance was observed with alloy 431 for which a definite improvement was shown by the lower strength temper. For the PH15-7Mo alloy, however, the lower strength RH1050 temper was not more resistant than the RH950 temper, but in this case the tensile

strengths of both tempers were over 200,000 psi and were quite similar (Table VII).

Specimens with three different orientations (L, T and S) were exposed to investigate possible directional effects with rolled bars of the three basic alloy types: AM355 SCT850, 431 HT200 and PH13-8Mo H950. In the case of the PH13-8Mo H950 alloy there was no failure. In the case of the 431 HT200 alloy, failure occurred only with the long-transverse (T) specimens at the 75% Y.S. stress level. With the AM355 SCT850 alloy bar failures occurred with specimens of all three orientations stressed even at the lowest stress level (27 ksi). Although long-transverse (T) specimens from the plate of AM355 SCT850 did not fail at stresses up to 114 ksi, it is not clear whether this improved performance can be related to a difference in directionality in grain structure of the 1.25" thick rolled plate and the 2" x 6" rolled bar or a difference in prior thermal history (Table VI). Micrographs in the one year summary report<sup>(12)</sup> comparing the two products do not show a marked difference in directionality. On the other hand, the microstructure of plate in the SCT850 temper, Figure 20 in the Eighth Quarterly Report<sup>(17)</sup>, showed a relatively large amount of precipitate similar to that in the SCT1000 temper of the bar.

The fractures of several of the atmospheric failures were examined with the scanning electron microscope to determine the nature of failure. The environmental cracking was predominantly intergranular in nature as shown in Figure 74 for a specimen of 431 HT200 alloy that failed after 141 days. The entire fracture surface of the 1/8" diameter tensile bar is shown with stepped regions of SCC and tensile failure. Enlarged regions from top

center of this surface indicate the intergranular nature of the SCC.

The results observed to date for the tests in the seacoast atmosphere are in reasonable agreement with the marine atmospheric data cited by Slunder<sup>(43)</sup> in his DMIC review and by Denhard<sup>(44)</sup> in his review of the stress corrosion characteristics of high strength stainless steels presented at the Twenty-Fourth Meeting of AGARD.

b. Industrial Atmosphere

A comparison of the data for the two atmospheric exposures indicates, as in the case of the aluminum alloys, that the seacoast environment is more aggressive in causing SCC than the inland industrial atmosphere. For example, specimens of alloy AM355 in the SCT850 temper failed when stressed in all three directions as low as 27 ksi and exposed to the seacoast atmosphere, but in the industrial atmosphere failures were observed for specimens stressed in just the two transverse directions, and only at 75% Y.S. (124.7 ksi). Long-transverse (T) specimens of alloy PH15-7Mo in the RH900 temper stressed to 75% Y.S. (152.6 ksi) were the only other failures in the industrial atmosphere (Table XXVI).

2. Alternate Immersion in 3.5% NaCl

A similar set of smooth tensile specimens was exposed 205 days to the 3.5% NaCl alternate immersion test. The following specimens failed within the first seven days, except for AM355 SCT1000:

<u>Alloy</u>	<u>Temper</u>	<u>Direction</u>	<u>Stress % Y.S.</u>	<u>F/N</u>	<u>Days</u>
PH15-7Mo	RH950	T	75	2/3	1,1
PH15-7Mo	RH1050	T	75	5/5	1,1,1,1,1
PH15-7Mo	RH1050	T	50	3/3	1,2,4
431	HT200	S	75	1/4	5
AM355 Bar	SCT850	L	75	2/4	4,4
AM355 Bar	SCT850	T	75	1/4	7
AM355 Bar	SCT850	S	75	2/4	3,7
AM355 Bar	SCT1000	T	75	1/5	138

These materials also failed in the seacoast atmospheric exposure; however, some that failed in the seacoast atmosphere did not fail in the laboratory test. One such item was 17-7PH RH1050 alloy, which was surprising because Humphries<sup>(45)</sup> reported failures of transverse specimens from 2.5-in. diameter bar stock of this alloy and temper in the same type of test. Therefore, it was decided to test additional specimens. Because rapid crack growth occurred in the precracked specimens immersed in 20% NaCl solution this corrodent was used for the repeat tests. Transverse tensile bars of both alloys 17-7PH RH1050 and 15-5PH RH900 were stressed to 75% Y.S. and exposed to 20% NaCl solution by total immersion for one year without failure. Thus, the difference with Humphries' results was not resolved; it may have been an inherent difference in the materials, or it could merely reflect differences in test conditions.

Several of the failures were examined fractographically to determine the nature of failure. As in the case of the atmospheric specimens, the failures resulted from SCC which was predominantly intergranular. Figure 75 is a composite of SEM fractographs of the fracture surface of a specimen of AM355 alloy in the SCT850 temper which failed after 3 days in the alternate immersion test.

The view at left shows the entire fracture surface of the 0.125" diameter tensile bar at a low magnification of about 20X. The jagged region is the region of intergranular SCC which initiated the fracture. Thus, failures in both the atmosphere and the accelerated test were similar and resulted from intergranular SCC.

Tensile losses due to corrosion were obtained on all specimens that completed test without failure. The losses were very small (<2%) in all cases except the short-transverse (S) specimens of alloys 431 and AM355. These specimens had losses of 11 to 15% and visual examination indicated that the losses were caused by local pitting.

#### B. Tests With Bolt Loaded Precracked Specimens

##### 1. Exploratory Tests

Exploratory stress corrosion tests were performed with fatigue precracked specimens of alloy 15-5PH in the H900 and H1150M tempers to determine which of several sodium chloride solutions discussed in the literature <sup>(30,31,32)</sup> would give the more rapid test.

- A. 3.5% NaCl made with Reagent Grade NaCl and distilled water
- B. 20% NaCl with Reagent Grade NaCl and distilled water
- C. Synthetic sea water (ASTM D1141-52, without heavy metals)

Specimens loaded to 95, 75 and 50%  $K_{Ic}$  for the H900 temper and to 95 and 75%  $K_Q$  for the H1150M temper were immersed in each of the solutions. Once a week the crack lengths were measured and fresh solutions were placed in the glass dishes.

Crack growth initiated only in H900 temper specimens exposed to the 20% NaCl solution, after definite incubation times that increased with decreasing  $K_{I1}$ , as shown in Figure 76. Because at the end of 56 days no crack growth had started in H900 temper specimens in the other two solutions, or in any of the H1150M temper specimens, the load on five selected specimens was increased to "pop-in": one of the two H1150M temper initially loaded to 95%  $K_{Ic}$  in each of the three solutions and one of the two H900 temper initially loaded to 50%  $K_{Ic}$  in the two 3.5% NaCl solutions (A & C). However, even at these high stress intensities no crack growth was observed after an additional 154 day exposure, when the test was discontinued.

Exposure of all but one of the specimens was terminated at the end of 211 days when it appeared that crack growth in the H900 temper specimens had ceased. Continued exposure of one of the two 50%  $K_{Ic}$  specimens for an additional 154 days confirmed that an arrest had been reached (growth rate less than  $10^{-6}$  in./hr.).

Residual stress intensities determined for the specimens exposed to the 20% NaCl solution are given in Table XXVII. The  $K_{I1}$  values for the two 50%  $K_{Ic}$  specimens checked closely, indicating a  $K_{Isc}$  of about 27 ksi  $\sqrt{\text{in}}$ . The specimen loaded to 95%  $K_{Ic}$  and one of the two loaded to 75%  $K_{Ic}$  developed crack growth extending to the point where valid K values could not be determined. Metallographic examination of the specimen loaded to 75%  $K_{Ic}$  that did not develop any crack growth showed that the fatigue crack had been broadened by corrosion but there was no indication of crack initiation.

Because valid  $K_{Ic}$  values had not been obtained with specimens in the H1150M temper, a  $K_{Ic}$  value of 100,000 psi  $\sqrt{\text{in.}}$  was assumed, and the H1150M specimens were supposedly loaded to 95 and 75% of that value. Although these specimens did not experience any crack growth the  $K_{I_r}$  values were 20 to 30 ksi  $\sqrt{\text{in.}}$  below the intended  $K_{I_1}$  values. The intended initial stress intensities may not have been developed as it appears that the specimens deformed plastically during loading.

From the results of these exploratory tests and the experience of Freedman<sup>(32)</sup> it was decided to use the 20% NaCl solution for the accelerated test in the general test program.

## 2. Atmospheric Exposures

Replicate specimens loaded to several nominal stress intensity levels were exposed to the atmosphere at the seacoast and at an inland industrial location to determine threshold stress intensities for the various stainless steels. Although most emphasis was placed upon long-transverse (T-L) specimens, longitudinal (L-T) and short-transverse (S-L) specimens also were exposed for alloys PH13-8Mo, 431 and AM355, the same ones as for smooth specimens to investigate possible effects of specimen orientation. A complete listing of all the specimens and their disposition is given in Tables D-7 and D-8 in the Appendix.

### a. Seacoast Atmosphere (28 mo.)

No crack growth was visible in the 15-5PH H1150M specimens loaded to 95%  $K_Q$ , the highest level of  $K_{I_1}$ , after 28 months at the seacoast. However, cracking started within a few months in specimens of all of the other alloys and tempers at  $K_{I_1}$  values of

95, 75 and in some cases 50% of  $K_{Ic}$ . Cracking propagated 0.2 to 0.8 in. within three months, and, as summarized in Table XXVIII for long-transverse (T-L) specimens loaded to 95%  $K_{Ic}$ , the average cracking velocity was about  $2$  to  $9 \times 10^{-4}$  in./hr. The velocities were not appreciably lower for  $K_{I1}$  values of 75 and 50%  $K_{Ic}$ . Details regarding crack lengths, final  $K_I$  values, etc. are given in Table D-7 of the Appendix.

It is evident from Table D-7 that except for 15-5PH H1150M, 431 HT125, and AM355 SCT1000 (plate and bar), the  $K_{I_{SCC}}$  must be less than 50%  $K_{Ic}$ . Additional specimens of 17-7PH RH1050 were loaded at 35 and 25%  $K_{Ic}$  to obtain a closer estimate of  $K_{I_{SCC}}$ . Crack growth occurred in both specimens within 7.6 months, so that the  $K_{I_{SCC}}$  for this material appears to be less than 25%  $K_{Ic}$  ( $< 12 \text{ ksi}\sqrt{\text{in.}}$ ) in the seacoast atmosphere.

With regard to the effect of specimen orientation the resistance to SCC was equally low in all three directions for alloys 431 HT200 and AM355 SCT850. For the third alloy, PH13-8Mo H950, the resistance to SCC was equally low in the longitudinal (L-T) and long-transverse (T-L) directions, but crack growth did not occur with the short-transverse (S-L) specimens.

In most instances SCC advanced in the plane of the precrack and followed an intergranular path as shown in Figures 77-79 for each of the three types of stainless steel. In some instances, such as specimens of AM355 SCT850, PH13-8Mo H950, and 431 HT200 alloy, crack branching occurred, as shown in Figure 80. Measurement of crack growth was impracticable in these instances.

Both of the AM355 SCT850 (bar) specimens exposed with no

applied load showed crack growth during exposure to the seacoast atmosphere. This also occurred with a specimen exposed to 20% NaCl solution as illustrated in Figure 81. The crack growth followed an abnormal course along both faces but not in the center; also small cracks were observed at the back end running perpendicular to the plane of the fracture. Although every effort had been made to keep residual stresses to a minimum, the thermal treatment for AM355 alloy involved a water quench, which would be an unavoidable source of residual stress. Specimens of the other alloys were either air cooled or oil quenched (431 alloy) and would be less likely to develop appreciable residual stress. Thus, specimens of AM355 alloy, and to a lesser extent 431 alloy, may have been subjected to some additional load in the form of residual stresses from the quench. An example of the complicating influence of residual quenching stress on tests with precracked specimens was illustrated by Hyatt<sup>(46)</sup> for a heat treated aluminum alloy.

Fractographic examinations were made on specimens of several of the alloys and will be discussed in more detail in a later section covering tests in 20% NaCl solution.

b. Industrial Atmosphere (29 Mo.)

SCC did not occur with as many alloys in the industrial atmosphere as in the seacoast atmosphere. The following items showed no crack growth, as indicated in Table D-8:

15-5PH H950 and H1150M  
PH13-8Mo H950 and H1050  
431 HT125  
AM355 (Plate) SCT850 and SCT1000  
AM355 (Bar) SCT1000

SCC started quickly in specimens of 17-7PH RH1050 and

PH15-7Mo RH950 and RH1050. Average crack velocities for specimens loaded to 95%  $K_{Ic}$  were relatively high, as shown in Table XXVIII, with the 17-7PH RH1050 and PH15-7Mo RH950 having an average velocity of about  $1 \times 10^{-2}$  in./hr. While the average velocity for the PH15-7Mo RH950 appears greater in the industrial atmosphere than in the seacoast atmosphere,  $1 \times 10^{-2}$  in./hr. vs.  $5 \times 10^{-4}$  in./hr., it is probable that higher velocities would have been noted in the seacoast atmosphere if the crack growth measurements could have been made frequently enough to have observed the early stages of growth. In all probability the crack growth velocities for these alloys are similar in both atmospheres, with the main difference in SCC performance being the stress intensity level at which cracking is initiated. For instance, cracking was not observed for alloy 17-7PH RH1050 at 50%  $K_{Ic}$  during 29 mo. in the industrial atmosphere, but did occur within 7.6 mo. in the seacoast atmosphere at  $K_{I1}$  as low as 25%  $K_{Ic}$ .

### 3. Continuous Immersion in 20% NaCl Solution

As in the case of atmospheric tests replicate specimens were loaded to several nominal stress intensity levels as identified in Table D-9 along with details regarding their exposure.

Cracking started quickly and grew rapidly in specimens of those alloys shown by the outdoor exposures to have the lowest resistance to SCC. Graphs of environmental crack growth for all of the alloys are presented in Figures 82-88. With the more resistant alloys there was a marked inconsistency in the crack growth behavior, as can be seen in Figures 83, 84, 86 and 88. For example, there were instances of very rapid crack growth in one of a pair of

specimens and no crack growth in the duplicate, or crack growth at 50 and 75%  $K_{Ic}$  but no cracking at 95%  $K_{Ic}$ . The most erratic behavior was for specimens loaded to an intended  $K_{I1}$  value of 95%  $K_{Ic}$ . Presumably certain of the specimens that were being loaded so close to  $K_{Ic}$  were inadvertently overloaded and the precrack blunted by plastic deformation. Six of the specimens that showed no environmental crack growth at the end of the 200-day exposure were re-cracked by fatigue or tension and re-exposed (refer to the last section of Table D-9 for details). Rapid crack growth occurred in each specimen, as shown for certain ones in Figures 84, 86 and 88. It is concluded from this experience that when testing steel alloys of this type complete reliance should not be placed in single test specimens, and that considerable care must be exercised in applying high stress intensities.

Additional graphs with crack growth rate plotted as a function of stress intensity are presented in Figures 89-93. As discussed in detail for the aluminum alloys (Section VI-B2), the latter graphs were derived from the first set by determining the slope of constant regions of the crack growth curves and calculating the stress intensity factor for the crack length at each end of the region of constant slope. A composite graph of the K-Rate data for the various stainless steel alloys and tempers is shown in Figure 93. A summary of estimated threshold stress intensities and the highest sustained initial crack velocities derived from these graphs is given in Table XXVIII with the data discussed previously for specimens exposed to the seacoast and industrial atmospheres.

Again, as noted in the seacoast atmospheric tests, the effect of specimen orientation on the SCC behavior was negligible, as shown in Figures 83, 85 and 87. This is in agreement with other rather limited data in the literature (p. 122, Ref. 42).

#### 4. Evaluation and Interpretation

Specimens of the three types of stainless steel alloys were photographed to show typical forms of environmental crack growth that were observed in the seacoast atmosphere and 20% NaCl solution. Because fewer failures occurred in the industrial atmosphere, a direct comparison in all three environments was not feasible. The comparison of fractured surfaces in the two environments is shown in the left portion of Figures 94-96. In general, the fatigue crack fronts were reasonably straight or slightly convex, as shown in Figure 94. The environmental crack growth tended to extend in a contour parallel to the front of the precrack; however, there were some exceptions with the alloys which showed crack branching, such as PH13-8Mo, 431 and AM355 (Fig. 78, 79, 80, 95).

There was rust present on the surface of the environmental crack growth region in the seacoast atmosphere and the 20% NaCl solution, but not thick deposits of oxide like those observed in the aluminum alloy specimens. Thus, there was the possibility of corrosion-product wedging and this phenomenon probably accounts for the acceleration of cracking after extended periods (over 4,500 hr.) of exposure in the 20% NaCl solution in several instances. However, there was no indication of corrosion-product wedging with exposures as long as 2,000 hr. which appear to be necessary to initiate SCC in specimens at lower  $K_{I1}$  values.

A comparison of the performance of the various alloys and tempers in the three environments is shown by the data summarized in Table XXVIII. Comparison of the average initial velocities shows that the velocity differs with the environment as was also observed for the aluminum alloys. The SCC velocities were significantly higher in the 20% NaCl solution than in the atmospheric environments. Comparison of threshold values showed that the accelerated test in 20% NaCl solution ranked the alloys and tempers in about the same order as the seacoast atmosphere. The seacoast atmosphere indicated a lower threshold for PH13-8Mo H950 and H1050 than the 20% NaCl solution and would be considered the most critical test environment for these particular stainless steel alloys; the inland industrial atmosphere was the least critical.

Specimen orientation did not influence the SCC performance of any of the three stainless steel alloys in either the accelerated or atmospheric test environments.

### C. Fractographic Examination

A composite of photographs and SEM fractographs was prepared for each of the three types of stainless steels and are shown in Figures 94-96. All of the SCC fractures, regardless of the alloy type or test environment, were intergranular and typical of stress-corrosion cracking in these alloys. The tension fracture surfaces exhibited the dimple rupture typical of most ductile tensile fractures; one exception was the fracture in 17-7PH RH1050 alloy (Figure 94).

Alloy 15-5PH H1150M showed no visible evidence of crack growth on the fracture surface of the compacts exposed to the 20%

NaCl solution, but residual stress intensities determined for these specimens were lower than the applied  $K_{I_1}$ . The transition region between the fatigue precrack and the tension fracture was studied with the SEM for evidence of crack growth, but none was observed (Figure 97). As was concluded for the aluminum alloys 5456-H117 and 6061-T651, the apparent reduction in K probably was the result of plastic deformation during loading or creep and possibly the combination.

#### D. Comparison of Alloys

The six stainless steel alloys included in this investigation can be classified into three types: Martensitic precipitation hardening alloys 15-5PH and PH13-8Mo; Semi-austenitic precipitation hardening alloys 17-7PH, PH15-7Mo and AM355; and Martensitic alloy 431. Two tempers were evaluated in most instances, with one temper representing the highest tensile strength and the other representing a combination of higher fracture toughness and stress corrosion resistance with some reduction in tensile strength.

##### 1. Martensitic Precipitation Hardening Alloys

In 1967 Denhard<sup>(44)</sup> on the basis of smooth specimen tests, cited alloy PH13-8Mo as being the most resistant of the martensitic precipitation hardening alloys and capable of sustaining relatively high stresses without cracking. In the present investigation smooth specimens of alloys 15-5PH in the H900 and H1150M tempers, as well as PH13-8Mo in the H950 and H1050 tempers, showed no evidence of stress-corrosion cracking in any of the three test environments. The results of tests with precracked specimens, however, indicated that only 15-5PH H1150M showed no evidence of crack growth in any

of the test environments, and appeared to be virtually immune to stress-corrosion cracking. This material also had the lowest strength of any of the alloys and tempers evaluated. Definite susceptibility to SCC was observed with precracked specimens of the H900 temper of 15-5PH alloy and of the H950 and H1050 tempers of PH13-8Mo alloy. Carter, et. al.<sup>(47)</sup> also reported susceptibility for 15-5PH H900 alloy using fatigue precracked single edge notched specimens loaded in cantilever bending and exposed to 3.5% NaCl solution, but found no evidence of crack growth for PH13-8Mo in the H950 temper.

An interesting phenomenon for precracked specimens of PH13-8Mo alloy in the cantilever-beam test was observed by Sandoz<sup>(48)</sup> and for Custom 450 alloys\* by Henthorne<sup>(49)</sup>. Crack initiation occurred away from the notch and the precrack at the junction of the solution container and the specimen. This was attributed to lowering of pH in the crevice between the corrosion cell and the specimen by crevice corrosion which then leads to hydrogen cracking.

## 2. Semi-Austenitic Precipitation Hardening Stainless Steels

Except for the SCT1000 temper of AM355 alloy this group of steels had a relatively low resistance to SCC when tested as both smooth and precracked specimens. The least resistant of all the stainless steels based on the precracked specimens was alloy 17-7PH in the RH1050 temper. It exhibited an extremely high initial velocity of  $4 \times 10^{-1}$  in./hr. in the 20% NaCl solution, whereas the other alloys had initial velocities ranging from  $2 \times 10^{-3}$  in./hr.

-----  
\*Typical Composition of Custom 450<sup>(49)</sup>:  
.03C, .3Mn, .3Si, .015P, .005S, 15Cr, 6.5Ni, .8Mo, 1.5Cu, .7Cb

to  $5 \times 10^{-2}$  in./hr. However, when evaluated with smooth specimens it appeared more resistant to SCC than the other two semi-austenitic precipitation hardening alloys, PH15-7Mo in the RH950 and RH1050 tempers and AM355 in the SCT850 temper. These results are consistent with tests of smooth specimens of sheet (0.025-0.050 in.) that showed SCC of PH15-7Mo RH1075 and AM355 SCT1000 alloys<sup>(50)</sup>.

The resistance to SCC of AM355 alloy was improved by aging to the lower strength, high toughness SCT1000 temper, but it did not give the alloy immunity to SCC. A smooth specimen failure was observed in the 3.5% NaCl alternate immersion test and crack growth was observed with precracked specimens. Although tests of precracked specimens by Carter, et. al.<sup>(47)</sup> failed to develop SCC in AM355 SCT1000 rolled bar (2-1/2" x 2-1/2"), tests of precracked specimens in the present investigation, which included rolled bar (2" x 6") and the same item of 1.25 in. plate tested by Freedman<sup>(32)</sup>, produced SCC in both the 20% NaCl solution and the seacoast atmosphere. These results thus corroborate the results obtained by Freedman and differ with those obtained by Carter, et. al.

### 3. Martensitic Stainless Steels

Alloy 431 represented this classification of stainless steels. Its resistance to SCC was less than that of the martensitic precipitation hardening stainless steels and similar to the semi-austenitic precipitation hardening stainless steels. The resistance to SCC of the HT125 temper which is aged past peak tensile properties was very similar to that of AM355 SCT1000, although much lower in strength.

#### 4. Summary

To compare the SCC characteristics of various high strength steels Sandoz in Chapter 3 of Ref. 42 plotted the  $K_{I_{SCC}}$  and yield strengths in a graph which also contains reference lines for certain assumed critical crack depths. If one assumes a long, thin flaw at the surface and the existence of a yield-point stress, then SCC would be expected to propagate if the flaw depth exceeded  $a_{cr}$ , given by  $a_{cr} = 0.2 \left( \frac{K_{I_{SCC}}}{Y.S.} \right)^2$ . The value of  $a_{cr}$  may thus be regarded as a figure of merit which incorporates both the SCC resistance,  $K_{I_{SCC}}$ , and the contribution which yield strength stress levels can make to the SCC hazard by virtue of high residual or fit-up stresses. All of the data for a given alloy representing various products, tempers, fabricating practices, stressing direction, etc. were circumscribed by Sandoz with an "envelope". The data for precipitation hardening stainless steels summarized in Ref. 42 were reproduced in Figure 98. Just the envelopes were transferred for alloys PH13-8Mo and 17-4PH, plus individual data points for other materials with only a few tests. Superimposed on this background are the results of the present investigation and other pertinent data from Freedman<sup>(32)</sup> and Henthorne<sup>(49)</sup>.

For the alloys with relatively low resistance to SCC, such as 17-7PH, PH15-7Mo and AM355-SCT850, the data from this investigation agreed well with that from other investigations. However, for alloys and tempers with improved resistance, data from this investigation tended to be more conservative; i.e., indicated lower values for  $K_{I_{SCC}}$ . Particularly striking examples were alloys PH13-8Mo and 15-5PH. One reason might be related to differences

in concentration of sodium chloride solution used, as it was found in the exploratory tests with 15-5PH alloy that crack growth did not occur in 3.5% NaCl or synthetic ocean water; most data in the literature were obtained with 3.5% NaCl or sea water. Another difference in testing procedure that may be especially significant for these stainless steel alloys is the compact tension specimen versus the cantilever beam used by most other investigators. The crevice present in the compact tension specimen with the chevron notch is much deeper than that of the cantilever beam with the straight notch, and as mentioned earlier, these steels are especially vulnerable to SCC in crevice situations. There are possibly other reasons that might be related to the test materials.

The significance of the accelerated test data obtained in the present investigation is affirmed by the excellent agreement with the results of the outdoor atmospheric exposures.

#### VII. RESULTS OF STRESS CORROSION TESTS OF TITANIUM 6Al-4V ALLOY

##### Tests with Smooth Specimens

Long-transverse 0.125-in. diameter tension specimens stressed to 70% of the actual yield strengths were exposed concurrently with the stainless steel specimens to the same test environments as the aluminum alloys. There have been no SCC failures of the titanium specimens to date in any environment; i.e., 28 mo. in the seacoast and industrial atmospheres and 12 mo. in the 3.5% NaCl alternate immersion test. The atmospheric tests will be continued for an exposure of at least four years, but the alternate immersion test was discontinued after 12 mo. and the specimens were tensile tested. The losses in tensile strength due to corrosion were negligible (Table XXIX).

B. Performance of Precracked Compact Tension Specimens

Fatigue precracked specimens loaded to 95, 75 and 50%  $K_{Ic}$  were exposed to the seacoast and industrial atmosphere and immersed in 3.5% NaCl solution. Detailed data for the individual test specimens are given in Table D-10 in the Appendix.

1. Atmospheric Exposures

a. Seacoast Atmosphere

No crack growth has been observed to date (812 days) in specimens from the beta forged material, but crack growth occurred at all levels of applied stress intensity in specimens from the alpha-beta forging. In the alpha-beta specimen loaded to 95%  $K_{Ic}$  crack growth started immediately, before it could be exposed to the seacoast atmosphere. At the first inspection after 141 days of exposure, the crack had grown 0.7 in. and the specimen was removed for determination of the residual stress intensity and fractographic examination. After about one year crack growth also started in specimens loaded to 75 and 50%  $K_{Ic}$ . At 75%  $K_{Ic}$  one crack grew 0.11 in. in 73 days and the other grew 0.24 in. in 57 days, with average crack growth rates of  $6 \times 10^{-5}$  in./hr. and  $2 \times 10^{-4}$  in./hr. In the single specimen loaded to 50%  $K_{Ic}$  there was 0.03 in. crack growth in 73 days, with an average rate of  $2 \times 10^{-5}$  in./hr. Exposure of the 75%  $K_{Ic}$  specimen with 0.24 in. crack growth was terminated at 483 days for a check of the residual stress intensity and a metallographic examination of the environmental crack. Exposure of the other 75%  $K_{Ic}$  specimen was continued, but no further crack growth was noted after an additional 11 months.

Residual stress intensity measurements for the two alpha-beta

specimens that were removed, showed good agreement, with  $K_{I_P}$  values of 65 and 66%  $K_{I_C}$ . There may be some question as to the accuracy of the  $K_{I_P}$  value for the specimen loaded to 95%  $K_{I_C}$  due to the large amount of crack growth (0.7 in.). However, the  $K_{I_P}$  value for the specimen loaded to 75%  $K_{I_C}$  can be considered a candidate for  $K_{I_{SCC}}$  if it is assumed that crack growth had ceased. This is questionable since crack growth did not start in the specimen loaded to 50%  $K_{I_C}$  until after 13 months exposure. Thus, a  $K_{I_{SCC}}$  value less than 50%  $K_{I_C}$  (24 ksi  $\sqrt{in.}$ ) is indicated for the alpha-beta processed forging.

Microscopic examination of a cross-section at the tip of the crack in the alpha-beta specimen loaded to a  $K_{I_1}$  of 75%  $K_{I_C}$  confirmed the presence of typical SCC, with the crack alternately progressing transgranularly across alpha grains and along alpha and beta interfaces (Figure 99). A similar specimen from the beta forging was removed for examination after 483 days even though no crack growth had been observed. Microscopic examination of a section at mid-thickness of the specimen confirmed that no environmental crack growth had occurred (Figure 100).

Exposure of the beta processed specimens is being continued to determine whether SCC will be initiated at a later date. Exposure of the remaining alpha-beta processed specimens is also continuing to see whether crack growth will be renewed, after an apparent arrest, due to corrosion wedging. It is considered significant, however, that there has been no indication of such wedging in either these tests or accelerated tests of 5000 hours duration in 3.5% NaCl solution.

b. Industrial Atmosphere

No crack growth has been observed to date (861 days) in any specimen from the beta forging or in alpha-beta specimens loaded to 75 or 50%  $K_{Ic}$ . Crack growth started immediately in the alpha-beta specimen loaded to 95%  $K_{Ic}$  but stopped growing after three days, and did not appear to have extended after 483 more days, so the exposure was terminated and the residual stress intensity was determined. During the first three days the crack growth was 0.34 in. with an average growth rate of  $5 \times 10^{-3}$  in./hr. If it is assumed that the crack had come to a true arrest, then the  $K_{Ic}$  value of 31 ksi  $\sqrt{\text{in.}}$  (85%  $K_{Ic}$ ) could be considered as an estimate of  $K_{Isc}$  for this environment. However, longer exposure is needed to confirm this in view of: (1) the indication of slight crack growth at the surface of one of the specimens loaded to 75%  $K_{Ic}$  and, (2) the initiation of SCC at 75 and 50%  $K_{Ic}$  after an induction period of about one year in the seacoast atmosphere. Exposure of the 75%  $K_{Ic}$  specimen with slight crack growth at the surface was discontinued at 486 days and the specimen was sectioned for metallographic examination. Although the applied stress intensity appeared to have decreased a small amount (to 70%  $K_{Ic}$ ), there was no crack growth detected at the interior of the specimen.

Similarly one of the duplicate beta forged specimens loaded to 75%  $K_{Ic}$  was removed after 486 days for examination. The results were the same as for the specimen from the alpha-beta forging.

Exposure of the remaining specimens is being continued to determine whether SCC will be initiated at a later date.

2. Immersion in 3.5% NaCl Solution

Crack growth occurred in specimens from both beta processed and alpha-beta processed forgings at applied stress intensities of 95 and 75 per cent of  $K_{Ic}$ , but no growth occurred in specimens of either material loaded to 50%  $K_{Ic}$ , as shown in Figure 101. The stress-corrosion cracking was very rapid, with all growth ceasing by the end of 2 to 2-1/2 hours and not resuming, at least for 5000 hours when the exposure was concluded (Figure 102). During the 2 to 2-1/2 hours of crack growth the average rate of propagation was 0.04 to 0.15 in./hr. for the beta forging and 0.14 to 0.24 in./hr. for the alpha-beta forging. These results are consistent with published data<sup>(51)</sup> which show that aqueous stress corrosion crack propagation in titanium alloys is extremely rapid.

A comparison of crack growth rates in specimens of the alpha-beta forging exposed to the various environments is shown below:

Intended $K_{I1}$	Avg. Initial Crack Growth Rate, in./hr.		
	Seacoast	Industrial	3.5% NaCl
95% $K_{Ic}$	$5 \times 10^{-3}$ *	$5 \times 10^{-3}$ *	$2 \times 10^{-1}$
75	$6 \times 10^{-5}$ $2 \times 10^{-4}$	None	$1 \times 10^{-1}$
50	$2 \times 10^{-5}$	None	None

\*SCC growth started and stopped before specimen could be placed in the test environment.

These rates are estimated values averaged over the hours or days during which growth was occurring, and the initial crack growth no doubt proceeded at higher rates than indicated above. The most meaningful rates probably are those observed for  $K_{I1}$  of 75%  $K_{Ic}$ .

Comparison of the residual stress intensity values for the accelerated test specimens (Table D-10) with the intended  $K_{I1}$  values of 95 and 75%  $K_{Ic}$  shows marked discrepancies, particularly obvious with the alpha-beta specimen supposedly loaded to 75%  $K_{Ic}$ . In this instance  $K_{I_r}$  exactly equalled  $K_{I1}$  and yet there was 0.3 in. crack growth that should have reduced  $K_{I1}$  by a significant amount (approx. 15% or  $5.5 \text{ ksi} \sqrt{\text{in.}}$ ). The  $K_{I_r}$  values should be the most reliable because they are calculated from actual measurements of both load and crack length. Thus, it appears that all of the specimens intended for 95 or 75%  $K_{Ic}$  may have been inadvertently overloaded. This could account for the immediate initiation of crack growth in the room atmosphere when the intended initial stress intensity of 95%  $K_{Ic}$  was applied to the alpha-beta specimens. Inasmuch as there was no crack growth during the last 208 days of exposure (less than  $10^{-6}$  in./hr.) cracking may be considered to have arrested and the  $K_{I_r}$  values regarded as candidates for  $K_{I_{scc}}$ . The more conservative values from the 75%  $K_{Ic}$  specimens indicate  $K_{I_{scc}}$  values in 3.5% NaCl of 77%  $K_{Ic}$  ( $34 \text{ ksi} \sqrt{\text{in.}}$ ) and 74%  $K_{Ic}$  ( $27 \text{ ksi} \sqrt{\text{in.}}$ ) for the beta processed and alpha-beta processed forgings, respectively. The value for the alpha-beta forging is higher than the value indicated above for the seacoast atmosphere.

The data from this investigation are compared in Figure 103 with a compilation by Blackburn, Smyrl and Feeney (Chapter 5, Ref. 42) of  $K_{Ic}$ ,  $K_{I_{scc}}$  and yield strength data for the alloy Ti-6Al-4V. The data are for a variety of plates, extrusions and forgings, 0.5 to 1.5 in. thick, and the wide variation in properties obtained for

the different products and tempers is clearly illustrated. The  $K_{Ic}$  and  $K_{Isc}$  values for the forgings from this investigation, which are superimposed on the published data, were somewhat lower than most of the values shown for materials of similar yield strength.

Blackburn, et. al., noted that the  $K_{Ic}$  and  $K_{Isc}$  values of Ti-6Al-4V alloy products can be influenced by a number of metallurgical variables such as composition, material thickness and preferred orientation or texture. They also observed that  $K_{Isc}$  values can vary as a result of test procedure. Several of these factors could be influencing the comparison of the data from this investigation and the published data. Factors considered most likely responsible for the low values for these forgings are probably related to their greater thickness (2.25 in.) and to their oxygen content (0.19%). Blackburn, et. al. (p. 319, Ref. 42) have shown that as the oxygen content of Ti-6Al-4V alloy was increased from 0.10 to 0.19 per cent, that  $K_{Ic}$  and  $K_{Isc}$  values decreased approximately 50 ksi  $\sqrt{\text{in.}}$  with corresponding increases in yield strength of only 12 to 15 ksi. This effect of oxygen level was seen with material from two different heat treatments which provided different levels of strength.

Results of the present investigation confirm the published information in showing that beta processed material can be expected to have a higher resistance to SCC than alpha-beta processed material. The difference was most definite in the seacoast atmospheric exposure.

### C. Fractographic Examination

The appearance of the fracture faces of specimens from both forgings after the aqueous chloride SCC tests is illustrated in Figure 101. Visually, the texture of the environmental growth portion of the fracture appears somewhat different for the two forgings. TEM fractographic examination, however, showed that the mode of fracture in the environmental growth region of both the beta and alpha-beta forgings was mixed intergranular, cleavage and ductile mode. Figure 104 illustrates typical fracture characteristics for the titanium alloy precracked specimens. Similar fracture features have been observed on sheet and plate of Ti-6Al-4V and other alpha-beta type alloys (p. 336, Ref. 42).

## IX. GENERAL DISCUSSION

### A. Comparison of Alloy Ranking by Precracked and Smooth Specimen Tests

The most useful forms of SCC data for ranking alloys and tempers are estimates of threshold stress from smooth specimens and threshold stress intensity and SCC propagation rate (velocity) from tests of precracked specimens in specific environments. These forms of data have the advantage that they are useful not only for comparing materials of construction, but for some situations can be used in design. However, for the data to be meaningful it is essential that the specific test conditions be associated with the data and that proper consideration be given to any differences in test conditions when materials are compared. Because of the basic difference in procedure used for tests of precracked and smooth specimens, one of the main objectives of this investigation was to compare the rankings of a wide variety of alloys and tempers by the

two procedures. A summary of data for the purpose of comparison is given in Table XXX and shown graphically in Figures 105-107.

1. Aluminum Alloys

The data for fatigue precracked compact tension specimens and smooth 0.125-in. tensile specimens exposed to the seacoast atmosphere are summarized in Figure 105. It is apparent that both the precracked specimen and the smooth specimen tests separated the group of six high resistance alloys at the left side of the graph from the low resistance alloys at the right. This is shown by the relatively high estimated threshold stresses and stress intensities and the absence of crack growth or the occurrence of low crack growth rates for the high resistance alloys (in most cases resulting from tensile overload) contrasted to opposite trends for the other alloys. In the group of high resistance alloys there were two discrepancies between the two test methods: for 7075-T7351 the precracked specimen developed a slight amount of intergranular SCC and the smooth specimen did not, but for 2024-T851 the performances were reversed. Ranking of the alloys in the low resistance group was not possible because specimens were not exposed at low enough stresses and stress intensities to obtain close estimates of the thresholds. Trends in the industrial atmosphere were similar (Table XXX).

The main body of accelerated test data for precracked specimens was obtained on compact tension specimens immersed in a salt-dichromate-acetate solution selected on the basis of exploratory tests described previously in Section VI-B1. Although the primary accelerated test for the smooth specimens was the 3.5% NaCl alternate immersion test, a set of the smooth tension specimens also was

exposed 90 days by continuous immersion in the salt-dichromate-acetate solution to provide a direct comparison with the precracked specimens. The smooth specimen test results agreed with the precracked specimen tests in identifying the four lowest resistance materials, but did not reveal susceptibility to SCC in several other materials shown to be susceptible in the precracked specimen tests (Figure 106). Also, this test of the smooth specimens was not as critical as the alternate immersion test in 3.5% NaCl solution (Tables XVI and XVII). Longer exposure of the smooth specimens or other variation of the procedure with the salt-dichromate-acetate solution, as discussed previously in Section VI-A3, might bring the two test procedures into closer agreement.

A more significant comparison of accelerated test data is shown in Figure 107 with tests of smooth specimens exposed to the commonly used 3.5% NaCl alternate immersion test versus tension precracked DCB specimens wet three times daily with 3.5% NaCl solution. The latter procedure was developed by Hyatt<sup>(26)</sup> as a practical substitute for the alternate immersion procedure. The estimated SCC thresholds were plotted both in actual stress or stress intensity units and as percentage of yield strength or of  $K_{I1}$ . The comparison of the two test methods was the same as that noted for the seacoast atmosphere. In the high resistance group there were again two discrepancies between the two methods. The 7075-T7351 precracked specimens indicated a definite but low degree of susceptibility to intergranular SCC which the smooth specimens stressed to 75% Y.S. did not show. It is possible that more highly stressed smooth specimens would have shown some susceptibility.

However, the situation is anomalous because smooth specimens that became pitted in the 3.5% NaCl alternate immersion test developed transgranular environmental crack growth instead of the typical intergranular environmental crack growth (SCC) in aluminum alloys (compare Figures 20 and 68). Additional studies will be required to determine whether this difference in crack mode is influenced more by the state of stress or by environmental factors. In the case of 2024-T851, smooth specimens showed a susceptibility to intergranular SCC at a stress of 75% Y.S. but precracked specimens stressed to pop-in did not. Environmental crack growth occurred in the DCB, but it was of the tensile overload type rather than SCC. In the group of low resistance aluminum alloys the performances of the various alloys were similar in both tests, and there was no consistent trend for one test to be more critical than the other.

An investigation of aluminum alloy hand forgings of a wide variety of alloys by Chu and Wacker<sup>(52)</sup> provided an opportunity to rank the SCC performances by precracked (cantilever beam) and smooth specimen (bent beam) tests. Ranking of the alloys and tempers with  $K_{I_{SCC}}$  values did not agree well with the threshold stresses estimated from the smooth specimen tests. The main discrepancy was the unrealistically high  $K_{I_{SCC}}$  values reported for alloys 2014-T6 and 2024-T352, which are known<sup>(22,26)</sup> to have low resistance to SCC when stressed in the short-transverse direction, as demonstrated again in the present investigation. Inasmuch as the estimates of  $K_{I_{SCC}}$  were based on relatively short (100-300 hr.) periods of immersion in sea water, it is possible that a longer period of exposure would have given more realistic threshold values.

In two European papers presented at the 33rd Meeting of the "Structures and Materials Panel" of AGARD at Brussels, Belgium in October, 1971, the investigators presented results of comparative tests with Boeing DCB specimens and smooth test specimens. Bollani<sup>(53)</sup> reported tests on short-transverse tests of 2-in. thick plate of 7075-T651 and 7075-T7351. Lehmann<sup>(54)</sup> compared the SCC performances of a die forging in alloys 7079-T6 and AZ74.61\*. In both investigations the two types of tests gave satisfactory distinctions between the high and low resistance products, and the authors concluded that for a complete evaluation of the resistance to SCC it is necessary to test precracked as well as smooth specimens.

A round robin stress corrosion testing program was carried out at seven divisions of the North American Rockwell Corporation to evaluate and compare various smooth specimen and precracked specimen techniques for assessing stress corrosion susceptibility<sup>(55)</sup>. Tests were conducted on a hand forging of 7049\* alloy heat treated and artificially aged to four different levels of strength and anticipated resistance to SCC. Results of the conventional tests indicated that the susceptibility to SCC decreased regularly with increased aging time and decreased strength. However, crack growth measurements on fracture mechanics specimens (bolt-loaded DCB's) differentiated the four tempers into two groups; there was no significant difference in growth rate between the underaged and T6 temper, or between the T73 and the overaged temper.

On the basis of many tests of a variety of aluminum alloys

-----  
\*Typical compositions:

AZ74 6.0Zn, 2.3Mg, 0.8Cu, 0.2Cr, 0.4Ag  
7049 7.7Zn, 2.5Mg, 1.6Cu, 0.16Cr

and tempers with bolt loaded DCB specimens Hyatt<sup>(26)</sup> concluded that, "trends derived from DCB specimen data agree with established trends derived from smooth specimen threshold data. However, in many cases, the data from DCB specimens are more discriminating than smooth specimen data, and growth rates at the higher stress intensity levels can be used as a new basis for comparing and rating new alloys and heat treatments". In a subsequent article<sup>(56)</sup> Speidel and Hyatt regarded such precracked specimen data as a valuable addition to the smooth specimen threshold data in the same way that fatigue crack growth data are a valuable addition to the standard S-N fatigue curves for different alloys. Also, in their work with the "overaging" of 7075 and 7178\* alloy plate the SCC plateau velocity decreased regularly with increased aging time.

Thus, from a consideration of the results of the present investigation and the published literature it is concluded that the use of precracked specimens is not essential for a reliable evaluation of the resistance to SCC of aluminum alloys, but this technique does afford a practical method for determining SCC velocity. A more complete evaluation of the resistance to SCC of a material can be obtained by testing precracked as well as smooth specimens.

## 2. Stainless Steel and Titanium Alloys

The data for the steel and titanium alloys are summarized with that for the aluminum alloys in Figures 105 and 106. In the seacoast atmosphere there were eight instances (7 of the 13 steels and 1 of the 2 titanium items) in which the precracked specimens showed a marked susceptibility to SCC whereas the smooth specimens

-----  
\*Typical composition:

6.8Zn, 2.8Mg, 2.0Cu, 0.2Cr

have not failed during the 27 mo. exposure to date. It is possible, of course, that continued exposure of the smooth specimens will reduce this rather striking difference. For five of the steel alloys with lowest resistance to SCC both kinds of specimens failed, and for the most resistant steel alloy, 15-5PH H1150M and the beta-forged Ti-6Al-4V alloy neither type of specimen cracked. SCC in the precracked specimens of all of the steel alloys except 15-5PH H1150M propagated at a high velocity similar to that of the low resistance aluminum alloys. For the accelerated tests in sodium chloride solution the comparison was similar to that in the seacoast atmosphere except that even fewer materials failed as smooth specimens.

This behavior of the steel alloys and the titanium is consistent with the experience of most other investigators<sup>(4,42,48)</sup>, and, in fact, reflects the reason for the rapid acceptance of the fracture mechanics approach to SCC testing. It, therefore, appears to be essential that alloys of this type be evaluated with tests of precracked specimens as well as with smooth specimens.

In contrast with these tests of relatively thick sections, however, it was found in accelerated tests of thin sheet (0.025-0.050 in.) of several high strength stainless steels (including AM355 SCF1000, PH15-7Mo RH1075, and PH14-8Mo SRH950) that the presence of a pre-existing fatigue crack had no effect on the susceptibility to SCC<sup>(50)</sup>. Thus, it should be recognized that the tests of thin sheet should not be used to predict the performance of relatively thick components of a structure and vice versa.

B. Design Implications of Stress Corrosion Test Data

1. Theory

If the estimate of the environment to be encountered in service is reasonably accurate, the stress corrosion test data obtained with smooth specimens yields useful engineering data that will alert the design and shop engineers to the maximum sustained tensile stress that can be tolerated by a material. Theoretically at least, the stress corrosion data developed from precracked specimens utilizing fracture mechanics principles could be more useful because two pieces of information are obtained: (1) the limiting stress intensity factor ( $K_{I_{SCC}}$ ) and (2) the rate of environmental crack growth ( $da/dt$ ). These two types of information would be used to analyze a typical situation in the manner shown by the following example.

For material X,  $K_{I_c}$  and  $K_{I_{SCC}}$  are known, and there is a  $K_I$  versus  $da/dt$  curve, as represented by the diagram in Figure 108(a). The operating stress for a structural component is known, and the maximum size of crack or flaw that may exist in the structure without detection can be established, which together can be used to calculate an initial stress intensity,  $K_{I_1}$ , for the structure. The chosen initial flaw size will be the largest one that could exist in the structure without having been detected by the NDT methods which are employed, which may be limited by accessibility as well as precision. With the  $K_{I_1}$ , an initial judgement of the situation is established, and three possibilities exist:

a. If  $K_{I_1}$  is less than  $K_{I_{SCC}}$ , such as A in Figure 108(a), there will be no stress corrosion crack growth and the structure is safe unless other factors (e.g., fatigue stressing) cause the

crack or flaw to grow to a size where  $K_{I_1}$  equals or exceeds  $K_{I_{SCC}}$ .

b. If  $K_{I_1}$  is greater than  $K_{I_{SCC}}$ , such as B, environmental crack growth can be expected and the designer must consider how soon cracking will initiate (Figure 108(b)), how fast the crack will grow and the likely consequences. The rate of crack growth can be determined from the  $K_I$  versus  $da/dt$  relationship, and the length of time for the crack to grow to a size large enough that  $K_I$  equals or exceeds  $K_{I_c}$  can be calculated (with some assumption about crack incubation time). The designer then must consider the possibility that complete fracture will occur, and determine whether the time period over which it develops is acceptable or whether some change in material or design parameters is called for.

In calculating the time for the crack to grow, it is important to note that the  $K_I$  level, and hence the rate, will likely change as the crack grows. In a constant load situation where one deals with a gross stress that is assumed to be independent of crack size,  $K_I$  increases as the crack grows. In many instances, such as tight fitups, the gross stress really does not remain constant, but will decrease as the crack grows. Depending upon the rate of decrease, this could have the effect of decreasing the  $K_I$  level and, therefore, of decreasing the crack growth rate as seen from Figure 108(a). Although the designer is rarely in a position to be sure that this is taking place, it does explain why some cracks arrest without causing complete fracture. Thus, the determination of total time to reach a critical situation is an integration and the type of gross stress situation should be taken into account when considering the consequences.

c. If  $K_{I1}$  exceeds  $K_{Ic}$ , the operating stress obviously is too high and some redesign or change of materials is indicated.

When both fatigue and stress corrosion crack growth are concurrent, both must be considered. The resultant rate of flaw growth may be not merely the additive effects of pure fatigue and pure SCC but perhaps a synergistic stress-corrosion-fatigue effect. The actual rate will depend upon the relative crack growth rates due to SCC and fatigue (i.e., whether or not one is strongly dominant) and the degree of synergistic effect for the individual alloy and temper. Evaluation of the latter effect is beyond the scope of this investigation.

## 2. Practice

The procedures outlined above would seem quite practical, but for two important points: (1) designers do not desire to use alloys which stress corrosion crack to any appreciable degree under the sustained tension stress anticipated in the structure, so the use of crack growth rates to calculate life rarely, if ever, comes into play, and (2) the stress-intensity type of analysis implies that no stress corrosion crack growth will take place below  $K_{Isc}$ , but this is not supported by practical experience.

The first point concerns the reticence of designers to use any material in which a stress corrosion crack propagates at an appreciable rate. For example, current tendencies are to shun aluminum alloys such as 7079-T651 which stress-corrosion crack rapidly when structures are stressed in the short-transverse direction relative to the grain structure. One reason is that the stress situations that have caused SCC in service, at

least with aluminum alloys, usually are unknown to the designer as they involve sustained tension stresses that are not anticipated and can not be precisely measured; these situations result from fit-up during assembly of structural components or from residual stresses locked in during quenching following heat treatment, forming, straightening, welding, etc. Another reason for this is that SCC propagation rates have not been well defined -- except for limited information indicating that the rates can be relatively high, depending upon the specific conditions. It can be correctly noted that this is in contrast to the situation in designing for fatigue, where significant rates of growth must be dealt with. However, in the case of fatigue, the time to failure is related to the magnitude of the operating stress and the period of operation, which can be recorded; whereas with SCC the measurement of time to failure must be started when the part is machined or assembled into the structure, and depends more upon the age of the structure, the magnitude of the sustained tension stress, and the environment than upon the period of operation. Moreover, in the case of fatigue, there is little choice, as there are no "immune" or "highly resistant" alloys, whereas with regard to SCC, the problem can usually be avoided by a change in design and assembly practices or by a change in alloy or temper.

On the second point, the concept of  $K_{I_{SCC}}$  clearly implies that so long as the combination of operating stress and flaw size is such that the applied stress intensity is less than a certain level, no stress corrosion crack growth will take place. But experience has shown that this is not realistic for some aluminum

alloys. Consider the situation with 7079-T651 plate, for which the  $K_{I_{SCC}}$  value is about  $4 \text{ ksi}\sqrt{\text{in.}}$  in salt-dichromate-acetate solution (Table XXIV). As Figure 109 (developed in this example for long thin surface cracks, though any other crack type and shape could be used with the appropriate stress intensity relationship) shows, even a value as low as  $4 \text{ ksi}\sqrt{\text{in.}}$  implies that in the presence of a 0.01 in. deep crack a tension stress of 20 ksi may be safely sustained indefinitely. This is not true, as smooth specimens containing no visible cracks will fail as a result of SCC within a short time at that stress. The  $K_{I_{SCC}}$  analysis fails to take into account that cracks can initiate as a result of electrochemical reactions at metallurgical sites, such as grain boundaries, that are not classifiable in the initial analysis as flaws in the material. Another possible explanation is that for low resistance alloys such as 7079-T651 there may not be a real  $K_{I_{SCC}}$  and the number assumed for it is too high.

These facts prompted the previous proposal<sup>(29)</sup> that a dual approach to design must be considered in dealing with thresholds - both the limiting stress and stress intensity must be considered, as shown in Figure 110. In such a chart, the "safe" region (that in which stress corrosion free service would be expected) is that indicated to be SCC free both by the threshold stress from smooth specimen tests and the threshold stress intensity factor from precracked specimen tests. There is a region above the stress-limited region but to the left of the stress-intensity line in which safety would be indicated by the stress-intensity approach, but tests of smooth specimens and service experience indicate that

SCC will occur. Comparisons of such charts in Figure 111 for the various aluminum alloys included in the present investigation not only illustrate the superiority of the high resistance group of alloys, but also show that the threshold stress intensity may not be as restrictive, or as realistic for aluminum alloys, as the threshold stress. On the other hand, for several of the stainless steel alloys tested, such as the 15-5PH H900, PH13-8Mo H950 and H1050, 431 HT125, and the 6Al-4V titanium alloy forgings, the threshold stress intensity appeared to be more restrictive than the threshold stress.

#### C. Problems in Interpretation of Accelerated SCC Test Data

Accelerated SCC tests are necessary for alloy development because it is not practical to perform such tests only in natural environments, which may require long exposure periods. Unfortunately, all accelerated corrosion tests are subject to limitations that are related to the material and the environment. In the case of SCC tests there is the additional limiting factor in the mechanics of the stress situation. Test procedures must be sensitive enough to detect a low degree of susceptibility to SCC, yet not so drastic that materials with low and high susceptibility cannot be differentiated. The definition of a significant "low degree of susceptibility" must be based on the requirements of the intended structures. Thus it is inevitable that there will be problems with interpretation of accelerated test data.

Problems have arisen in defining "intermediate" resistance to SCC because variables in the SCC test procedure can have a marked effect on the test data. The choice of test conditions can profoundly influence the relative rankings of alloys and tempers

and the selection of materials of construction<sup>(57)</sup>. The ideal test will provide unambiguous test data free from extraneous corrosion and mechanical effects that are neither a part of the SCC process nor involved in practical situations. Following is a discussion of some of the problems in interpretation that were observed in smooth and precracked specimen tests in this investigation.

1. Smooth Specimen Tests

Times to failure (i.e., specimen lives) are, per se, of limited use in ranking alloys except under special circumstances. To obtain an estimate of the more useful "threshold" stress,  $\sigma_{th}$ , to initiate SCC in a smooth specimen exposed to a given environment a large number of test specimens is required, particularly if the threshold is to be determined with a high level of confidence. It is evident from results of the smooth specimen tests in this investigation that a great many more specimens would have to be tested to obtain close estimates of threshold stresses for the materials tested. Although estimates of threshold stresses plotted in Figures 105-107 could only be shown as "greater than" or "less than" a specific test stress, such data nevertheless are useful in developing general characterizations of materials.

Apparent threshold stresses are influenced by the cross-section area of the test specimen, the loading method, corrosiveness of the environment and the length of exposure. These factors are especially likely to determine whether or not a specimen will fail when testing materials with an intermediate resistance to SCC. Test media that are too mild and exposure periods that are too short will lead to threshold estimates that are unrealistically high.

Such was the case for certain of the aluminum alloy tensile specimens that were continuously immersed in the salt-dichromate-acetate solution (Refer to Figures 105 and 106). Increased sensitivity was gained with the more corrosive 3.5% NaCl alternate immersion test as shown in Figure 107. But when a test specimen becomes pitted appreciably and the net section stress increases above that of the nominal gross section stress (Figure 8), the threshold stress to initiate SCC in a smooth surface becomes indeterminate. Estimates of  $\sigma_{th}$  thus tend to be unrealistically low. Also, there is the problem that pitting of the small specimens may result in tensile overload failures that become confused with failures caused by SCC and again leads to threshold estimates that are unrealistically low. Metallographic or fractographic examinations are required to determine the real cause of the fracture of pitted test specimens.

There is still the question as to the most realistic size of test specimen to be used.

## 2. Precracked Specimen Tests

There are a number of experimental difficulties with tests of precracked compact tension and DCB specimens that must be overcome if meaningful threshold stress intensities and accurate K-Rate curves are to be obtained. Most of these have been illustrated and discussed in detail by Smith and Piper<sup>(42)</sup> and by Speidel and Hyatt<sup>(56)</sup>, including such factors as residual stresses, corrosion-product wedging, specimen orientation and grain flow, crack branching and delamination. Some other procedural difficulties not given as much emphasis in the literature were encountered in the present

investigation.

a.  $K_{I_{SCC}}$  by Crack Initiation

Estimating  $K_{I_{SCC}}$  by testing specimens under constant load at various applied  $K_I$  values appeared to be the most reliable method but it is not free from problems of interpretation. For example, as shown schematically in Figure 108(b), the time for incubation of SCC ( $t_{inc}$ ) and the time for the specimen to fracture ( $t_F$ ) are not equal, especially at lower  $K_{I_1}$  values approaching  $K_{I_{SCC}}$ . A more meaningful estimate of  $K_{I_{SCC}}$  would be obtained from the  $t_{inc}$  curve because it should be free from the effects of specimen size and fracture toughness of the material that will influence  $t_F$ . However, it generally is not feasible to determine the  $t_{inc}$  curve, as the first evidence of SCC is difficult to obtain. Because a  $t_F$  curve is the usual substitute it is advisable to check all "run-out" tests to determine whether SCC has initiated. This practice, which was followed in the present investigation, will tend to give lower estimates of  $K_{I_{SCC}}$  than if failures are only recorded for fractured specimens.

The chief problems involved in the determination of  $K_{I_{SCC}}$  by crack initiation are long incubation times at  $K_{I_1}$  levels close to the apparent threshold, possible blunting of the precrack at high  $K_{I_1}$  levels and corrosion product wedging. Evidence of long incubation times was noted with both the ring-loaded aluminum alloy specimens and the bolt-loaded steel specimens. In the tests of the steel alloys, some inconsistency was observed at the high  $K_{I_1}$  levels with the result that environmental crack growth would not start.

Corrosion-product wedging, which could cause lower apparent  $K_{I_{SCC}}$  values, did not appear to be a problem with the ring loaded aluminum alloy specimens in this investigation.

b.  $K_{I_{SCC}}$  by Crack Arrest

Determination of  $K_{I_{SCC}}$  by the arrest method in a decreasing-K (constant deformation) test requires that the SCC induced at a high level of  $K_I$  will decelerate as the crack lengthens until SCC ceases (i.e., crack arrest), or until the rate of crack growth becomes vanishingly small. One advantage of this method in most cases is the avoidance of long incubation times. Nevertheless this procedure also is time-dependent, and it is necessary to have an explicit interpretation of the term "arrest". To be of engineering significance the crack growth rate used to denote an arrest also should be relatable to service performance. Speidel and Hyatt<sup>(56)</sup> recommended for aluminum alloys a velocity of  $10^{-8}$  cm/sec., or about  $1.4 \times 10^{-5}$  in./hr. as a convenient indicator of  $K_{I_{SCC}}$ .

A SCC growth rate of about  $1.4 \times 10^{-5}$  in./hr. in the accelerated tests used in this investigation appears to provide a reasonable estimate of  $K_{I_{SCC}}$  for high strength aluminum alloys if it is assumed that a SCC growth rate in a seacoast atmosphere of  $10^{-6}$  in./hr. (approx. 0.1" in 10 years) is tolerable in an unprotected structure; i.e., it will assure a satisfactorily low probability of SCC trouble. However, with a measurement limitation of 0.01 in., an undesirably long exposure of more than one year in the atmosphere during which there is no measurable crack growth would be required to demonstrate crack arrest. In an accelerated test giving an SCC growth rate ten times that in the atmosphere (as the tests

in this investigation did) only 1000 hours (41 days) would be required. But in this investigation it was shown that with exposures longer than 300 hours (12.5 days) in the 3.5% NaCl test or 600 hours (25 days) in the salt-dichromate-acetate test corrosion-product wedging becomes dominant, with the result that calculations of stress intensity become meaningless. Thus, the estimates of  $K_{I_{SCC}}$  in these tests must be based on growth rates of about  $3 \times 10^{-5}$  in./hr. for the 3.5% NaCl test and about  $1.7 \times 10^{-5}$  in./hr. for the SDA test. These rates do not differ much from the rate proposed by Speidel and Hyatt.

Unfortunately, the determination of  $K_{I_{SCC}}$  by the arrest method may be impracticable for many alloys and tempers because of corrosion-product wedging. This problem is especially acute with aluminum alloys because of the relatively insoluble and voluminous nature of the corrosion products. With the low resistance alloys the corrosion product wedges drive the crack onward in the same manner that exfoliation corrosion advances. All different degrees of arrest and temporary arrest were observed, as shown in Figures 50 and 51, rendering the estimates of  $K_{I_{SCC}}$  very inaccurate as indicated in Figures 53 and 54. There may not, in fact, be a true  $K_{I_{SCC}}$  for a product with a very directional grain structure, such as 7079-T651 plate, when it is loaded in the short-transverse (S-L) direction. An indication of this is shown in Figure 30 by the initiation of SCC in specimens exposed with no applied load for just a few months in a seacoast atmosphere. Experimental evidence of a threshold stress intensity will certainly depend upon the test environment. With the high resistance alloys the corrosion products

build up into compact wedges that actually force the metal apart, as if in a very slow tear test, even if it is not susceptible to SCC. Any slight susceptibility to SCC probably will be evident. However, under such severe wedging conditions it becomes impossible without a metallographic examination to distinguish between materials with slight susceptibility to SCC and those which are just being torn apart (Refer to Figures 105-107).

c. Invalid  $K_{I_{SCC}}$  Values

Invalid  $K_{I_{SCC}}$  data can be derived for materials with a relatively high resistance (or immunity) to SCC in two other situations. One such source is the misinterpretation of residual stress intensities measured in bolt loaded specimens after exposure. A  $K_{I_P}$  value that is lower than the intended  $K_{I_1}$  value is not necessarily a measure of  $K_{I_{SCC}}$ , and should not be regarded as such until it is established that SCC really occurred<sup>(58)</sup>. In previous sections it was pointed out how  $K_{I_P}$  values might seem to be low as a consequence of either inaccuracies in applying high  $K_{I_1}$  values close to  $K_{I_C}$  that result in small amounts of plastic deformation, relaxation of the stress during exposure, or a small amount of corrosion product wedging. The effect of any of these events would be to cause part of the COD to be inelastic and give the effect of a reduced load when the specimen is unloaded to measure the final COD. Such behavior was noted for aluminum alloys 5456-H117 and 6061-T651 and the steel alloy 15-5PH H1150M, and specific values for  $K_{I_{SCC}}$  therefore were not indicated. It would be meaningless to report a  $K_{I_{SCC}}$  value in the absence of actual environmental crack growth.

Novak<sup>(59,60)</sup> has pointed out that invalid  $K_{I_{SCC}}$  data also can be obtained for materials with a very high fracture toughness when the fracture tests reflect a  $K_I$ -suppression effect. This is of especial concern because the  $a_{cr}$  value corresponding to the onset of fracture ( $K_{Ic}$ ) or SCC ( $K_{I_{SCC}}$ ) may be underestimated by more than a factor of ten when such values are calculated on the basis of invalid  $K_Q$  or apparent  $K_{I_{SCC}}$  values. Novak's analysis<sup>(60)</sup> provides a framework of  $K_{I_{SCC}}$  classifications for placing such data in perspective. Examination of the data for the highest toughness alloys tested in the present investigation indicates that  $K_I$ -suppression effects were not involved.

d. Measurement of da/dt

One of the problems in determining  $K_{I_{SCC}}$  by the arrest method involves the experimental difficulties in measuring very small amounts of crack growth and the interpretation of the erratic growth curves that are obtained (Figure 38). A more sophisticated technique is needed to measure the original precrack and to monitor crack growth, as measurements on the surface sometimes provide only a crude estimate of actual crack growth at the interior of the specimen. While special techniques have been devised for mechanistic studies of small numbers of specimens, a simple economical procedure is needed for the many tests required for alloy development work.

A possible approach for the latter need is to run a set of replicate bolt loaded specimens for a fixed period, determine the amount of crack growth at the end of that time and calculate the average growth rate for the test duration. The period of

exposure should be chosen so as to permit ample time to initiate SCC of slightly susceptible materials and short enough to avoid appreciable cracking by tensile overload as a result of corrosion-product wedging. The optimum combination of corrosive environment and test period must be based on trial test data for materials that can be related to service performance.

#### X. SUMMARY AND CONCLUSIONS

The following summary statements and conclusions are based upon the work performed in this investigation to evaluate SCC susceptibility using fracture mechanics techniques and a review of published literature. Tests were performed on a variety of aluminum alloys, precipitation-hardening stainless steels and 6Al-4V titanium alloy with wedge-opening load precracked compact tension and DCB specimens exposed both to accelerated tests and to the outdoor atmosphere. First are some general statements about the test methods and then statements related to the particular alloys tested in this investigation. Specific needs are mentioned along the way as guide posts pointing to future work.

##### A. Test Methods

1. Despite claims of early advocates of precracked test specimens, there still is no single, fool-proof stress corrosion test method that is free from special limitations on test conditions and free from problems of interpretation of the test results. Thus, it is highly desirable to develop guidelines or recommended practices that will lead to uniform procedures for stress corrosion testing with the relatively new fracture mechanics method with precracked specimens as well as with the older conventional method with smooth specimens. Several reviews of methods for determining susceptibility

to SCC with smooth and precracked specimens are available and are listed in the Bibliography. Moreover, a number of task groups under ASTM Subcommittees G01.06 and E24.04 are now preparing recommended practices for use with the more widely used specimens of both types and test environments.

2. The advantages proposed for tests with precracked specimens are that, (a) the uncertainties associated with initiation of SCC are minimized, (b) a flaw geometry is provided for which a stress analysis is available through fracture mechanics, and (c) data are provided in terms of SCC growth rate and the related crack-tip stress intensity factor, that are potentially more useful for predicting the behavior of large structural components containing macroscopic flaws. The threshold stress intensity,  $K_{I_{SCC}}$ , quantifies the resistance to SCC with a single number that has predictive capabilities with respect to combinations of pre-existing crack depths and gross section stresses which would cause SCC in a specified environment. However, Wei, et. al. <sup>(61)</sup> have cautioned that:

"Because the apparent  $K_{I_{SCC}}$  are so dependent on test procedures and conditions, its practical utility must be carefully re-evaluated".

3. The most common way to determine  $K_{I_{SCC}}$  is by exposing to a given corrosive environment a number of replicate specimens loaded to various  $K_{I_1}$  levels to observe a minimum  $K_I$  value at which stress corrosion crack growth will occur during an arbitrarily selected time. The main disadvantage of this method is that long incubation times may be required at  $K_{I_1}$  levels close to the threshold. Long incubation times often can be avoided with a specimen loaded by constant deformation to a high  $K_I$  level to initiate SCC and then

monitoring the SCC velocity as the crack grows, causing the gross stress and  $K_I$  to decrease;  $K_{I_{SCC}}$  then is designated by an arbitrarily selected low crack velocity (or when crack growth is considered to have stopped). Although this method of determining  $K_{I_{SCC}}$  by "crack arrest" seems very attractive, it is not feasible in many instances because of the interference of corrosion products formed near the crack tip. These products create high unknown wedge forces that influence  $K_I$  so that it cannot be calculated simply from the crack length.

4. For a given alloy and environment the SCC propagation rate is closely related to and varies with the stress intensity at the crack tip  $K_I$ ; hence, to characterize the stress corrosion behavior of an alloy by its SCC propagation rate it is necessary to consider the  $K_I$ -rate relationship over the full range of  $K_I$  from  $K_{Ic}$  to  $K_{I_{SCC}}$  (Figure 108a). Nevertheless, it appears that the relative resistance to SCC of alloys can be ranked fairly efficiently by comparing the SCC propagation rates (plateau velocities) at high levels of  $K_I$  close to the respective critical stress intensities.

5. There are a number of formidable experimental difficulties with tests of precracked specimens that must be overcome if meaningful threshold stress intensities and accurate  $K$ -Rate curves are to be obtained for all types of alloys and product forms. Factors such as residual stresses, crack branching and materials with very high toughness present particularly difficult problems. Therefore, it seems that at this time tests with precracked specimens and fracture mechanics analyses should be coordinated with smooth specimen tests to more fully describe the stress corrosion resistance of an alloy.

6. Comparative rankings of the relative resistance to SCC by tests of precracked and smooth specimens were found to vary with the alloy and temper. Materials with a low threshold stress for initiating SCC in a smooth surface,  $\sigma_{th}$ , also showed a low  $K_{I_{SCC}}$  and a tendency for a relatively high SCC velocity under plane strain conditions. On the other hand certain steel and titanium alloys with a high  $\sigma_{th}$  showed a relatively low  $K_{I_{SCC}}$  and high SCC velocity under plane-strain conditions (Figures 105-107). The existence of a plane-strain stress state, however, is not a prerequisite for SCC of most of the materials that have been known to give SCC problems in service. For many thin components information regarding the threshold stress to initiate SCC in a smooth surface is likely to be more relevant than test data obtained with precracked test specimens; hence, there is need for a fuller development of the practical significance of the test data and the application of it to the design of engineering structures.

#### B. Tests of Aluminum Alloys

##### 1. Smooth Specimens

The SCC behavior of the 13 alloy and temper combinations tested with smooth specimens was representative of the performance of these materials established by service experience and previous lab tests of smooth specimens. Exposures of three months to 3.5% NaCl by alternate immersion and three years in seacoast and inland industrial atmospheres have been completed. There were no SCC failures of longitudinal specimens of any of the materials. With short-transverse specimens the performance varied widely, as anticipated, ranging from no susceptibility at 75% Y.S. (highest

stress tested) to marked susceptibility at about 15% Y.S. (lowest stress tested). The data are summarized in Tables XIII-XVI, XXX and Figures 105-107. Although no long-transverse tests were made in this investigation other experience has shown that the resistance to SCC of long-transverse specimens from rolled plate is very high, nearly equal to that of longitudinal specimens<sup>(22,34,42)</sup>.

## 2. Precracked Specimens

a. Trends derived from the precracked specimens agree with established trends derived from smooth specimen  $\sigma_{th}$  data, and it appears that SCC growth rates at the higher  $K_I$  levels (i.e., plateau velocity in Figure 108a) can be used as a supplementary basis for comparing and rating new alloys and thermal treatments.

b. Stress corrosion data in terms of estimated  $K_{I_{SCC}}$  and SCC growth rates for the various alloys and tempers tested are summarized in Tables XIX, XX and XXX, and shown graphically in Figures 43, 53, 54, 105, 106, 107. In general, estimates of  $K_{I_{SCC}}$  for S-L oriented tests in seacoast or industrial atmosphere were greater than 80%  $K_{I_C}$  for high resistance alloys such as 5456-H117, 6061-T651, 2219-T87, 2021-T81, 2024-T851 and 7075-T7351 and in the range of about 20 to 50%  $K_{I_C}$  for alloys such as 2014-T651, 2024-T351, 2219-T37, 7075-T651, 7039-T6351, 7079-T651 and 5456-Sens. SCC growth rates for S-L oriented specimens stressed close to  $K_{I_C}$  in a seacoast atmosphere were about 1 to  $5 \times 10^{-4}$  in./hr. (1 to 5 in./yr.) for the low resistance alloys and less than about 0.03 in./yr. for a highly resistant alloy such as 7075-T7351.

c. To investigate the K-Rate relationship for an alloy in

a decreasing-K test the most suitable specimen appears to be a double-bolt loaded DCB specimen with a chevron notch similar to that described by Speidel and Hyatt<sup>(56)</sup> and presented in a draft of a proposed method of test presently under consideration by ASTM Subcommittees G01.06.04 and E24.04. A sketch of the proposed specimen is shown in Figure 112. Other (unpublished) data obtained at Alcoa Research Laboratories supplementing the work in this contract investigation have shown that this modification will produce the same results as the slightly modified Boeing DCB used in the present contract (Figures 9, 26, 27). An advantage of the new modification is in the ease of producing a mechanical pop-in with minimum plastic deformation of the tougher alloys. Although a minimum specimen thickness is not required to initiate SCC, it is desirable to maintain plane strain conditions when feasible to facilitate pop-in.

d. Estimates of  $K_{I_{SCC}}$  can best be approached by the crack-initiation procedure. A "constant" load applied with an elastic ring (or dead weight) appears to be the most practicable method because of the convenience in automatic monitoring and recording of crack initiation and growth (Figure 12-15). A fatigue precracked compact tension specimen is preferred over a tension precracked specimen because of higher precision in applying the initial stress intensity  $K_{I_1}$ . For this type of test continuous immersion in a salt-dichromate-acetate solution has the advantage over plain 3.5% NaCl because it causes more rapid SCC crack growth and less rapid general corrosion of the precrack (Figures 21, 24, 50, 51).

e. Discriminating between highly resistant tempers, however, still poses a problem because of difficulties associated with identification of extremely slow crack growth rates. One difficulty is associated with the actual measurement of slight amounts of localized or uneven growth (Figures 44, 45, 55). Another difficulty arises because the small amounts of sub-critical crack growth resulting from corrosion product wedging and tensile overload cannot be distinguished from equally small amounts of growth resulting from SCC without metallographic or fractographic examination of the crack tip (compare alloys 2219-T87 and 7075-T7351 in Figures 105-107).

f. Meaningful tests can be obtained only with S-L or S-T oriented specimens; i.e., with load applied in the short-transverse direction relative to the grain structure and crack growth directed in either the longitudinal or the long-transverse direction. Attempts to test specimens with other orientations, such as L-T, with load applied in the longitudinal direction will result in stress corrosion cracks growing out of the plane of the precrack and rendering calculations of both  $K_I$  and crack growth rate impossible (Figure 28, 29, 47).

### 3. SCC Ranking of Alloys and Tempers

Because of experimental difficulties associated with the determination of precise SCC thresholds ( $\sigma_{th}$  and  $K_{I_{SCC}}$ ) and SCC growth rates, a method of classifying the SCC ranking of materials into broad groups based on accelerated tests of both smooth and precracked specimens appears to be advantageous. An example of such

an approach for aluminum alloy products tested in the short-transverse direction (S-L) is shown below:

Typical Alloy	General SCC Rating(1)	SCC Threshold		SCC Velocity In./Hr.(4)
		Gross Stress % G.Y.S.(2)	Stress Intensity % $K_{Ic}$ (3)	
6061-T6	A	>90	>95	$<1 \times 10^{-5}$
7075-T73	B	>75	>80	$<5 \times 10^{-5}$
7075-T76	C	>40	>50	$<5 \times 10^{-4}$
7075-T6	D	<40	<50	$>5 \times 10^{-4}$

(1) Practical significance of ratings:

- A - No known instance of SCC in service or in standard laboratory tests
- B - No known instance of SCC in service; limited failures in standard laboratory tests of short-transverse specimens under extreme stress (intensity).
- C - No known instance of SCC in service. SCC not anticipated in service at short-transverse tension stress resulting from heat treatment and quenching or from design and assembly stresses kept below about 40-50% of the guaranteed yield strength. Higher sustained tension caused by forming or assembly of misfit components must be avoided.
- D - Limited SCC in service principally when component stressed in short-transverse or transverse direction relative to grain flow; SCC unlikely if tension stress sustained only in direction parallel to grain flow.

(2) 0.225-in. tension specimen; ARL frame; 30 days 3.5% NaCl A.I. (M823)

(3) Compact tension specimen, fatigue precracked; constant load; 2000 hr. salt-dichromate-acetate.

(4) DCB; 2-bolt load to mechanical pop-in; 300 hr. 3.5% NaCl dropwise; average velocity at 95-80%  $K_{I1}$ .

To determine the rating for a material, check the SCC velocity and at least one of the two SCC thresholds and use the lowest of the criteria to establish the SCC rating. The use of such a system, of course, would require standardization of the test procedures.

## C. Tests of Precipitation Hardening Stainless Steels

### 1. Smooth Specimens

Exposures of 7 mo. to 3.5% NaCl by alternate immersion and 28 mo. in seacoast and inland industrial atmospheres have been completed, and the results are summarized in Tables XXV, XXVI, XXVII and Figures 105 and 106. The SCC behavior of the 13 alloy and temper combinations tested with smooth specimens generally fell into line with published results of other smooth specimen tests of these alloys. The most susceptible alloys were the AM355 SCT850 bar, PH15-7Mo RH950 and RH1050, 17-7PH H1050 and 431 HT200. Specimens of AM355 SCT850, 431 HT200 and PH13-8Mo H950 removed from the 2 or 2.25" x 6" rolled bar in three orientations parallel to the three major axes L, T and S, showed no appreciable difference in behavior. The seacoast atmosphere was distinctly more aggressive in causing SCC than the inland industrial atmosphere and slightly more aggressive also than the 3.5% NaCl alternate immersion test.

### 2. Precracked Specimens

a. Stress corrosion data in terms of estimated  $K_{I_{SCC}}$  and SCC growth rates for the various alloys and tempers are summarized in Tables XXVIII and XXX, and shown graphically in Figures 93, 105 and 106. In the seacoast atmosphere crack growth started almost immediately in T-L specimens loaded to 95%  $K_{I_C}$  for all of the materials except 15-5PH H1150M, and propagated 0.2 to 0.8 in. within three months; the average crack growth rate was about 2 to 9 x 10<sup>-4</sup> in./hr., similar to that of short-transverse (S-L) specimens of the low resistance aluminum alloys (Figure 105). Estimates of  $K_{I_{SCC}}$  were below 50%  $K_{I_C}$  for nine of the alloys, between 50 and 75%  $K_{I_C}$

for 431 HT125, and AM355 SCT1000 (plate and bar), and above about 95%  $K_Q$  for the 15-5PH H1150M which did not show any crack growth within the 28-mo. exposure.

b. Within 29 mo. in the inland industrial atmosphere crack growth initiated in only five alloys (17-7PH RH1050, PH15-7Mo RH950 and RH1050, 431 HT200 and AM355 SCT850 bar), and except in the case of 17-7PH RH1050 the amount of crack growth was slight even at 95%  $K_{Ic}$  (Appendix Table D-8). Estimates of  $K_{Isc}$  in this environment were about 50%  $K_{Ic}$  or above, but it is probable that SCC will start at lower  $K_{I1}$  values with continued exposure. It seems noteworthy that the five alloys and tempers just mentioned are the only ones that failed as smooth specimens in the seacoast atmosphere; only three of these failed as smooth specimens in the industrial atmosphere (PH15-7Mo RH950 and RH1050 and AM355 SCT850 bar (Tables XXV and XXVI)).

c. The performance of the various alloys and tempers in the 20% NaCl exposure was about the same as in the seacoast atmosphere except that there was a marked inconsistency in behavior of replicate specimens of the more resistant alloys (Figures 83-88). Although estimates of  $K_{Isc}$  for some of the alloys were handicapped because specimens were not exposed at low enough  $K_I$  values, closer estimates based on "crack-arrest" were possible in many instances (Figure 93).

d. Orientation of the test specimens had no appreciable effect on the SCC performance of the three alloys tested, just as in the case of the smooth specimens.

e. Both the crack-arrest and the crack-initiation procedures appear to be suitable for testing these steel alloys. Corrosion-product wedging did not appear to be a problem in tests extended at least to 2000 hr. The type of specimen shown in Figure 112 should be practical for steel alloys although tension precracking may not be feasible for some higher strength alloys, and side grooving to minimize crack branching should be considered.

f. Because the tests with precracked specimens gave a decidedly lower ranking for certain martensitic precipitation hardening alloys and tempers that showed a high threshold stress for initiation of SCC in a smooth surface, it appears to be essential that tests of both types be used to investigate the resistance to SCC of such alloys. It should be considered that for components of thin sections not involving discernible pre-existing flaws, the more optimistic smooth specimen test data would be more applicable. Henthorne<sup>(49)</sup> has cautioned that the use of  $K_{Isc}$  as a design criterion for martensitic precipitation hardening stainless steels (Custom 450, 455) is questionable in view of the probability that design factors in service could cause the corrosion aspect of cracking (e.g. generation of hydrogen in crevices) to dominate and produce cracking at lower stress intensities. The same concern should be given to the use of  $\sigma_{th}$  as a design criterion.

## D. Tests of Titanium 6Al-4V Alloy

### 1. Smooth Specimens

Both the beta-forged and the alpha-beta forged materials demonstrated a high threshold stress for initiation of SCC in a smooth surface, as indicated by the absence of failures under stress of 75% Y.S. during exposures of 12 mo. to 3.5% NaCl by alternate immersion and 28 mo. in seacoast and inland industrial atmospheres.

### 2. Precracked Specimens

a. The beta-forged material also showed high threshold stress intensity for initiation of SCC as indicated by absence of SCC in fatigue precracked specimens at a stress intensity of 75 and about 95%  $K_{Ic}$  during exposures of 27 mo. in seacoast and inland industrial atmospheres. Alpha-beta forged material, on the other hand, developed SCC at 75 and 50%  $K_{Ic}$  in the seacoast atmosphere but not in the industrial atmosphere.

b. Crack growth occurred in 3.5% NaCl solution for specimens from both the beta-forged and the alpha-beta forged materials at applied stress intensities of approximately 95%  $K_{Ic}$  and 75%  $K_{Ic}$  but not at 50%  $K_{Ic}$  (Figure 102). The SCC was very rapid, with all growth ceasing by the end of 2 to 2.5 hr. and not resuming during 5000 hr. subsequent exposure. During the short period of crack growth the average rate of propagation was 0.04 to 0.15 in./hr. for the beta forging and 0.14 to 0.24 in./hr. for the alpha-beta forging.

Table I

LIST OF MATERIALS AND SOURCES OF SUPPLY

Alloy	Manufactured Form	Source	As Received	Ultimate Temper	ARL sample no.
<u>Aluminum Alloys</u>					
2014	Rolled Plate 2-1/2" thick	Alcoa Mill	T651	T651	366335
2021	Rolled Plate 2-1/2" thick	ARL (1)	T81	T81	326400
2024	Rolled Plate 2-1/2" thick	Williams & Co., Pgh.	T351	T351	366206
2024	Rolled Plate 2-1/2" thick	Williams & Co., Pgh.	T351 (2)	T851	366207
2219	Rolled Plate 2" thick	ARL (1)	T37	T37	344793
2219	Rolled Plate 2" thick	ARL (1)	T37 (2)	T87	338148
7039	Rolled Plate 2-1/2" thick	ARL (1)	T6351	T6351	314758
7075	Rolled Plate 2-1/2" thick	Alcoa Mill	T651	T651	366259
7075	Rolled Plate 2-1/2" thick	Williams & Co., Pgh.	T651	T651	366209
6061	Rolled Plate 2-1/2" thick	Williams & Co., Pgh.	T651 (2)	T351	366210
5456	Rolled Plate 2-1/2" thick	Williams & Co., Pgh.	T651	T651	366208
5456	Rolled Plate 2-1/2" thick	Alcoa Mill	H117	H117	366656
2024	Rolled Plate 2-1/2" thick	Alcoa Mill	H321	(3)	366657
2024	Rolled Plate 2-1/2" thick	Williams & Co., Pgh.	T351	T351	366936
7075	Rolled Plate 2-1/2" thick	Williams & Co., Pgh.	T351 (2)	T851	366937
7075	Rolled Plate 2-1/2" thick	Williams & Co., Pgh.	T651	T651	366938
7075	Rolled Plate 2-1/2" thick	Williams & Co., Pgh.	T651 (2)	T751	366939
<u>Steel Alloys</u>					
17-7 PH	Rolled Bar 1-1/4" x 6"	Armco	R100	RH 1050	366665
PH 15 - 7 Mo	Rolled Bar 1-1/4" x 6"	Armco	R100	RH 950	366666
PH 15 - 7 Mo	Rolled Bar 1-1/4" x 6"	Armco	"A"	RH 1050	366666
5-5 PH (VAC-CE)	Rolled Bar 2-1/4" x 6"	Armco	"A"	H900	366668
15-5 PH (VAC-CE)	Rolled Bar 2-1/4" x 6"	Armco	H1150M	H1150M	366667
PH 13 - 8 Mo	Rolled Bar 2-1/4" x 6"	Armco	"A"	H950	366669
PH 13 - 8 Mo	Rolled Bar 2-1/4" x 6"	Armco	"A"	H1050	366669
431	Rolled Bar 2-1/4" x 6"	Armco	"A"	HT 125	366670
431	Rolled Bar 2-1/4" x 6"	Armco	"A"	HT 200	366670
AM 355	Rolled Plate 1-1/8" thick	MSFC (NASA)	"A"	PHSCT 850	366671
AM 355	Rolled Plate 1-1/8" thick	MSFC (NASA)	"A"	PHSCT 1000	366671
AM 355	Rolled Bar 2" x 6"	Allegheny-Luxium	"A"	PHSCT 850	366672
AM 355	Rolled Bar 2" x 6"	Allegheny-Luxium	"A"	PHSCT 1000	366673
<u>Titanium Alloy</u>					
6Al - 4V	β Forged Bar 2-1/4" x 6"	Alcoa Mill	Annealed	Annealed	366965
6Al - 4V	α-β Forged Bar 2-1/4" x 6"	Alcoa Mill	Annealed	Annealed	366966

Notes: (1) Plant fabricated and heat treated material available at Alcoa Research Laboratories from stock procured for another investigation.  
 (2) To be artificially aged to specified condition at Alcoa Research Laboratories.  
 (3) Stress corrosion susceptible temper produced by heating the plate at 300°F.

Table II

## CHEMICAL COMPOSITION OF ALUMINUM ALLOY FLATE

Alloy- Temper	S. No.	Thick. In.	Composition - Per Cent (1)													
			Si	Fe	Cu	Mn	Mg	Zn	Cr	Ni	Ti	Be	V	Sn	Zr	Cd
2014-T651	366335	2.5	0.93	0.52	4.21	0.83	0.51	0.07	0.01	0.01	0.05	0.000	---	---	---	---
2021-T81	326400	2.5	0.06	0.14	6.30	0.31	0.01	0.02	0.01	0.06	---	0.08	0.05	0.13	0.13	
2024-T351	366206	2.5	0.09	0.33	4.78	0.66	1.37	0.04	0.00	0.02	0.001	---	---	---	---	
2024-T351	366936	2.5	0.14	0.31	4.61	0.58	1.51	0.15	0.02	0.04	0.001	---	---	---	---	
2024-T851	366207	2.5	0.09	0.33	4.81	0.65	1.39	0.04	0.00	0.02	0.001	---	---	---	---	
2024-T851	366937	2.5	0.14	0.31	4.54	0.58	1.48	0.14	0.02	0.05	0.001	---	---	---	---	
2219-T37	344793	2.0	0.10	0.21	6.35	0.26	0.00	0.05	0.00	0.06	---	0.09	---	0.15	---	
2219-T87	338148	2.0	0.10	0.21	6.35	0.26	0.00	0.05	0.00	0.06	---	0.09	---	0.15	---	
5456- HL17	366656	2.5	0.12	0.28	0.06	0.78	5.40	0.05	0.10	0.03	0.000	---	---	---	---	
5456- Sens.	366657	2.5	0.12	0.28	0.06	0.78	5.40	0.05	0.10	0.03	0.000	---	---	---	---	
6061-T651	366208	2.5	0.69	0.35	0.26	0.04	1.01	0.04	0.19	0.05	0.000	---	---	---	---	
7039-T6351	314756	2.5	0.13	0.25	0.04	0.25	2.93	4.30	0.21	0.03	0.000	---	---	---	---	
7079-T651	366259	2.25	0.10	0.20	0.77	0.17	3.57	4.68	0.17	0.03	0.001	---	---	---	---	
7075-T651	366209	2.5	0.12	0.26	1.80	0.07	2.42	6.07	0.19	0.03	0.002	---	---	---	---	
7075-T651	366938	2.5	0.08	0.31	1.80	0.02	2.38	6.02	0.19	0.03	0.002	---	---	---	---	
7075-T7351	366210	2.5	0.12	0.26	1.82	0.07	2.41	6.09	0.19	0.03	0.002	---	---	---	---	
7075-T7351	366939	2.5	0.08	0.31	1.81	0.02	2.38	6.01	0.19	0.03	0.002	---	---	---	---	

Note: (1) Quantometric analysis on a remelted disc sample.

Table III

TYPICAL HEAT TREATMENT PRACTICES FOR ALUMINUM ALLOY PLATES(1)

<u>Alloy</u>	<u>Solution Heat Treatment</u>		<u>Precipitation Heat Treatment</u>		
	<u>Metal Temp. Deg. F</u>	<u>Temper Designation</u>	<u>Metal Temp. Deg. F</u>	<u>Time at Temp., Hrs.</u>	<u>Temper Designation</u>
2014	925-945	T451	320	18	T651
2021	975-995	T31	325	24	T81
2024	910-930	T351	375	12	T851
2219	985-1005	T37	350	18	T87
6061	960-1025	T451	320	18	T651
7039	840-860	W51	(2)	(2)	T6351
7079	820-875	W51	240	48	T651
7075	860-910	W51	250	24	T651
		W51	(3)	(3)	T7351

Notes: (1) Detailed information pertaining to heat treatment practices may be found in the following references:

- (a) Specification MIL-H-6088E, dated Feb. 5, 1971, Heat Treatment of Aluminum Alloys.
  - (b) Alcoa Green Letter No. 210, April, 1968, Alcoa Aluminum Alloy 2021.
- (2) Two stage treatment comprised of 8 hrs. at 225°F plus 16 hrs. at 300°F.
  - (3) Two stage treatment comprised of 6 hrs. at 225°F plus 8 hrs. at 350°F.

Table IV

## TENSILE PROPERTIES OF ALUMINUM ALLOY PLATES

Alloy-Temper	S. No.	Thick. In.	Longitudinal (1)		Long-Transverse (2)		Short-Transverse (1)				
			T.S. ksi	El. % in 4D	T.S. ksi	Y.S. (3) ksi	El. % in 4D	T.S. ksi	Y.S. (3) ksi	El. % in 4D	
2014-T651	336335	2.5	70.8	64.4	8.0	69.9	63.5	7.8	66.5	59.6	3.0
2021-T81	326400	2.5	68.3	57.8	10.5	68.8	59.5	4.8	68.6	59.1	5.0
2024-T351	366206	2.5	70.7	53.9	12.0	67.5	47.1	17.0	55.4	42.4	3.5
2024-T351	366936	2.5	-----	-----	-----	68.9	47.6	17.8	59.1	43.5	3.5
2024-T851	366207	2.5	67.2	60.0	8.0	68.6	62.2	7.5	63.9	61.8	1.0
2024-T851	366937	2.5	-----	-----	-----	70.4	64.4	7.0	65.1	62.3	1.0
2219-T37	344793	2.0	54.2	45.1	18.5	58.7	42.5	17.5	57.9	42.1	12.0
2219-T87	338148	2.0	69.2	56.7	12.5	71.6	58.2	9.5	69.1	57.7	5.5
5456-H117	366656	2.5	50.1	39.1	17.0	49.5	33.5	16.5	44.1	30.3	9.0
5456-Sens.	366657	2.5	50.0	31.7	17.5	49.2	29.5	18.2	43.7	28.4	9.0
6061-T651	366208	2.5	43.2	41.5	17.0	45.7	45.4	11.5	46.8	41.6	12.0
7039-T6351	314758	2.5	67.2	57.6	12.0	64.4	55.1	12.0	62.6	54.2	6.0
7079-T651	366259	2.25	82.7	75.6	11.0	78.9	70.1	12.8	77.2	66.6	5.5
7075-T651	366209	2.5	85.6	77.2	10.0	81.9	71.9	8.5	75.3	66.7	2.0
7075-T651	366938	2.5	-----	-----	-----	80.2	71.7	8.0	74.8	66.6	2.0
7075-T7351	366210	2.5	70.6	59.6	11.0	69.7	58.6	10.0	65.0	55.1	4.0
7075-T7351	366339	2.5	-----	-----	-----	68.0	56.6	9.5	65.0	54.4	4.0

Notes: (1) Duplicate 0.125-in. dia. specimens centered in plate thickness.  
(2) Duplicate 0.500-in. dia. specimens taken at quarter-plane per ASTM Standards.  
(3) Offset equal to 0.2 per cent.

Table V

## CHEMICAL COMPOSITION OF STEEL ALLOY PRODUCTS

Alloy	Product	S. No.	Source (1.)	Composition - Per Cent													
				C	Mn	P	S	Si	Cr	Ni	Mo	Ta	Al	Cu	Cb	N	
17-7 PH	1-1/4" x 6" Bar	366665	Cast Bar	0.065	0.64	0.017	0.010	0.31	16.98	7.20	---	---	---	---	---	---	---
				0.076	0.66	0.018	0.011	0.37	17.04	7.03	---	---	1.33	---	---	---	---
15-7 Mo	1-1/4" x 6" Bar	366666	Cast Bar	0.065	0.68	0.022	0.010	0.36	15.22	7.28	2.30	---	---	---	---	---	---
				0.080	0.68	0.021	0.010	0.39	15.25	7.10	2.36	---	1.22	---	---	---	---
15-5 PH (H1150M)	2-1/4" x 6" Bar	366667	Cast Bar	0.037	0.28	0.017	0.009	0.35	15.13	4.50	---	---	---	---	---	---	---
				0.050	0.24	0.012	0.010	0.39	15.35	4.64	---	0.01	---	3.38	0.27	---	---
15-5 PH	2-1/4" x 6" Bar	366668	Cast Bar	0.037	0.28	0.017	0.009	0.35	15.13	4.50	---	---	---	---	---	---	---
				0.050	0.23	0.012	0.009	0.40	15.35	4.67	---	0.01	---	3.38	0.27	---	---
PH13-8 Mo	2-1/4" x 6" Bar	366669	Cast Bar	0.045	0.01	0.002	0.003	0.01	12.76	8.20	2.13	---	---	---	---	---	0.004
				0.035	0.01	0.003	0.003	0.015	12.90	7.87	2.18	---	0.91	---	---	---	---
431	2-1/4" x 6" Bar	366670	Cast Bar	0.16	0.48	0.018	0.009	0.48	16.19	2.49	---	---	---	---	---	---	0.048
				0.13	0.51	0.019	0.010	0.48	16.25	2.51	---	---	---	---	---	---	---
AM55	1-1/8" Plate	366671	Plate	0.10	0.84	0.020	0.010	0.23	15.83	4.07	2.72	---	---	---	---	0.080	
AM55	2" x 6" Bar	366673	Cast Bar	0.11	0.87	0.020	0.015	0.20	15.14	4.23	2.89	---	---	---	---	---	0.037
				0.10	0.75	0.020	0.010	0.23	15.50	4.12	2.81	---	---	---	---	---	---

NOTE: (1) Cast analyses furnished by the manufacturer; product analyses were made by the Spectrochemical Laboratories, Inc. of Pittsburgh, Pennsylvania.

Table VI

## HEAT TREATMENT PRACTICES USED FOR THE STEEL ALLOY PRODUCTS

Alloy	As Received	Heat Treatment(1)	Precipitation Treatment(2)	Ultimate Temper
A. Specimens Finish Machined In As-Received Condition				
17-7 PH	R100	-----	Aged at ARL to Final Temper(3)	RH 1050
PH15-7 Mo	R100	-----	1 hr./1050°F 1 hr./950°F 1 hr./1050°F	RH 950 RH 1050
15-5 PH	Condition A	-----	1 hr./900°F	H900
PH13-8 Mo	Condition A	-----	4 hr./950°F 4 hr./1050°F	H950 H1050
B. Sawed Blanks				
431	Condition A	Heat Treated And Aged to Ultimate Temper By Allegheny Inalum Research Center	2 hr./1175°F 2 hr./525-575°F, air-cooled to R.T., retempered 2 hr./525-575°F	HT 125 HT 200
C. Sawed Blanks				
AM 355	Annealed Plate	Heat Treated By Allegheny Inalum Research Center → Machined → Aged To Ultimate Temper By Allegheny Inalum Research Center(3)	3 hr./850°F 3 hr./1000°F	SCT 850 SCT 1000
	CS, E, + OF Bar (Condition A)	1-3 hr./1900°F, water quenched, soaked 3 hr./-100°F; 10 min.-1 hr./1750°F, water quenched, soaked 3 hr./-100°F 10 min.-1 hr./1750°F, water quenched, soaked 3 hr./-100°F	3 hr./850°F 3 hr./1000°F	SCT 850 SCT 1000
D. Typical Thermal Treatment (Sample Received in Ultimate Temper)				
15-5 PH	H1150 M	30 min./1900°F, oil quench or air cool	2 hr./1400°F, air cool to R.T., retemper 4 hr./1150°F	H1150 M

- Notes: (1) All heat treated samples held for unspecified intervals at room temperature prior to precipitation treatment.  
(2) All samples air-cooled to room temperature subsequent to precipitation treatment.  
(3) Oxide film removed by polishing tensile bars with fine aloxite cloth, and grinding compacts to size with fine carborundum wheel.

Table VII

## TENSILE PROPERTIES FOR HIGH STRENGTH STEEL ALLOY ROLLED BAR AND PLATE

Alloy	Product	S. No.	Condition	Tensile Properties (1)														
				Longitudinal			Long Transverse			Short Transverse								
				T.S. ksi	Y.S.(2) ksi	El. % in 4D	T.S. ksi	Y.S.(2) ksi	El. % in 4D	T.S. ksi	Y.S.(2) ksi	El. % in 4D						
17-7PH	1-1/4" x 6" Bar	366665	RH1050	---	---	---	208.7	190.5	10.0	---	---	---	---	---	---	---	---	---
PH15-7MO	1-1/4" x 6" Bar	366666	RH950	---	---	---	223.4	203.5	3.0	---	---	---	---	---	---	---	---	---
PH15-7MO	1-1/4" x 6" Bar	366666	RH1050	---	---	---	210.3	195.0	8.0	---	---	---	---	---	---	---	---	---
15-5PH	2-1/4" x 6" Bar	366668	H900	---	---	---	192.7	171.2	14.0	---	---	---	---	---	---	---	---	---
15-5PH	2-1/4" x 6" Bar	366667	H1150M	---	---	---	131.4	93.1	24.0	---	---	---	---	---	---	---	---	---
PH13-8MO	2-1/4" x 6" Bar	366669	H950	224.2	201.6	14.0	224.6	196.7	14.0	225.0	203.3	11.0	---	---	---	---	---	---
PH13-8MO	2-1/4" x 6" Bar	366669	H1050	189.8	171.6	18.0	192.1	178.5	18.0	190.9	175.5	14.0	---	---	---	---	---	---
431	2-1/4" x 6" Bar	366670	HT200	222.9	165.5	18.0	222.3	165.4	9.0	215.4	153.7	7.0	---	---	---	---	---	---
431	2-1/4" x 6" Bar	366670	HT125	133.2	103.7	19.0	136.3	107.4	14.0	133.8	105.0	10.0	---	---	---	---	---	---
AM355	1-1/8" Th. Plate	366671	SCT850	---	---	---	219.0	152.5(3)	16.0	---	---	---	---	---	---	---	---	---
AM355	1-1/8" Th. Plate	366671	SCT1000	---	---	---	184.5	169.7	20.0	---	---	---	---	---	---	---	---	---
AM355	2" x 6" Bar	366673	SCT850	224.1	186.1	20.0	225.3	190.3	15.0	226.9	186.6	8.0	---	---	---	---	---	---
AM355	2" x 6" Bar	366673	SCT1000	185.2	163.7	20.0	192.7	172.4	18.0	189.3	171.2	10.0	---	---	---	---	---	---

Note: (1) Results are average of duplicate 0.125" dia. tensile bars from center of bar or plate thickness.

(2) Offset equal to 3.2 per cent.

(3) Anomalous test result; a value of about 180 would be expected.

TABLE VIII

CHEMICAL COMPOSITION(1) AND TENSILE PROPERTIES OF  
TITANIUM 6 AL - 4 V ALLOY FORGED 2 1/4" x  
6" BARS

Forging Condition	S. No.	Longitudinal(2)			Long-Transverse(2)			Short-Transverse(2)		
		T.S. ksi	Y.S.(3) ksi	El. % in 4D	T.S. ksi	Y.S.(3) ksi	El. % in 4D	T.S. ksi	Y.S.(3) ksi	El. % in 4D
Beta-Forged	366965	146.3	134.8	18.8	147.8	137.6	10.9	140.3	118.9	14.1
		135.2	122.1	17.2	138.7	122.9	14.1	141.5	122.1	14.1
		146.0	133.6	17.2	153.2	144.1	15.6	136.3	122.1	12.5
	Avg.	142.5	130.2	17.7	146.6	134.9	13.5	139.4	121.0	13.6
Alpha-Beta Forged	366966	147.1	135.8	18.8	154.7	145.8	17.2	148.8	138.2	14.1
		144.0	134.3	18.8	154.2	139.1	17.2	145.8	132.6	14.1
		149.5	138.8	18.8	158.7	149.8	15.6	146.3	135.0	14.1
	Avg.	146.9	136.3	18.8	155.9	144.9	16.7	147.0	135.3	14.1

Notes: (1) Composition of ingot from which both forgings were made:

0.012% C, 0.17% Fe, 0.011% N, 6.3% Al, 3.9% V, 0.0075% Ti, 0.0075% H, 0.19% O.

Hydrogen content was 0.004% (35-38 ppm) in both forged bars.

(2) 0.160 inch diameter specimens removed near the center of the bar.

(3) Offset equal to 0.2 per cent.

Table IX

RESULTS OF PLANE-STRAIN FRACTURE TOUGHNESS TESTS OF LONGITUDINAL (L-T)  
AND SHORT-TRANSVERSE (S-L) COMPACT TENSION SPECIMENS FROM ALUMINUM ALLOY PLATE

Alloy-Temper	S. No.	Plate Thick. In.	Longitudinal (L-T)				Valid K <sub>IC</sub>	Short-Transverse (S-L)				Valid K <sub>IC</sub>
			Specimen Thick. In.	Load P <sub>Q</sub> lb.	Crack Length In.	K <sub>Q</sub> ksi√in.		Specimen Thick. In.	Load P <sub>Q</sub> lb.	Crack Length In.	K <sub>Q</sub> ksi√in.	
2014-T651	366335	2.5	1.00	3650	0.97	23.6	Yes	1.00	2500	1.050	18.3	Yes
			1.00	3560	0.97	23.4	Yes	1.00	2470	1.035	19.1	Yes
					Avg.				Avg.	18.7		
2021-T81	366400	2.5	1.00	5050	0.94	31.4	Yes (1)	1.00	2990	0.965	19.3	Yes
			1.00	4840	0.96	30.8	Yes (1)	1.00	3140	0.956	19.9	Yes
					Avg.				Avg.	19.6		
2024-T351	366206	2.5	1.00	4120	1.03	29.2	Yes (1)	1.00	3050	1.087	22.1	Yes
			1.00	4450	0.99	30.0	Yes	1.00	3360	0.933	20.0	Yes
					Avg.				Avg.	21.0		
2024-T851	366207	2.5	1.00	3490	1.01	23.9	Yes	1.00	2430	1.014	16.8	Yes
			1.00	3650	0.96	22.7	Yes (1)	1.00	2490	0.990	16.6	Yes
					Avg.				Avg.	16.7		
2219-T37	344793	2.0	0.75	2820	0.76	29.8	No (2)	0.75	2310	0.817	27.6	No (2)
			0.75	2460	0.79	27.8	No (2)	0.75	2160	0.832	26.6	No (2)
					Avg.				Avg.	27.1		
2219-T87	338148	2.0	1.00	3860	1.00	26.3	Yes	0.75	1860	0.752	19.4	Yes
			1.00	3680	1.01	25.4	Yes	0.75	1690	0.758	19.9	Yes
					Avg.				Avg.	19.6		
5456-H117	366656	2.5	1.00	3510	1.02	24.7	No (3)	1.00	3270	0.995	22.0	No (2)
			1.00	3100	1.04	22.3	No (3)	1.00	2950	1.050	21.6	No (2)
					Avg.				Avg.	21.8		
5456-Sens.	366657	2.5	1.00	3000	1.05	21.9	No (3)	1.00	3400	0.965	21.9	No (2)
			1.00	2890	1.05	21.3	No (3)	1.00	3250	0.962	20.8	No (2)
					Avg.				Avg.	21.4		
6061-T651	366208	2.5	1.00	5320	0.98	35.1	No (2)	1.00	3450	0.930	21.2	Yes
			1.00	5120	0.95	32.2	No (2)	1.00	3440	0.951	21.7	Yes
					Avg.				Avg.	21.4		
7039-T6351	314758	2.5	1.00	3850	1.02	27.2	Yes (1)	1.00	3230	0.950	20.3	Yes
			1.00	3770	1.04	27.2	Yes (1)	1.00	2720	1.070	20.5	Yes
					Avg.				Avg.	20.4		
7075-T651	366209	2.5	1.00	4250	0.97	27.8	Yes	1.00	2670	1.063	19.4	Yes
			1.00	4220	0.98	27.8	Yes	1.00	2810	1.007	19.7	Yes
					Avg.				Avg.	19.5		
7075-T7351	366210	2.5	1.00	4540	0.97	29.6	Yes (1)	1.00	3030	1.035	21.6	Yes
			1.00	4450	0.97	29.6	Yes	1.00	3070	0.994	20.5	Yes
					Avg.				Avg.	21.0		
7079-T651	366259	2.25	1.00	3610	1.03	25.6	Yes (1)	1.00	2560	1.068	19.3	Yes
			1.00	3780	1.03	26.9	Yes (1)	1.00	2440	1.088	19.0	Yes
					Avg.				Avg.	19.1		

NOTES: (1) Considered meaningful and useful, although not technically valid according to ASTM criteria.  
(2) Not valid for K<sub>IC</sub>. Did not meet ASTM criteria for specimen thickness or plastic deformation of the specimen.  
(3) Technically valid according to ASTM criteria, but these values appear to be low.

TABLE X

RESULTS OF PLANE-STRAIN FRACTURE TOUGHNESS TESTS OF LONGITUDINAL (L-T)  
 COMPACT TENSION SPECIMENS FROM 2.0-IN. THICK 2219 ALUMINUM ALLOY PLATE

Alloy & Temper	S. No.	Nominal Specimen Thickness In.	Load, lb.	Crack Length, In.	K <sub>Q</sub> ksi.in.	Valid K <sub>IC</sub> Value
2219-T37	344793	0.75	2740	0.762	29.1	No (1)
			2520	0.792	28.5	No (1)
			2820	0.76	29.8	No (1)
			2460	0.79	27.8	No (1)
2219-T87	338148	1.00	4760	0.953	30.0	No (1)
			4400	1.023	30.7	No (1)
			14500	2.076	37.0	No (1)
2219-T87	338148	2.00	15000	2.049	37.5	No (1)
			14700	2.047	36.7	No (1)
			2460	0.766	26.4	Yes
2219-T87	338148	0.75	2460	0.754	25.8	Yes
			3910	0.975	25.5	Yes
			3860	1.00	26.3	Yes
2219-T87	338148	1.00	3680	1.01	25.4	Yes
			11100	2.044	27.7	Yes
			11000	2.039	27.5	Yes
2219-T87	338148	2.00	11400	1.998	27.4	Yes

Note: (1) Not valid for K<sub>IC</sub>. Specimen did not meet ASTM criteria for specimen thickness or plastic deformation of the specimen.





Table XII

RESULTS OF FRACTURE TOUGHNESS TESTS OF LONG-TRANSVERSE (T-L) COMPACT TENSION SPECIMENS OF TITANIUM - 6AL-4V ALLOY HAND FORGINGS

	0.5" Thick			1.0" Thick			1.5" Thick					
	Load P <sub>Q</sub> lb.	Crack Length, In.	K <sub>Q</sub> ksi √In.	Valid K <sub>IC</sub>	Load P <sub>Q</sub> lb.	Crack Length, In.	K <sub>Q</sub> ksi √In.	Valid K <sub>IC</sub>	Load P <sub>Q</sub> lb.	Crack Length, In.	K <sub>Q</sub> ksi √In.	Valid K <sub>IC</sub>
Beta Forged S. No. 366965	1360	0.532	28.7	Yes	6350	1.038	45.5	Yes	10,500	1.471	37.8	Yes
	1470	0.512	29.2	Yes	6425	1.046	46.8	Yes				
		AVG.	28.9		5425	1.058	40.2	Yes				
						AVG.	44.2					
Alpha-Beta Forged S. No. 366966	1620	0.521	33.0	Yes	5150	1.065	38.6	Yes	8,200	1.556	32.2	Yes
	1560	0.518	31.7	Yes	4760	1.071	36.0	Yes				
		AVG.	32.3		4600	1.074	34.9	Yes				
						AVG.	36.5					

TABLE XIII

ALUMINUM ALLOY SMOOTH TENSILE SPECIMENS SCHEDULED FOR 4 YEARS EXPOSURE TO SEACOAST ATMOSPHERE AT POINT JUDITH, RHODE ISLAND (EXPOSURE STARTED SEPTEMBER 22, 1969)

Alloy	Longitudinal Specimens			Str. 754 Y.S.			Short-Transverse Specimens		
	Str. ksi	Spec.	Days	Str. ksi	Spec.	Days	Str. 27 ksi	Spec.	Days
5456-H117	L10	29		N18	23			N21	
	L11			N19				N22	
	L12			N20				N23	
6061-T651	L10	31		N15				N18	
	L11			N16				N19	
	L12			N17				N20	
7075-T7351	L10	45		N15	41				
	L11			N16					
	L12			N17					
2219-T87	L10	43		N15	43				
	L11			N16					
	L12			N17					
2021-T81	L10	43		N15	44				
	L11			N16					
	L12			N17					
2024-T851	L10	45		N15	46	35			
	L11			N16		304			
	L12			N17					
Alloys With Low Resistance to Stress-Corrosion Cracking									
2014-T651	L10	48		N18	45	35			
	L11			N19		35			
	L12			N20		FIT			
2024-T351	L10	40		N18	32	35			
	L11			N19		35			
	L12			N20		35			
2219-T37	L10	34		N18	32	35			
	L11			N19		35			
	L12			N20		35			
7075-T651	L10	58		N18	50	35			
	L11			N19		35			
	L12			N20		35			
7039-T6351	L10	43		N18	41	FIT			
	L11			N19		FIT			
	L12			N20		FIT			
7079-T651	L10	57		N18	50	FIT			
	L11			N19		FIT			
	L12			N20		35			
5456-Sens.	L10	24		N15	21	35			
	L11			N16		35			
	L12			N17		35			

Notes: (1) In addition to the stressed specimens, duplicate unstressed specimens (L8, L9 and either N13, N14 or N16, N17) were exposed for each alloy-temper.  
 (2) Removed because of severe exfoliation.  
 (3) Unstressed specimens L8 and L9 also removed because of severe exfoliation 631 days.  
 (4) Unstressed specimens N16, N17 also removed because of severe corrosion 631 days.  
 (5) Removed September 15, 1971, for a stress check; strains were erratic and low indicating that during original shipment of the stressed specimens to Pt. Judith vibrations caused relaxation of the stressing frames. The specimens were restressed to 10 ksi and re-exposed November 15, 1971.

FIT = Failed in Transit - not exposed.

TABLE XIV

ALUMINUM ALLOY SMOOTH TENSILE SPECIMENS SCHEDULED FOR 4 YEARS EXPOSURE TO INDUSTRIAL ATMOSPHERE AT NEW KENSINGTON, PA. (EXPOSURE STARTED MAY 29, 1959)

Alloy	Longitudinal Specimens			Alloys With High Resistance to Stress-Corrosion Cracking			Short-Transverse Specimens			
	Str., ksi	Str., 75% Y.S. Spec.	Days	Str., ksi	Str., 75% Y.S. Spec.	Days	Str., 27 ksi Spec.	Str., 20 ksi Spec.	Str., 10 ksi Spec.	Days
5456-H117	29	L15		2.	N29	--	--	N32	--	--
		L16			N30	--	--	N33	--	--
		L17			N31	--	--	N34	--	--
6061-T651	31	L15		31	N23	--	--	N26	--	--
		L16			N24	--	--	N27	--	--
		L17			N25	--	--	N28	--	--
7075-T7351	45	L15		41	N23	N26	--	--	--	--
		L16			N24	N27	--	--	--	--
		L17			N25	N28	--	--	--	--
2219-T87	43	L15		43	N23	N26	--	--	--	--
		L16			N24	N27	--	--	--	--
		L17			N25	N28	--	--	--	--
2021-T81	43	L15		44	N23	N26	--	--	--	--
		L16			N24	N27	--	--	--	--
		L17			N25	N28	--	--	--	--
2024-T851	45	L15		46	N23	N26	--	--	--	--
		L16			N24	N27	--	--	--	--
		L17			N25	N28	--	--	--	--
2014-T651	48	L15		45	N29	134	N32	215	N35	249
		L16			N30	75	N33	202	N36	253
		L17			N31	29	N34	222	N37	253
2024-T351	40	L15		32	N29	19	N32	103	N35	249
		L16			N30	26	N33	75	N36	253
		L17			N31	29	N34	22	N37	253
2219-T37	34	L15		32	N29	34	N32	64	N35	249
		L16			N30	29	N33	64	N36	253
		L17			N31	34	N34	69	N37	253
7075-T651	58	L15		50	N29	43	N32	98	N35	1020
		L16			N30	22	N33	98	N36	347
		L17			N31	40	N34	113	N37	103
7039-T6351	43	L15		41	N29	6	N32	19	N35	615
		L16			N30	34	N33	6	N36	579
		L17			N31	11	N34	11	N37	103
7079-T651	57	L15		50	N29	13	N32	63	N35	615
		L16			N30	11	N33	34	N36	356
		L17			N31	19	N34	57	N37	326
5456-Sens.	24	L15		21	N23	163	--	--	N26	83
		L16			N24	83	--	--	N27	83
		L17			N25	83	--	--	N28	83

Notes: (1) In addition to the stressed specimens, duplicate unstressed specimens (L13, L14 and either N21, N22 or N27, N28) were exposed for each alloy-temper.

TABLE XV

PER CENT LOSSES IN TENSILE STRENGTH FROM CORROSION OF 0.125" DIAMETER TENSILE SPECIMENS EXPOSED 84 DAYS TO 3.5% NaCl BY ALTERNATE IMMERSION

		Longitudinal				Short Transverse			
Alloy	Temper	No Stress	Str. 75% Y.S.	No Stress	Str. 75% Y.S.	Str. 27 ksi	Str. 20 ksi	Str. 10 ksi	
<u>Alloys With High Resistance to Stress-Corrosion Cracking</u>									
5456	H17	0	0	0	0	--	0	--	
6061	T651	0	0	5	26 (6)	--	12	--	
7075	T7351	9	8	22	45 (7)	42 (7)	--	--	
2219	T87	18	18	47	51 (7)	42	--	--	
2021	T81	16	18	35 (1)	48 (3)	45	--	--	
2024	T851	15	14	42 (1)	35 (4)	42 (2)	--	--	
<u>Alloys With Low Resistance to Stress-Corrosion Cracking</u>									
2014	T651	15	24	37 (1)	SCC	SCC	--	50	
2024	T351	26	33	54 (1)	SCC	SCC	--	SCC	
2219	T37	43	53	70 (1)	SCC	SCC	--	SCC	
7075	T651	10	15	19 (1)	SCC	SCC	--	SCC	
7039	T6351	0	0	28 (1)	SCC	SCC	--	24	
7079	T651	5	7	13 (1)	SCC	SCC	--	19 (2)	
5456	Sens.	0	0	(5)	SCC	--	SCC	--	

## Notes:

- (1) Tensile tested after only 30 days of exposure
- (2) Data for two specimens
- (3) Data for one specimen tested after 29 days
- (4) Data for one specimen tested after 13 days
- (5) Severely corroded specimens broke while dismantling after exposure
- (6) Severe localized corrosion.
- (7) Transgranular cracks emanating from pits.

TABLE XVI

NUMBER FAILURES/NUMBER EXPOSED (F/N) AND DAYS TO FAILURE 0.125" DIAMETER SHORT-TRANSVERSE TENSILE SPECIMENS EXPOSED 84 DAYS TO 3.5% NaCl BY ALTERNATE IMMERSION

Alloy	Temper	Str. 75% Y.S.		Str. 27 ksi		Str. 20 ksi		Str. 10 ksi		
		Str. ksi	F/N	Days	F/N	Days	F/N	Days	F/N	Days
<u>Alloys With High Resistance to Stress-Corrosion Cracking</u>										
5456	H117	23	0/5	5 OK 84	---	---	0/3	3 OK 84	---	---
6061	T651	31	0/5	5 OK 84	---	---	0/3	3 OK 84	---	---
7075	T1351	41	1/5	80(t), 4 OK 84	0/3	3 OK 84	---	---	---	---
2219	T87	43	2/5	42, 76, (t), 3 OK 84	0/3	3 OK 84	---	---	---	---
2021	T81	44	3/5	14, 16, 29, (t) (*)	0/3	3 OK 84	---	---	---	---
2024	T851	46	3/5	4, 8, 13, (i) (*)	1/3	17(t), 2 OK 84	---	---	---	---
<u>Alloys With Low Resistance to Stress-Corrosion Cracking</u>										
2014	T651	45	5/5	1, 1, 1, 1, 1	3/3	1, 1, 1	---	---	1/3	84, 2 OK 84
2024	T351	32	3/5	4, 4, 4 (*)	3/3	1, 4, 4	---	---	3/3	4, 7, 13
2219	T37	32	5/5	1, 1, 1, 1, 1	3/3	1, 1, 1	---	---	3/3	1, 1, 1
7075	T651	50	5/5	4, 4, 4, 4, 4	3/3	4, 4, 4	---	---	3/3	12, 12, 12
7039	T6351	41	5/5	7, 7, 7, 7, 9	3/3	9, 84, 84	---	---	0/3	3 OK 84
7079	T651	50	5/5	4, 4, 4, 4, 4	3/3	4, 4, 4	---	---	1/3	5, 2 OK 84
5456	Sens.	21	5/5	1, 1, 2, 2, 2	---	---	3/3	1, 1, 2	---	---

Notes: (\*) The remaining two specimens removed from test at the time of the third failure.

(t) Failures examined metallographically, results indicated failures most likely occurred by tensile overload from reduction in cross section area and not by stress-corrosion cracking.

(i) Failures examined metallographically, results indicated failures occurred by stress-corrosion cracking.

Table XVII

RESULTS OF STRESS CORROSION TESTS OF 0.125" DIAMETER SHORT TRANSVERSE TENSILE SPECIMENS CONTINUOUSLY IMMersed IN SODIUM CHLORIDE-DICHROMATE-ACETATE SOLUTION FOR 90 DAYS

Alloy & Temper	75% Y.S.		27 ksi		20 ksi		10 ksi	
	F/N(I)	Days	F/N	Days	F/N	Days	F/N	Days
Alloys With High Resistance to Stress-Corrosion Cracking								
5456-EL17	0/3	OK 90	---	---	0/3	OK 90	---	---
6061-T651	0/3	OK 90	---	---	0/3	OK 90	---	---
7075-T7351	1/3	61(3), 20K 90	0/3	OK 90	---	---	---	---
2219-T87	0/3	OK 90	0/3	OK 90	---	---	---	---
2021-T81	0/3	OK 90	0/3	OK 90	---	---	---	---
2024-T851	0/3	OK 90	0/3	OK 90	---	---	---	---
Alloys With Low Resistance to Stress-Corrosion Cracking								
2014-T651	0/3	OK 90	0/3	OK 90	---	---	0/3	OK 90
2024-T351	0/3	OK 90	0/3	OK 90	---	---	0/3	OK 90
2219-T37	0/3	OK 90	1/3	90(2), 2 OK 90	---	---	0/3	OK 90
7075-T651	3/3	29, 90(2), 90(2)	1/3	90(2), 2 OK 90	---	---	0/3	OK 90
7039-T6351	3/3	4, 4, 4	2/3	16, 43, 1 OK 90	---	---	0/3	OK 90
7079-T651	3/3	50, 69, 90(2)	3/3	50, 61, 90(2)	---	---	0/3	OK 90
5456-Sens.	3/3	2, 2, 2	---	---	3/3	2, 2, 2	3/3	2, 2, 9

- Notes: (1) F/N denotes the number of specimens that have failed over the number of specimens exposed.  
 (2) Specimen was found to be broken under the protective coating upon disassembly of stressing frame. Exact data of failure is not known.  
 (3) Metallographic examination revealed a mixed mode crack and a large pit associated with the fracture.

Table XVIII

LONGITUDINAL (L-T) COMPACT TENSION SPECIMENS OF ALUMINUM  
ALLOYS EXPOSED TO SALT-DICHROMATE-ACETATE SOLUTION

Alloy	Hours Exposure	K <sub>I</sub> Values as % K <sub>Ic</sub>			Visual Crack Growth, In.	
		K <sub>Ix</sub> (1)	K <sub>I1</sub> --	K <sub>I2</sub> --	Surface	Fracture (5)
<u>Alloys With High Resistance to Stress-Corrosion Cracking</u>						
5456-H117	2184	112(2)	95	73,80	No	No
6061-T651	2184	81(2)	95	80,82	No	No
7075-T7351	2184	91	95	68,86	No	No
2219-T87	2184	90	95	82,83	No	~0.02
2021-T81	2184	88(2)	95	92,92	No	~0.02
2024-T851	2184	97	95	76,88	No	~0.15
<u>Alloys With Low Resistance to Stress-Corrosion Cracking</u>						
2014-T651	2328	(4)	95	83,87	0.04	0.04
	2328		75	70	0.02	0.01
2024-T351	2328	(4)	95	80,81	0.04	0.04
	2328		75	67	0.01	0.01
2219-T37	528(3)	95(2)	95	76	0.14	0.06
	528(3)		75	54	0.14	(4)
7075-T651	1008(3)	(4)	95	73,80	0.02	0.00
	1008(3)		75	62	0.01	0.00
7039-T6351	2304	98	95	80,84	0.01	0.02
	2304		75	63	0.00	0.02
7079-T651	2304	(4)	95	79,82	0.01	0.00
	2304		75	59	0.00	0.00
5456-Sens.	1008(3)	113(2)	95	71,72	0.01	0.02
			75	57	0.00	0.02

## Notes:

- (1) Tested in air after exposure with no applied load.
- (2) Not valid per E399 criteria for K<sub>Ic</sub>.
- (3) Exposure discontinued because of severe exfoliation.
- (4) Not determined.
- (5) Not including lengths of cracks perpendicular to plane of precrack in specimens of low resistance alloys (Figure 29).

Table XIX

SHORT-TRANSVERSE (S-L) COMPACT TENSION SPECIMENS OF HIGH RESISTANCE ALUMINUM ALLOYS EXPOSED TO VARIOUS ENVIRONMENTS

Alloy	Exposed At No Load		Incubation Time (1), Mo.	Initial Crack Growth (1)		Exposed At Load 95% K <sub>IC</sub>		K <sub>IC</sub> (% K <sub>IC</sub> )	Avg. Velocity Interior In./Hr.	SUCCESS
	Mo.	K <sub>IC</sub> (% K <sub>IC</sub> )		Surface In.	Mo.	AVG. Velocity In./Hr.	No.			
<u>Seacoast Atmosphere (8 Mo.)</u>										
5456-H117	16	104(2)	>24	---	---	---	0	0.05, 0.09	2, 18 X 10 <sup>-6</sup>	NO
6061-T651	18	110	>24	---	---	---	0	0, 0	---	NO
7075-T7351	18	97	3, 21 (4)	7, 3	6, 30 X 10 <sup>-6</sup>	8	0	0.04, 0.06	9 X 10 <sup>-6</sup>	Yes
2219-T67	18	94	3, 8 (5)	5, 7	5, 10 X 10 <sup>-6</sup>	8	0.01, 0	0.04, ---	7 X 10 <sup>-6</sup>	NO
2021-T81	18	106	3	5	15 X 10 <sup>-6</sup>	8	0.06, 0.06	0.06, 0.08	12 X 10 <sup>-6</sup>	NO
2024-T851	18	101	3	5	9 X 10 <sup>-6</sup>	8	0.07, 0.01	0.04, 0.04	7 X 10 <sup>-6</sup>	NO
<u>Industrial Atmosphere (12 Mo.)</u>										
5456-H117	15	(103) <sup>2</sup>	>26	---	---	12	0	0	---	NO
6061-T651	28	99	>28	---	---	12	0	0	---	NO
7075-T7351	28	95	>28	---	---	12	0	0	---	NO
2219-T67	28	91	>28	---	---	12	0	~0.05	6 X 10 <sup>-6</sup>	NO
2021-T81	28	106	>28	---	---	12	0	~0.05	6 X 10 <sup>-6</sup>	NO
2024-T851	28	100	>28	---	---	12	0	~0.07	5 X 10 <sup>-6</sup>	NO
<u>Salt-Dichromate-Acetate Solution (2000 Hr.)</u>										
5456-H117	3	100(2)	>3	---	---	3	0	0	---	NO
6061-T651	3	95	1, 5	0.5	2.5 X 10 <sup>-5</sup>	3	0	0.08, 0.07	3 X 10 <sup>-5</sup>	NO
7075-T7351	3	88	0.2	0.5	2.5 X 10 <sup>-4</sup>	3	0.02	0.05, 0.05	2 X 10 <sup>-5</sup>	Yes
2219-T67	3	101	2	0.2	6 X 10 <sup>-5</sup>	3	0.10	0.10, 0.06	4 X 10 <sup>-5</sup>	NO
2021-T81	3	104	1	0.5	2.5 X 10 <sup>-4</sup>	3	0.05	0.08, 0.08	4 X 10 <sup>-5</sup>	NO
2024-T851	3	96	1	0.5	2.5 X 10 <sup>-4</sup>	3	0.14	0.08, 0.08	4 X 10 <sup>-5</sup>	Yes

Notes: (1) Average crack extension visible on surfaces of specimen.

(2) Not valid per ASTM E199 criteria for K<sub>IC</sub>.

(3) Established on basis of metallographic examination of unbroken specimens removed from test after 15 mo. at seacoast, 18 mo. in industrial atmosphere and 3 mo. in salt-dichromate-acetate solution.

(4) In one specimen crack extension occurred between 8 and 15 mo., and between 21 and 24 mo. In another; the other two removed at 8 mo. showed no crack growth.

(5) In one specimen crack extension occurred between 3 and 8 mo., and between 8 and 15 mo. In another; the other two showed no crack growth at 8 mo. (removed) or at 24 mo.

Table XX

ENVIRONMENTAL CRACK VELOCITY IN ALUMINUM ALLOYS EXPOSED TO VARIOUS ENVIRONMENTS  
SHORT-TRANSVERSE (S-L) BOEING DCB SPECIMENS BOLT LOADED TO POP-IN

Alloy	Average Initial Crack Velocity - In./Er.			3.5% NaCl Dropwise
	Outdoor Atmosphere (2)	Salt-Dichromate-Acetate Solution	Industrial	
<u>Alloys With High Resistance to Stress-Corrosion Cracking</u>				
5456-H117	0	8 x 10 <sup>-5</sup> (1)	0	6 x 10 <sup>-5</sup> (1)
6061-T651	0	0	0	6 x 10 <sup>-5</sup> (1)
7075-T7351	0	0	0	4 x 10 <sup>-4</sup> (1)
2219-T87	4 x 10 <sup>-5</sup> (1)	2 x 10 <sup>-5</sup> (1)	1 x 10 <sup>-5</sup> (1)	3 x 10 <sup>-4</sup> (1)
2021-T81	7 x 10 <sup>-5</sup> (1)	9 x 10 <sup>-5</sup> (1)	2 x 10 <sup>-5</sup> (1)	4 x 10 <sup>-4</sup> (1)
2024-T851	1 x 10 <sup>-5</sup> (1)	4 x 10 <sup>-5</sup> (1)	4 x 10 <sup>-5</sup> (1)	1 x 10 <sup>-4</sup> (1)
<u>Alloys With Low Resistance to Stress-Corrosion Cracking</u>				
2014-T651	2 x 10 <sup>-4</sup>	2 x 10 <sup>-4</sup>	2 x 10 <sup>-4</sup>	1 x 10 <sup>-3</sup>
2024-T351	2 x 10 <sup>-4</sup>	2 x 10 <sup>-4</sup>	2 x 10 <sup>-4</sup>	8 x 10 <sup>-4</sup>
2219-T37	3 x 10 <sup>-4</sup>	3 x 10 <sup>-4</sup>	3 x 10 <sup>-4</sup>	2 x 10 <sup>-3</sup>
7075-T651	2 x 10 <sup>-4</sup>	1 x 10 <sup>-4</sup>	1 x 10 <sup>-4</sup>	9 x 10 <sup>-4</sup>
7039-T6351	2 x 10 <sup>-4</sup>	3 x 10 <sup>-4</sup>	3 x 10 <sup>-4</sup>	4 x 10 <sup>-3</sup>
7079-T651	4 x 10 <sup>-4</sup>	1 x 10 <sup>-2</sup>	1 x 10 <sup>-2</sup>	2 x 10 <sup>-2</sup>
5456-Sens.	5 x 10 <sup>-4</sup>	5 x 10 <sup>-5</sup>	1 x 10 <sup>-2</sup>	3 x 10 <sup>-3</sup>

Note: (1) Transgranular mechanical fracture rather than intergranular SCC.  
(2) Based on the first six months of exposure.

Table XXI

## POP-IN EXPERIMENTS WITH SHORT-TRANSVERSE (S-L) BOEING DCB SPECIMENS

Alloy	Test	Measurements in Inches (1)			Crack Opening Displacement (V)		E psi (x10 <sup>6</sup> )	Crack Length, In.		K <sub>I</sub> , ksi √in. (V-Total)		K <sub>I</sub> , ksi √in. (V-Elastic)		K <sub>Ic</sub> ksi √in.
		H	d <sub>1</sub>	d <sub>2</sub>	d <sub>0</sub>	d <sub>1</sub> -d <sub>2</sub>		Total Plastic d <sub>0</sub> -d <sub>2</sub>	Surface	Fracture	Surface	Fracture	Surface	
2014-T651	1	0.500	1.000	1.018	1.003	0.018	0.015	0.003	0.695	25.4	25.4	21.1	21.2	19
	2	0.500	1.000	1.019	1.002	0.019	0.017	0.002	0.735	24.9	20.6	22.3	18.4	
	AVG.	0.500	1.000	1.018	1.002	0.018	0.016	0.002	0.773	25.1	22.7	21.7	19.7	
2021-T81	1	0.500	1.000	1.025	1.003	0.025	0.022	0.003	0.715	34.0	---	29.9	---	20
	2	0.500	1.000	1.024	1.004	0.024	0.020	0.004	0.745	30.9	24.5	25.8	20.4	
	AVG.	0.500	1.000	1.024	1.004	0.024	0.020	0.004	0.730	32.4	---	27.8	---	
2024-T351	1	0.495	0.990	1.032	1.005	0.042	0.027	0.015	0.775	51.6	---	33.4	---	21
	2	0.490	0.980	1.027	1.003	0.047	0.024	0.023	0.715	62.9	46.6	32.1	23.8	
	AVG.	0.492	0.985	1.030	1.004	0.045	0.026	0.019	0.745	57.1	---	32.9	---	
2024-T851	1	0.492	0.985	1.014	1.000	0.029	0.014	0.015	0.700	40.7	28.8	20.0	18.2	17
	2	0.490	0.990	1.017	1.000	0.027	0.017	0.010	0.755	33.7	---	21.2	---	
	AVG.	0.490	0.988	1.016	1.000	0.028	0.016	0.012	0.728	37.0	---	20.7	---	
2219-T37	1	0.495	0.990	1.054	1.018	0.064	0.036	0.028	0.730	84.7	---	47.9	---	27(3)
	2	0.495	0.990	1.053	1.017	0.063	0.036	0.027	0.735	82.0	57.8	46.9	33.0	
	AVG.	0.495	0.990	1.054	1.018	0.064	0.036	0.028	0.733	83.3	---	47.4	---	
2219-T87	1	0.500	1.000	1.030	1.006	0.029	0.024	0.005	0.710	39.8	28.6	32.9	23.7	20
	2	0.498	0.995	1.066	1.038	0.073	0.030	0.043	0.897(2)	36.3	26.7	21.2	23.7	
	AVG.	0.495	0.990	1.062	1.034	0.072	0.028	0.044	0.904	38.1	27.7	20.7	23.7	
5456-Sens.	1	0.492	0.985	1.057	1.029	0.072	0.038	0.044	0.685	100.2	---	39.0	---	21(3)
	2	0.498	0.995	1.066	1.038	0.073	0.030	0.043	0.750	90.6	67.7	36.2	27.1	
	AVG.	0.495	0.990	1.062	1.034	0.072	0.028	0.044	0.718	95.1	---	37.5	---	
5456-H117	1	0.500	1.000	1.058	1.026	0.058	0.032	0.026	0.755	71.5	66.7	39.2	26.6	22(3)
	2	0.490	0.980	1.049	1.022	0.069	0.027	0.042	0.785	88.9	---	35.4	---	
	AVG.	0.495	0.990	1.053	1.024	0.065	0.029	0.034	0.740	80.1	---	37.3	---	
6061-T651	1	0.495	0.990	1.046	1.012	0.056	0.034	0.022	0.680	77.3	---	47.2	---	21
	2	0.490	0.980	1.058	1.016	0.078	0.042	0.036	0.740	95.0	59.9	50.6	21.9	
	AVG.	0.490	0.983	1.054	1.016	0.069	0.037	0.032	0.723	86.9	58.4	41.9	27.3	
7039-T6351	1	0.500	1.000	1.029	1.005	0.029	0.024	0.005	0.735	37.3	27.5	30.9	22.8	20
	2	0.500	1.000	1.016	1.001	0.016	0.015	0.001	0.705	21.7	20.6	20.4	19.3	
	AVG.	0.500	1.000	1.016	1.001	0.016	0.015	0.001	0.705	21.7	20.7	20.4	19.4	
7075-T651	1	0.495	0.990	1.021	1.001	0.031	0.020	0.011	0.730	39.9	32.4	25.8	20.2	21
	2	0.500	1.000	1.020	1.001	0.020	0.019	0.001	0.745	25.3	20.7	24.0	19.6	
	AVG.	0.498	0.995	1.020	1.001	0.025	0.0195	0.006	0.738	32.5	26.5	24.9	20.3	
7079-T651	1	0.502	1.004	1.018	1.006	0.014	0.013	0.002	0.850	16.0	---	13.9	---	14
	2	0.500	1.001	1.019	1.004	0.018	0.015	0.003	0.835	16.8	14.1	14.0	11.8	
	AVG.	0.501	1.002	1.019	1.005	0.016	0.014	0.003	0.895	16.4	---	13.9	---	

Notes: (1) d<sub>0</sub> - 2H measured at bolt line before loading.d<sub>1</sub> - 2H measured at bolt line after loading.d<sub>2</sub> - 2H measured at bolt line after unloading.

(2) Fracture crack length based on average at T/2 and T/10 planes substituted for T/4 measurement.

(3) Not valid per ASTM criteria for K<sub>Ic</sub>.

Table XXII  
RESULTS OF TESTS OF RING LOADED COMPACT TENSION SPECIMENS  
OF HIGH RESISTANCE ALUMINUM ALLOYS

Alloy & Temper	Sample Number	Specimen Number	Initial Values			Values at Fracture				Time to Failure Hrs.	Evaluation of Run-outs						
			Target (1)		Crack Length, In.	Calculated (2)		Estimated (3)	Crack Length, In.		Load, lb.	K <sub>Ic</sub>	K <sub>Ic</sub>	K <sub>Ic</sub>	Top In Load	Crack Growth Micro	
			Crack Length, In.	Load, lb.		K <sub>Ic</sub>	K <sub>Ic</sub>										Crack Length, In.
5456-H117	366656	1	0.995	3075	20700	95	0.860(6)	3050	17000(6)	0.86	17000	0.833(4)	3320(4)	17900(4)	OK912(6)	NO	NO
		2	0.995	2970	20000	92	0.801	3330	17300	0.89	19300	0.833(4)	3320(4)	17900(4)	OK2328(4)	NO	NO
6061-T651	366208	1	0.990	3045	20400	95	---	---	---	---	---	---	---	---	OK2208(5)	NO	NO
		1A	0.990	3195	21400	100	0.988	3190	21300	0.93	19600	0.978(4)	3190(4)	21000(4)	OK2780(4)	NO	NO
7075-T7351	366210	1	0.985	3010	20000	95	---	---	---	---	---	---	---	---	OK2208(5)	---	---
		1A	0.985	3140	21000	100	0.909	3140	18700	1.01	21500	0.926(4)	3120(4)	19100(4)	OK2780(4)	NO	0.06
2219-T87	338148	1	0.740	1730	17700	90	0.758	1730	18400	---	---	0.803	1720	20100	OK1816(5)	NO	---
		2	0.750	1815	19000	97	0.782	1820	20400	0.74	18500	0.840	1790	22700	504	YES	0.06(7)
2021-T81	326400	1	1.025	2500	17700	90	1.030	2490	17700	1.14	20900	1.141	2440	20900	392	---	---
		2	1.000	2210	15000	76	1.054	2210	16300	0.99	14700	1.112(4)	2200(4)	17900(4)	OK2328(4)	NO	NO
2024-T851	366207	1	0.985	2855	15000	90	0.962	2270	14600	1.17	19800	1.137	2190	18600	240	---	---
		2	0.985	1805	12000	72	0.939	1810	11300	0.94	11300	0.979(4)	1810(4)	11900(4)	OK2400(4)	NO	NO

- Notes: (1) Target values based on side measurements of crack length.  
(2) Calculated values obtained from measurements of loads and crack opening displacements.  
(3) Final crack lengths measured on fracture surfaces. Estimate of K<sub>Ic</sub> based on last measured load.  
(4) Test terminated. Specimen intact and little or no evidence of crack growth on load-time curve.  
(5) Little or no evidence of crack growth. Load increased 5% and specimen renumbered 1A for continuation of the test.  
(6) Test terminated and specimen broken. No COD data available. Calculated initial values based on crack length measured after tensile fracture.  
(7) Visual examination of fracture indicated failure caused by tensile overload.

Table XXIII  
RESULTS OF TESTS OF RING LOADED COMPACT TENSION SPECIMENS  
OF LOW RESISTANCE ALUMINUM ALLOYS

Alloy & Temper	Sample Number	Specimen Number	Initial Values			Values at Fracture			Time to Failure Hrs.	Evaluation of						
			Crack Length, In.	Load, lb.	$K_{Ic}$	Crack Length, In.	Load, lb.	$K_{Ic}$		Drop In Load	Fracture	Micro				
2014-T651	366335	1	0.990	2095	14000	75	0.897	2100	12400	18600	1.178	1990	18300	456	---	---
		4	0.990	1676	11200	60	0.974	1680	11000	20600	1.309	1560	18900	352	---	---
		5	1.000	1473	10000	53	0.826	1440(5)	7700(5)	18000	1.302	1530	18300	464(5)	---	---
		3	1.000	1377	9400	50	0.905	1380	8200	8700	0.887(4)	1380(4)	8000(4)	OK1336(4)	No	No
		1	0.990	2360	15800	75	0.882	2360	13600	22000	1.223	2140	26800	664	---	---
2024-T351	366206	3	0.980	1820	12000	57	0.958	1900	12100	---	---	---	---	---	---	
		2	0.990	1573	10500	50	0.870	1570	8900	---	---	---	---	---	---	
2219-T37	344793	2	0.745	1309	13500	50	0.767	1311	14200	27900	1.118	1040	31100	376	---	---
		3	0.750	1300	13500	50	0.760	1330	14200	31700	1.116	900	36500	1280	---	---
		4	0.750	1148	12000	44	0.779	1160	12900	36600	1.122	810	33300	560	---	---
		1	0.990	2181	14700	75	0.888	2190	12700	19200	1.28	2040	21400	248	---	---
7075-T651	366209	2	0.980	1482	9800	50	0.910	1490	8900	19300	1.338	1350	17500	430	---	---
		4	0.995	1059	7000	36	0.852	1200	6600(9)	20600	1.52	980	17200	824	---	---
		3	0.985	883	5900	30	0.826	885	4700	5400	0.865	870	4900	OK2208(4)	Yes	Local
7039-T651	314758	1	0.990	2287	15300	75	0.886	2300	13300	24900	1.286	2110	24200	320	---	---
		2	1.020	1457	10200	40	0.972	1470	9600	25400	1.438	1250	21000	600	---	---
		3	1.010	1185	8200	40	1.000	1190	8200	---	---	---	---	---	---	
		4	0.990	1046	7000	34	0.888	1200	7000(9)	---	---	---	---	---	---	
7079-T651	366259	2	0.990	2152	14400	75	0.948	2150	13500	---	---	---	---	---	---	
		3	0.990	1435	9600	50	0.828	1440	8900	---	---	---	---	---		
		4	0.990	861	5800	30	0.875	860	4900	---	---	---	---	---		
		5	1.000	589	4000	21	0.920	600	3600	3700	---	---	---	---	---	
		1	1.000	2364	16000	75	0.904	2370	14000	---	---	---	---	---		
5456-Sens.	366657	1	0.990	1576	10700	50	0.899	1580	9300	---	---	---	---	---	---	
		2	0.990	800	5400	25	0.788	820	4200	---	---	---	---	---		
		3	0.990	448	3000	14	0.951	450	2900	3300	---	---	---	---	---	
		4	0.990	448	3000	14	0.951	450	2900	---	---	---	---	---		

Notes: (1) Target values based on side measurements of crack length.  
(2) Calculated values obtained from measurements of loads and crack opening displacements.  
(3) Final crack lengths measured on fracture surfaces. Estimate of  $K_{Ic}$  based on last measured load.  
(4) Test terminated. Specimen intact and little or no evidence of crack growth on load-time curve.  
(5) After 144 hrs. with no evidence of crack growth, K level increased to 10100 psi  $\sqrt{\text{in.}}$  and the specimen failed after 320 hr. at the new K level.  
(6) Clip gage failed during test.  
(7) Rapid crack growth. Calculations based on last readings taken.  
(8) Rapid fracture. Cracks too long for valid calculations.  
(9) Load was adjusted at beginning of test to obtain estimated level.  
(10) Specimen broken open several months after termination of test and about 0.25 in. SCC present on the fracture; probably caused by corrosion product wedging during storage after termination of test.

Table XXIV

ESTIMATED THRESHOLD STRESS INTENSITY FACTORS OF SOME ALUMINUM ALLOYS DETERMINED WITH COMPACT TENSION SPECIMENS UNDER RING LOADING - S-L SPECIMENS IMMERSSED IN SALT-DICHROMATE-ACETATE SOLUTION

<u>Alloy</u>	$K_{Ic}$ ksi $\sqrt{\text{in.}}$	$K_{Ith}$ ksi $\sqrt{\text{in.}}$	$K_{Ith}$ % $K_{Ic}$
<u>Alloys With High Resistance to SCC</u>			
5456-H117	21.8(1)	>18	>82
6061-T651	21.4	>21	>98
7075-T7351	21.0	18	86
2219-T87	19.6	>20	>100
2021-T81	19.6	17	87
2024-T851	16.7	13	78
<u>Alloys With Low Resistance to SCC</u>			
2014-T651	18.7	9	50
2024-T351	21.2	11	52
2219-T37	27.1(1)	12	45
7075-T651	19.6	4	20
7039-T6351	20.4	6	30
7079-T651	19.2	4	21
5456-Sens.	21.4(1)	2	9

Notes: (1) Regarded as  $K_{Ic}$  value (not valid for  $K_{Ic}$ )

Table XXV

STEEL ALLOY SMOOTH TENSILE SPECIMENS SCHEDULED FOR 4 YEARS EXPOSURE TO SEACOAST ATMOSPHERE  
 INDIVIDUAL SPECIMEN IDENTIFICATION (NO.) AND TIME TO FAILURE (Tf) IN DAYS(+)

Alloy	Temper	S. No.	Test Direction(1)	Str. 75% Y.S.			Str. 50% Y.S.			Str. 25% Y.S.			Str. 27 ksi	
				Str. ksi	No.	Tf	Str. ksi	No.	Tf	Str. ksi	No.	Tf	No.	Tf
17-7PH	H1050	366665	T	142.9	T15 T16 T17	141 141	95.3	T18 T19 T20						
PH15-7MO	RH950	366666	T	152.6	T15 T16	41 41			50.9	T17 T18			T19 T20	
PH15-7MO	RH1050	366666	T	146.3	T45 T46 T47	41 41 41	97.5	T48 T49 T50						
15-5PH	H1150M	366667	T	69.8	T15 T16 T17		20.4	T18 T19 T20						
15-5PH	H900	366668	T	128.4	T15 T16				42.8	T17 T18			T19 T20	
PH13-8MO	H950	366669	L	151.2	L15 L16 L17		100.8	L18 L19 L20						
PH13-8MO	H950	366669	T	147.5	T15 T16 T17		98.4	T18 T19 T20						
PH13-8MO	H950	366669	S	152.5	N15 N16 N17		101.7	N18 N19 N20						
PH13-8MO	H1050	366669	T	143.9	T45 T46 T47		89.3	T48 T49 T50						
431	HT200	366670	L	124.1	L15 L16				41.4	L17 L18			L19 L20	
431	HT200	366670	T	124.1	T15 T16	141 561			41.4	T17 T18			T19 T20	
431	HT200	366670	S	115.3	N15 N16				38.4	N17 N18			N19 N20	
431	HT125	366670	T	80.6	T45 T46 T47		53.7	T48 T49 T50						
AM355	SCT850	366671	T	114.4	T15 T16				38.1	T17 T18			T19 T20	
AM355	SCT1000	366671	T	127.3	T45 T46 T47		84.9	T48 T49 T50						
AM355	SCT850	366673	L	139.6	L15 L16	41 41			46.5	L17 L18	141 141		L19 L20	141
AM355	SCT850	366673	T	142.7	T15 T16	41 41			47.6	T17 T18	141 141		T19 T20	190 141
AM355	SCT850	366673	S	139.9	N15 N16	41 41			46.7	N17 N18	141 499		N19 N20	409 499
AM355	SCT1000	366673	T	129.3	T45 T46 T47		86.2	T48 T49 T50						

- Notes: (+) No entry in Tf column indicates specimen has not failed and is still in test.  
 (1) L = principal rolling or forging direction of product, T = width of product, and S = thickness of product.  
 (2) In addition to stressed specimens, duplicate unstressed specimens were exposed for each alloy-temper.  
 (3) All specimens exposed May 3, 1970.

Table XVI

STEEL ALLOY SMOOTH TENSILE SPECIMENS SCHEDULED FOR 4 YEARS EXPOSURE TO INDUSTRIAL ATMOSPHERE  
 INDIVIDUAL SPECIMEN IDENTIFICATION (NO.) AND TIME TO FAILURE(Tf) IN DAYS (+)

Alloy	Temper	S. No.	Test Direction(1)	Str. 75% Y.S.			Str. 50% Y.S.			Str. 25% Y.S.			Str. 27 ksi	
				Str. ksi	No.	Tf	Str. ksi	No.	Tf	Str. ksi	No.	Tf	No.	Tf
17-7PH	RH1050	366665	T	142.9	T23 T24 T25		95.3	T26 T27 T28						
PH15-7MO	RH950	366666	T	152.6	T23 T24	39 340			50.9	T25 T26			T27 T28	
PH15-7MO	RH1050	366666	T	146.3	T53 T54 T55		97.5	T56 T57 T58						
15-5PH	H1150M	366667	T	69.8	T23 T24 T25		20.4	T26 T27 T28						
15-5PH	H900	366668	T	128.4	T23 T24				42.8	T25 T26			T27 T28	
PH13-8MO	H950	366669	L	151.2	L23 L24 L25		100.8	L26 L27 L28						
PH13-8MO	H950	366669	T	147.5	T23 T24 T25		98.4	T26 T27 T28						
PH13-8MO	H950	366669	S	152.5	N23 N24 N25		101.7	N26 N27 N28						
PH13-8MO	H1050	366669	T	143.9	T53 T54 T55		89.3	T56 T57 T58						
431	HT200	366670	L	124.1	L23 L24				41.4	L25 L26			L27 L28	
431	HT200	366670	T	124.1	T23 T24				41.4	T25 T26			T27 T28	
431	HT200	366670	S	115.3	N23 N24				38.4	N25 N26			N27 N28	
431	HT125	366670	T	80.6	T53 T54 T55		53.7	T56 T57 T58						
AM355	SCT850	366671	T	114.4	T23 T24				38.1	T25 T26			T27 T28	
AM355	SCT1000	366671	T	127.3	T53 T54 T55		84.9	T56 T57 T58						
AM355	SCT850	366673	L	139.6	L23 L24				46.5	L25 L26			L27 L28	
AM355	SCT850	366673	T	142.7	T23 T24	501 173			57.6	T25 T26			T27 T28	
AM355	SCT850	366673	S	139.9	N23 N24	34 20			46.7	N25 N26			N27 N28	
AM355	SCT1000	366673	T	129.3	T53 T54 T55		86.2	T56 T57 T58						

Notes: (+) No entry in Tf column indicates specimen has not failed and is still in test.

(1) L = principal rolling or forging direction of product, T = width of product, and S = thickness of product.

(2) In addition to stressed specimens, duplicate unstressed specimens were exposed for each alloy-temper.

(3) All specimens exposed April 9, 1970.

Table XXVII

RESULTS OF EXPLORATORY TESTS OF COMPACT TENSION SPECIMENS  
(T-1) OF 15-5PH ALLOY IMMersed IN 20% NaCl SOLUTION

Temper	S. No.	Initial Values					Residual Values		
		Intended % $K_{Ic}$	Crack length, (1) in.	Load, lb.	$K_{Ii}$ psi in.	Days of Exposure	Crack length, (2) in.	Load, lb.	$K_{Ir}$ psi in.
H900	TC53	95	1.00	10,100	68,400	211	1.86	218	(3)
	TC54	75	1.00	7,950	54,000	211	1.76	406	(3)
	TC55	75	0.98	8,200	54,000	211	0.97	7,350	47,800
	TC56	50	0.98	5,420	36,000	211	1.23	2,680	27,500
	TC37	50	0.98	5,400	36,000	365	1.39	1,800	26,700
H1150M	TC19	95	0.98	14,400	95,000	211	0.97	10,000	65,200
	TC20	75	0.98	11,300	75,000	211	0.97	8,620	56,200

- Notes:   
 (1) Average length of crack measured on sides of the specimen.   
 (2) Average length of crack measured on fracture surface.   
 (3) Cracks too long for valid determination of stress intensity factor.

Table XXVIII

SUMMARY OF LONG-TRANSVERSE (T-L) TESTS OF COMPACT TENSION SPECIMENS OF STAINLESS STEEL ALLOYS FATIGUE PRECRACKED AND BOLF LOADED TO 95%  $K_{Ic}$ 

Alloy & Temper	$K_{Ic}$ ksi $\sqrt{in.}$	Seacoast Atmosphere (28 mo.)			Industrial Atmosphere (29 mo.)			20% NaCl Solution(2)		
		Incuba- tion, Mo.	$K_{Isc}$ (3) ksi $\sqrt{in.}$	Avg. Initial Crack Velocity In./Hr.	Incuba- tion, Mo.	$K_{Ith}$ (3) ksi $\sqrt{in.}$	Avg. Initial Crack Velocity In./Hr.	Incuba- tion, Mo.	$K_{Isc}$ ksi $\sqrt{in.}$	Avg. Initial Crack Velocity In./Hr.
17-7PH RH1050	47	----	<12	(4)	0	>24	$1 \times 10^{-2}$	0	<18	$4 \times 10^{-1}$
PH15-7Mo RH900	31	0	<15	$5 \times 10^{-4}$	0	>23	$1 \times 10^{-2}$	0	<15	$5 \times 10^{-2}$
PH15-7Mo RH1050	40	0	<20	$5 \times 10^{-4}$	0	>30	$3 \times 10^{-3}$	0	<20	$4 \times 10^{-2}$
15-5PH H900	72	>28	<36	$2 \times 10^{-4}$	>29	>68	-----	0.5	33	$2 \times 10^{-3}$
HL150M	76(1)	>28	>72	-----	>29	>72	-----	>6.7	>72	-----
PH13-8Mo H950	62	2.4	<31	$4 \times 10^{-4}$	>29	>59	-----	0	<46	$2 \times 10^{-2}$
HL050	88	2.4	<44	$5 \times 10^{-4}$	>29	>83	-----	0	<65	$2 \times 10^{-2}$
431 HF200	79	1.3	<40	$6 \times 10^{-4}$	>29	>40	-----	0	12	$8 \times 10^{-3}$
HT125	76(1)	4.7	>38	$3 \times 10^{-4}$	>29	>72	-----	1.2	43	$2 \times 10^{-3}$
AM355 SC1850	48	1.3	<24	$6 \times 10^{-4}$	>29	>45	-----	>6.7	8	$9 \times 10^{-3}$
SC11000	105	6.3	>52	$2 \times 10^{-4}$	>29	>99	-----	0.5	37	$6 \times 10^{-3}$
AM355 SC1850	37	1.3	<18	$9 \times 10^{-4}$	2	>18	$6 \times 10^{-5}$	0	6	$1 \times 10^{-2}$
SC11000	70	2.4	>35	$5 \times 10^{-4}$	>29	>66	-----	>6.7	28	$1 \times 10^{-2}$

Notes: (1) Not Valid per ASTM S399 criteria for  $K_{Ic}$ .

(2) Refer to Figure 93.

(3) Estimated from the  $K_{Ii}$  values at which SCC initiated.

(4) Failure occurred in laboratory atmosphere within four days after loading.

(5) Crack growth observed for specimens loaded at 75%  $K_{Ic}$ , but not for specimen loaded at 95%  $K_{Ic}$ .

Table XXIX

T1-6Al-4V ALLOY SMOOTH LONG-TRANSVERSE TENSILE SPECIMENS  
EXPOSED TO ACCELERATED TEST AND ATMOSPHERIC ENVIRONMENTS

Temper	Stressed 75% Y.S.			Stressed 50% Y.S.			Unstressed		
	Str.-ksi	Spec. Days(1)	% Loss T.S.(2)	Str.-ksi	Spec. Days(1)	% Loss T.S.(2)	No.	% Loss T.S.(2)	
Beta Forged	101	T13	Seacoast Atmosphere (Exposed May 3, 1970)(3)	72	T16		T11		
		T14			T17		T12		
		T15			T18				
Alpha-Beta Forged	109	T13		72	T16		T11		
		T14			T17		T12		
		T15			T18				
Beta Forged	101	Industrial Atmosphere (Exposed April 10, 1970)(3)			T24		T19		
		T21	T25	T20					
		T22	T26						
Alpha-Beta Forged	109	T21		72	T24		T19		
		T22			T25		T20		
		T23			T26				
Beta Forged	101	3.5% NaCl Solution by Alternate Immersion, One Year			T8		T1		
		T3	NF	3	T9		T2		
		T4		67	T10				
Alpha-Beta Forged	109	T3		72	T8		T1		
		T4			NF		4		T2
		T5							
		T6							
		T7							

Notes: (1) NF or no entry in this column indicates no failures to date.  
 (2) Results are average of tests of all specimens exposed at indicated stress.  
 (3) Test are continuing with completion tentatively scheduled for 4 years.



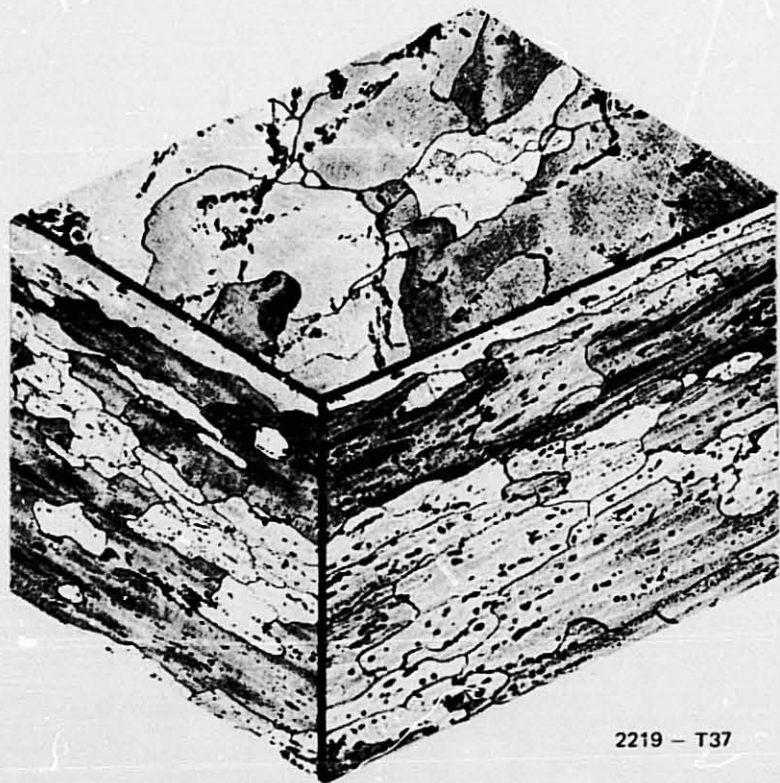
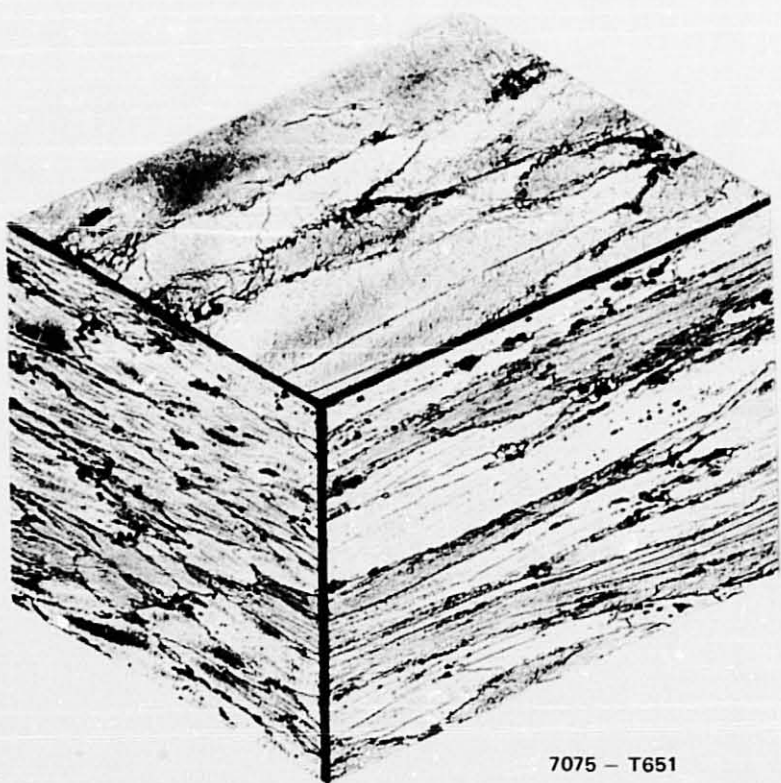
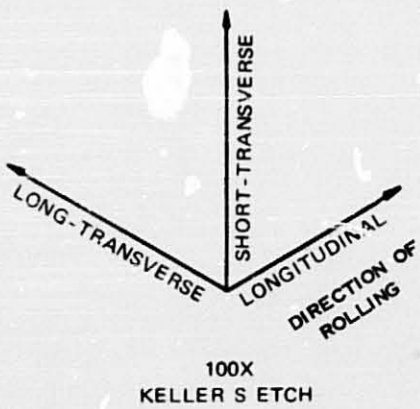
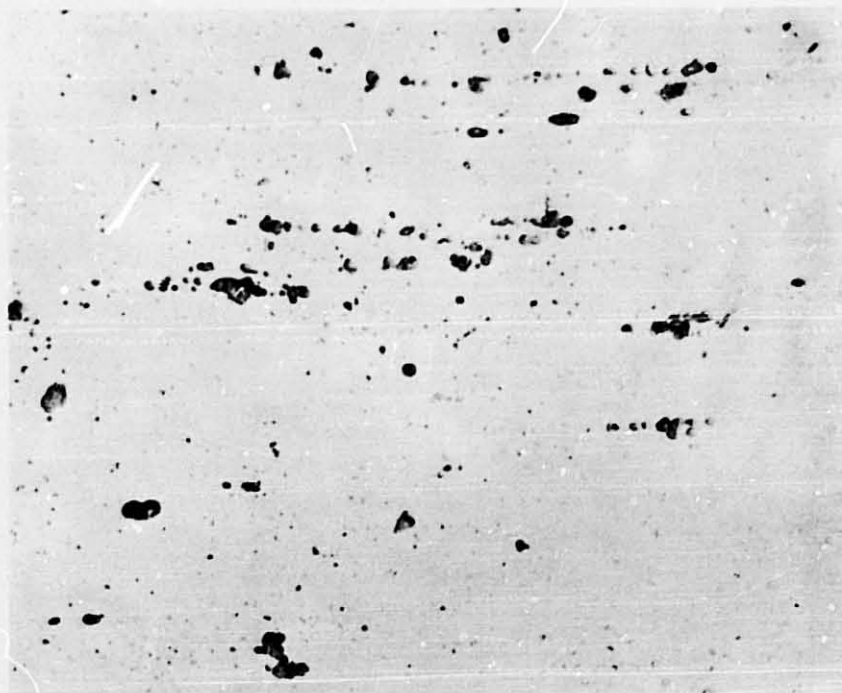
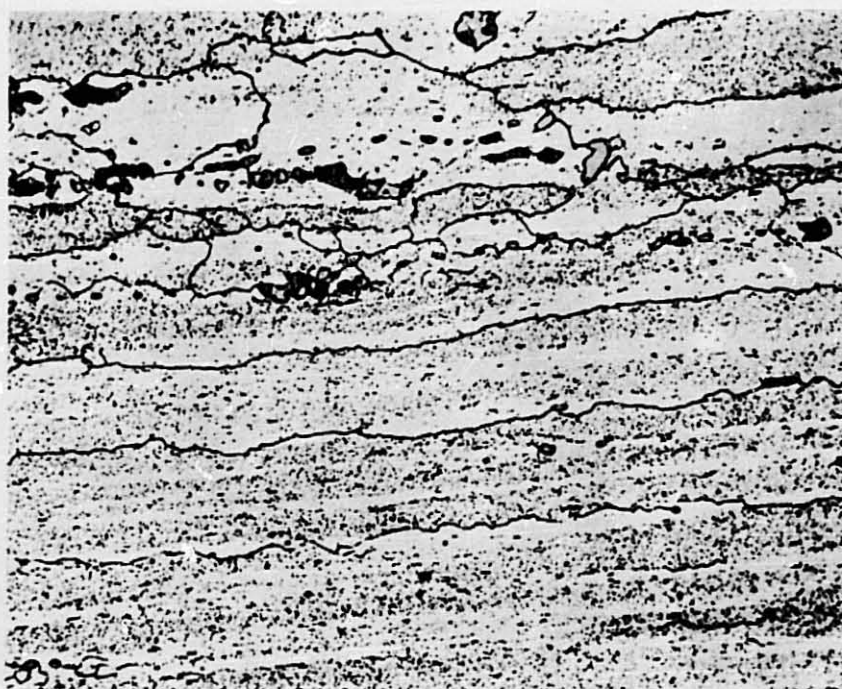


FIG. 1 GRAIN STRUCTURE AT MIDPLANE OF PLATE OF 7075 (2.500") AND 2219 (2.00") ALLOYS



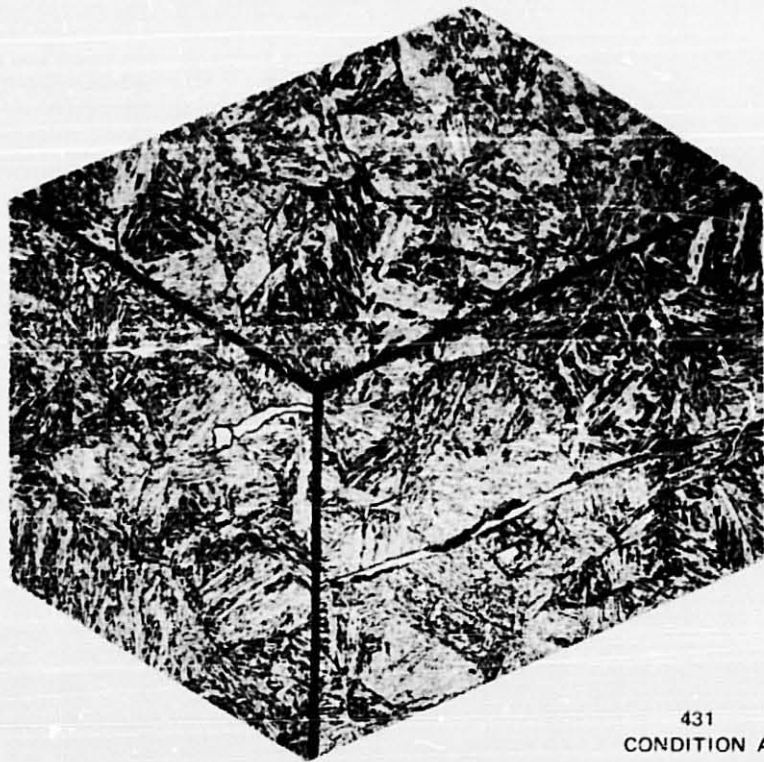
5456 - H117

500X  
40% H<sub>3</sub>PO<sub>4</sub>  
ETCH

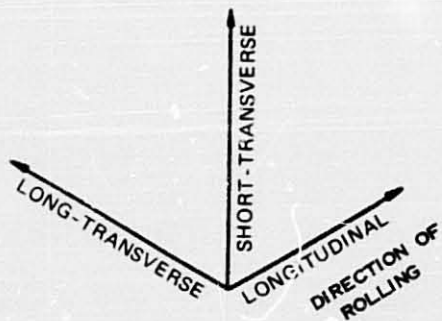


5456 - SENSITIZED

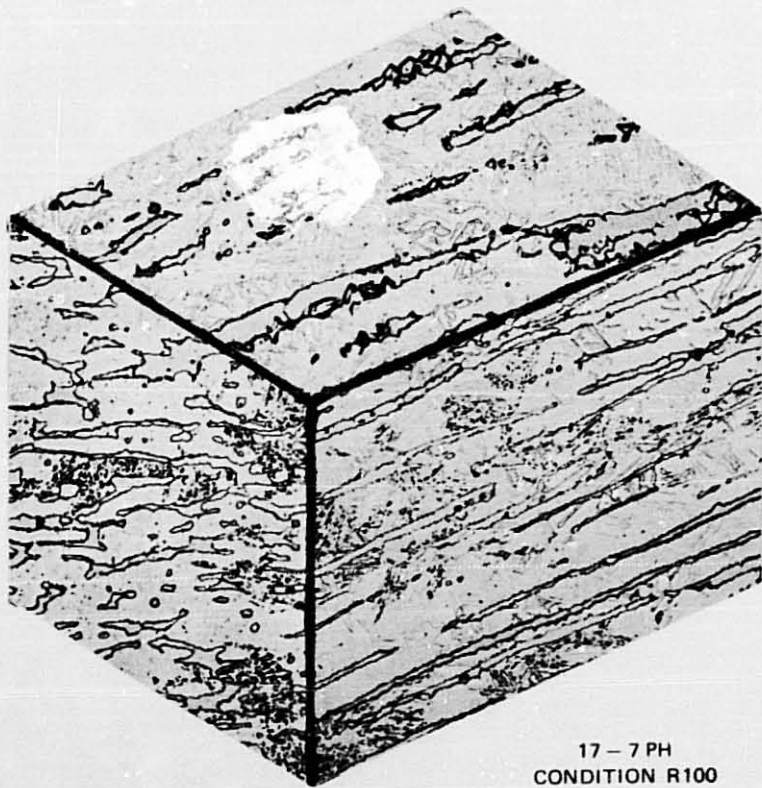
FIG. 2 LONGITUDINAL SECTION SHOWING PRECIPITATE STRUCTURE AT MIDPLANE OF 2.500" THICK 5456 - H117 AND 5456 - SENSITIZED PLATE



431  
CONDITION A

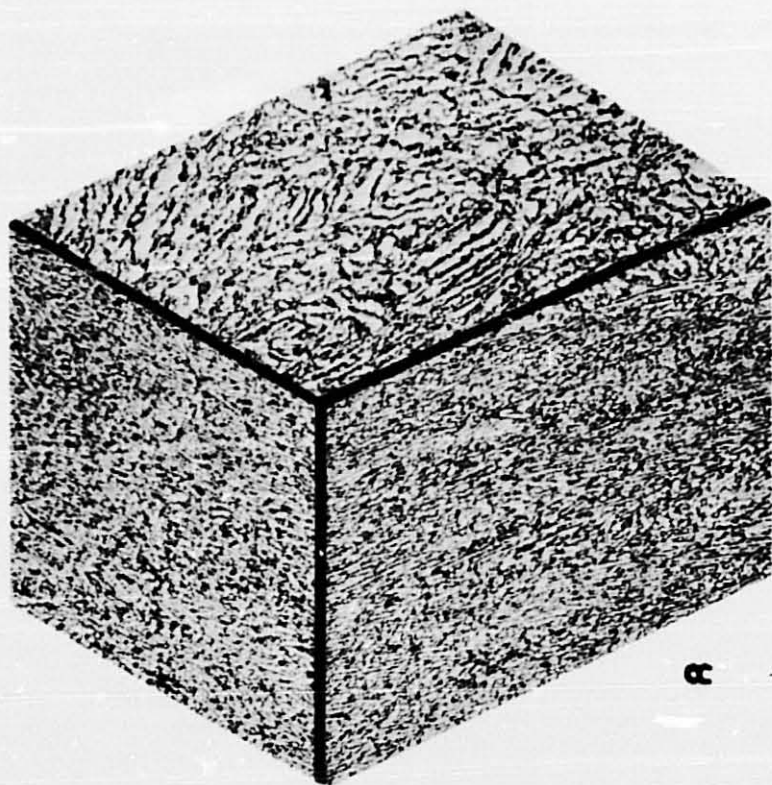


500X  
ETCH MIXED ACIDS  
IN GLYCEROL

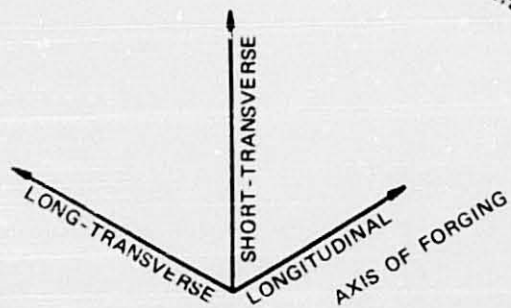


17 - 7 PH  
CONDITION R100

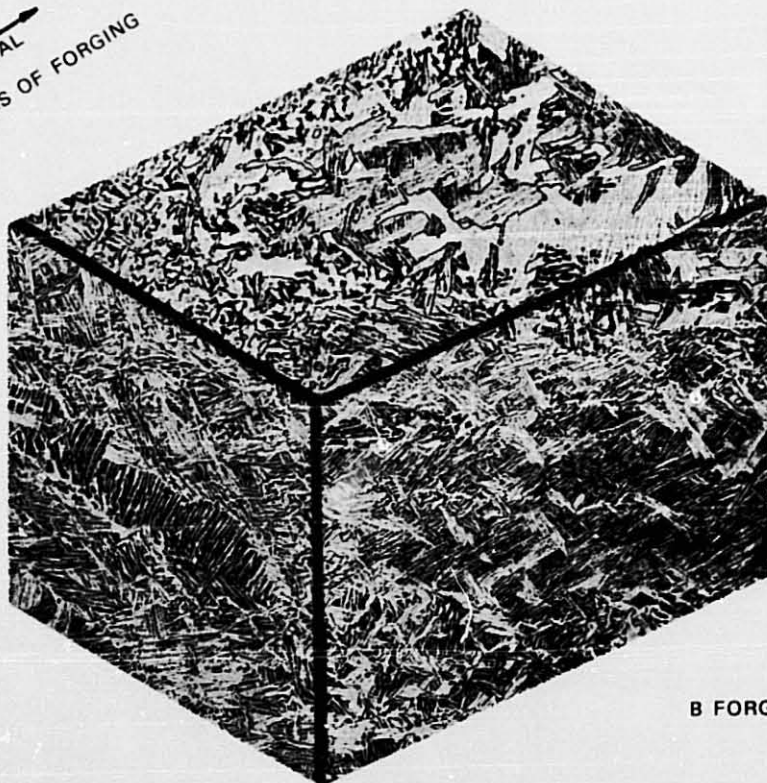
FIG. 3 GRAIN STRUCTURE AT MIDPLANE OF BAR OF 431 (2.250") AND 17 - 7 PH (1.250") ALLOYS



+ B FORGING



100X  
KELLER S ETCH



B FORGING

FIG. 4 GRAIN STRUCTURE AT MIDPLANE OF FORGED 2 1/4" X 6" BAR OF 6Al-4V ALLOY

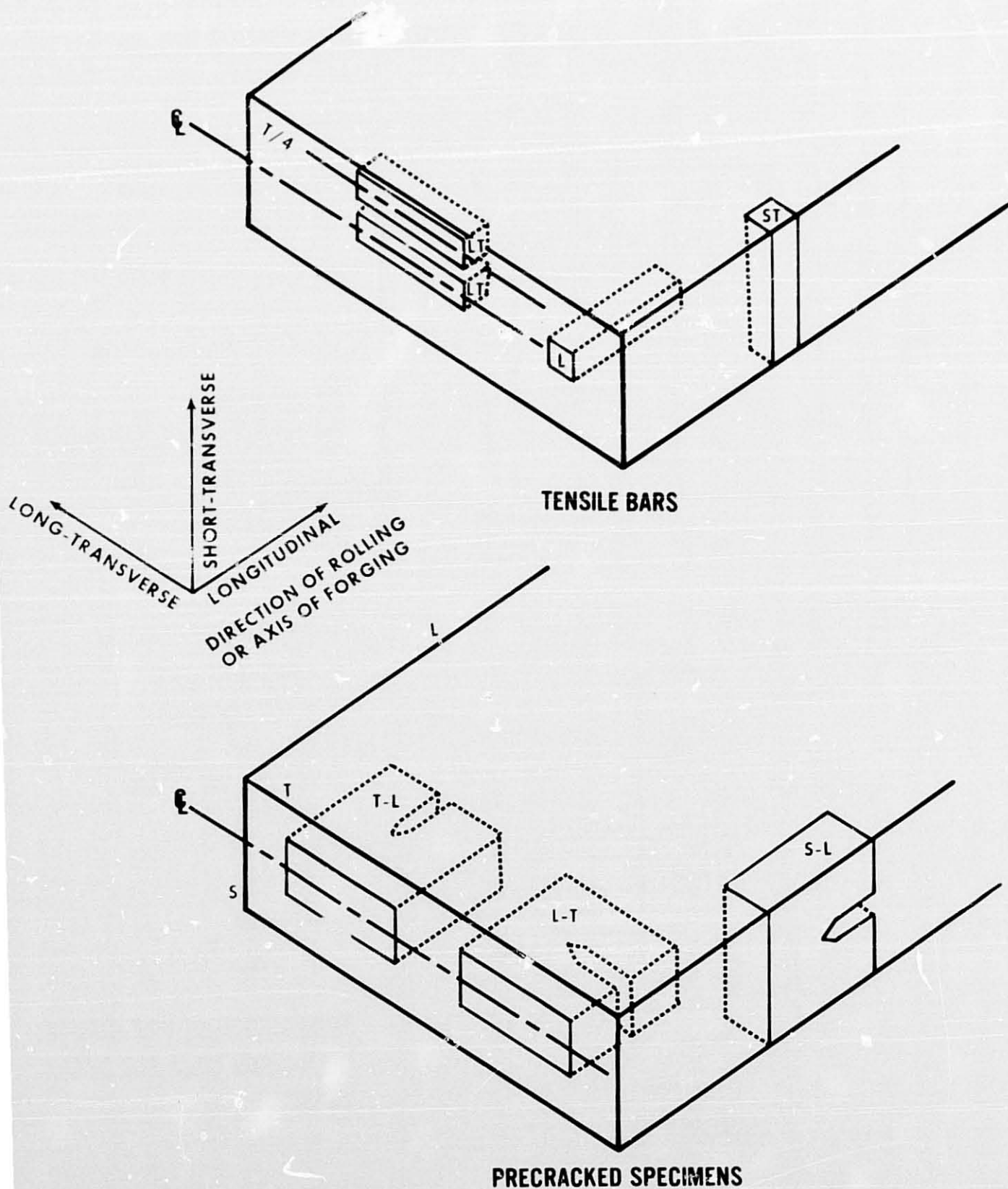
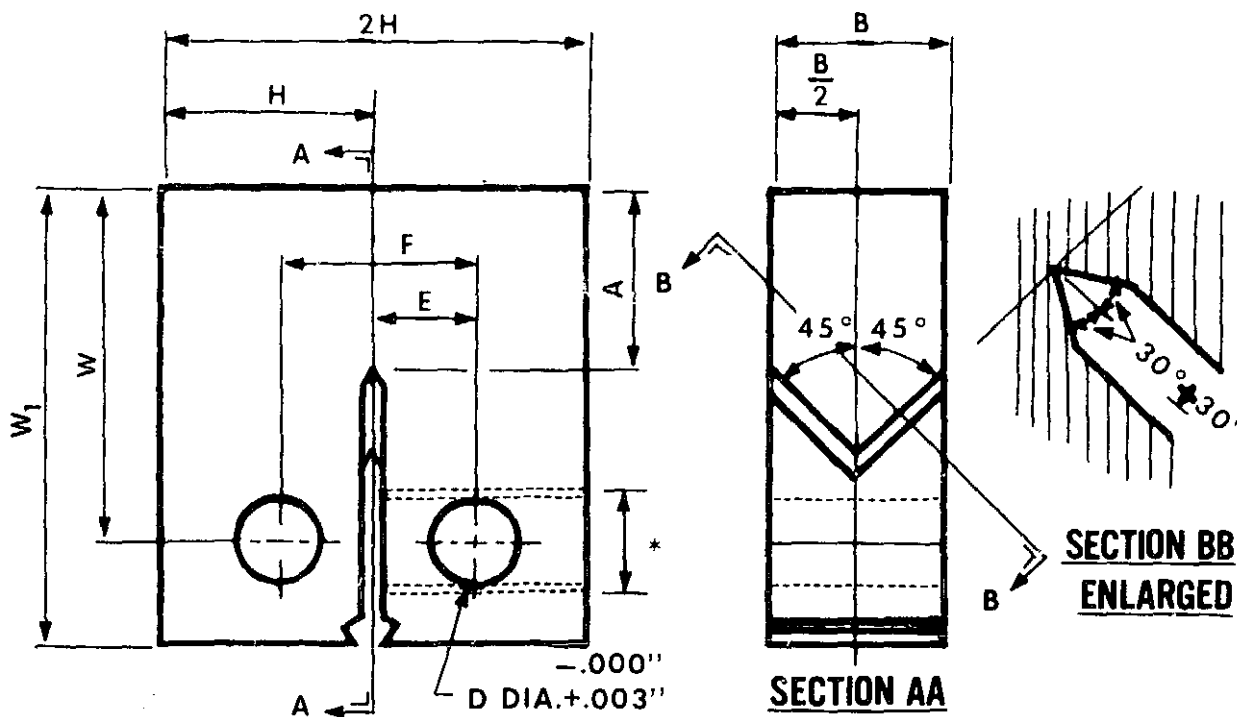
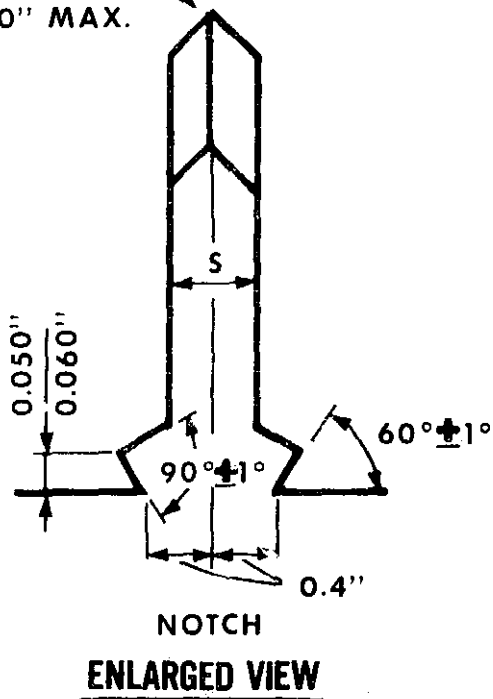


**Fig. 5** DIAGRAM OF SPECIMEN LOCATIONS AND ORIENTATIONS FOR MECHANICAL PROPERTY AND STRESS - CORROSION TESTS.



NOTCH ROOT  
RADIUS .010" MAX.

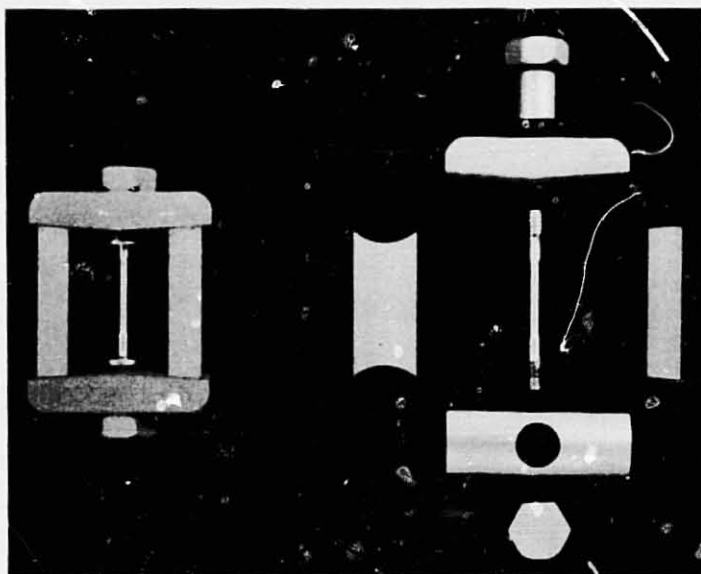


**PROPORTIONS**

- B = THICKNESS
- A = 1.1B
- W = 2B; W<sub>1</sub> = 2.5B
- S = 0.1B
- F = 1.10B
- H = 1.2B
- D = 0.5B

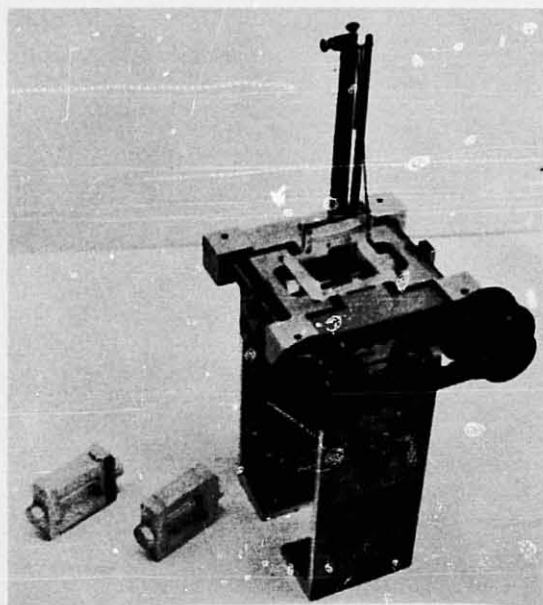
\* THREADED HOLE FOR LOADING  
BOLT WHEN USED FOR SCC  
TESTS.

**Fig. 6 COMPACT TENSION FRACTURE TOUGHNESS SPECIMEN**



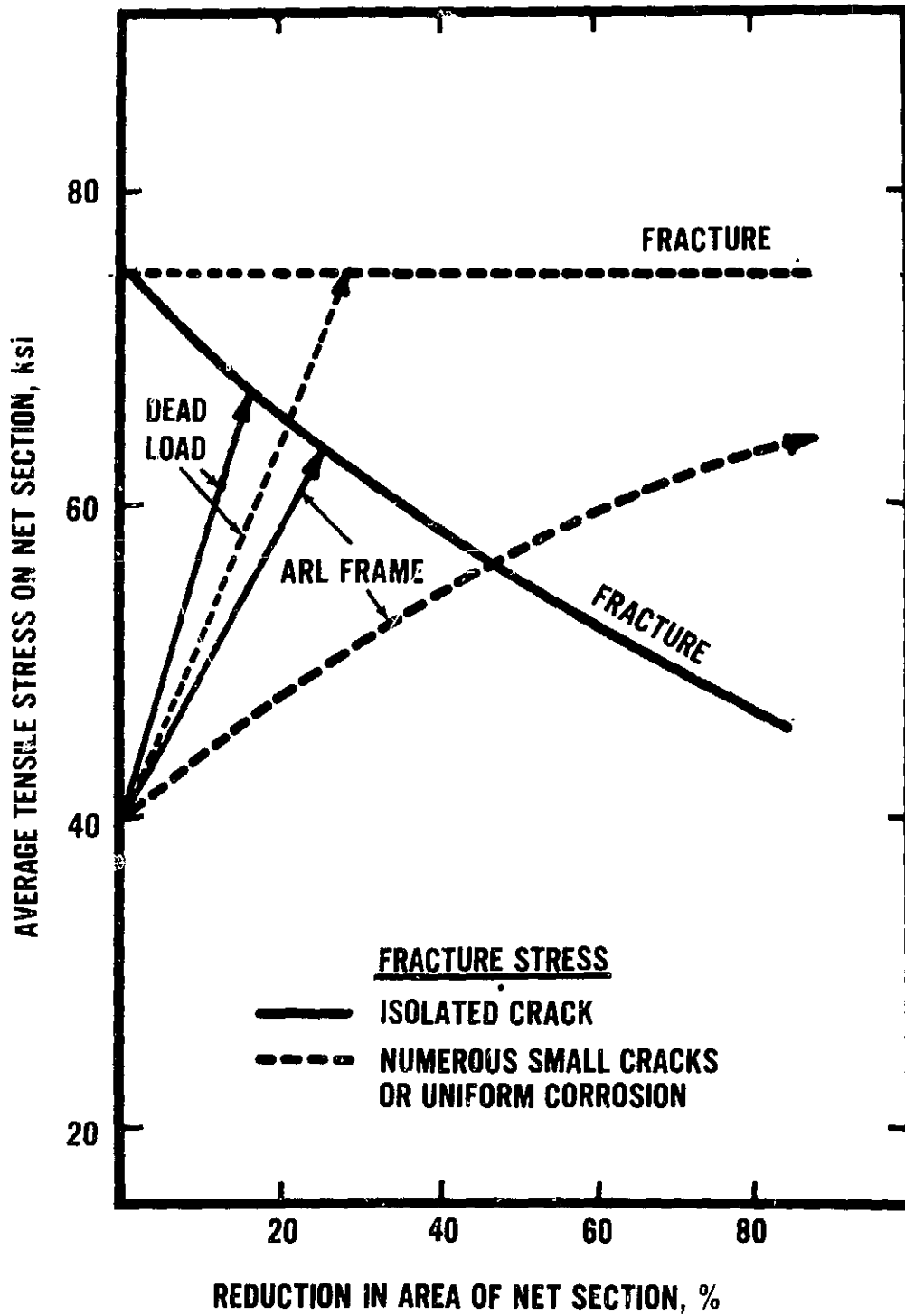
MAG: 1/2X

FIG. 7a SHOWS THE 1/8 IN. DIAMETER TENSION SPECIMEN, THE VARIOUS PARTS OF THE STRESSING FRAME AND THE FINAL STRESSED ASSEMBLY.



MAG: 1/5X

FIG. 7b SYNCHRONOUS LOADING DEVICE USED TO STRESS SPECIMENS. A STRESSED ASSEMBLY AND ONE ASSEMBLED FINGER-TIGHT READY FOR STRESSING ARE SHOWN TO THE LEFT. BOTH THE STRESSING FRAME AND THE LOADING DEVICE WERE DEVELOPED BY THE ALCOA RESEARCH LABORATORIES, PRIOR TO THIS CONTRACT.



**FIG. 8 EFFECT OF CORROSION PATTERN ON FRACTURE STRESS AND ON NET SECTION STRESS IN 0.125 in. DIA. ALUMINUM ALLOY SPECIMEN.**

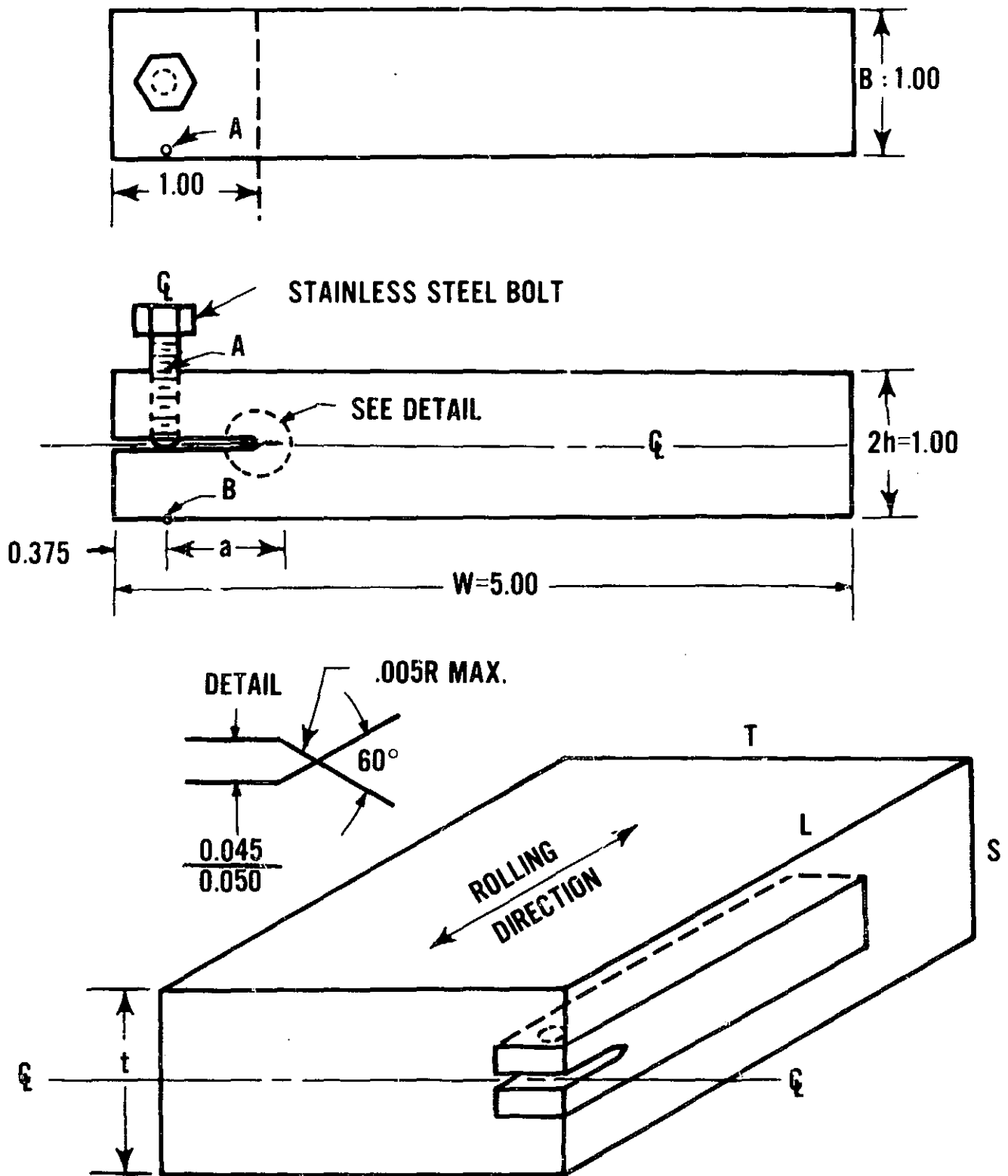


**Fig. 9 DOUBLE CANTILEVER BEAM SPECIMEN USED FOR STRESS CORROSION TESTING OF HIGH STRENGTH ALUMINUM ALLOYS**

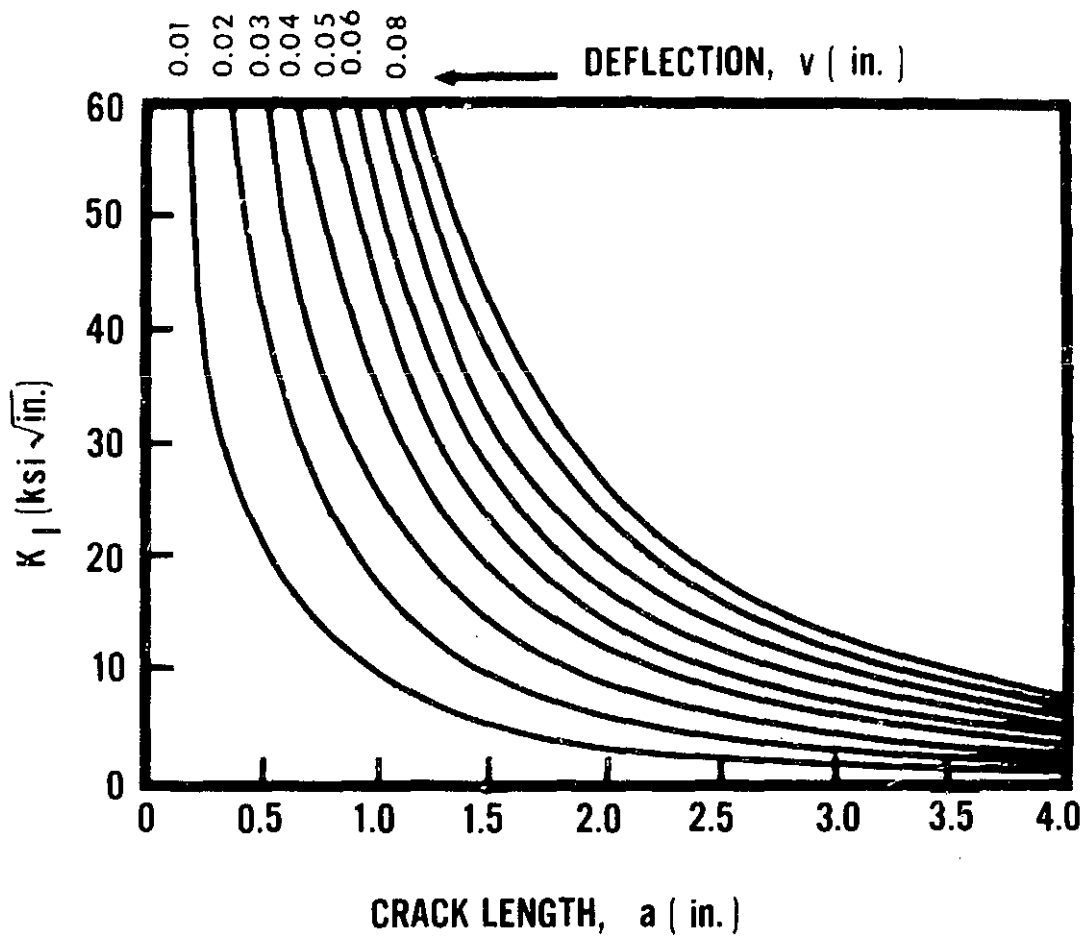


**Fig.10  $K_I$  VERSUS CRACK LENGTH FOR SEVERAL DEFLECTIONS IN ALUMINUM-ALLOY DCB SPECIMENS WITH A  $2h$  VALUE OF 1 in. ( AFTER HYATT (26) )**

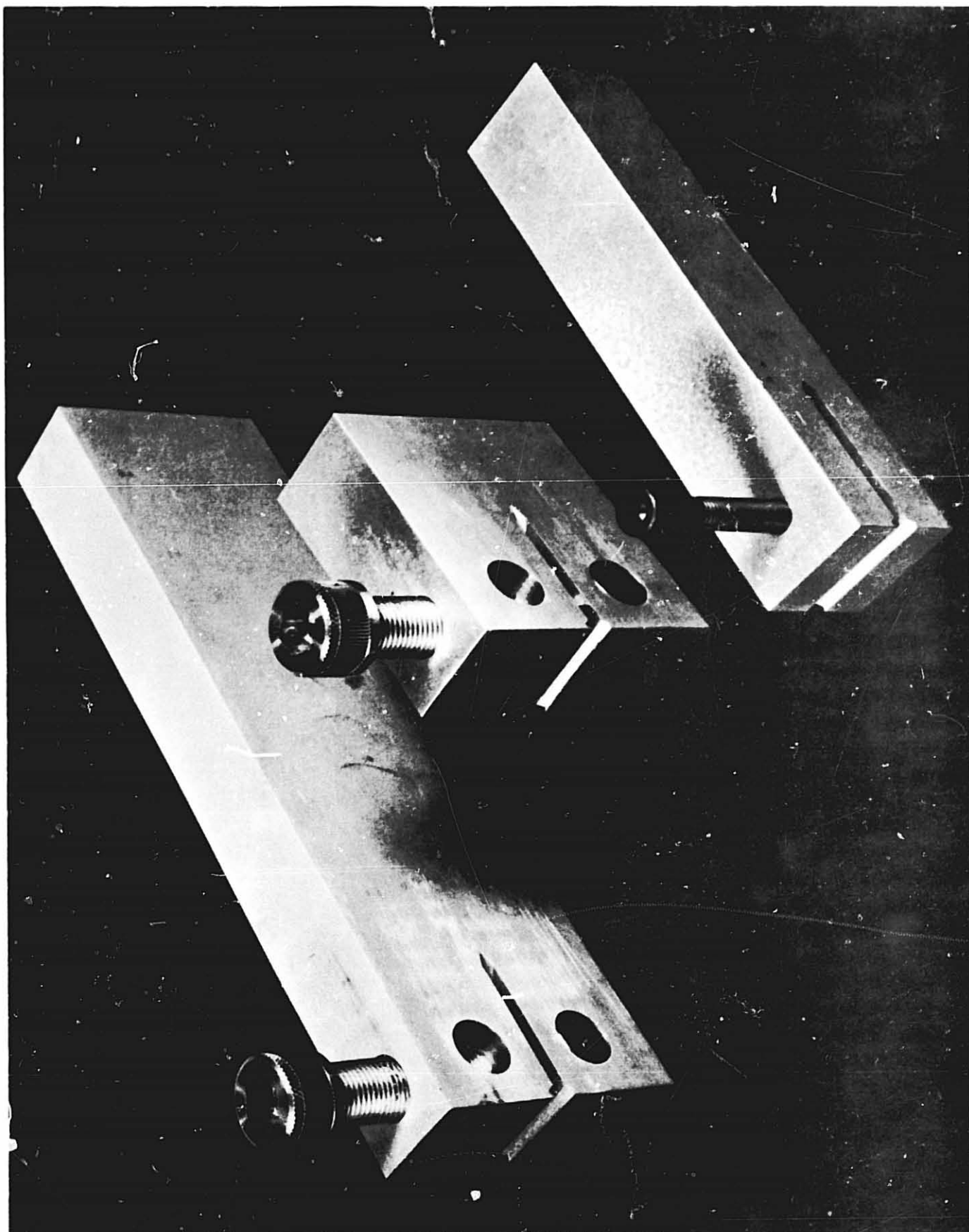


FIG. 11 DOUBLE CANTILEVER BEAM SPECIMENS OF ARL DESIGN (LEFT), BOEING DESIGN (RIGHT) AND COMPACT TENSION SPECIMEN (CENTER)

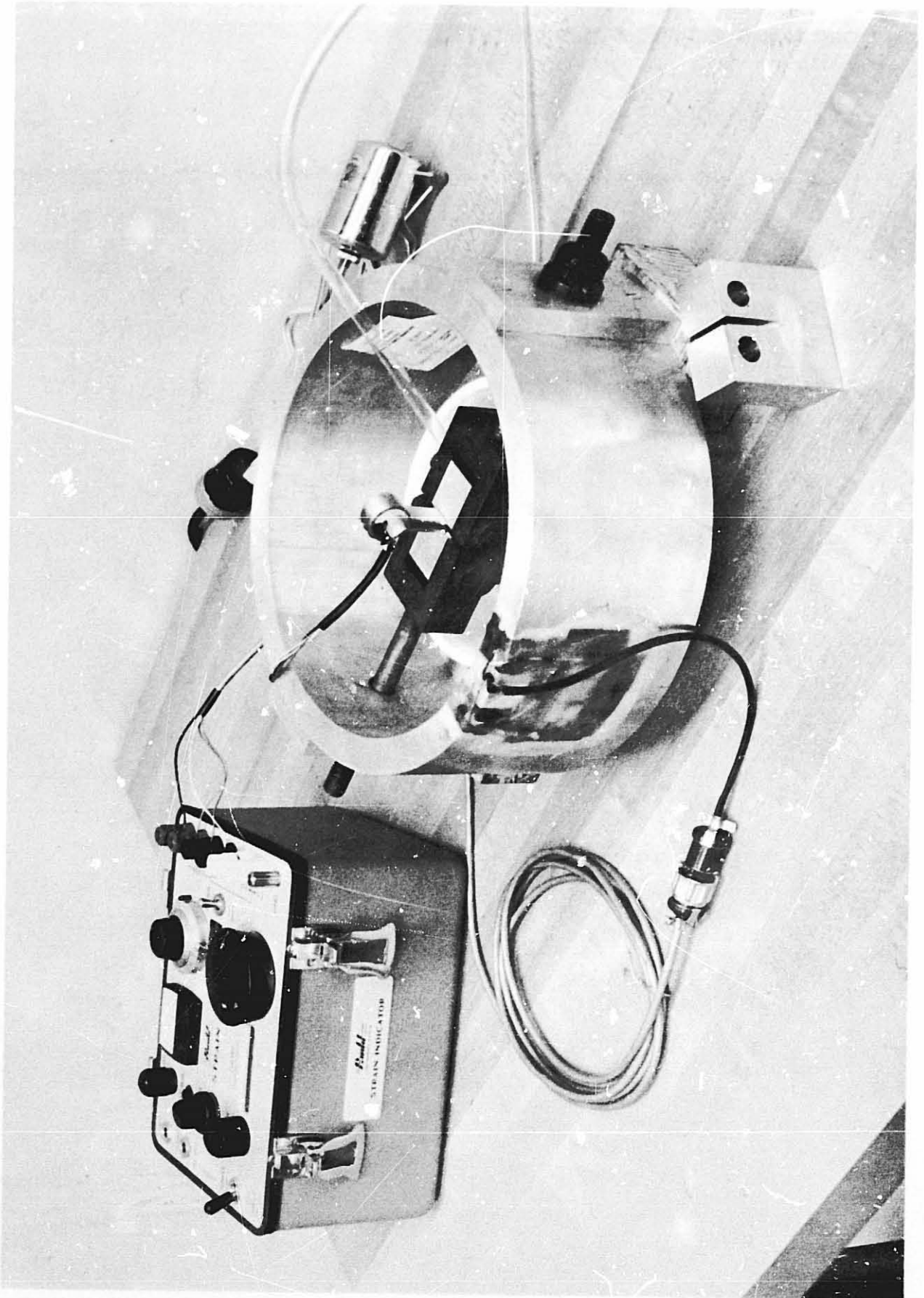


FIG. 12 RING-LOADED PRECRACKED COMPACT TENSION SPECIMEN

EVALUATION NUMBER 1 STRESS CORROSION FRACTURE TOUGHNESS DATA FOR RING LOAD IMPACT TENSION SPECIMENS

ALLOY + TEMPER 7075-T651 PRODUCT PLATE SIZE, IN 2.5 THICK SPEC. LOADED 03-23-71  
 SAMPLE NUMBER 566209 SPECIMEN NUMBER TL-1 MECH. TEST NUMBER 092768A TYPE TEST TI  
 SPECIMEN THICKNESS 1.000 IN SPECIMEN WIDTH 2.000 IN INITIAL CRACK LENGTH 0.990 IN TYPE PRECRACK FC 1/2  
 RING CONSTANT 0.500 IN/LB GAGE CONSTANT 100000. IN/IN MODULUS, KSI 10 0. INTL KI 14660 PSI-IN

TIME, HRS	LOAD(P), LBS	LOAD(V), IN	CRACK LENGTH (A), IN	CRACK GROWTH RATE (ΔA/DT), IN/HR	STR. INT. FACTOR (KI), PSI-IN(1/2)	REMARKS
0	2191.	0.00864	0.888	0.1216E-03	12715.	0.0000E-00
10	2190.	0.00877	0.893	0.7000E-03	12808.	0.5784E-03
20	2188.	0.00895	0.902	0.1011E-02	12943.	0.3116E-03
30	2185.	0.00918	0.912	0.1131E-02	13108.	0.1199E-03
40	2181.	0.00942	0.923	0.1125E-02	13288.	-0.5765E-05
50	2178.	0.00966	0.934	0.1050E-02	13469.	-0.7545E-04
60	2175.	0.00989	0.945	0.9507E-03	13642.	-0.9970E-04
70	2171.	0.01011	0.954	0.8614E-03	13802.	-0.8933E-04
80	2168.	0.01030	0.962	0.8063E-03	13948.	-0.5503E-04
90	2165.	0.01048	0.970	0.7993E-03	14088.	-0.7024E-05
100	2161.	0.01067	0.978	0.8446E-03	14229.	0.4527E-04
110	2157.	0.01087	0.987	0.9382E-03	14385.	0.9362E-04
120	2153.	0.01110	0.997	0.1069E-02	14546.	0.1312E-03
130	2148.	0.01138	1.008	0.1222E-02	14783.	0.1534E-03
140	2144.	0.01170	1.021	0.1380E-02	15043.	0.1573E-03
150	2138.	0.01208	1.036	0.1523E-02	15349.	0.1428E-03
160	2133.	0.01250	1.052	0.1636E-02	15700.	0.1129E-03
170	2127.	0.01295	1.069	0.1709E-02	16088.	0.7361E-04
180	2121.	0.01344	1.086	0.1744E-02	16504.	0.3448E-04
190	2114.	0.01394	1.103	0.1753E-02	16941.	0.9201E-05
200	2106.	0.01445	1.121	0.1769E-02	17396.	0.1569E-04
210	2097.	0.01499	1.139	0.1845E-02	17884.	0.7654E-04
220	2086.	0.01560	1.158	0.2064E-02	18445.	0.2193E-03
230	2074.	0.01638	1.181	0.2541E-02	19164.	0.4769E-03
240	2059.	0.01745	1.211	0.3429E-02	20184.	0.8880E-03
248	2045.	0.01868	1.242	0.4567E-02	21362.	0.1137E-02

CALCULATED SIF BASED ON MEASURED (A) AFTER FRACTURE

23089.

STANDARD ERROR = 0.4214052

LOAD = 0.1095E 04+ 0.3124E-01T+ -0.7680E-02T\*\*2+ 0.1433E-03T\*\*3+ -0.1393E-05T\*\*4+ 0.7107E-08T\*\*5  
 + -0.1822E-10T\*\*6+ 0.1815E-13T\*\*7+

CND = 0.8648E 03+ 0.4379E 00T+ 0.3715E-01T\*\*2+ -0.9484E-04T\*\*3+ -0.7191E-05T\*\*4+ 0.8756E-07T\*\*5  
 + -0.3743E-09T\*\*6+ 0.5561E-12T\*\*7+

A = 0.8882E 00+ 0.1216E-03T+ 0.3694E-04T\*\*2+ -0.5819E-06T\*\*3+ 0.3601E-08T\*\*4+ -0.5193E-11T\*\*5  
 + -0.2498E-13T\*\*6+ 0.6918E-16T\*\*7+

TYPICAL COMPUTER PRINT-OUT OF STRESS INTENSITIES AND CRACK GROWTH RATES AT VARIOUS INTERVALS DURING THE TEST

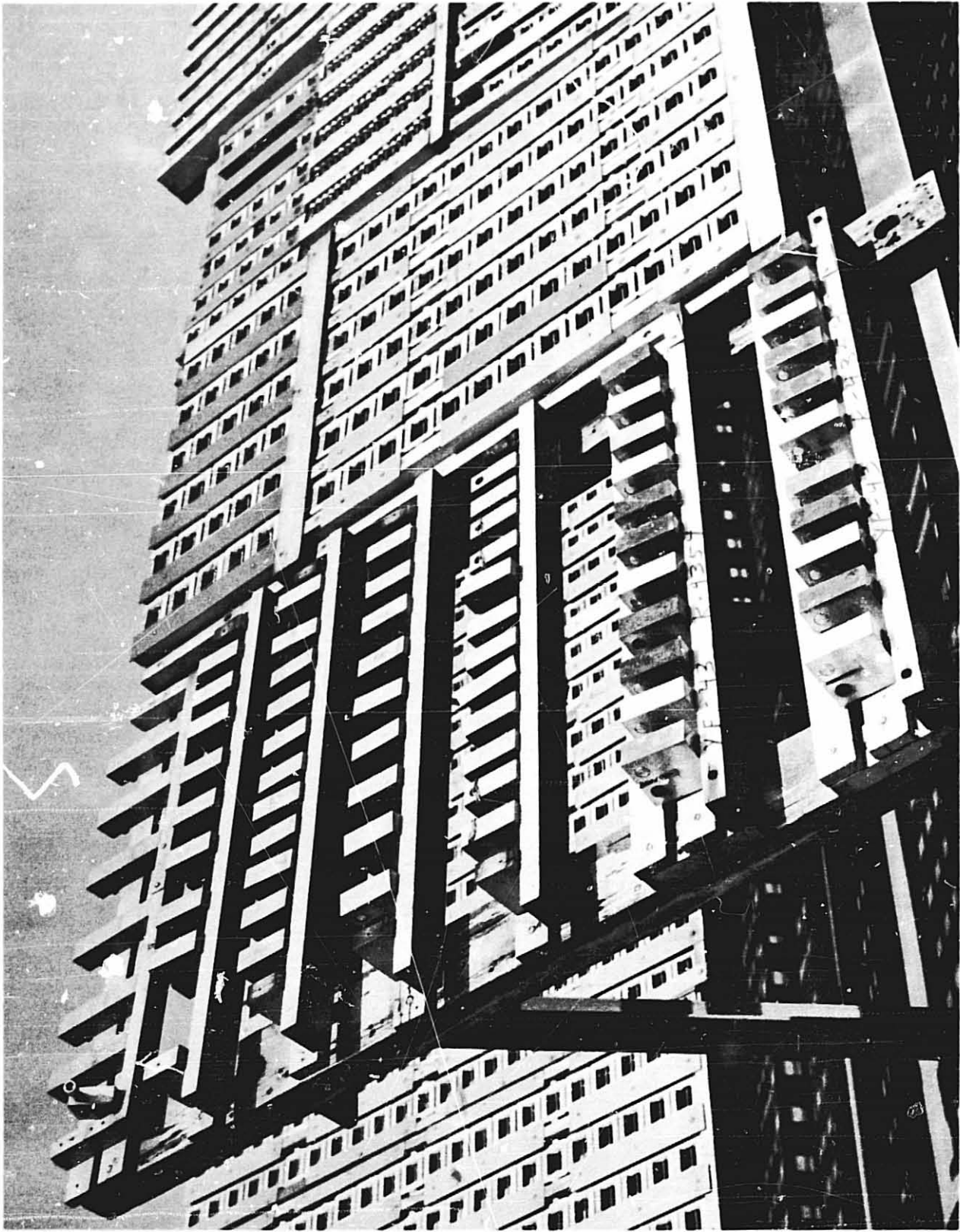


FIG. 16 VIEW OF PORTION OF AN EXPOSURE RACK IN THE INDUSTRIAL ATMOSPHERIC TEST SITE AT NEW KENSINGTON, PA., SHOWING MANNER OF EXPOSURE OF TEST SPECIMENS IN THIS INVESTIGATION.

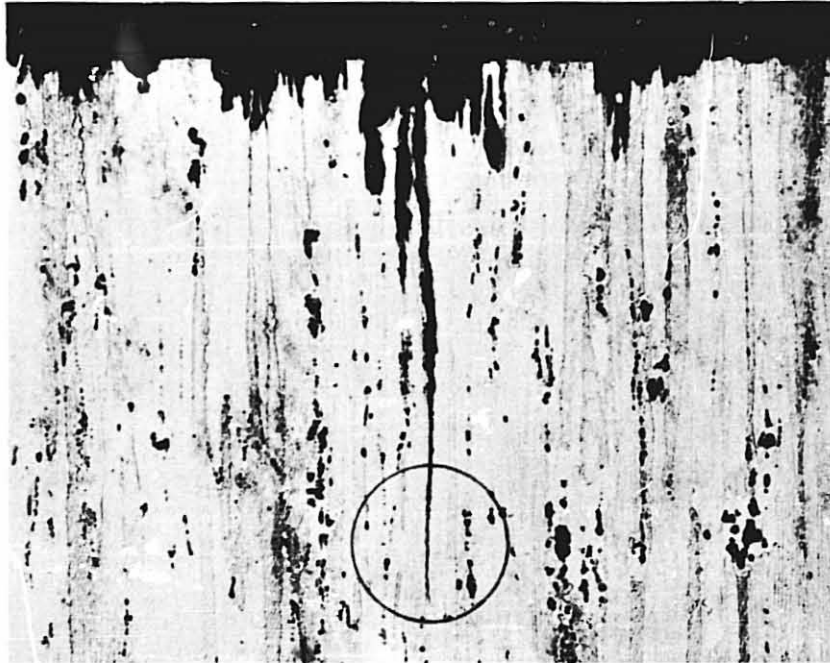


FIG. 17a DIRECTIONAL PITTING PLUS SECONDARY SCC IN S.T. TENSION SPECIMEN OF 2024 - T851 (366207 - N5) THAT FAILED AFTER 8 DAYS EXPOSURE TO 3.5% NaCl - A.I. AT A STRESS OF 75% Y.S. KELLER'S ETCH (100X)

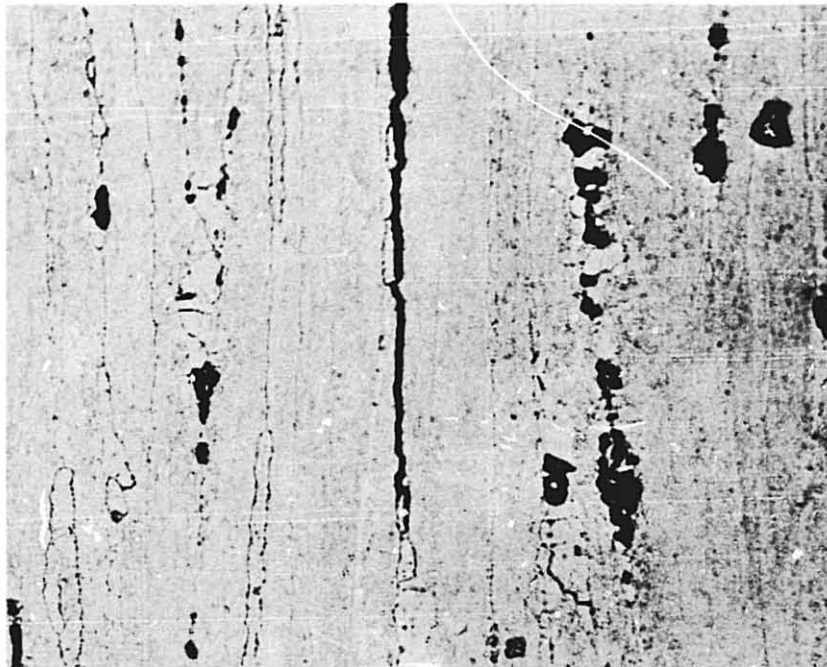


FIG. 17b HIGHER MAGNIFICATION (500X) OF THE REGION CIRCLED ABOVE SHOWING THE INTERGRANULAR NATURE OF THE SECONDARY CRACK. SEVERAL CRACKS OF THIS TYPE WERE DETECTED IN EACH OF THE THREE 2024 - T851 SPECIMENS THAT FAILED AT 75% Y.S.

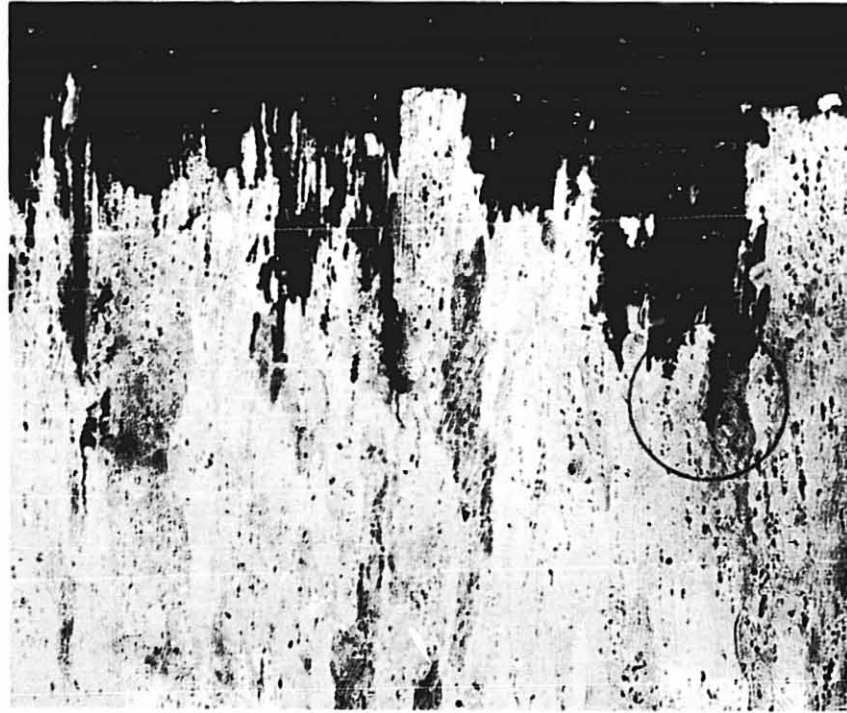


FIG. 18a DEEP DIRECTIONAL PITTING IN S.T. TENSION SPECIMEN OF 2219 - T87 (338148 - N8) THAT FAILED AFTER 42 DAYS EXPOSURE TO 3.5% NaCl - A.I. AT A STRESS OF 75% Y.S. KELLER'S ETCH (100X)

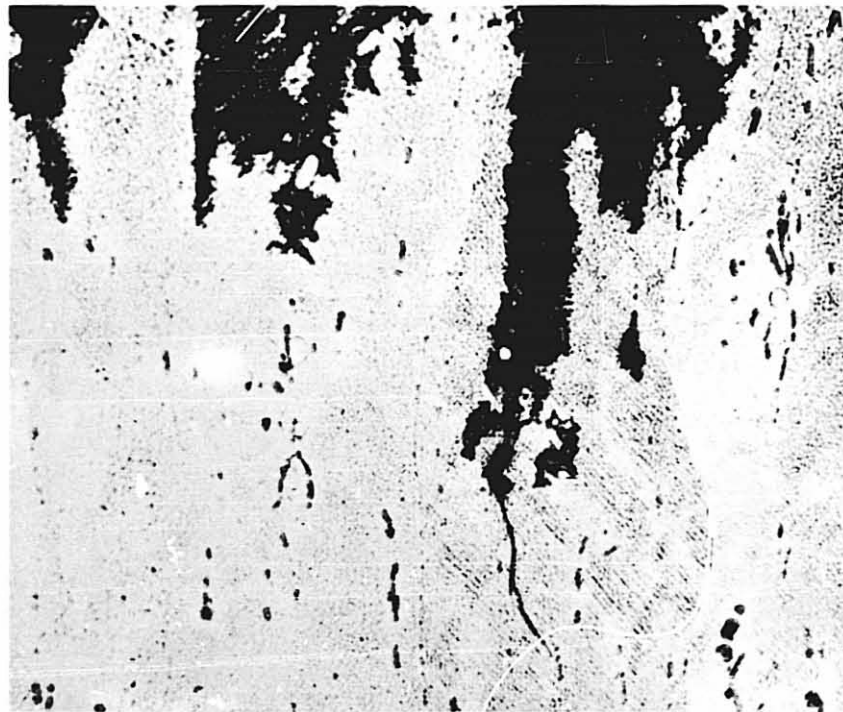


FIG. 18b HIGHER MAGNIFICATION (500X) OF THE REGION CIRCLED ABOVE SHOWING A TRANSGRANULAR CRACK EMANATING FROM A SITE OF DEEP PITTING. SIMILAR ATTACK AND TRANSGRANULAR CRACKING WAS FOUND IN THE 2219 - T87 SPECIMEN THAT FAILED AFTER 76 DAYS (SEE FIG. 20).

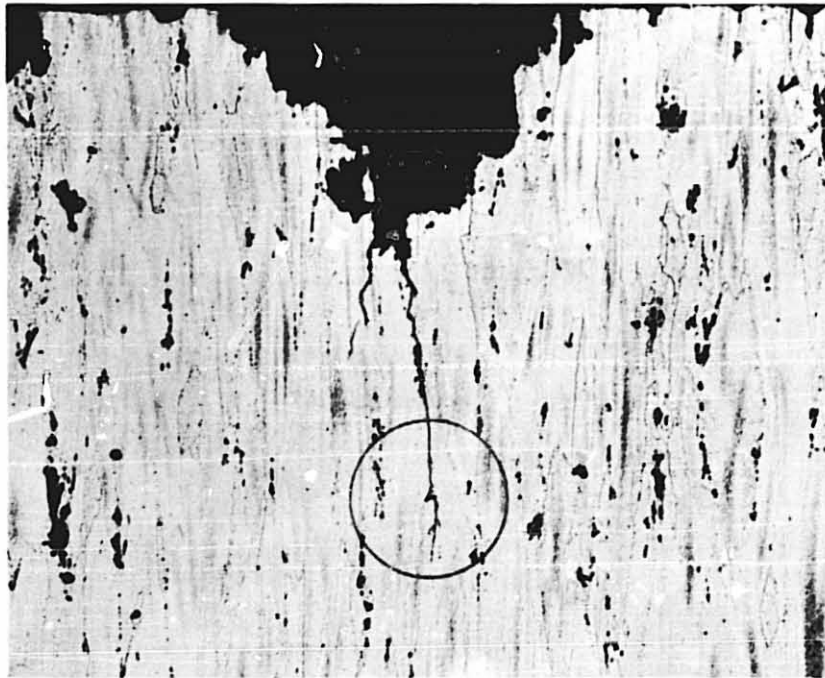
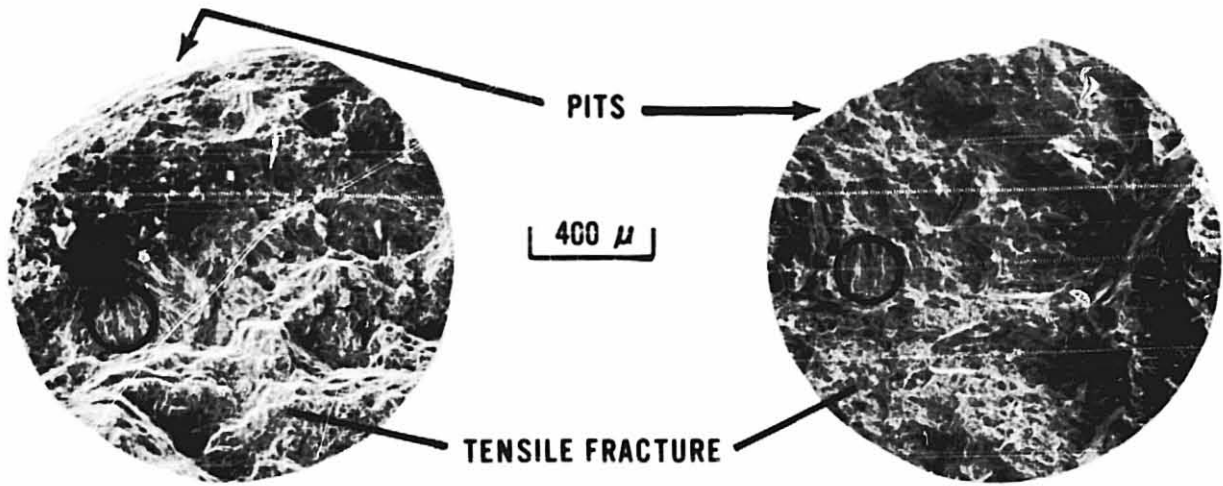


FIG. 19a DEEP PITTING IN THE S.T. TENSION SPECIMEN OF 7075 - T7351 (366210 - N6) THAT FAILED AFTER 80 DAYS EXPOSURE TO 3.5% NaCl - A.I. AT A STRESS OF 75% Y.S. TWO MIXED-MODE CRACKS EMANATE FROM THE PIT. KELLER'S ETCH (100X)



FIG. 19b HIGHER MAGNIFICATION (500X) OF THE REGION CIRCLED ABOVE SHOWING BOTH INTERGRANULAR AND TRANSGRANULAR TENDENCIES AT THE TIP OF THE CRACK (SEE FIG. 20).



2219-T87

7075-T7351

**Fig. 20 SEM FRACTOGRAPHS OF S.T. TENSION SPECIMENS STR. 75% Y.S. EXPOSED 84 DAYS TO 3.5% NaCl A.I. AND TENSILE TESTED. FRACTURE FACES OF TG CRACKS OF TYPE SHOWN IN Fig. 18b AND 19b.**

CORRODENTS

- ♦ - DISTILLED WATER (CONTROL) INITIAL pH 6.0
- △ - 0.6M NaCl (3.5%) (CONTROL) INITIAL pH 6.8
- ▽ - SYNTHETIC SEAWATER (CONTROL) INITIAL pH 8.2
- - 0.6M NaCl + 0.03M Na<sub>2</sub>CrO<sub>4</sub> INITIAL pH 7.8
- - 0.6M NaCl + 0.3M Na<sub>2</sub>CrO<sub>4</sub> INITIAL pH 8.2
- ▲ - 0.6M NaCl + 0.002M Na<sub>2</sub>Cr<sub>2</sub>O<sub>7</sub> + 0.07M NaC<sub>2</sub>H<sub>3</sub>O<sub>2</sub> + HC<sub>2</sub>H<sub>3</sub>O<sub>2</sub> TO pH 4.0
- ▼ - 0.6M NaCl + 0.03M K<sub>2</sub>Cr<sub>2</sub>O<sub>7</sub> + 0.07M CrO<sub>3</sub> INITIAL pH 1.3
- - 0.6M NaCl + 0.25M NaNO<sub>3</sub> + HNO<sub>3</sub> TO pH 3.0
- - 0.6M NaCl + 0.125M Na<sub>2</sub>SO<sub>4</sub> + H<sub>2</sub>SO<sub>4</sub> TO pH 3.0

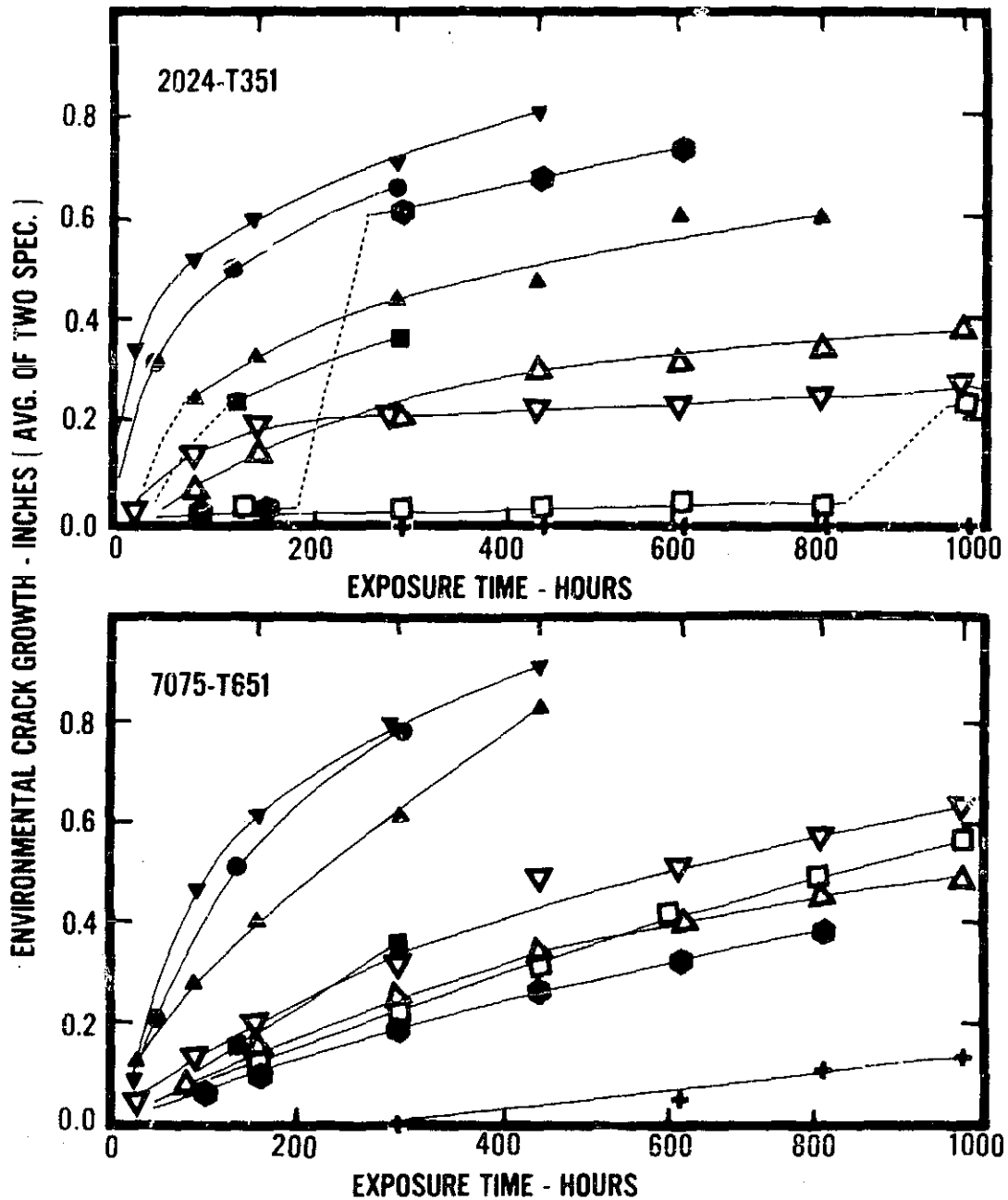


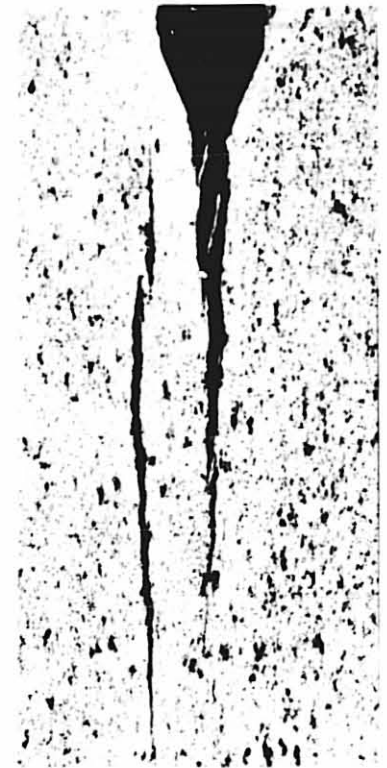
Fig. 21 COMPARISON OF ENVIRONMENTAL CRACK GROWTH IN VARIOUS CORRODENTS OF S-L COMPACT TENSION SPECIMENS BOLT LOADED TO POP-IN.



2024 - T351



2024 - T351



7075 - T651

FIG. 22 MACROGRAPHS ILLUSTRATING MULTIPLE CRACKING THAT OCCURRED ON THE COMPACT TENSION SPECIMENS IMMERSSED IN SOME CORRODENTS. THIS DID NOT OCCUR IN THE SALT-DICHROMATE-ACETATE SOLUTION CHOSEN FOR THE GENERAL TEST PROGRAM. (MAG. 3X)

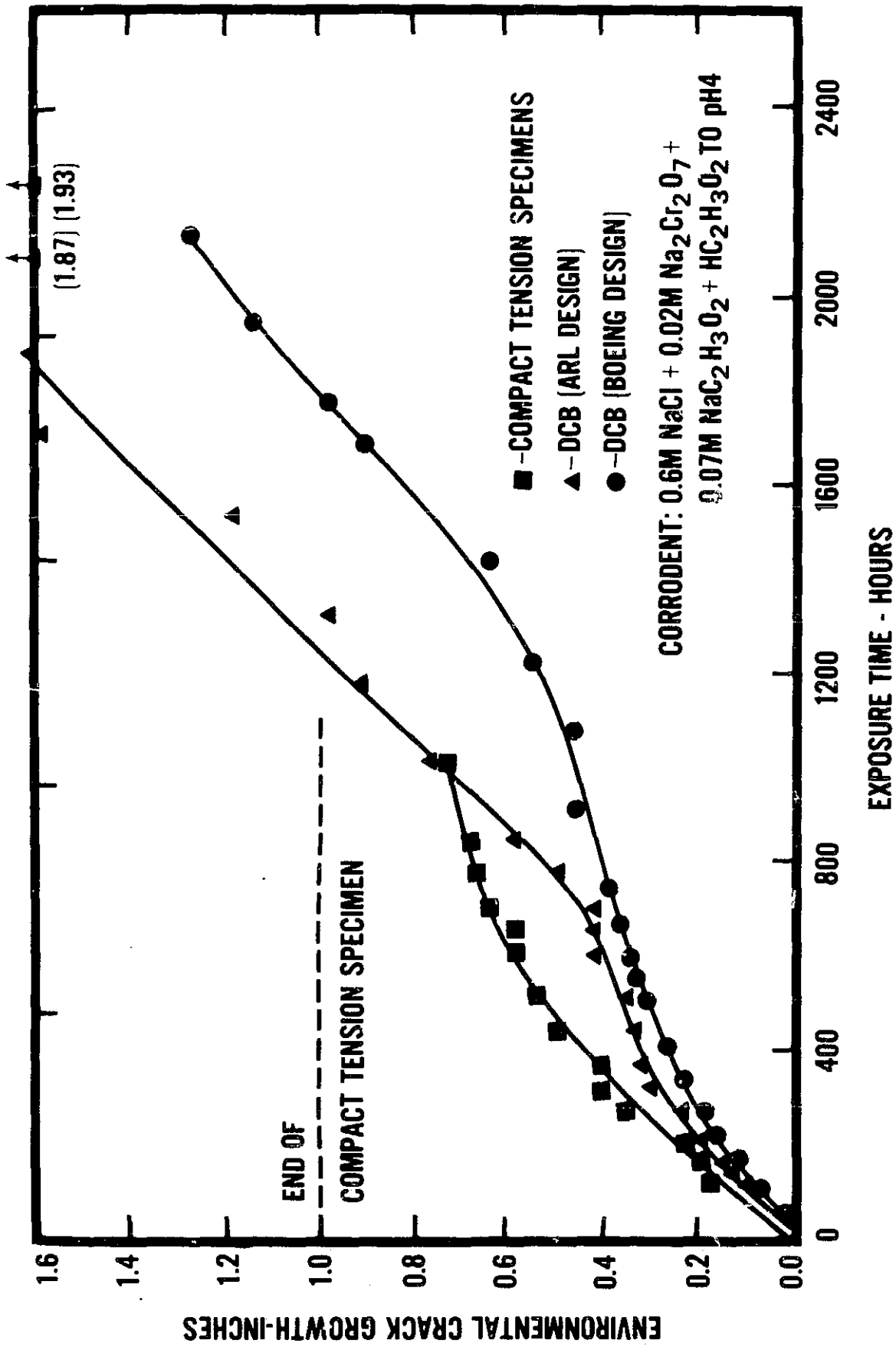


Fig.23 COMPARISON OF ENVIRONMENTAL CRACK GROWTH IN THREE TYPES  
 OF S-L SPECIMENS OF 7075-T651 BOLT LOADED TO POP-IN

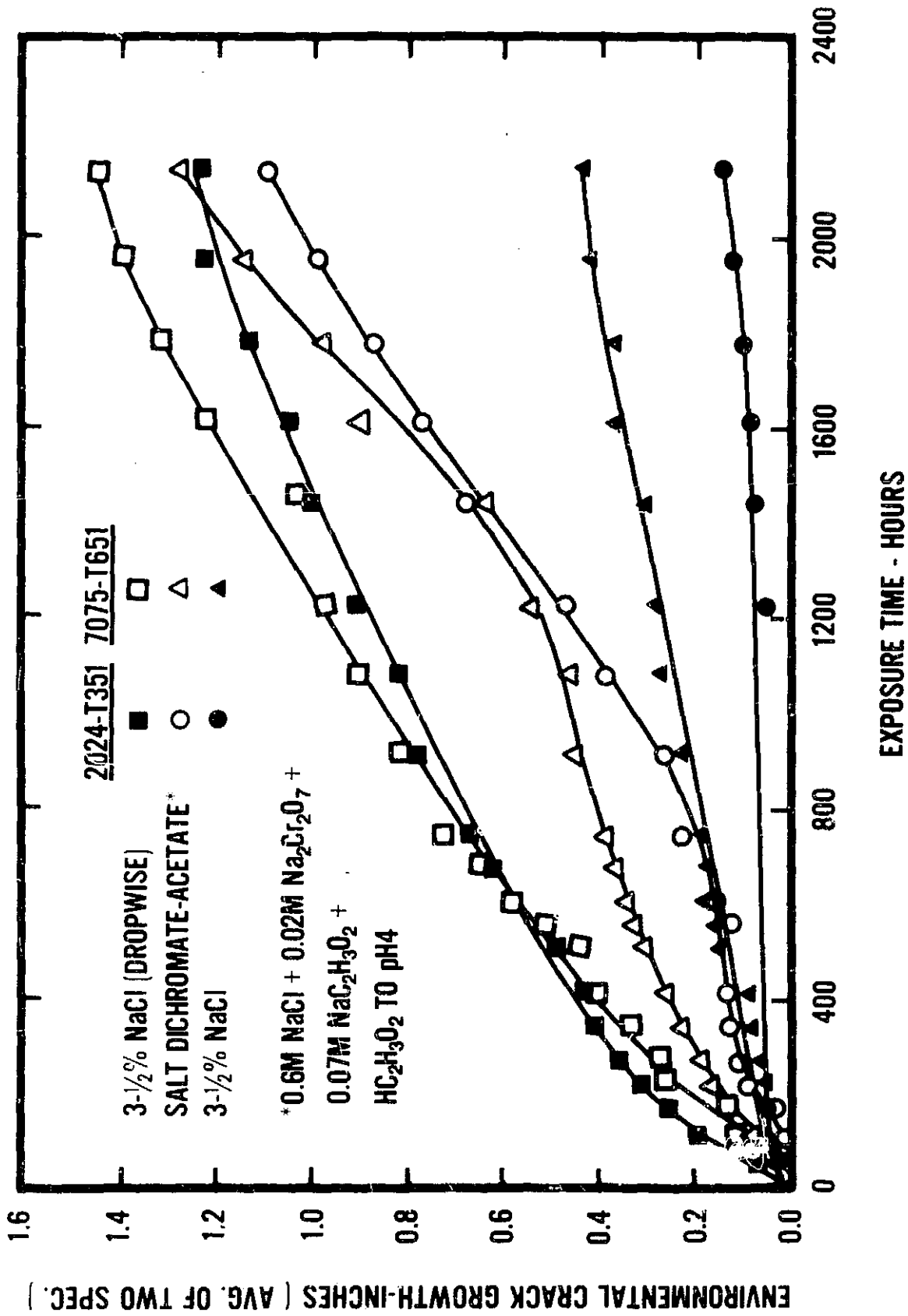
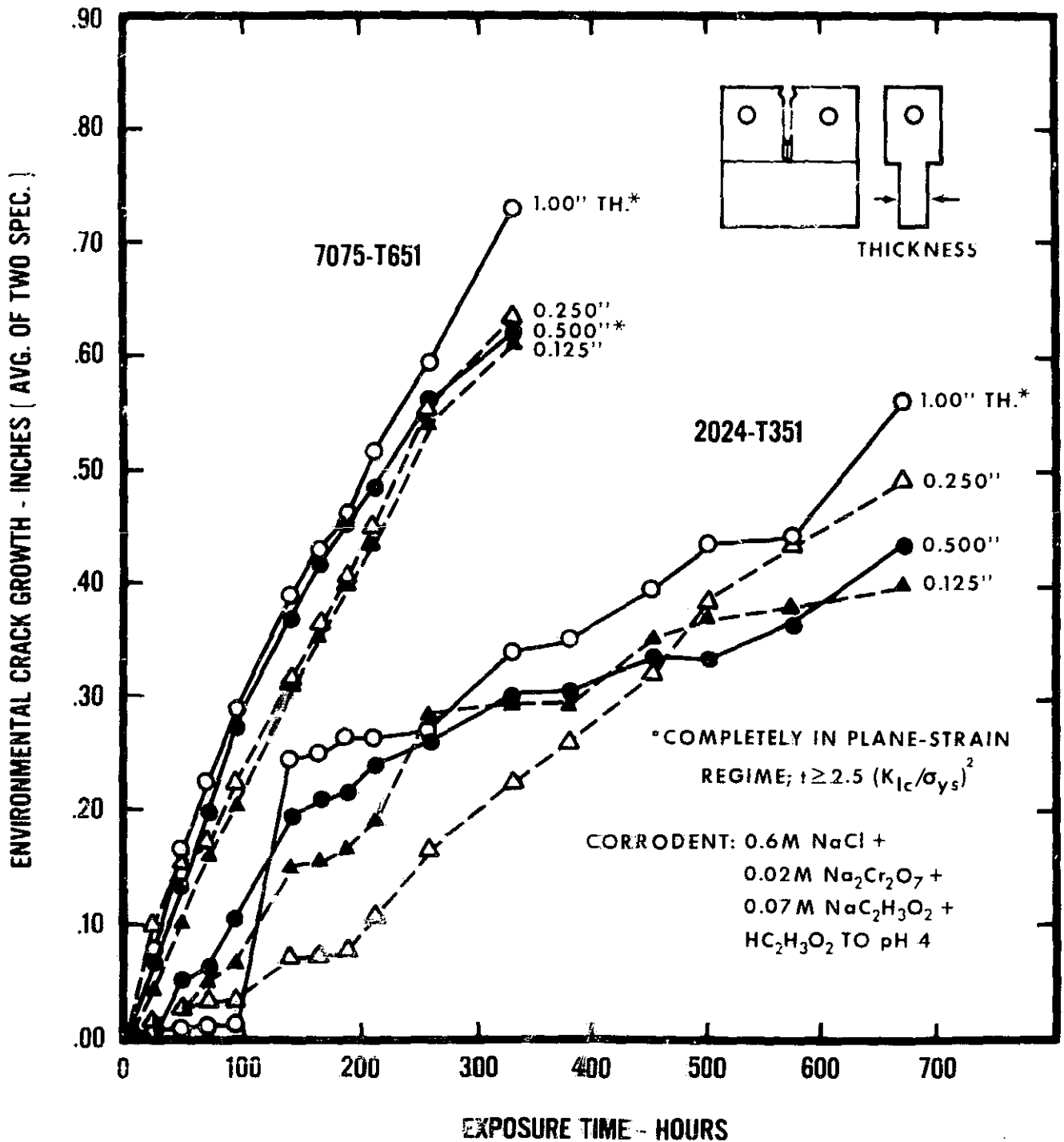


Fig.24 ENVIRONMENTAL CRACK GROWTH IN S-L DCB SPECIMENS ( BOEING DESIGN )  
 BOLT LOADED TO POP-IN AND EXPOSED TO VARIOUS CORRODENTS.



**Fig. 25 EFFECT OF SPECIMEN THICKNESS ON ENVIRONMENTAL CRACK GROWTH IN S-L COMPACT TENSION SPECIMENS BOLT LOADED TO POP-IN**

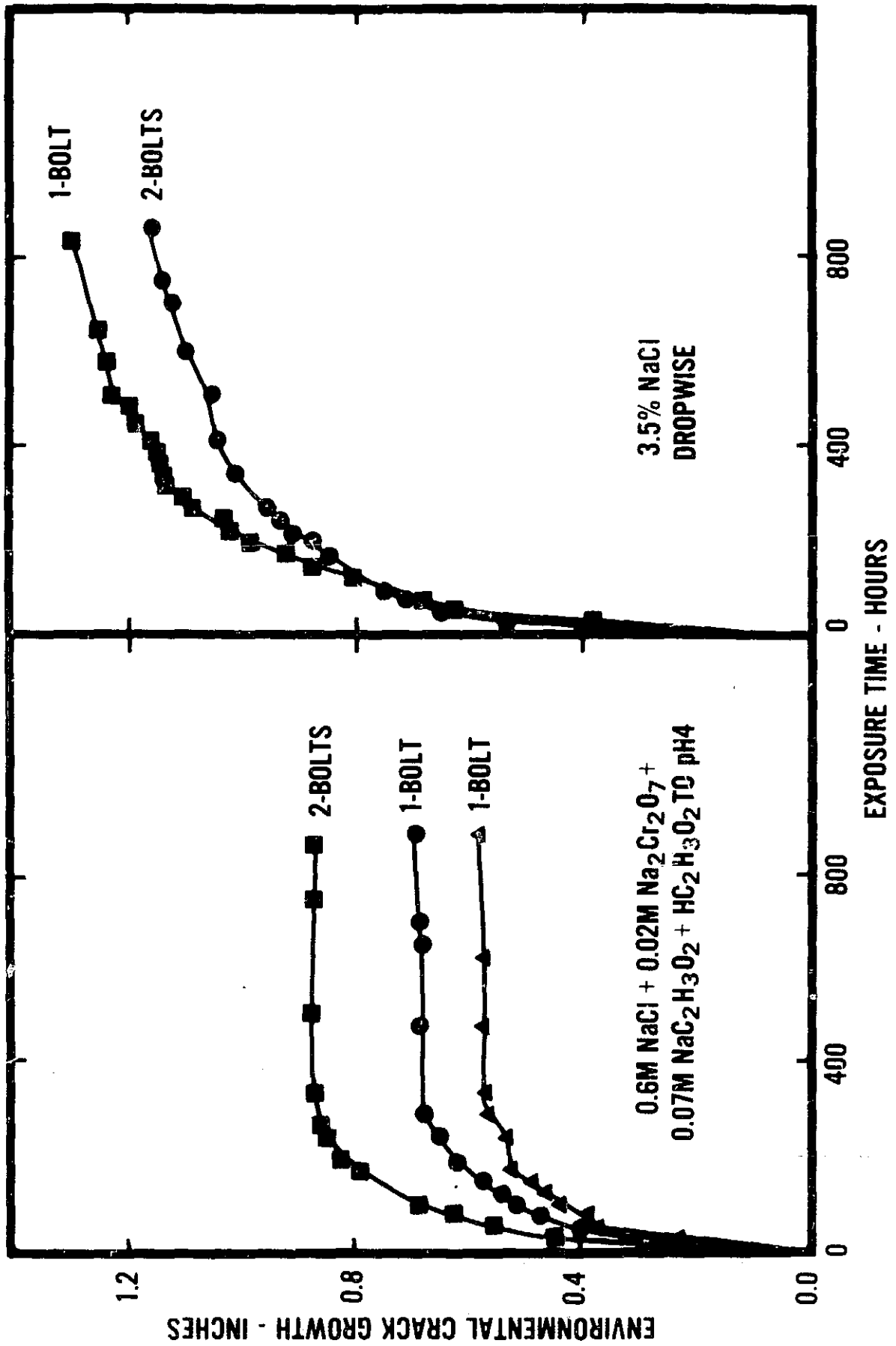
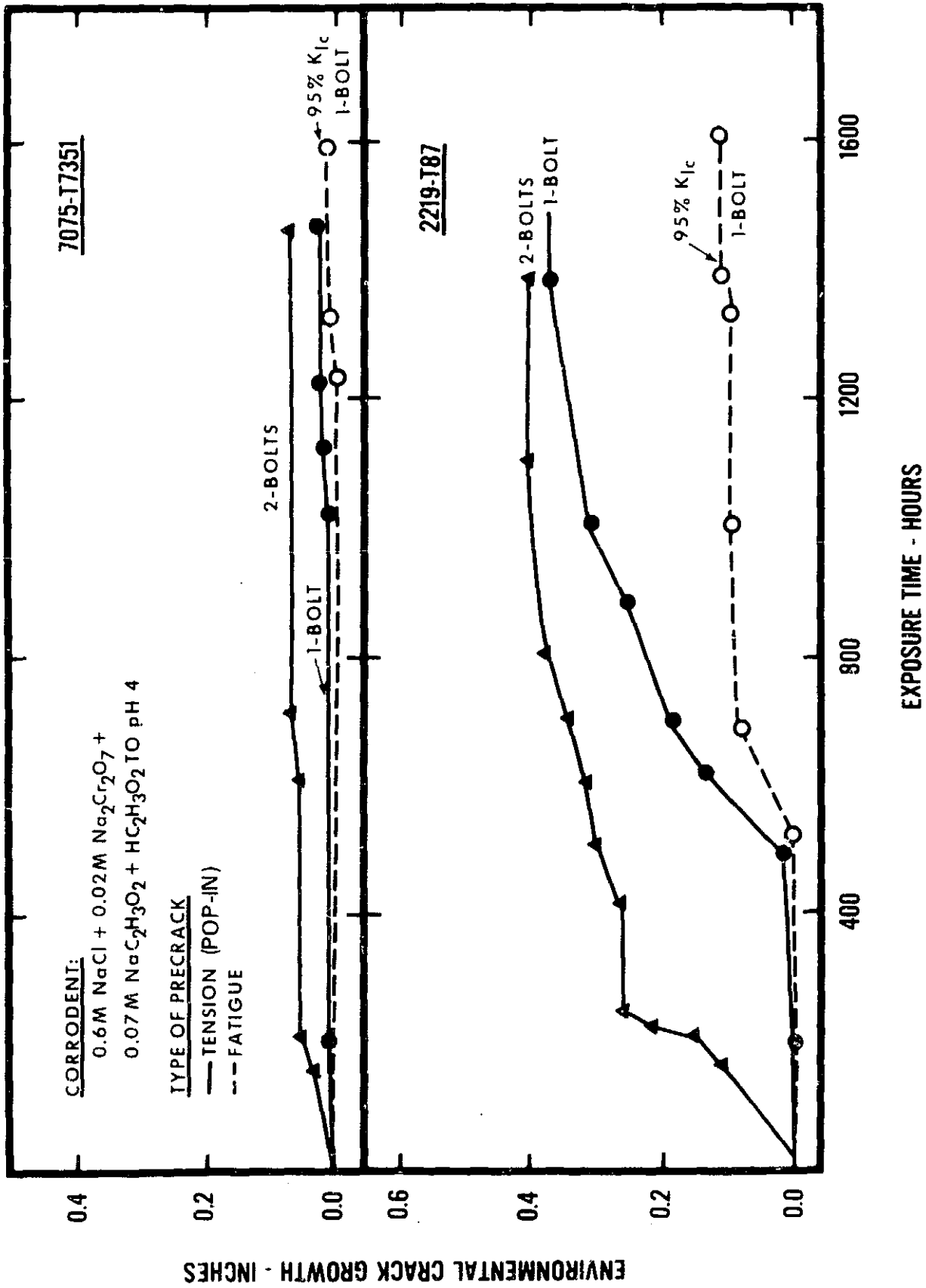
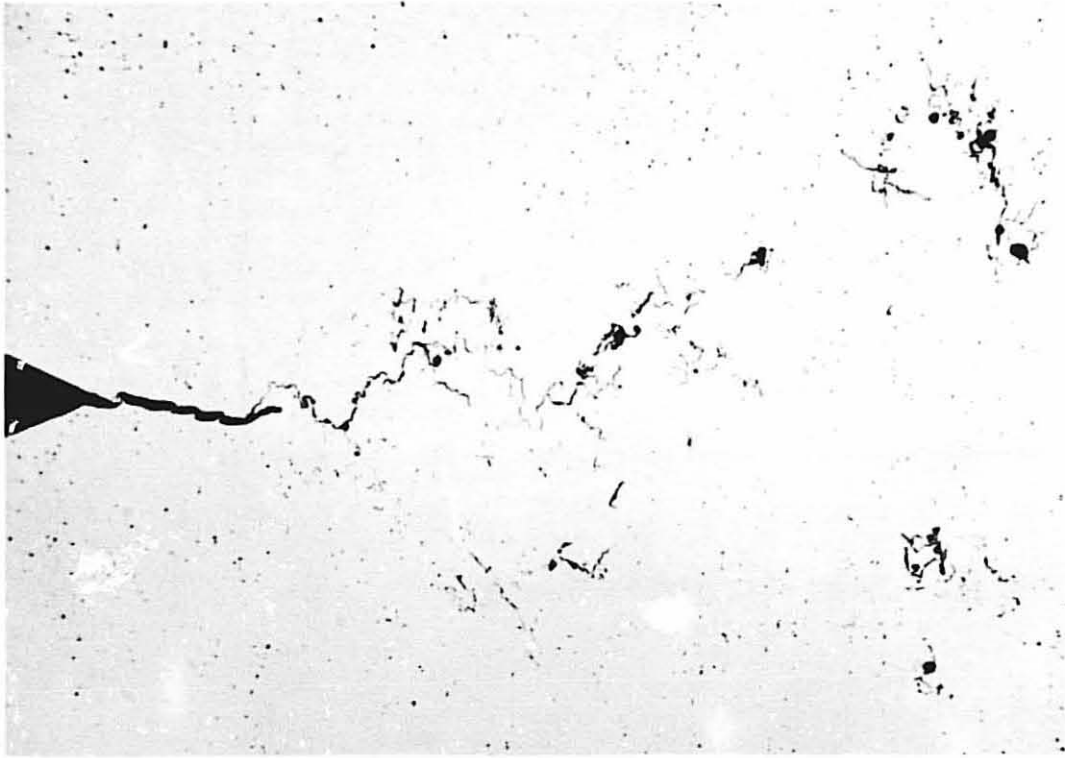


Fig. 26 COMPARISON OF 2-BOLT VS 1-BOLT LOADING FOR BOEING DCB SPECIMENS OF 7079-T651 S-L SPECIMENS BOLT LOADED TO POP-IN

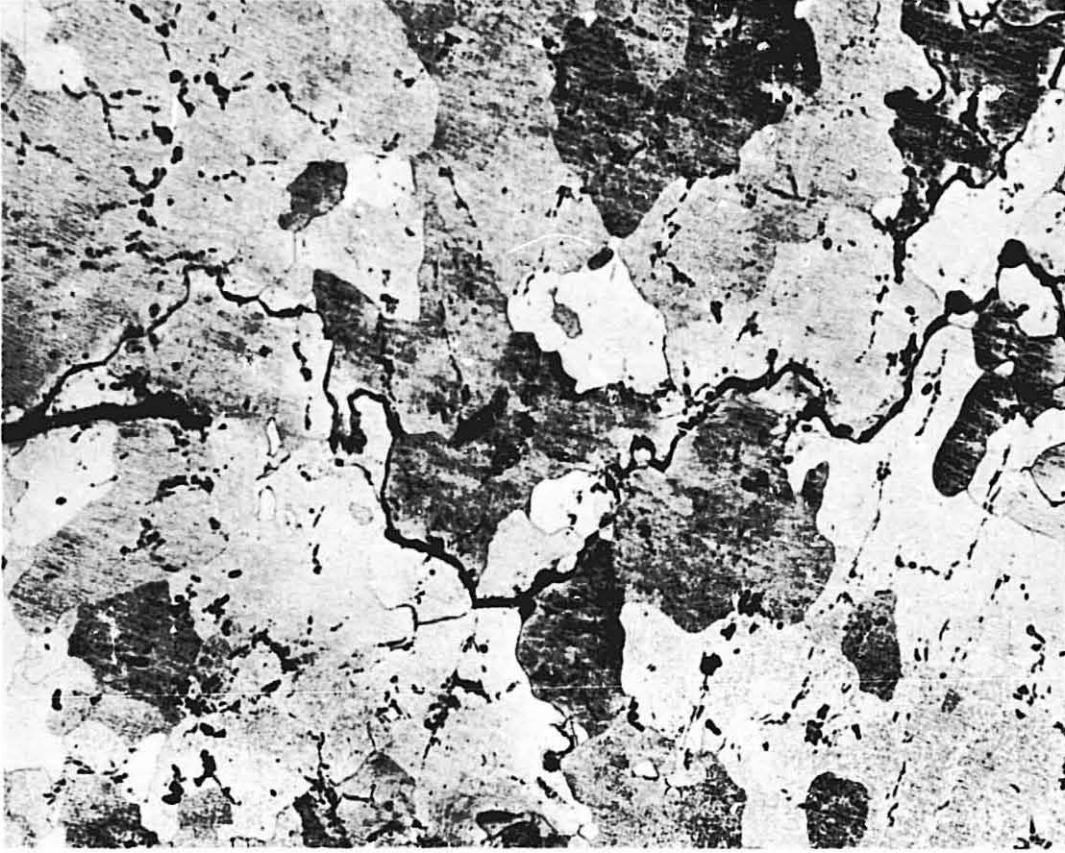


**Fig. 27 EFFECT OF TYPE OF PRECRACK AND METHOD OF LOADING ON ENVIRONMENTAL CRACK GROWTH IN S-L COMPACT TENSION SPECIMENS**



AS POLISHED

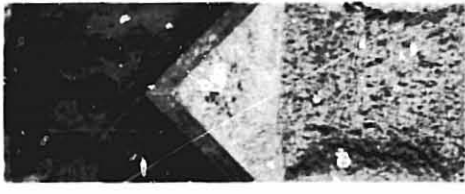
20x



KELLER'S ETCH

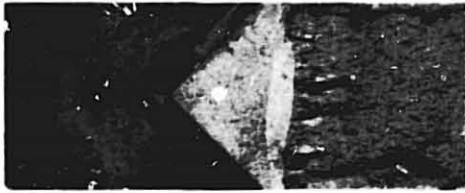
100x

**Fig. 28 BRANCHING INTERGRANULAR SCC AT TIP OF FATIGUE PRECRACK IN L-T COMPACT TENSION SPECIMEN OF 2219 -T37 LOADED TO 95%  $K_{Ic}$  AND EXPOSED 5 mo TO SEACOAST ATMOSPHERE**



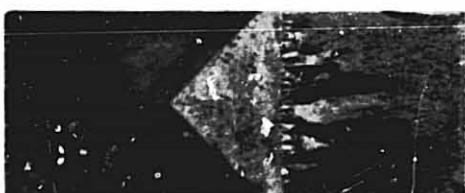
7075-T7351

96



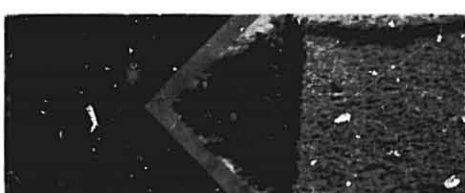
7075-T651

80



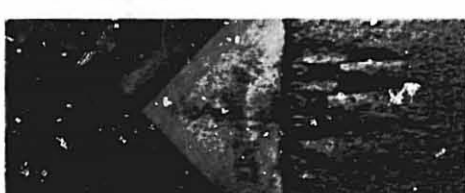
7039-T6351

84



2024-T851

80



2024-T351

81



2014-T651

87

**Fig .29 FRACTURE SURFACES OF L-T COMPACT TENSION SPECIMENS LOADED TO 95%  $K_{Ic}$  AND EXPOSED 90 DAYS TO SALT-DICHROMATE-ACETATE. THE  $K_{Ic}$  VALUE EXPRESSED AS %  $K_{Ic}$  IS SHOWN FOR EACH SPECIMEN.**



7039-T6351  
91

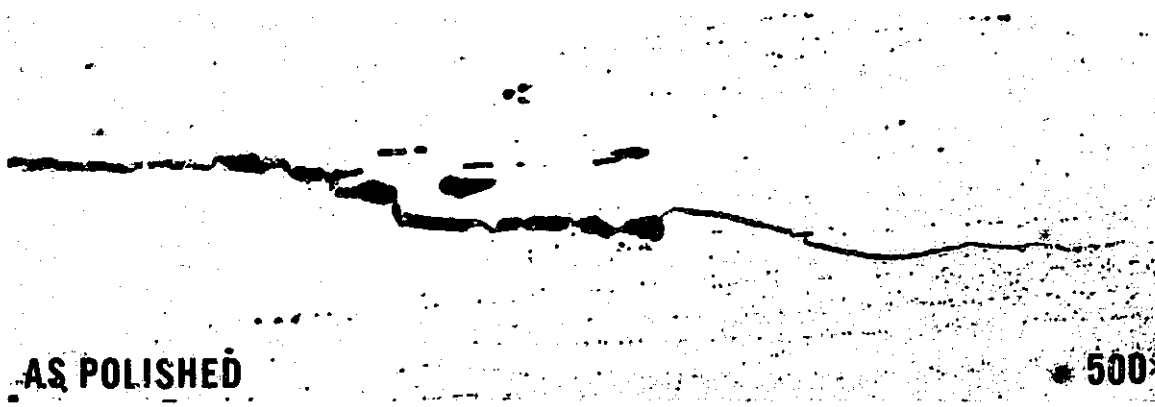
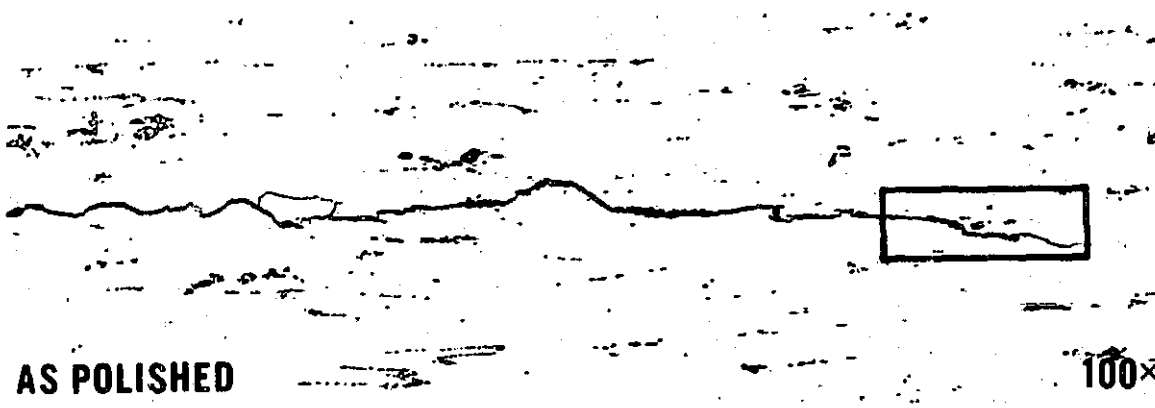


7075-T651  
94



7079-T651  
84

**Fig. 30 FRACTURE SURFACES OF S-L COMPACT TENSION SPECIMENS EXPOSED WITH NO LOAD FOR 8.3 mo TO SEACOAST ATMOSPHERE. THE  $K_{I,x}$  VALUE EXPRESSED AS %  $K_{Ic}$  IS SHOWN FOR EACH SPECIMEN.**



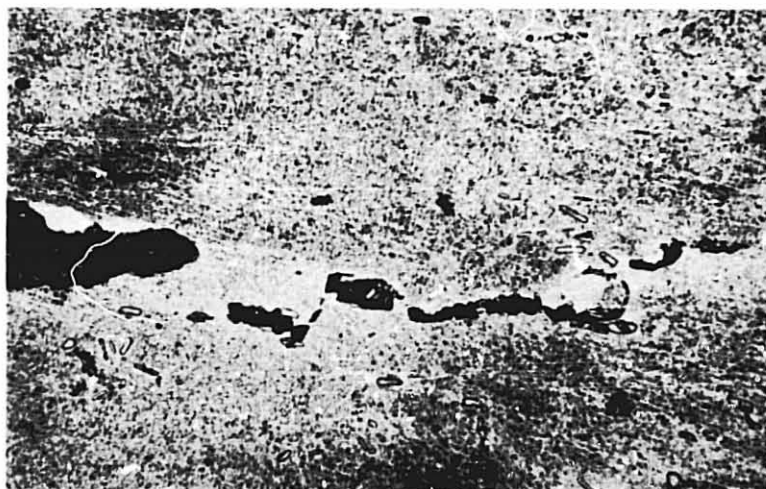
**Fig. 31 FATIGUE PRECRACK IN S-L COMPACT TENSION SPECIMEN OF 7075-T7351**



Fig. 32 S-L COMPACT TENSION SPECIMEN OF 7075-T7351 LOADED TO 95%  $K_{Ic}$  AND EXPOSED 15 mo TO SEACOAST ATMOSPHERE. INTERGRANULAR SCC EXTENDING BEYOND TIP OF FATIGUE PRECRACK.



100×



500×

**Fig. 33 S-L COMPACT TENSION SPECIMEN OF 2219-T87 LOADED TO 95%  $K_{Ic}$  AND EXPOSED 15 mo TO SEACOAST ATMOSPHERE. TRANSGRANULAR MECHANICAL TEARING EXTENDING BEYOND TIP OF THE CRACK. KELLER'S ETCH.**

**BOLT LOADED S-L COMPACT TENSION SPECIMENS**

$\Delta$  75%  $K_{Ic}$ ,  $\circ$  50%  $K_{Ic}$ ,  $\square$  25%  $K_{Ic}$

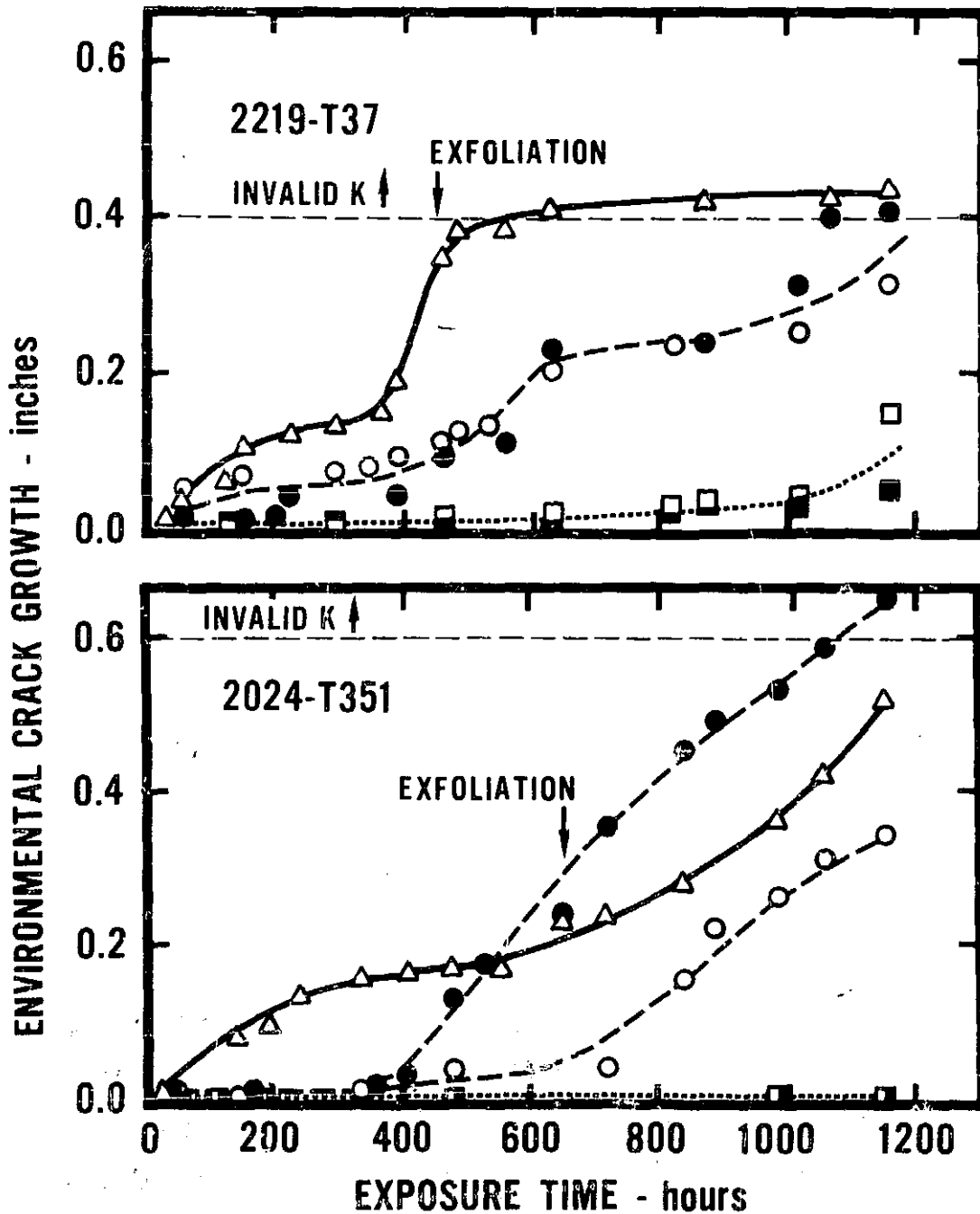


**Fig. 34 ENVIRONMENTAL CRACK GROWTH OF VARIOUS ALUMINUM ALLOYS IN SALT-DICHROMATE-ACETATE SOLUTION**

**BOLT LOADED S-L COMPACT TENSION SPECIMENS**

$\Delta$  75%  $K_{Ic}$ ,  $\circ$ ● 50%  $K_{Ic}$ ,  $\square$ ■ 25%  $K_{Ic}$

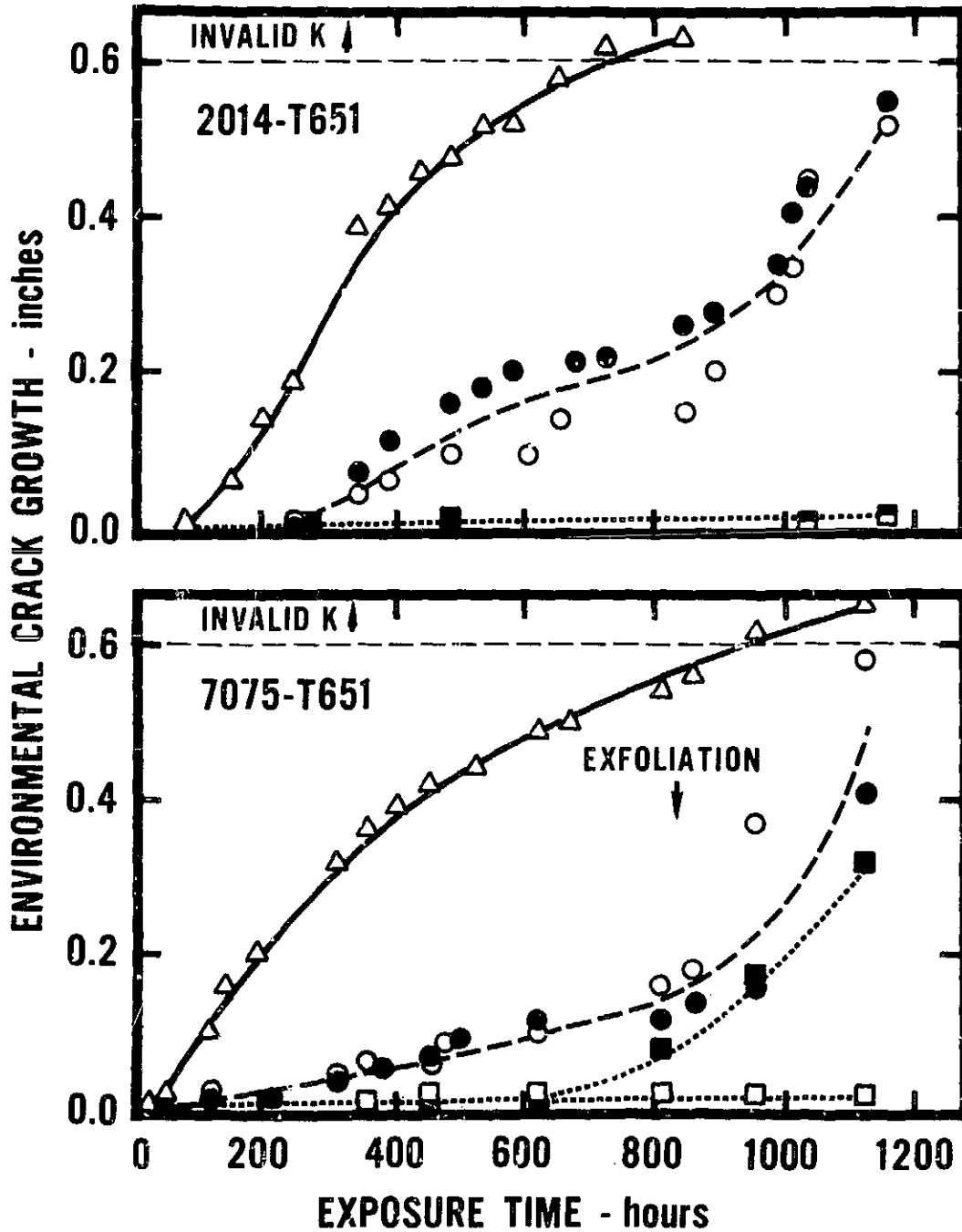


**Fig. 35 ENVIRONMENTAL CRACK GROWTH OF VARIOUS ALUMINUM ALLOYS IN SALT-DICHROMATE-ACETATE SOLUTION**

**BOLT LOADED S-L COMPACT TENSION SPECIMENS**  
 $\Delta$ 75%  $K_{Ic}$ ,  $\bullet$  $\circ$ 50%  $K_{Ic}$ ,  $\blacksquare$  $\square$ 25%  $K_{Ic}$

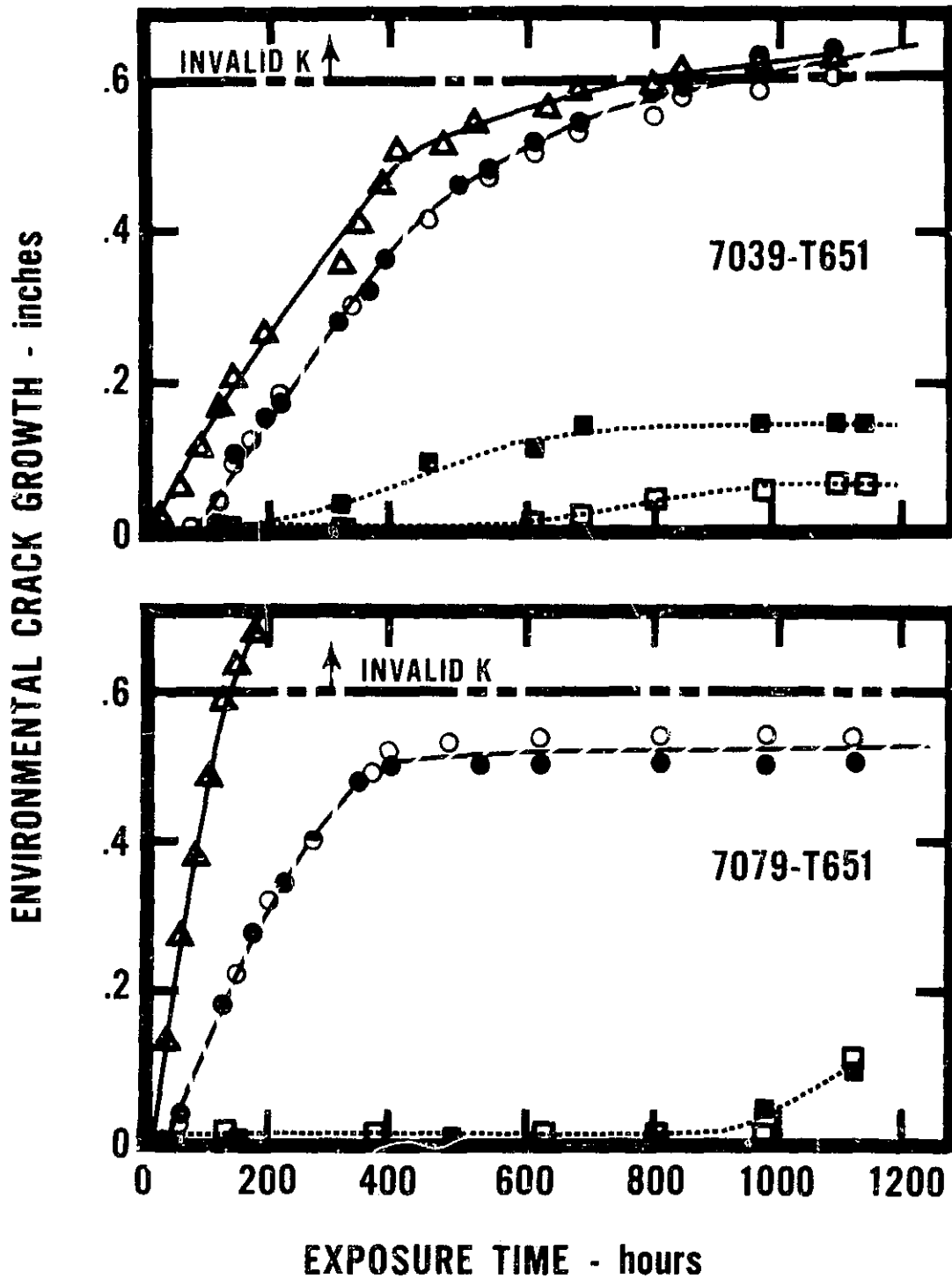


**Fig. 36 ENVIRONMENTAL CRACK GROWTH OF VARIOUS ALUMINUM ALLOYS IN SALT-DICHROMATE ACETATE SOLUTION**

**BOLT LOADED S-L COMPACT TENSION SPECIMENS**

**△ 75%  $K_{Ic}$ , ○● 50%  $K_{Ic}$ , □■ 25%  $K_{Ic}$**

**5456 - SENSITIZED**

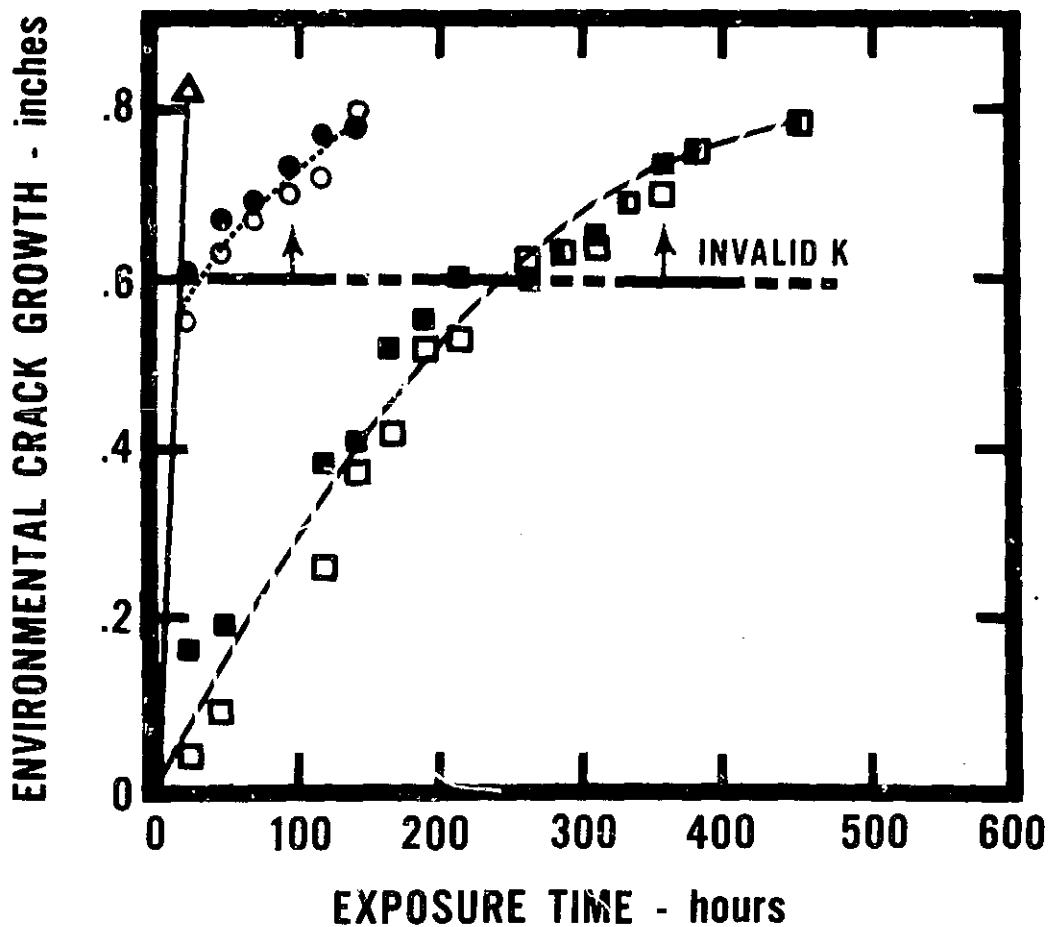


**Fig. 37 ENVIRONMENTAL CRACK GROWTH OF VARIOUS ALUMINUM ALLOYS IN SALT-DICHROMATE-ACETATE SOLUTION**

**BOLT LOADED SHORT TRANSVERSE (S-L) COMPACT TENSION SPECIMENS  
CORRODENT: 0.6MNaCl+0.02MNa<sub>2</sub>Cr<sub>2</sub>O<sub>7</sub>+0.07MNaC<sub>2</sub>H<sub>3</sub>O<sub>2</sub>+HC<sub>2</sub>H<sub>3</sub>O<sub>2</sub> TO pH4**

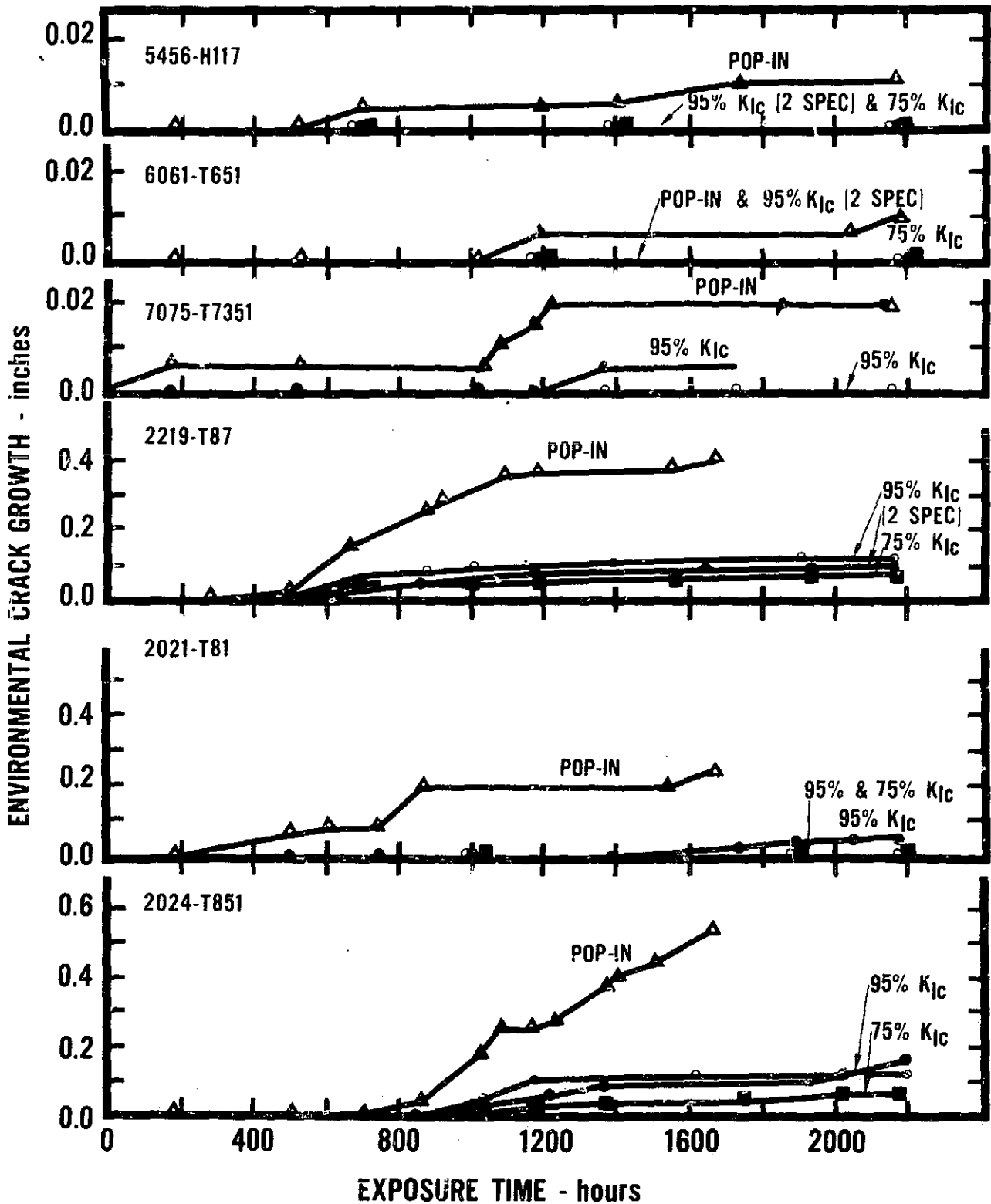
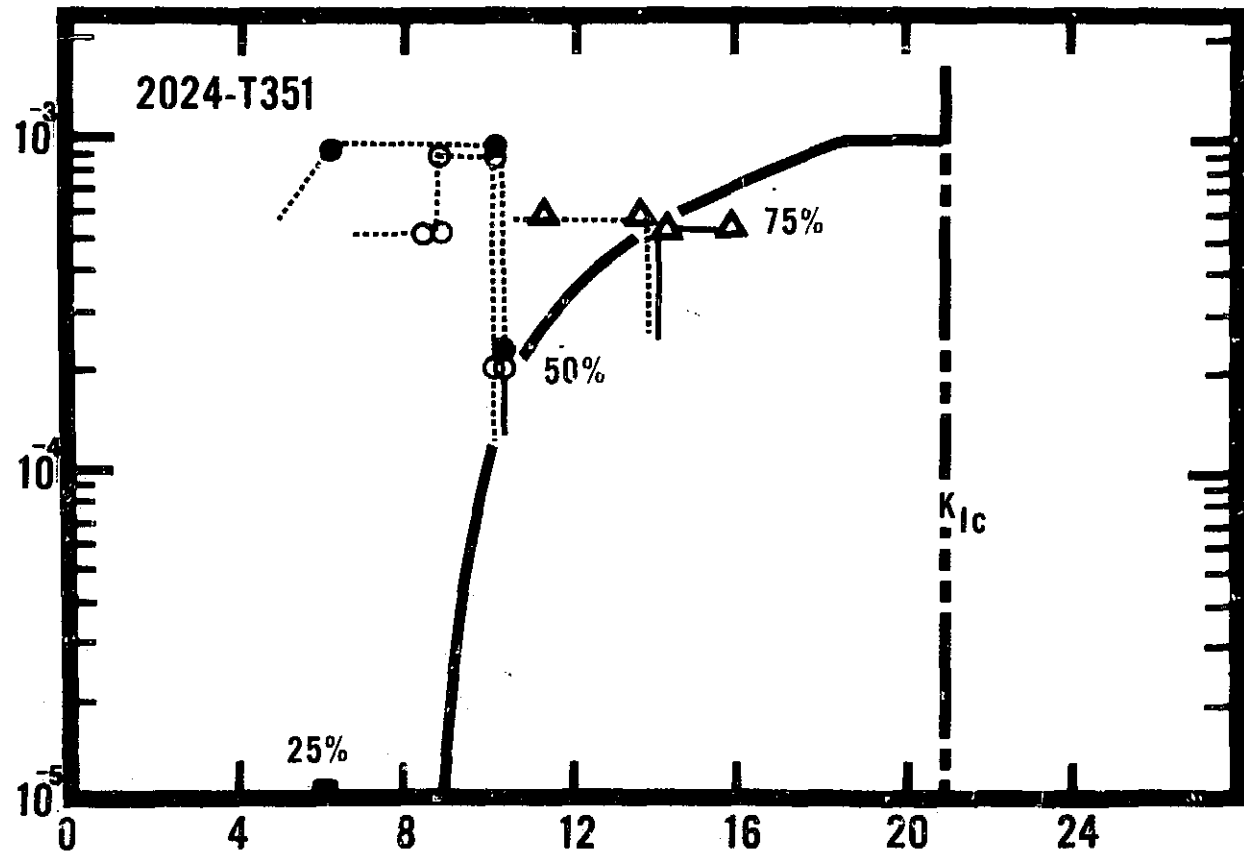
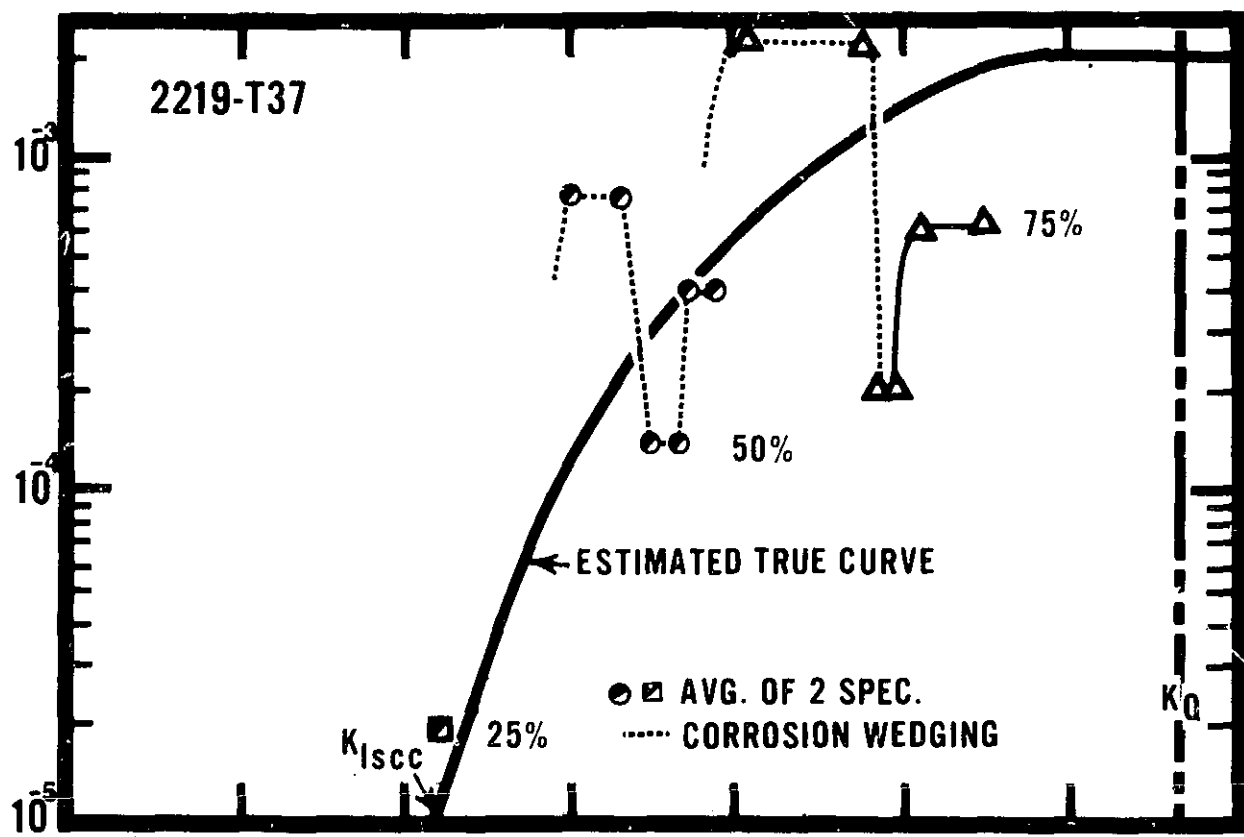


**Fig. 38 ENVIRONMENTAL CRACK GROWTH OF VARIOUS ALUMINUM ALLOYS IN SALT-DICHROMATE-ACETATE SOLUTION**

CRACK GROWTH RATE - in./yr



STRESS INTENSITY -  $ksi\sqrt{in.}$

Fig. 39 K-RATE CURVES FOR S-L COMPACTS

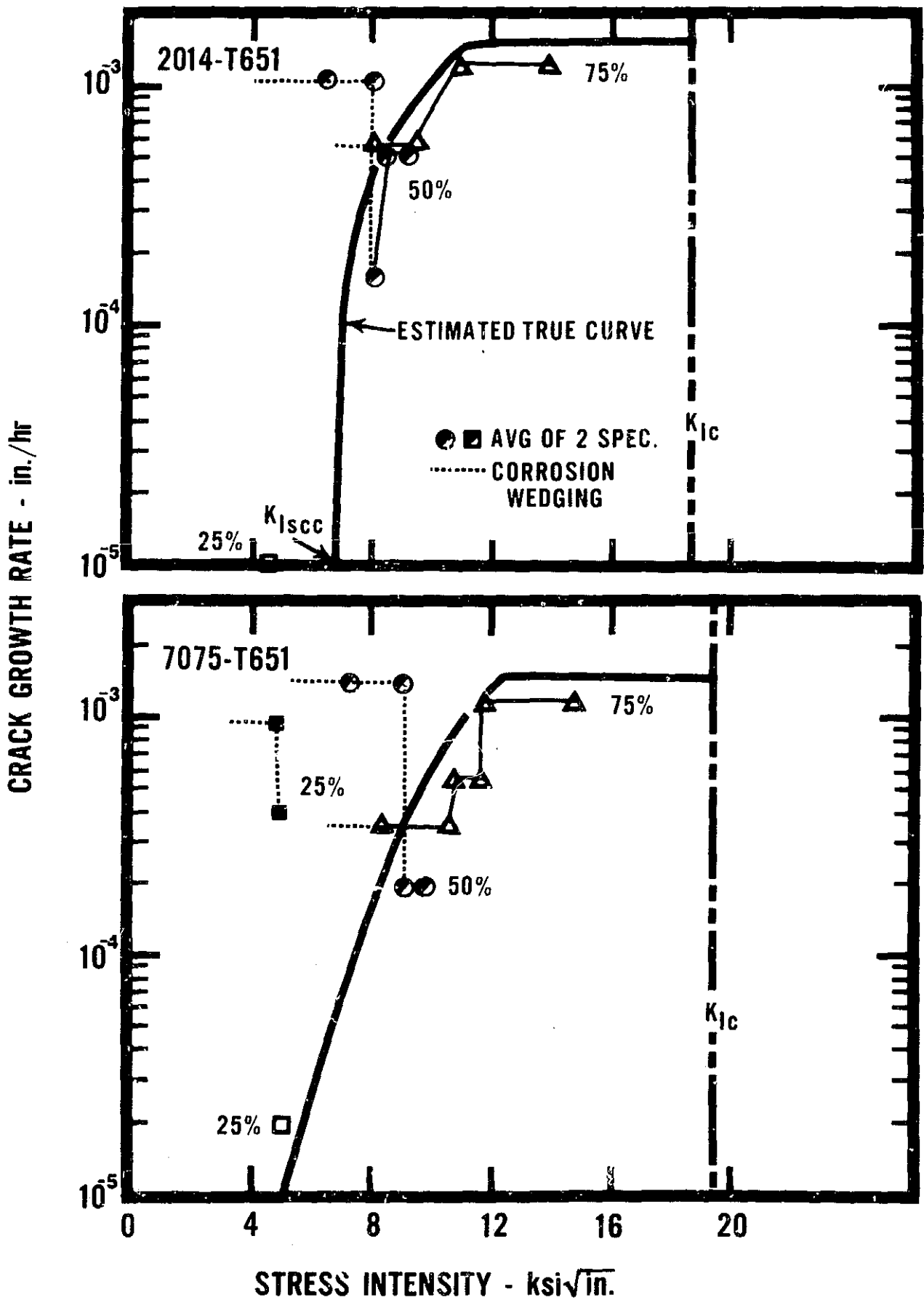


**Fig. 40 K-RATE CURVES FOR S-L COMPACTS**

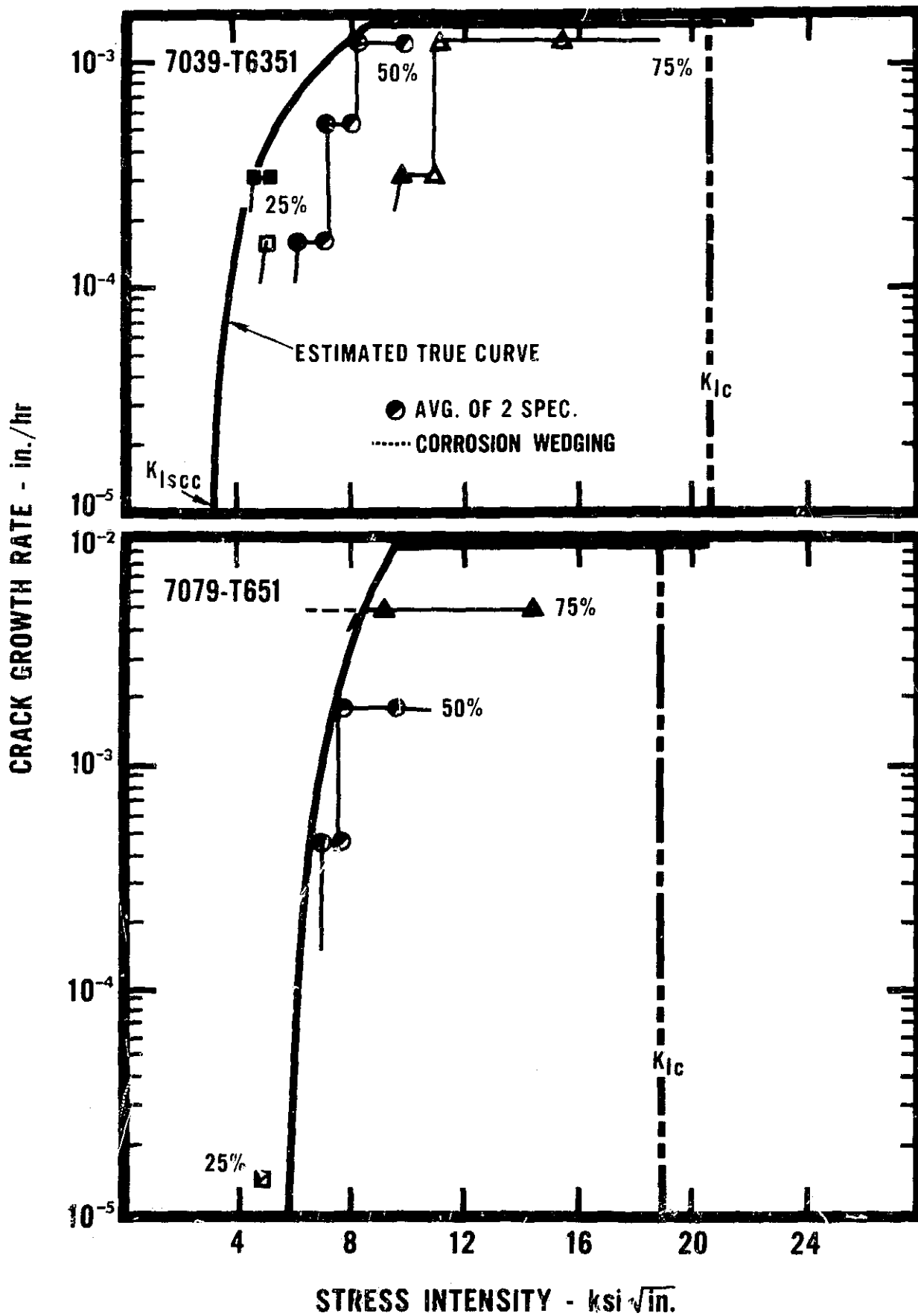
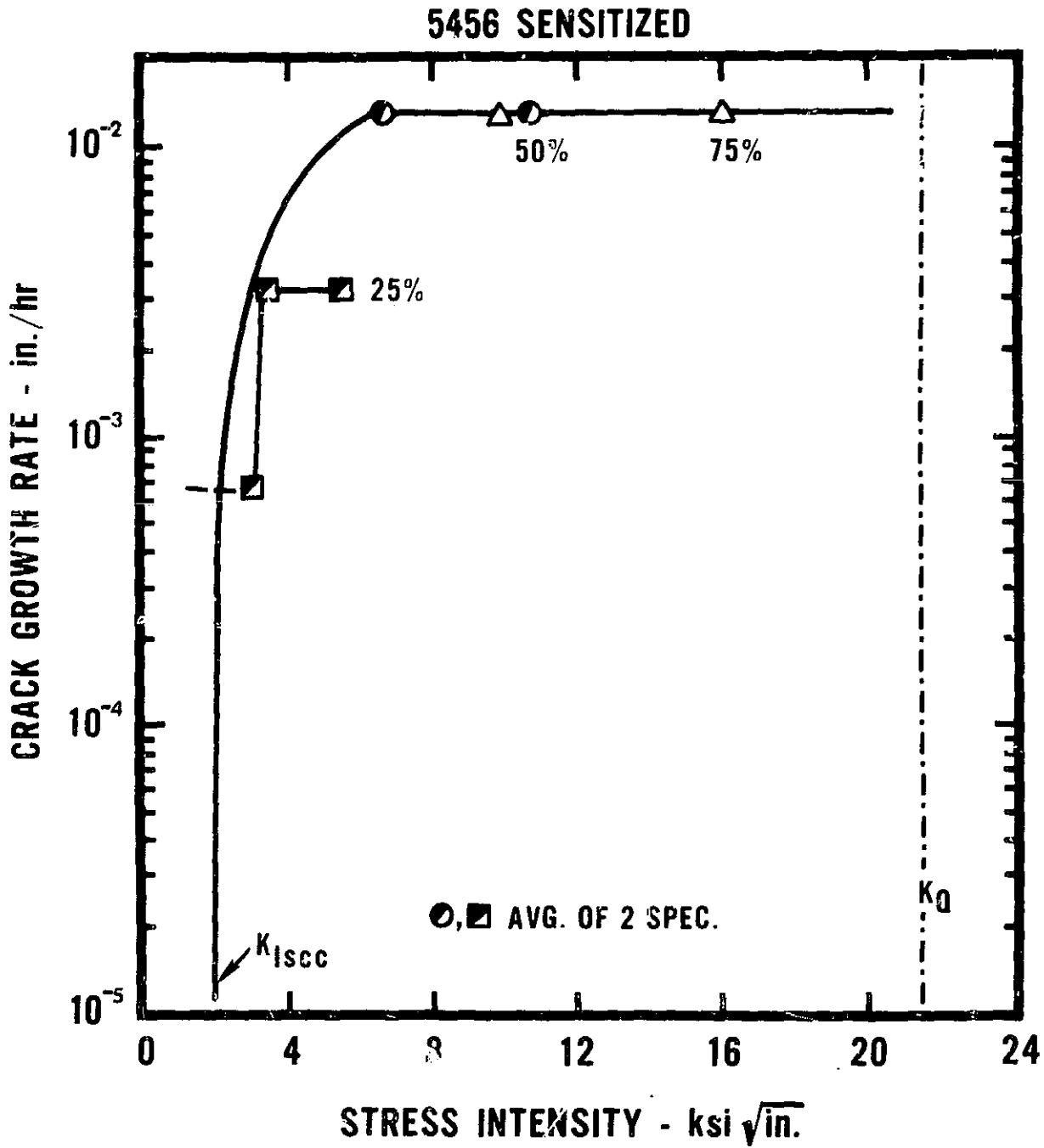
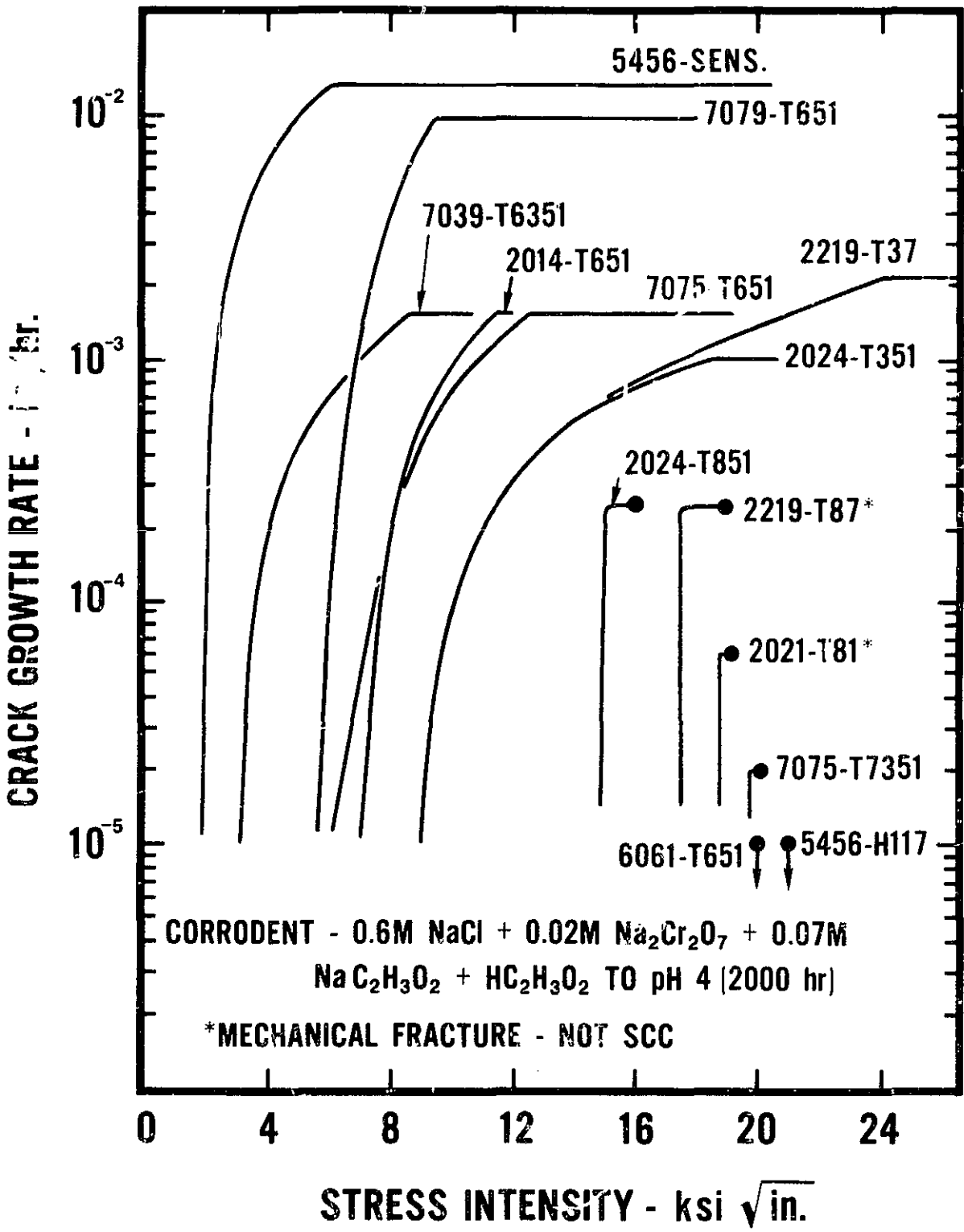


Fig. 41 K-RATE CURVES FOR S-L COMPACTS

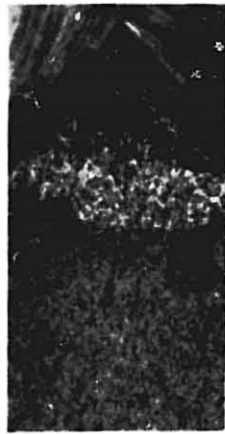


**Fig. 42 K-RATE CURVES FOR S-L COMPACTS**



**Fig. 43 K-RATE CURVES FOR S-L COMPACTS OF ALUMINUM ALLOYS (FATIGUE PRECRACKED)**

112



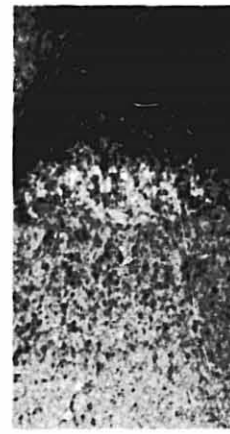
**FATIGUE  
PRECRACK**



**S-D-A  
47 DAYS**



**SEACOAST  
ATMOSPHERE  
120 DAYS**

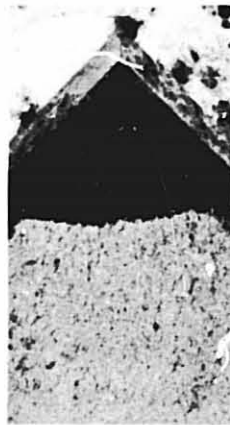


**INDUSTRIAL  
ATMOSPHERE  
540 DAYS**

**2024-T351**



**FATIGUE  
PRECRACK**



**S-D-A  
92 DAYS**



**SEACOAST  
ATMOSPHERE  
250 DAYS**



**INDUSTRIAL  
ATMOSPHERE  
365 DAYS**

**2024-T851**

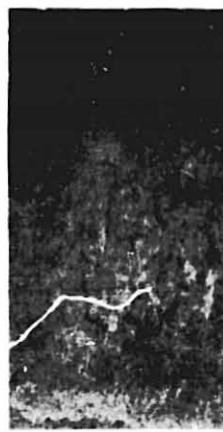
**Fig. 44 FRACTURE SURFACES OF S-L COMPACT TENSION SPECIMENS BOLT LOADED TO 95% $K_{Ic}$  SHOWING CRACK GROWTH IN VARIOUS ENVIRONMENTS**



FATIGUE  
PRECRACK



S-D-A  
47 DAYS



SEACOAST  
ATMOSPHERE  
90 DAYS

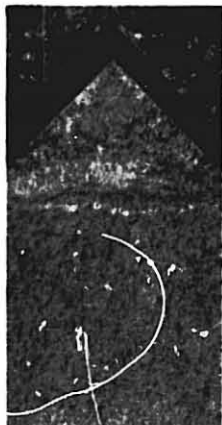


INDUSTRIAL  
ATMOSPHERE  
180 DAYS

7075-T651



FATIGUE  
PRECRACK



S-D-A  
92 DAYS



SEACOAST  
ATMOSPHERE  
250 DAYS



INDUSTRIAL  
ATMOSPHERE  
365 DAYS

7075-T7351

**Fig. 45 FRACTURE SURFACES OF S-L COMPACT TENSION SPECIMENS BOLT LOADED TO 95%  $K_{Ic}$  SHOWING CRACK GROWTH IN VARIOUS ENVIRONMENTS**

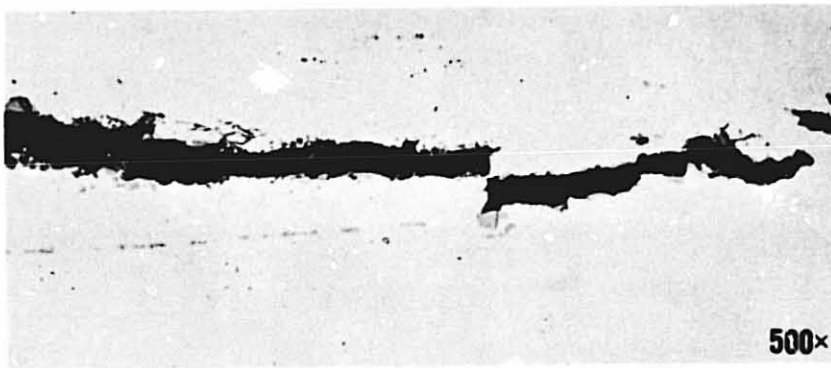
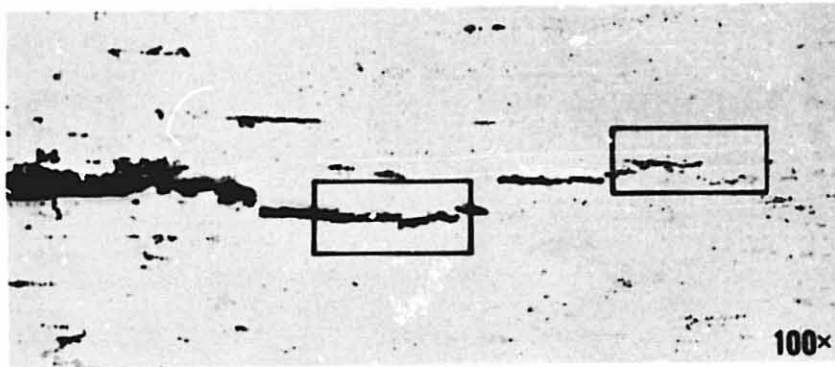


**FIG. 46 S-L COMPACT TENSION SPECIMEN OF 2024-T851 BOLT LOADED TO POP-IN AND EXPOSED 1656 hr. TO SALT - DICHROMATE - ACETATE SOLUTION. SHOWS CRACKING OF ALLOY CONSTITUENTS AHEAD OF THE CRACK TIP.**



**Fig. 47 LONGITUDINAL (L-T) DCB SPECIMENS WITH SCC  
IN LOCATIONS THAT INVALIDATE THE TEST:  
a - 7079-T551 SEACOST ATMOSPHERE  
b - 2219-T37 SALT-DICHROMATE-ACETATE  
SOLUTION**

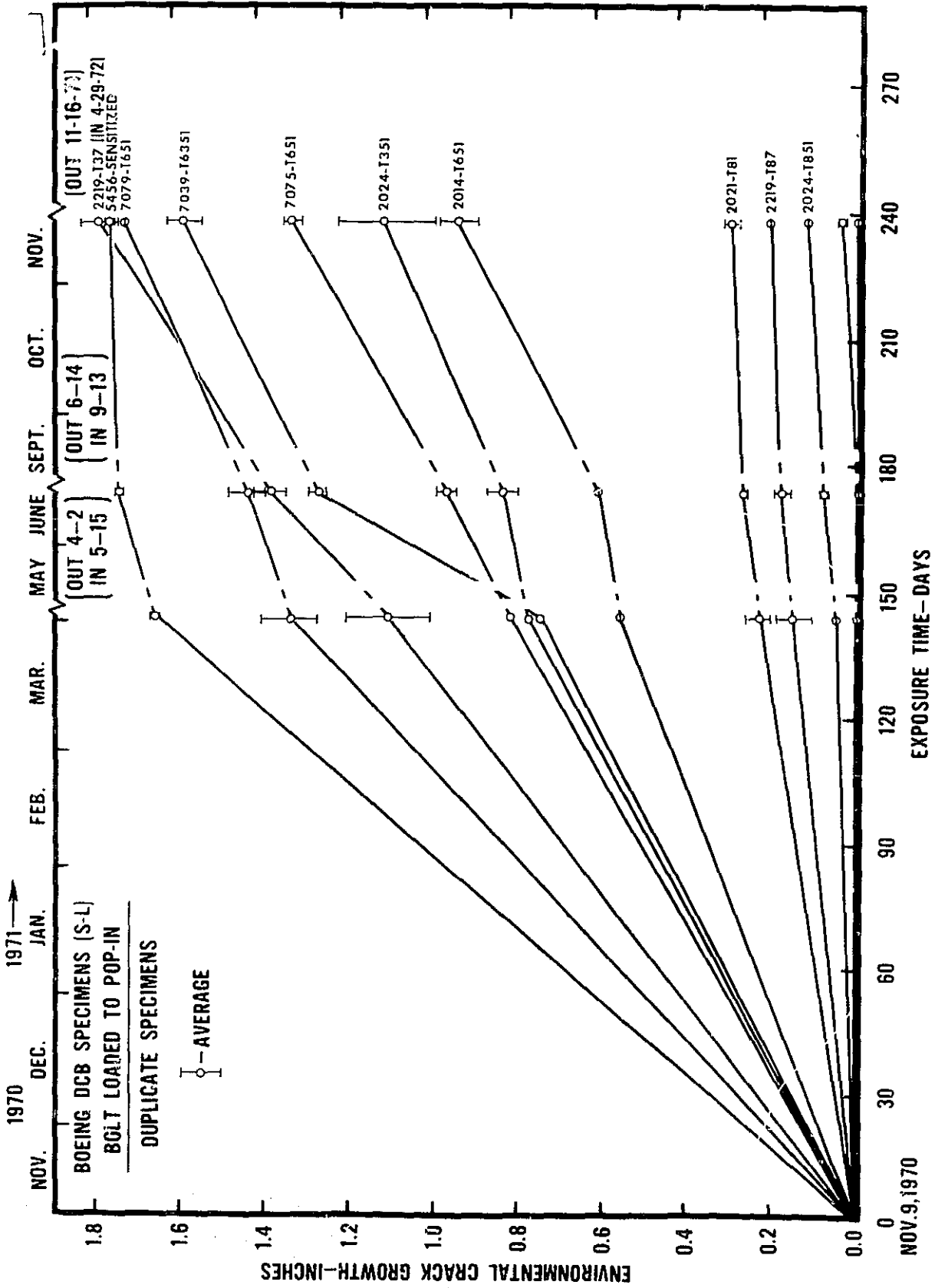


Fig. 48 ENVIRONMENTAL CRACK GROWTH OF VARIOUS ALUMINUM ALLOYS IN A SEACOAST ATMOSPHERE

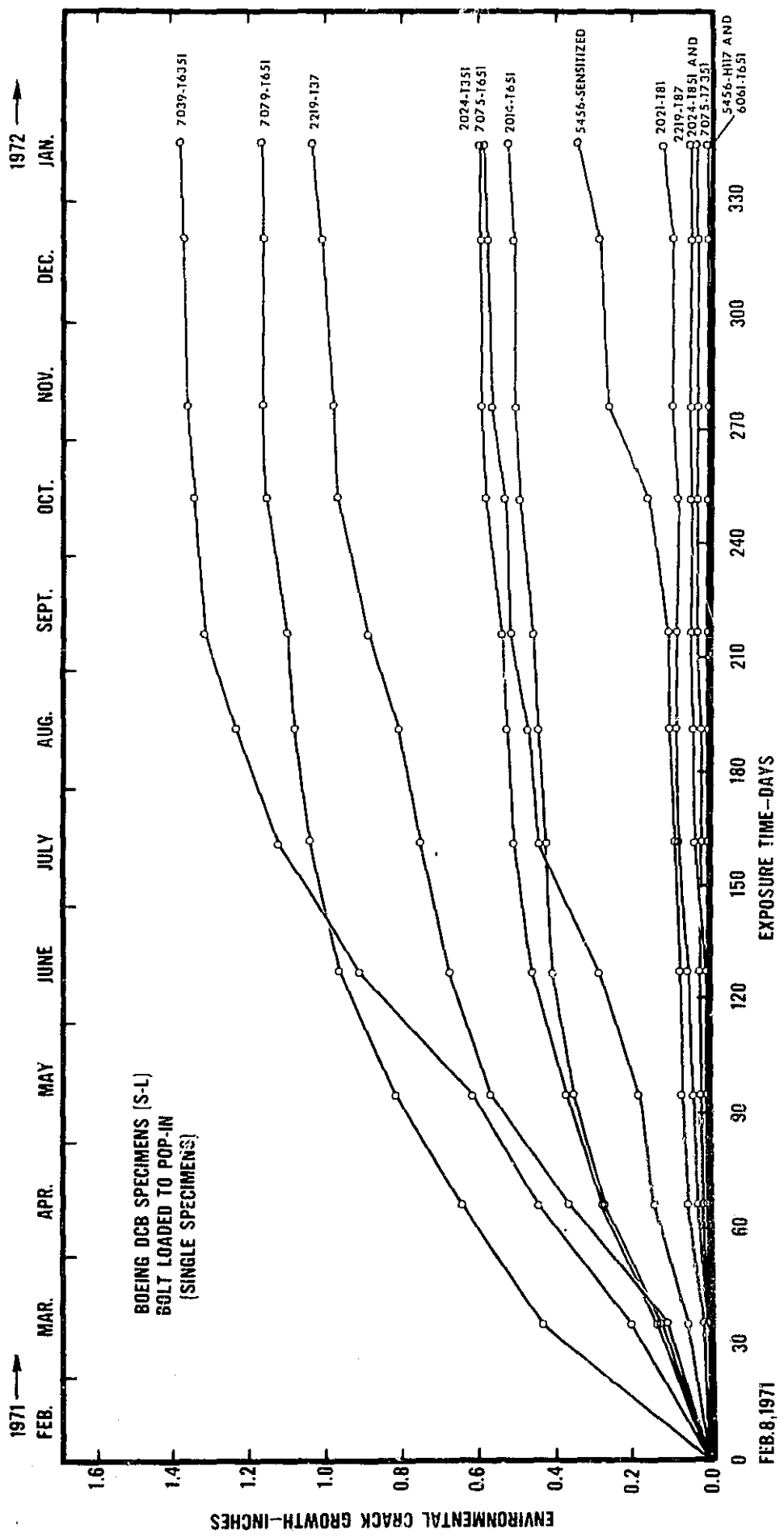


Fig. 49 ENVIRONMENTAL CRACK GROWTH OF VARIOUS ALUMINUM ALLOYS IN AN INDUSTRIAL ATMOSPHERE

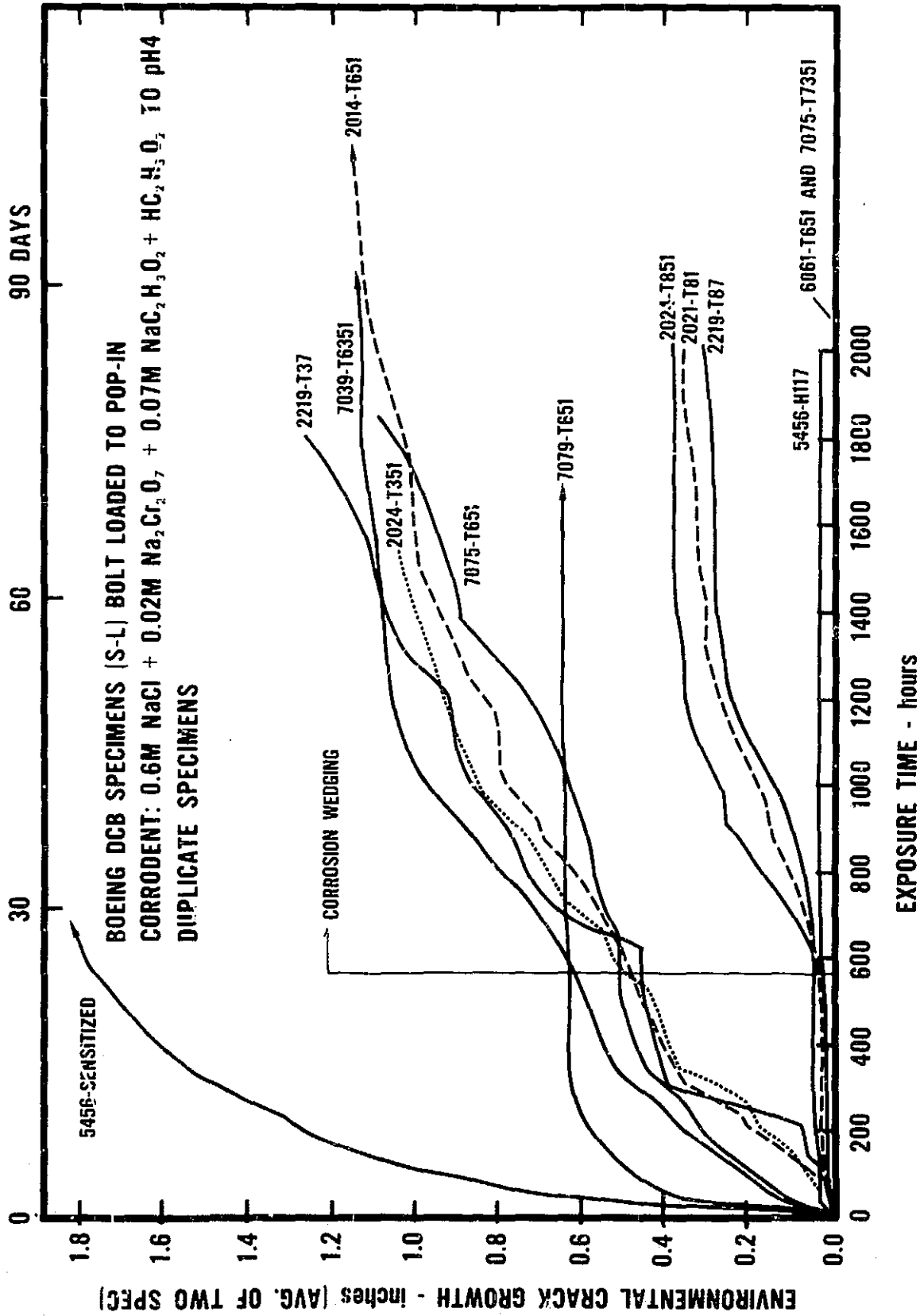


Fig. 50 ENVIRONMENTAL CRACK GROWTH OF VARIOUS ALUMINUM ALLOYS  
 IN SALT-DICHROMATE-ACETATE SOLUTION

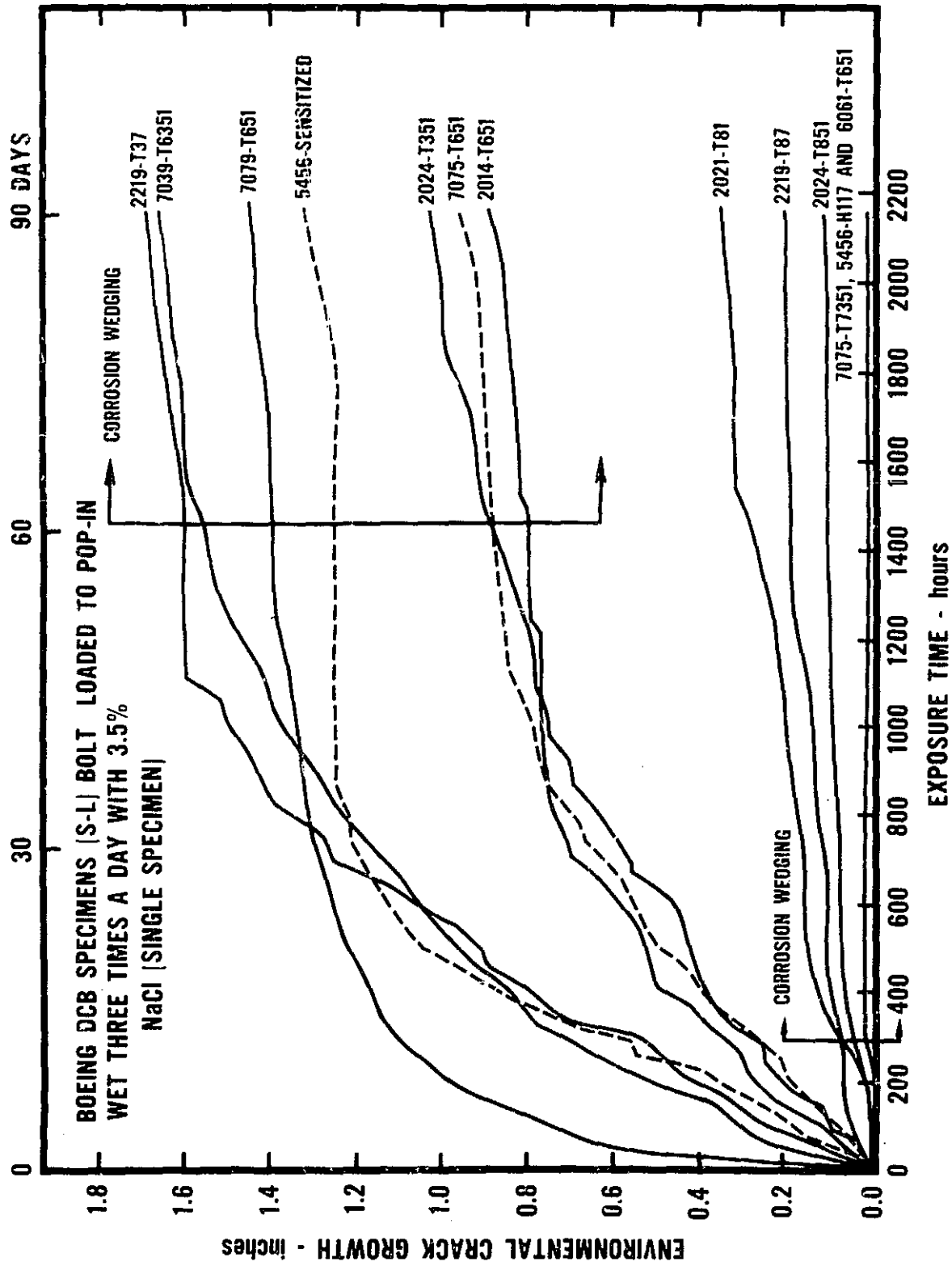


Fig. 51 ENVIRONMENTAL CRACK GROWTH OF VARIOUS ALUMINUM ALLOYS IN 3.5% NaCl

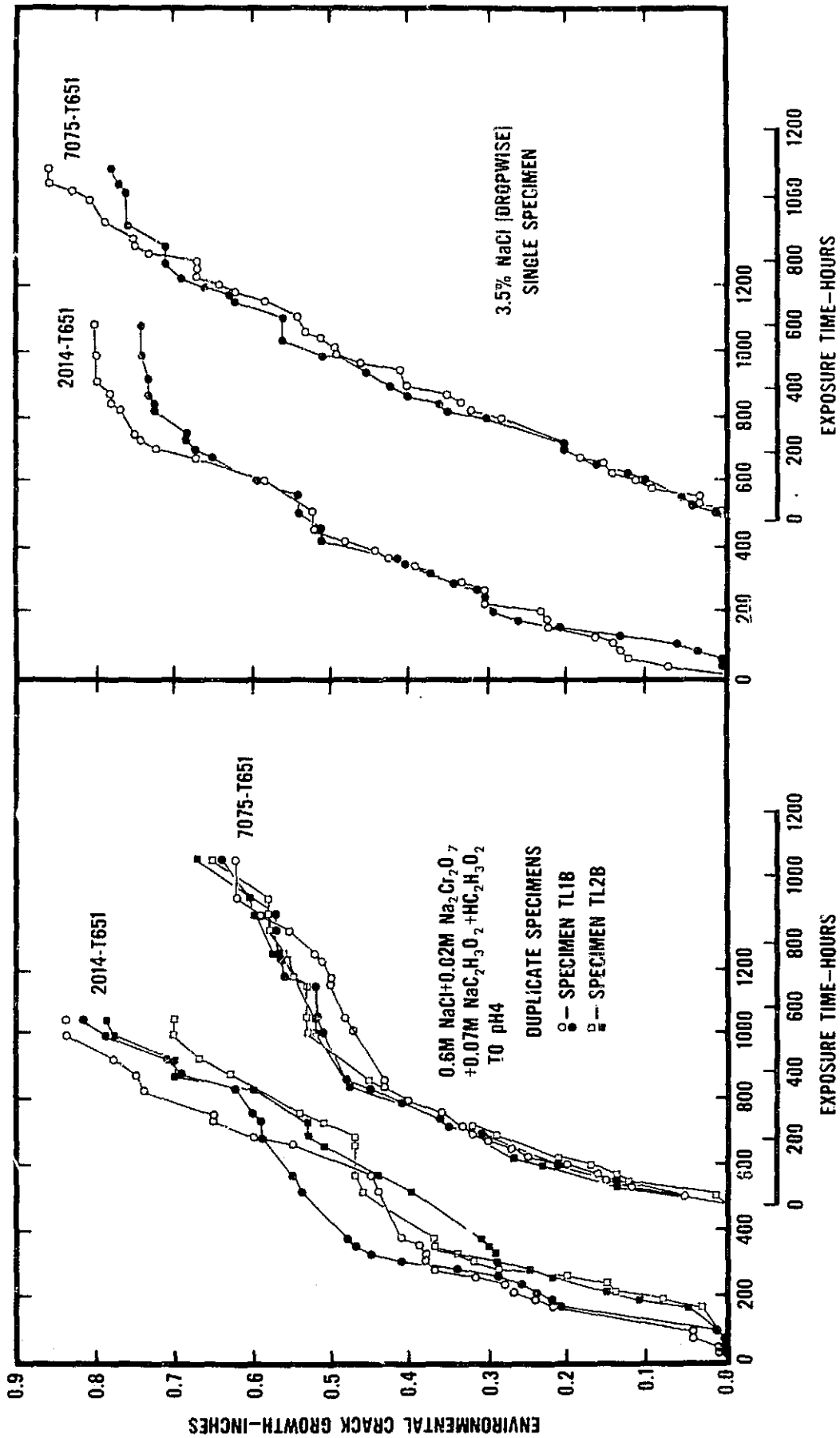
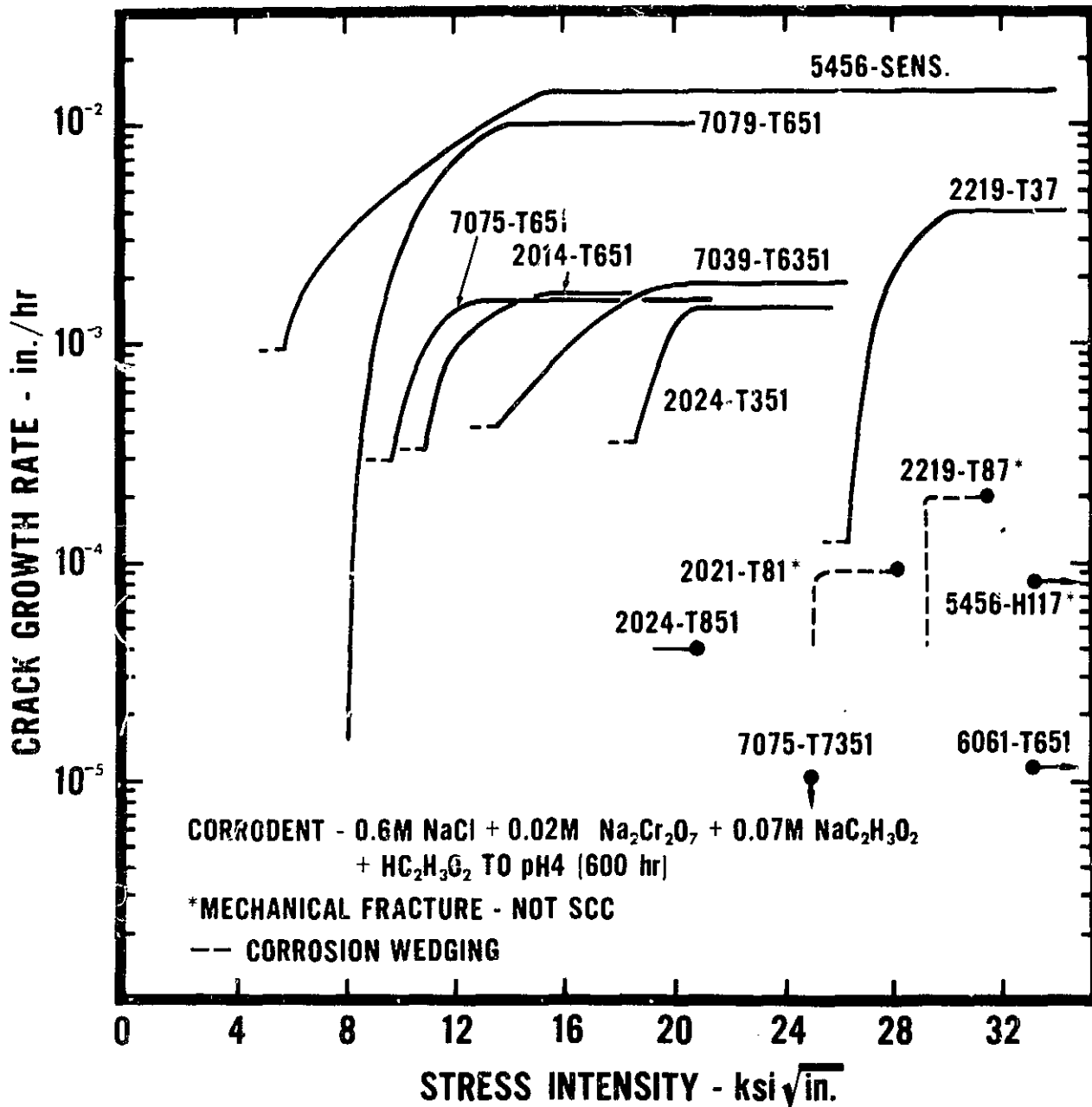
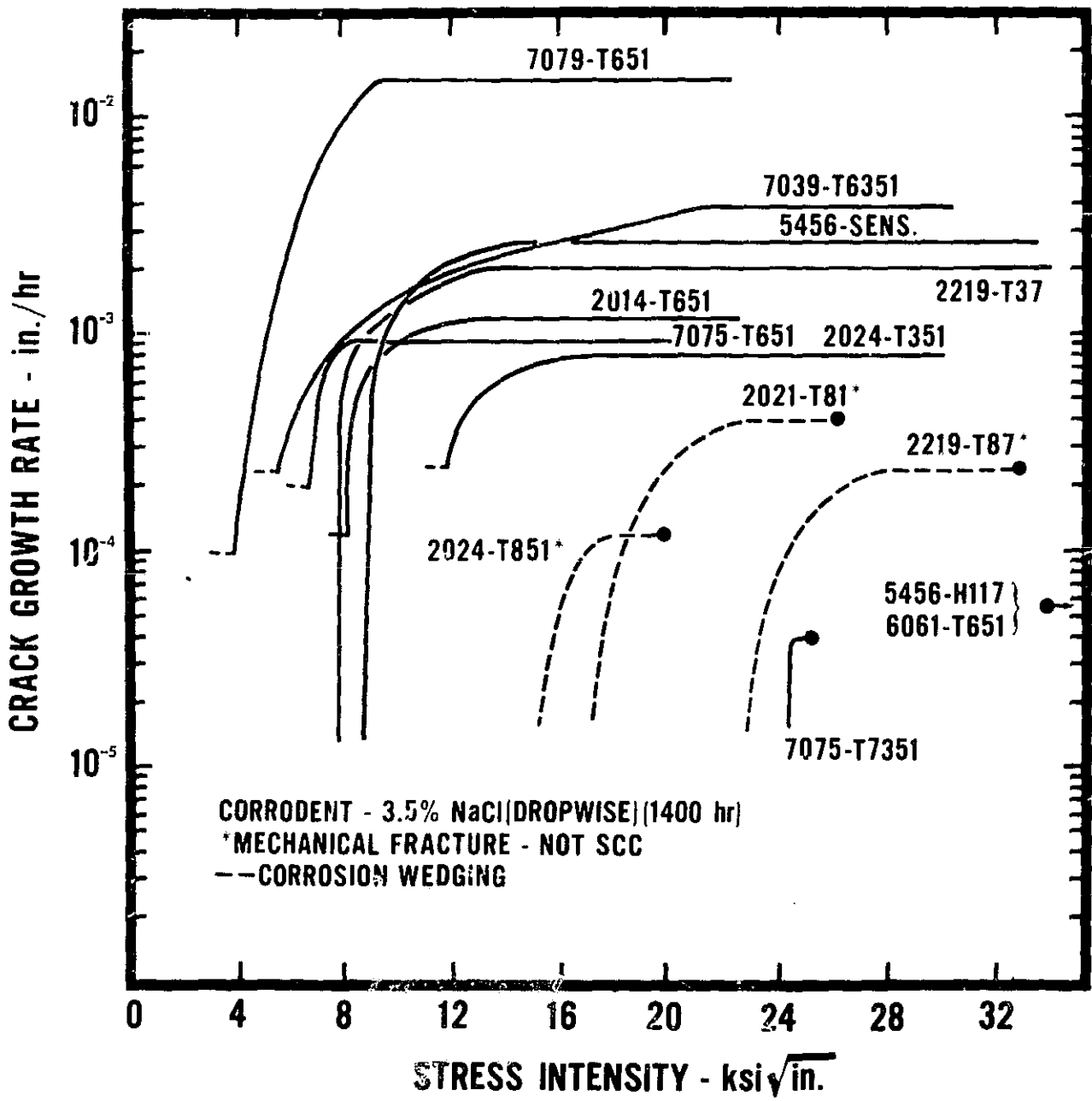


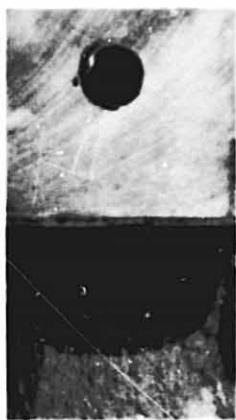
Fig. 52 VARIATION IN CRACK GROWTH ON OPPOSITE SIDES OF BOEING DCB SPECIMENS BOLT LOADED TO POP-IN



**Fig. 53 K-RATE CURVES FOR S-L DCB SPECIMENS OF ALUMINUM ALLOYS BOLT LOADED TO POP-IN**

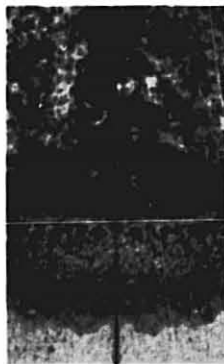
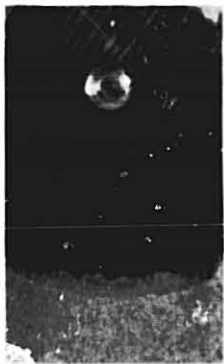


**Fig. 54 K-RATE CURVES FOR S-L DCB SPECIMENS OF ALUMINUM ALLOYS BOLT LOADED TO POP-IN**



← BOTTOM OF NOTCH

6061-T651



7075-T7351



2219-T87

TENSION  
PRECRACK

3.5% NaCl  
DROPWISE

SALT  
DICHROMATE  
ACETATE

**Fig.55 FRACTURE SURFACES OF BOEING DCB SPECIMENS OF RESISTANT ALLOYS SHOWING CRACK GROWTH IN ACCELERATED TESTS.**

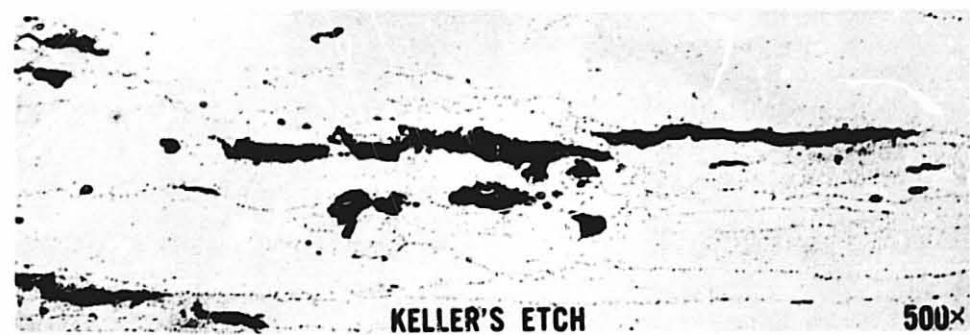
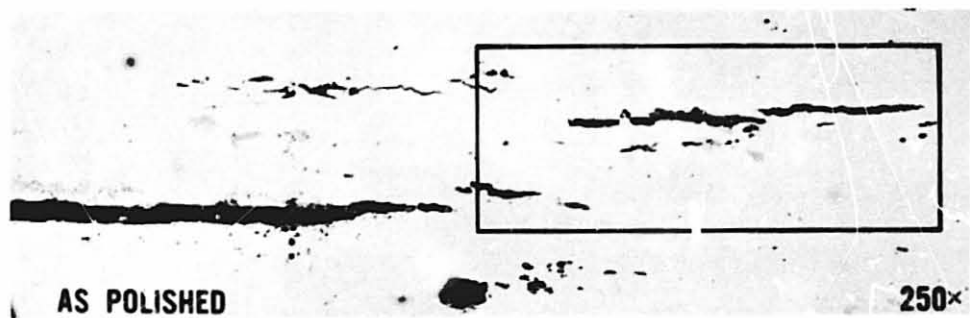
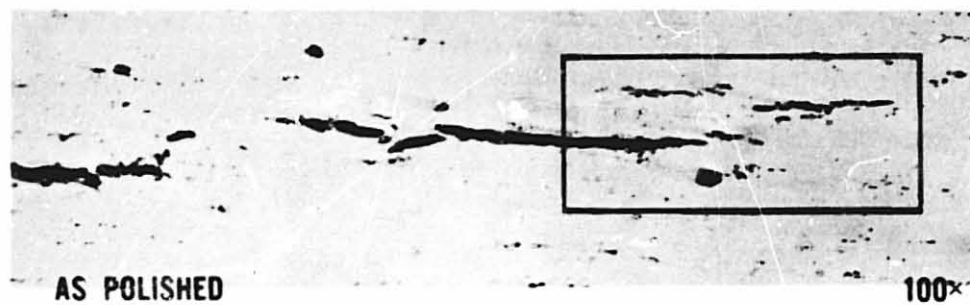
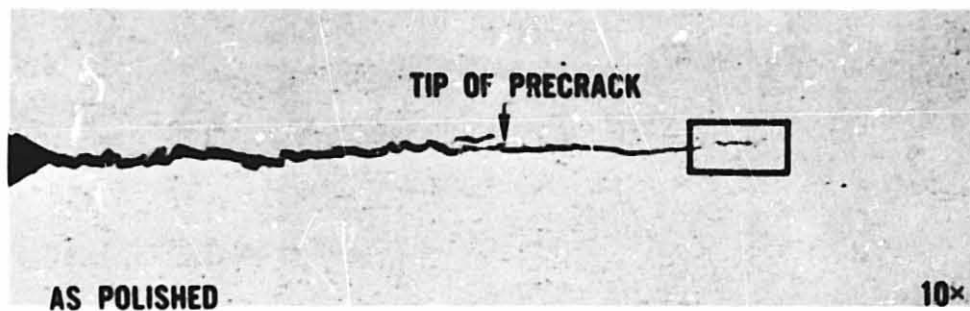


**Fig.56 S-L DCB SPECIMEN OF 7075-T7351 BOLT LOADED TO POP-IN AND EXPOSED 2200 HR. TO 3.5% NaCl ADDED DROPWISE. INTERGRANULAR SCC EXTENDING BEYOND TIP OF TENSION PRECRACK.**



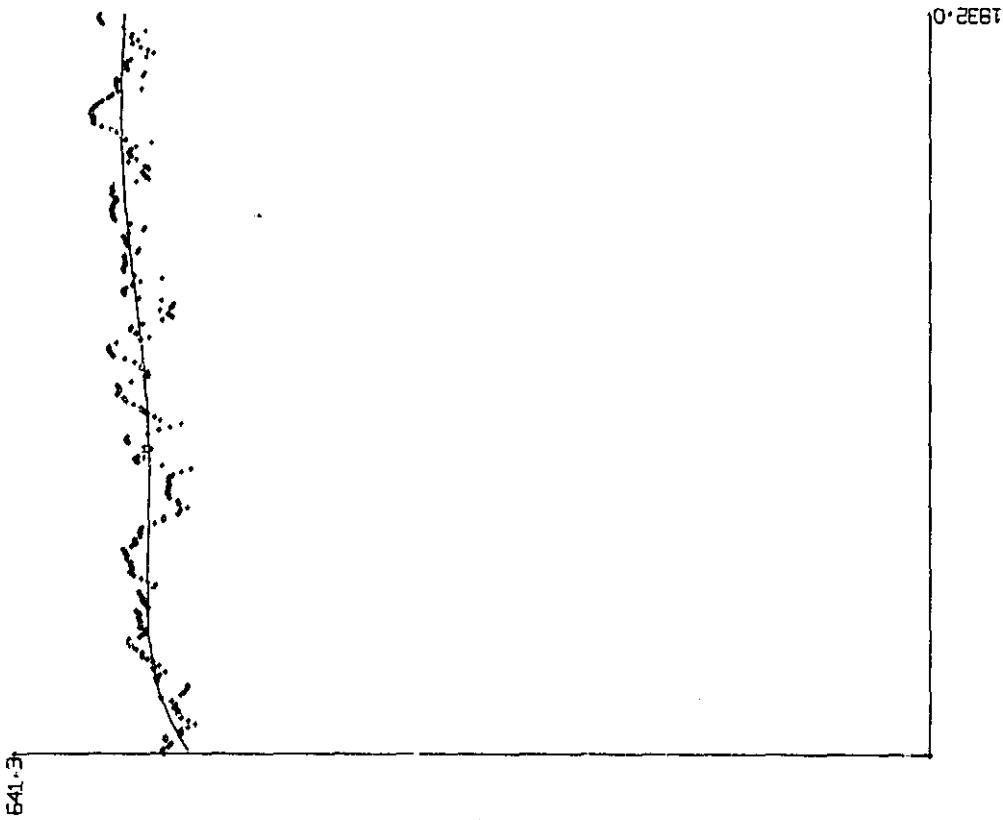
2219-T87



5456-H117



**Fig.57 S-L DCB SPECIMENS BOLT LOADED TO POP-IN AND EXPOSED 2200 hr. TO 3.5% NaCl ADDED DROPWISE. SHOWS EXTENSION OF MECHANICAL FRACTURE THROUGH ALLOY CONSTITUENTS THAT CRACKED AHEAD OF THE CRACK TIP.**



LOAD, LBx2

1633.7

641.3

1832.0

1832.0

TIME, hrs.

TIME, hrs.

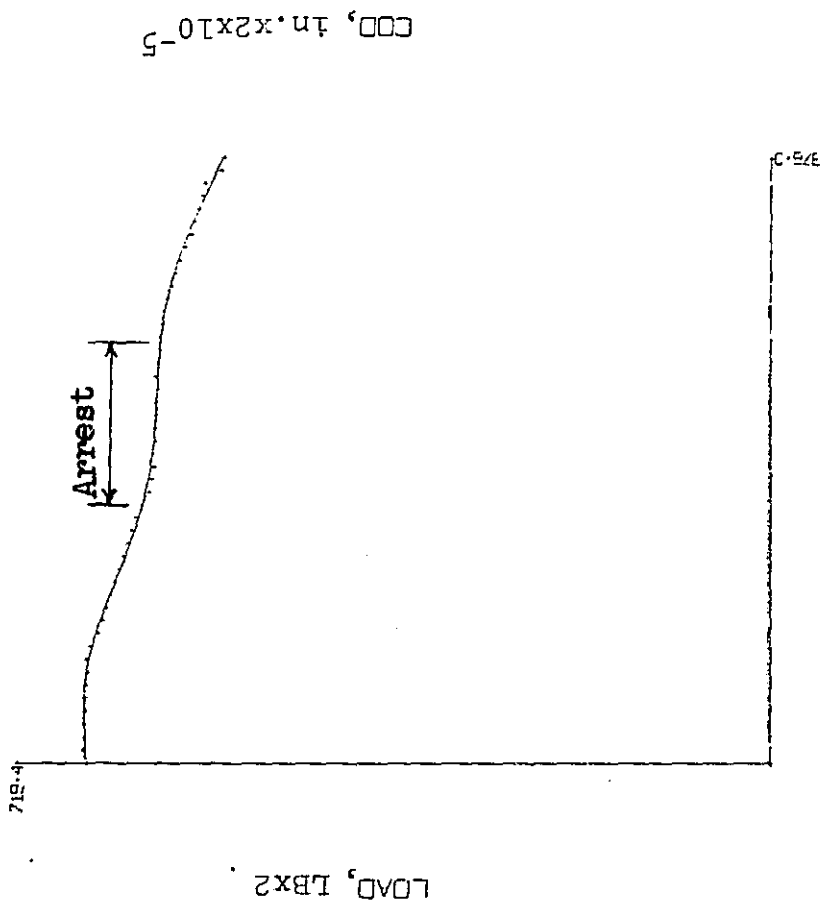
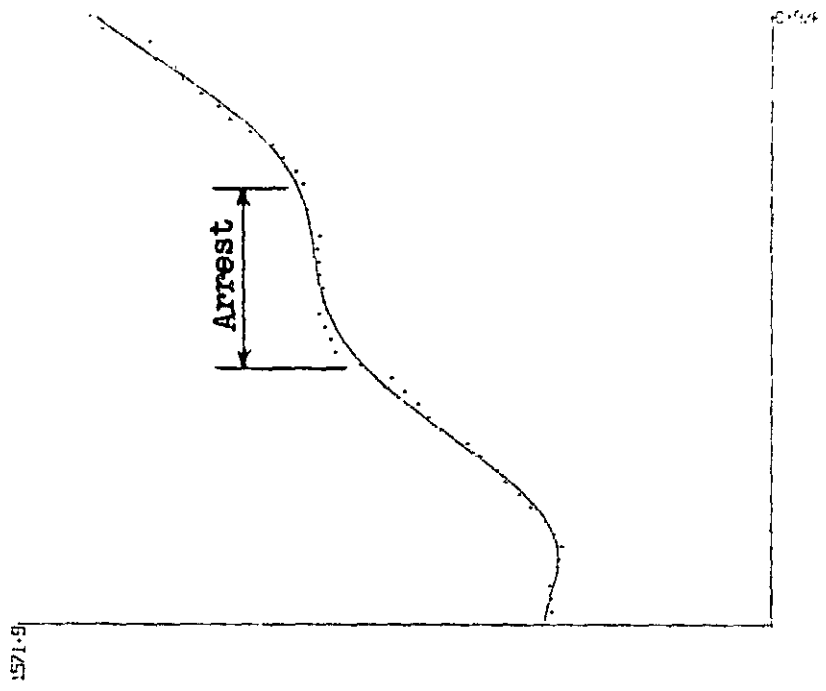
366656

TL- 2

366656

TL- 2

**Fig. 58** Ring Loaded Compact Tension Specimen of 5456-H117 Exposed in a Salt Dichromate Solution



TIME, hrs.

344793 TL- 2

TIME, hrs.

344793 TL- 2

**Fig. 59** Ring Loaded Compact Tension Specimen of 2219-T37  
Exposed in a Salt Dichromate Solution

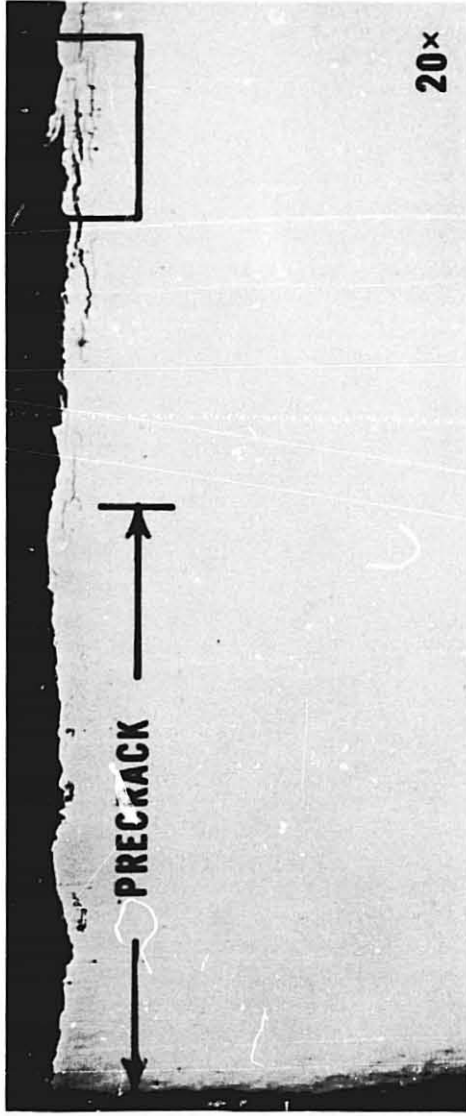
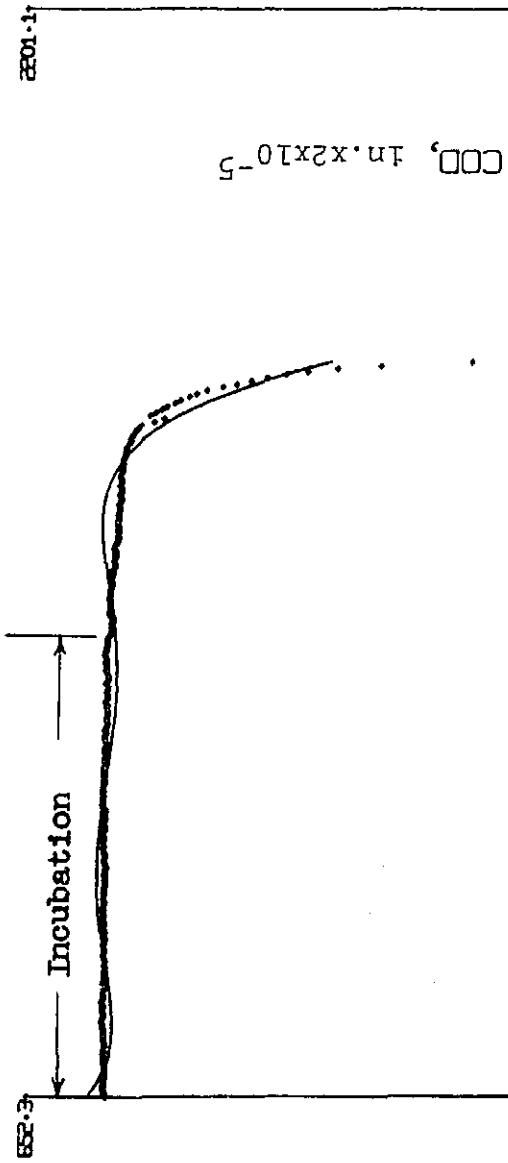


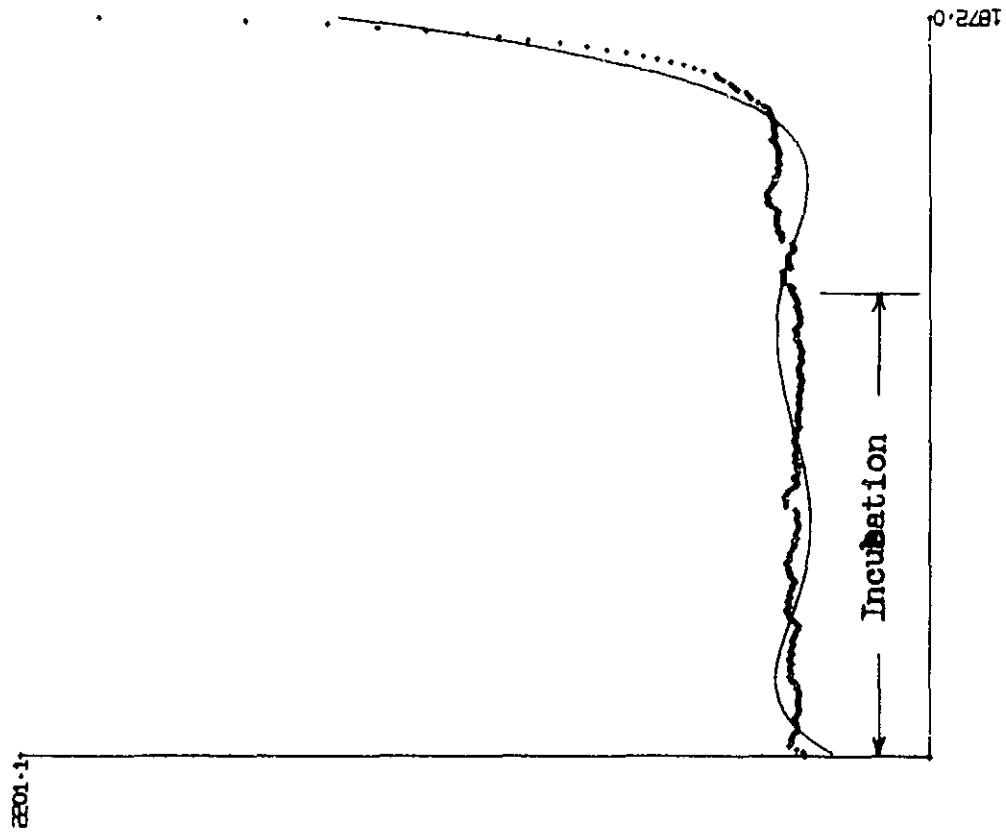
**Fig. 60 MICROGRAPHS SHOWING BRANCHING OF SCC IN RING LOADED COMPACT TENSION SPECIMEN OF 2219-T37 EXPOSED TO SALT-DICHROMATE-ACETATE SOLUTION.**



TIME, hrs.

314758

TL-3



TIME, hrs.

314758

TL-3

**Fig. 61** Ring Loaded Compact Tension Specimen of 7039-T6351 Exposed in a Salt Dichromate Solution

NOTE: SHORT TRANSVERSE (S-L) SPECIMENS, FATIGUE PRECRACKED  
 CORRODENT: 0.6 M NaCl + 0.02 M Na<sub>2</sub>Cr<sub>2</sub>O<sub>7</sub> + 0.07 M Na C<sub>2</sub>H<sub>3</sub>O<sub>2</sub> + HC<sub>2</sub>H<sub>3</sub>O<sub>2</sub> TO pH 4.

- 2014-T651      ◇ 2021-T81
- 2024-T351    ◇ 2024-T851
- △ 2219-T37     ○ 2219-T87

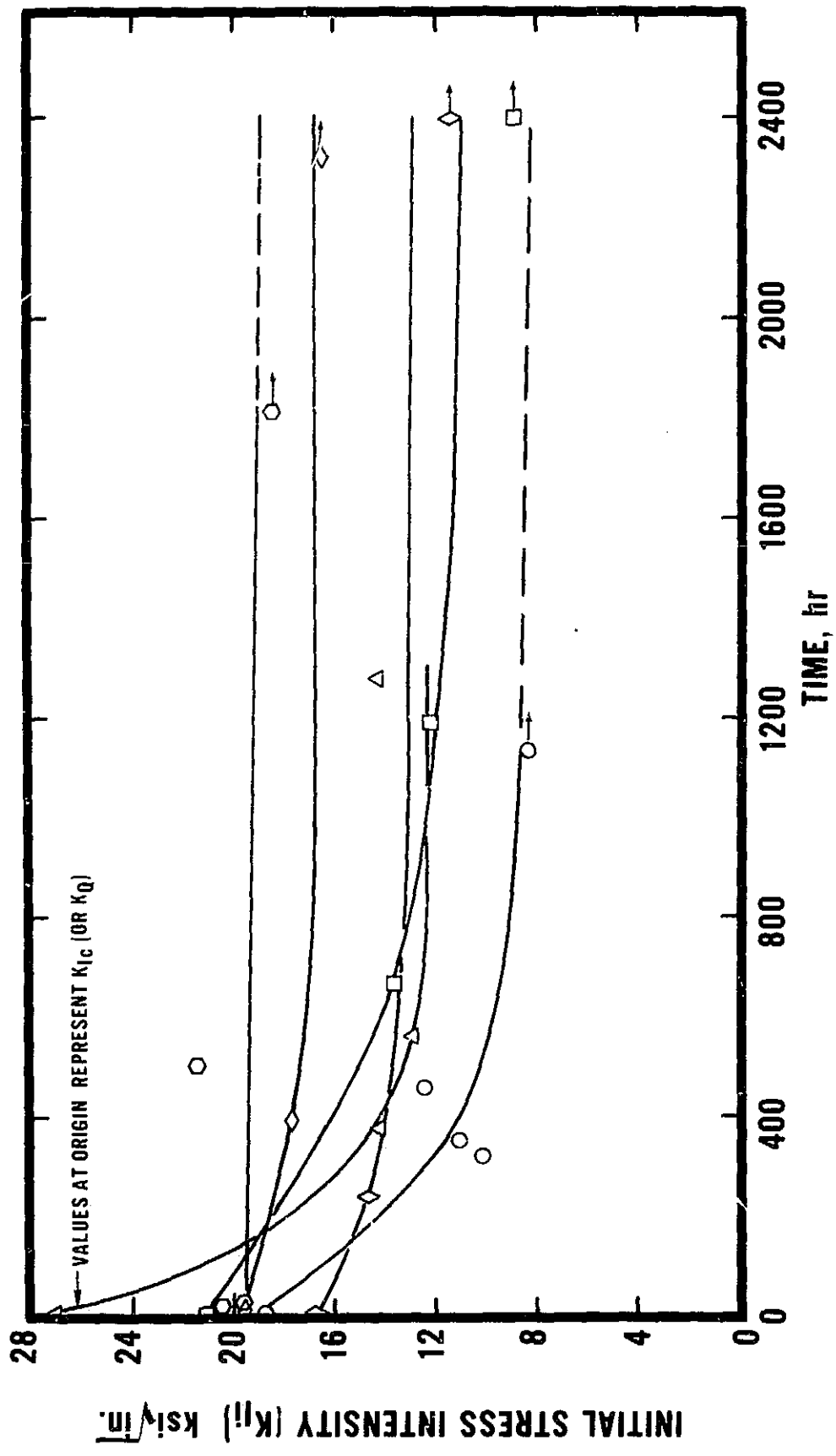


Fig. 62 INITIAL [APPLIED] STRESS INTENSITY VS TIME TO FAILURE FOR RING LOADED COMPACT TENSION SPECIMENS

NOTE: SHORT TRANSVERSE (S-L) SPECIMENS, FATIGUE PRECRACKED  
 CORRODENT: 0.6 M NaCl + 0.02 M Na<sub>2</sub>C<sub>2</sub>O<sub>4</sub> + 0.07 M Na<sub>2</sub>H<sub>2</sub>O<sub>7</sub> + HC<sub>2</sub>H<sub>3</sub>O<sub>2</sub> TO pH 4.

- ◇ 5456-H117    ▲ 7075-T651
- 5456-SENS.    ○ 7075-T7351
- ▽ 6061-T651    ◇ 7079-T651
- 7039-T6351

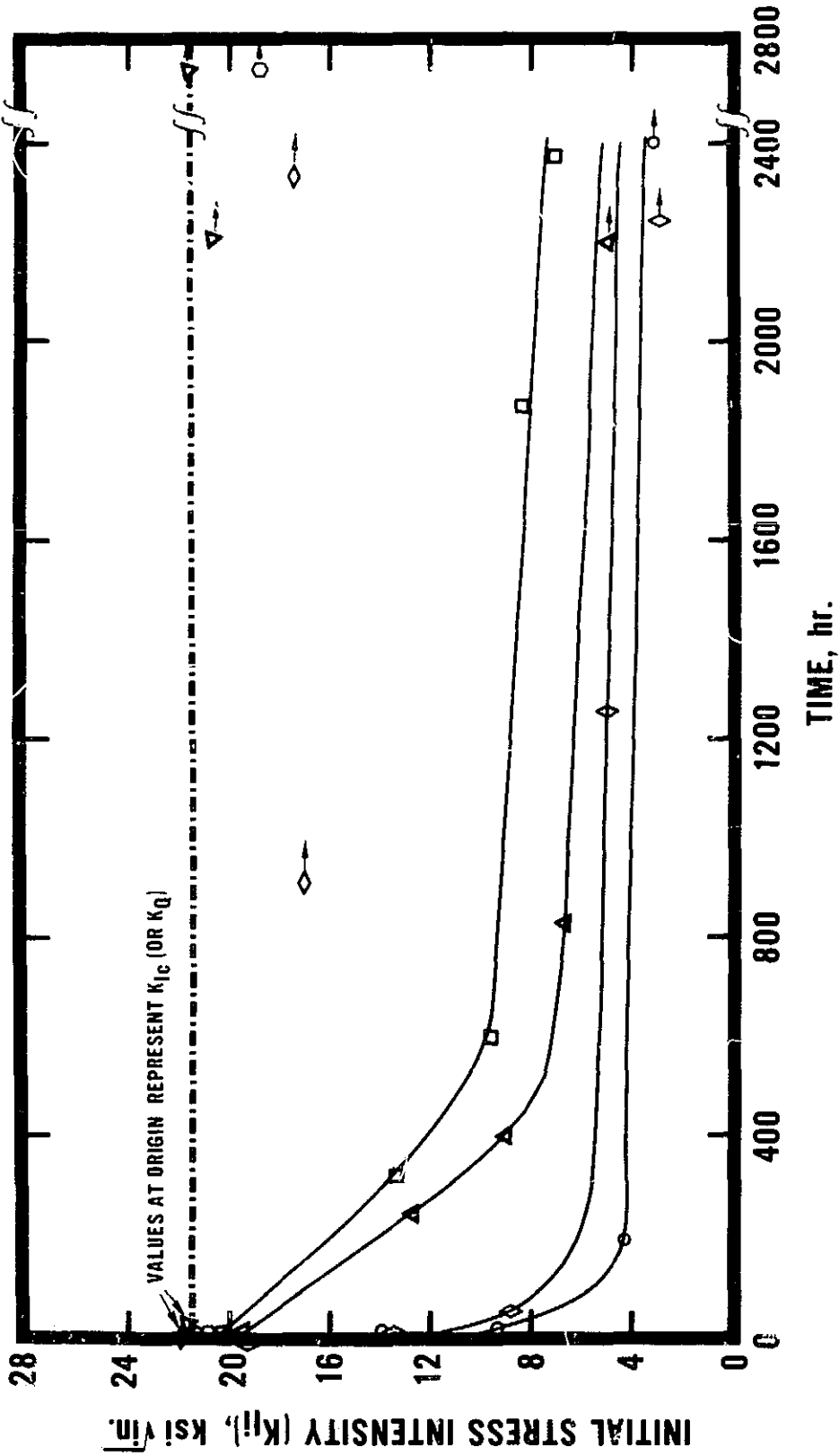
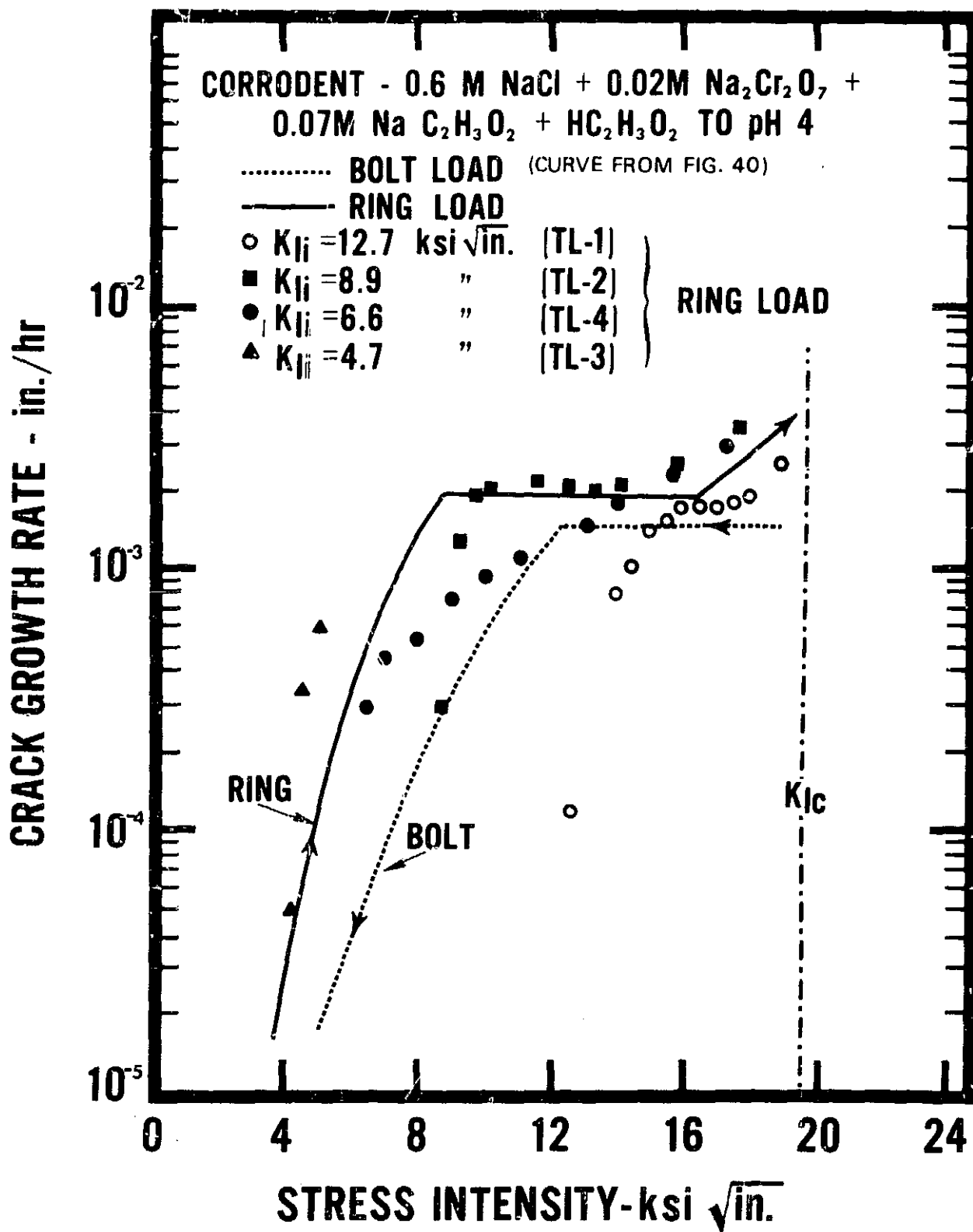


Fig. 63 INITIAL (APPLIED) STRESS INTENSITY VS TIME TO FAILURE FOR RING LOADED COMPACT TENSION SPECIMENS.



**Fig.64 K-RATE CURVES COMPARING RING AND BOLT LOADING. FATIGUE PRECRACKED S-L COMPACTS OF 7075-T651**

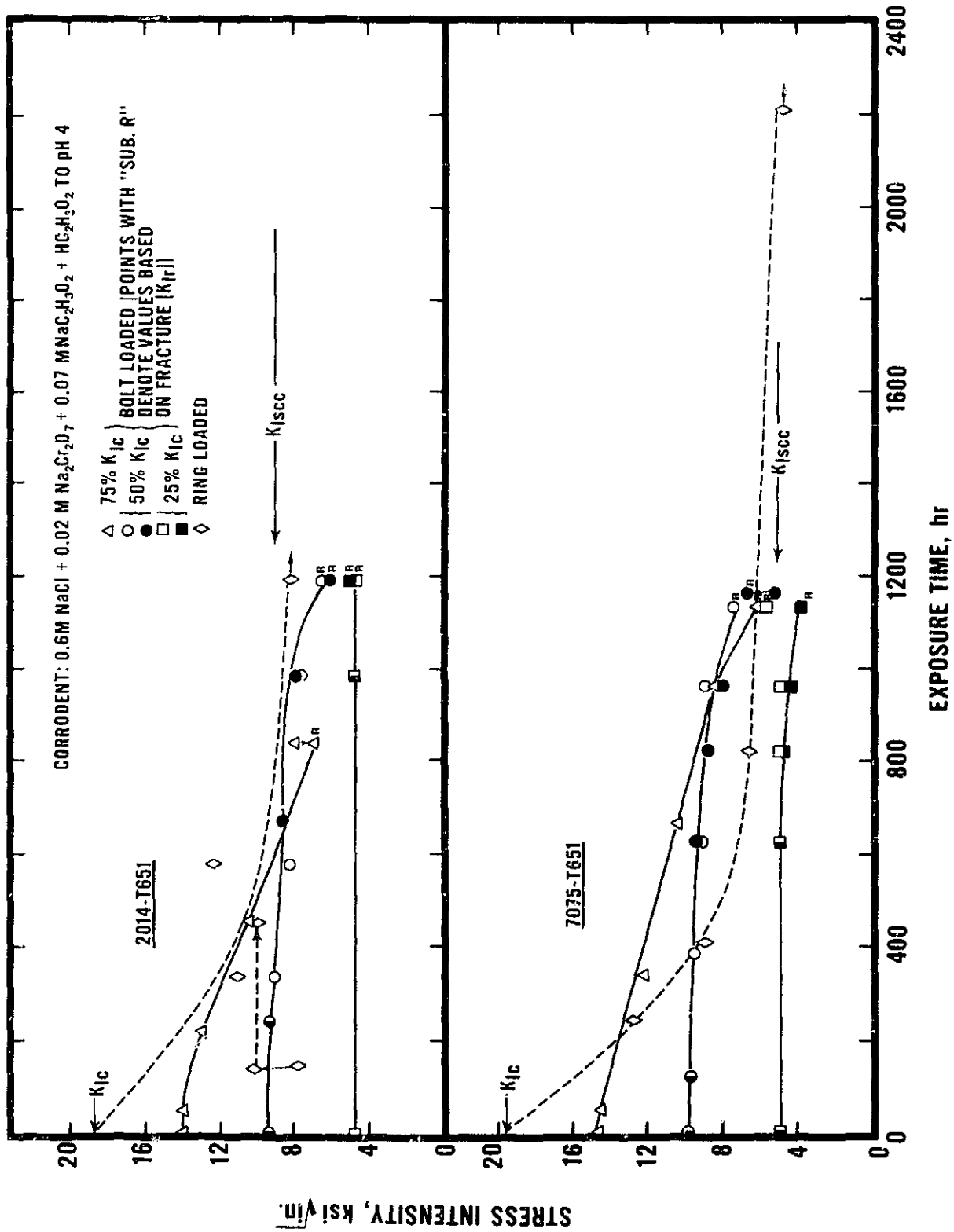


Fig. 65 K-TIME CURVES COMPARING RING AND BOLT LOADING. FATIGUE PRECRACKED S-L COMPACT TENSION SPECIMENS

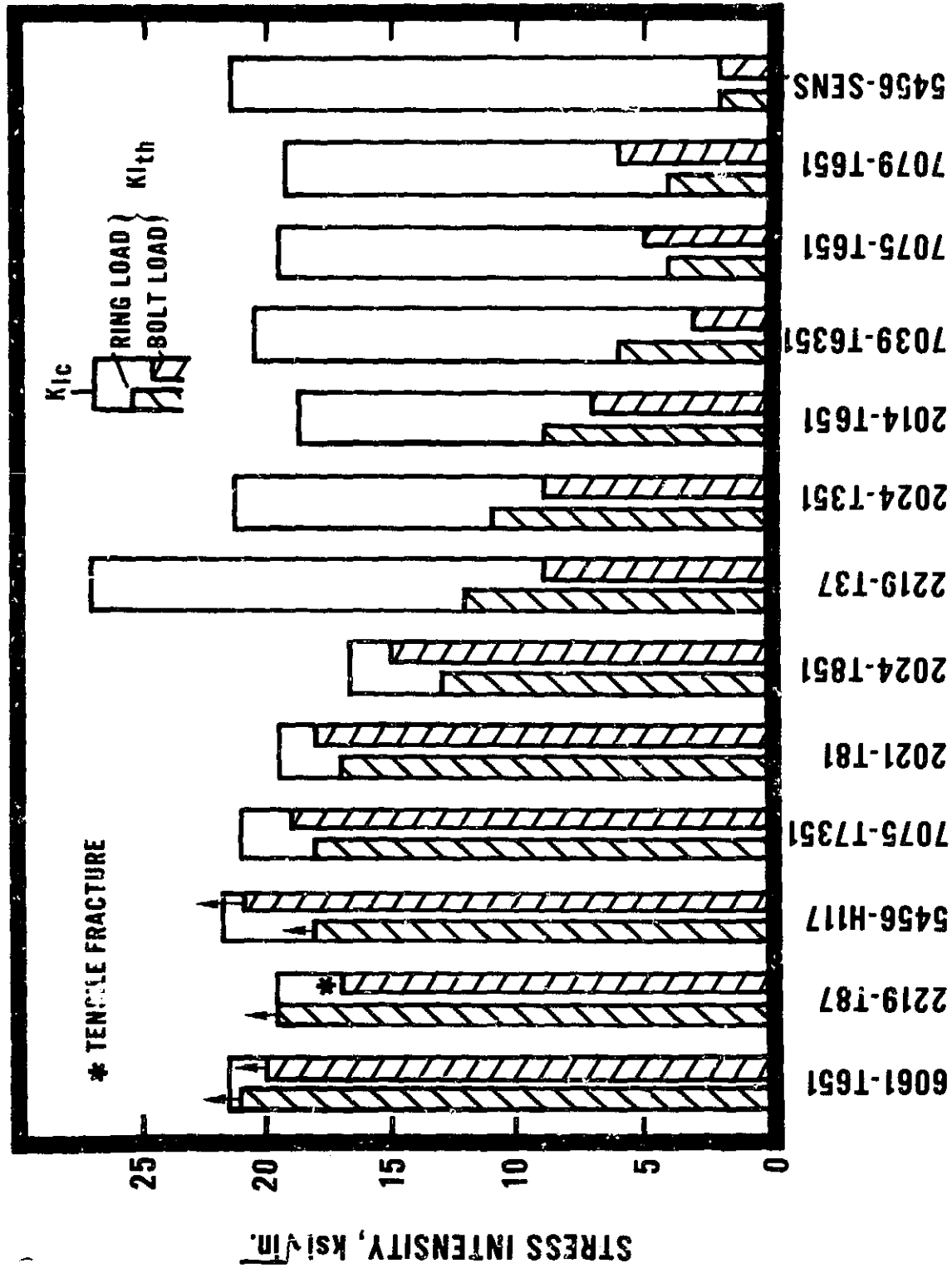
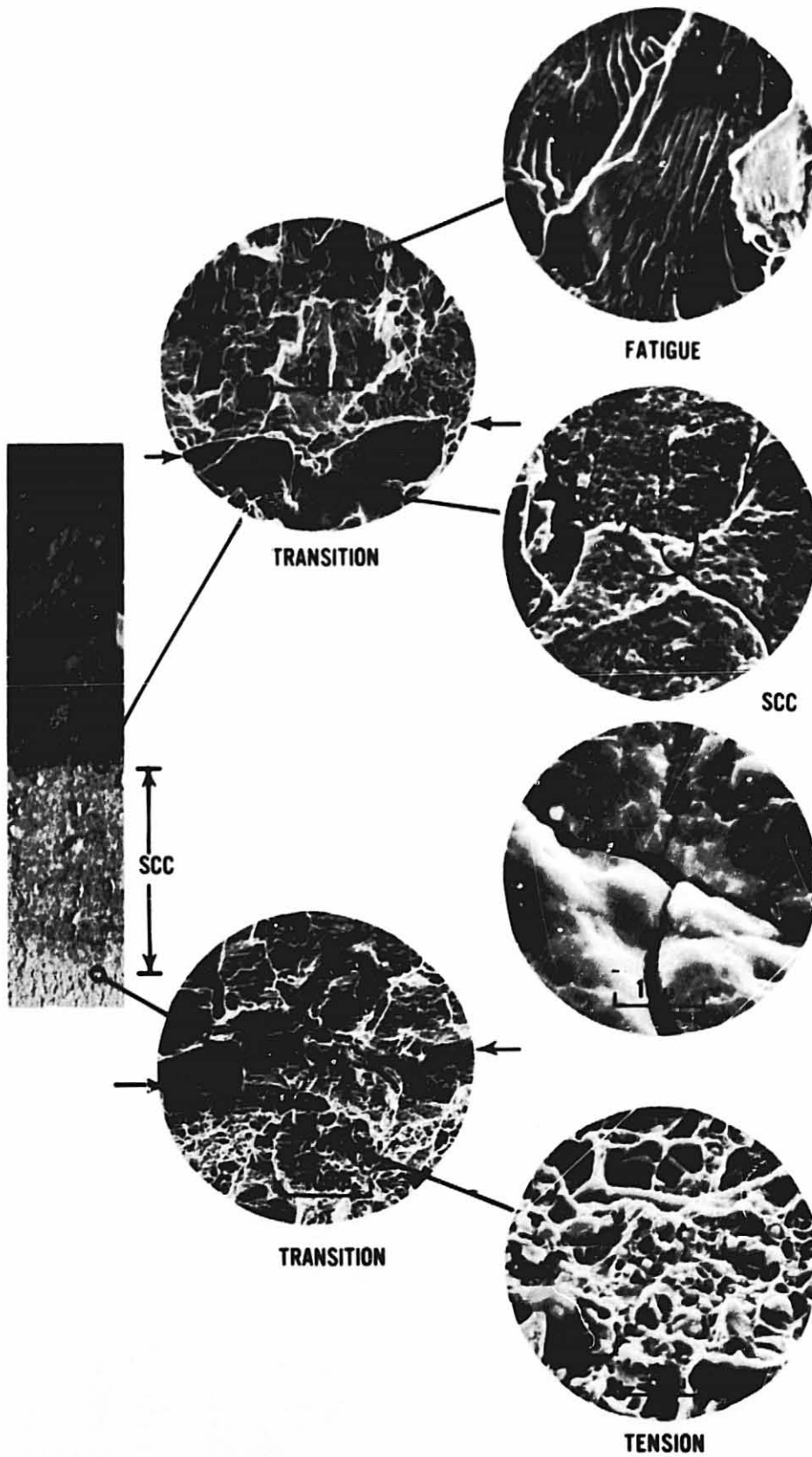
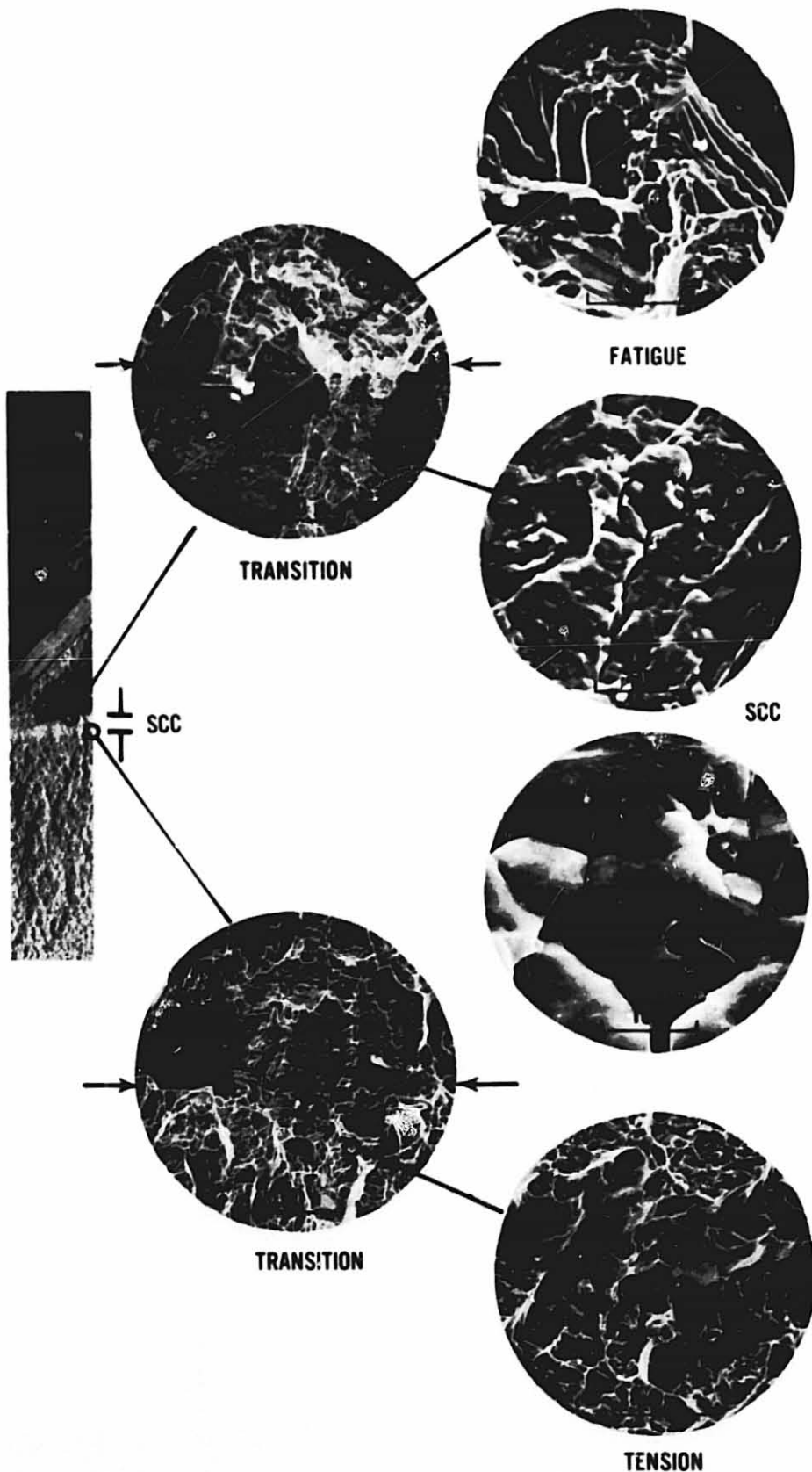


Fig. 66 RANKING OF ALUMINUM ALLOYS IN SALT-DICHROMATE-ACETATE SOLUTION S-L COMPACTS - RING VS BOLT LOADING.



**Fig. 67 SEM FRACTOGRAPHS OF S-L COMPACT TENSION SPECIMEN OF 7079-T651 BOLT LOADED TO 75%  $K_{Ic}$ . EXPOSED 4 mo INDUSTRIAL ATMOSPHERE**



**Fig. 68 SEM FRACTOGRAPHS OF S-L COMPACT TENSION SPECIMEN OF 7075-T7351 RING LOADED TO 95%  $K_{Ic}$ . EXPOSED 2780 hr TO SALT-DICHROMATE-ACETATE**

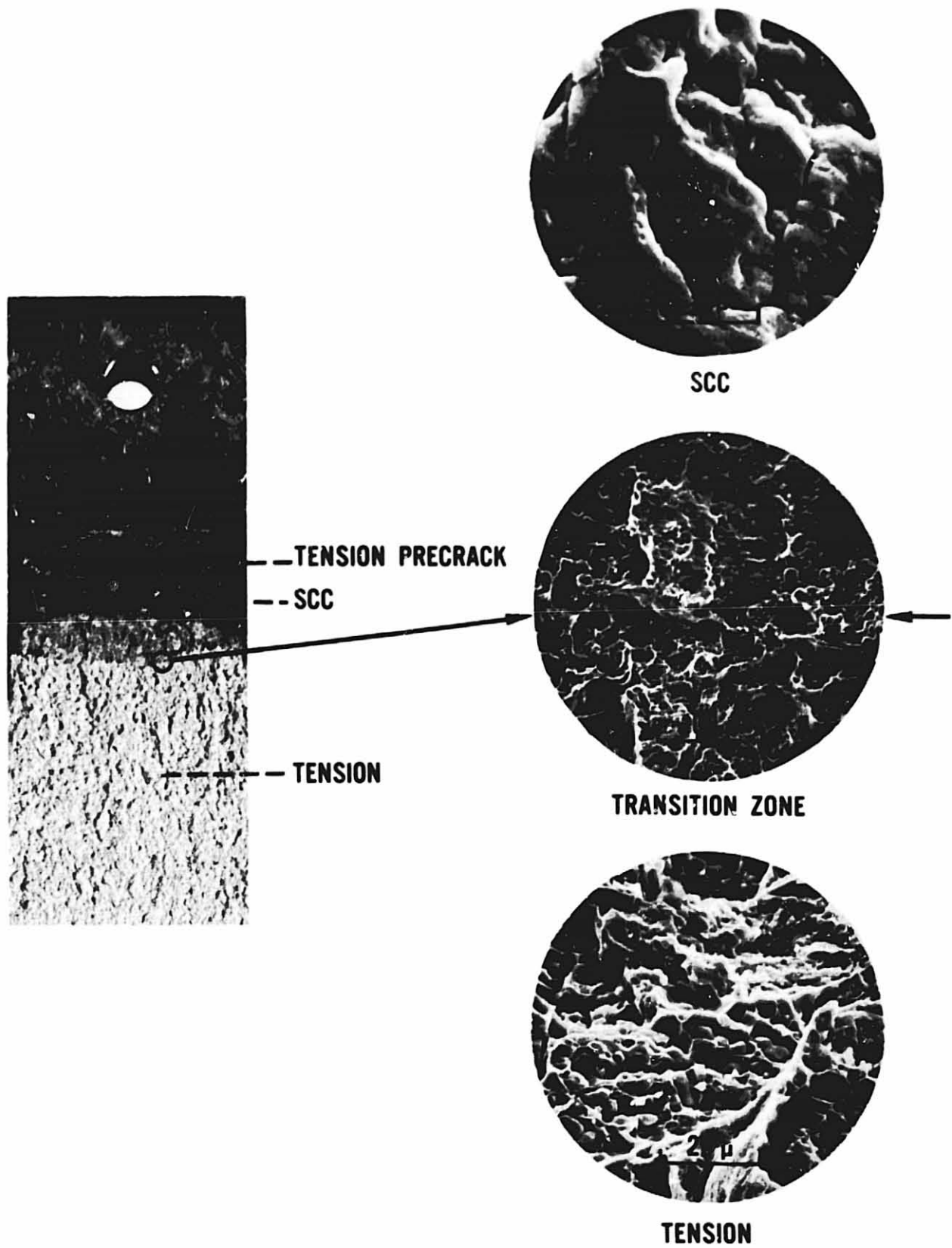


**Fig. 69 SEM FRACTOGRAPHS OF S-L DCB OF 2024-T851 BOLT LOADED TO POP-IN. EXPOSED 2352HR. TO SALT-DICHROMATE-ACETATE.**

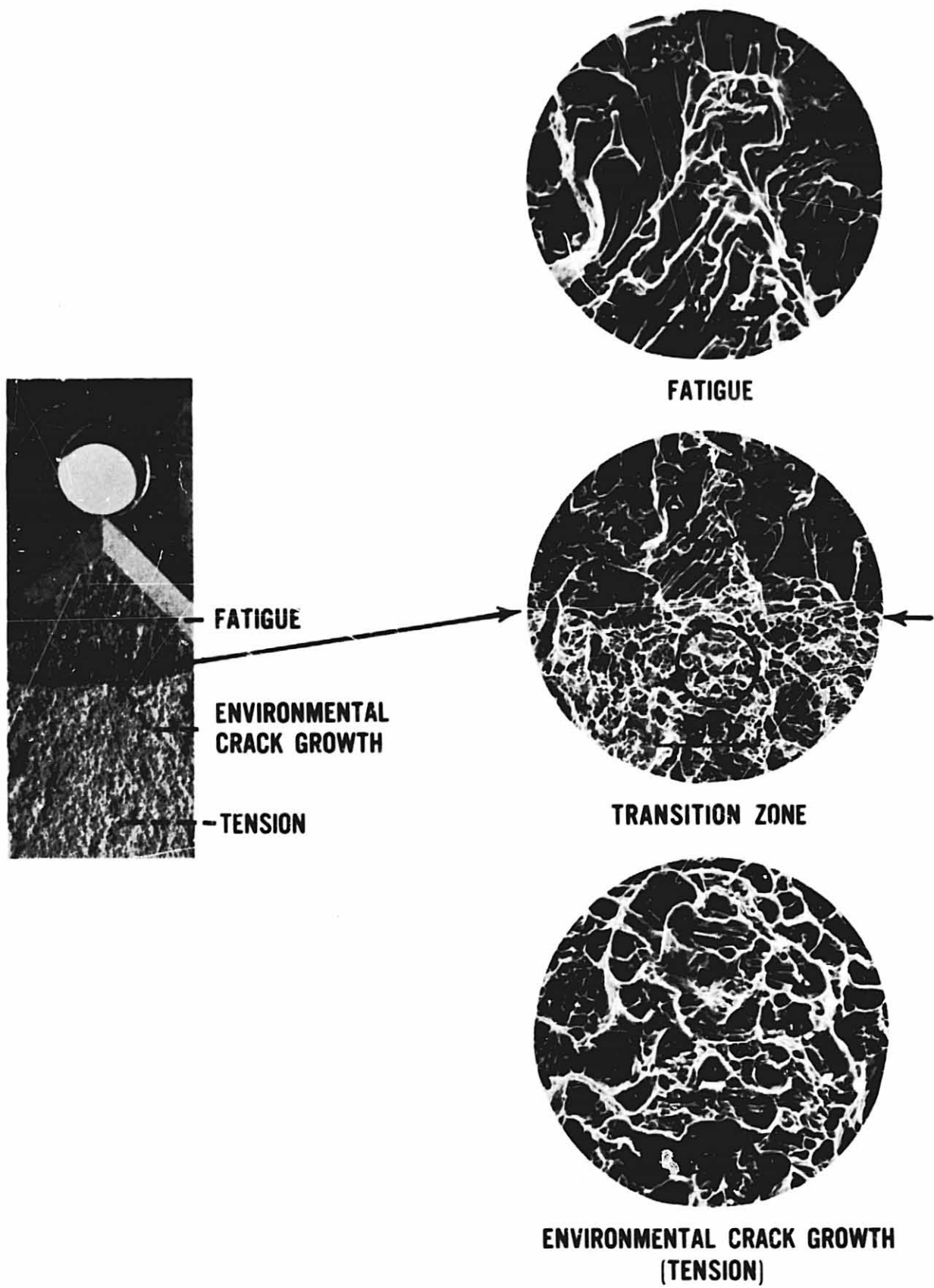


**Fig. 70 SEM FRACTOGRAPHS OF S-L COMPACT TENSION SPECIMEN OF 2219-T87 BOLT LOADED 95%  $K_{Ic}$ . EXPOSED 12 mo INDUSTRIAL ATMOSPHERE.**

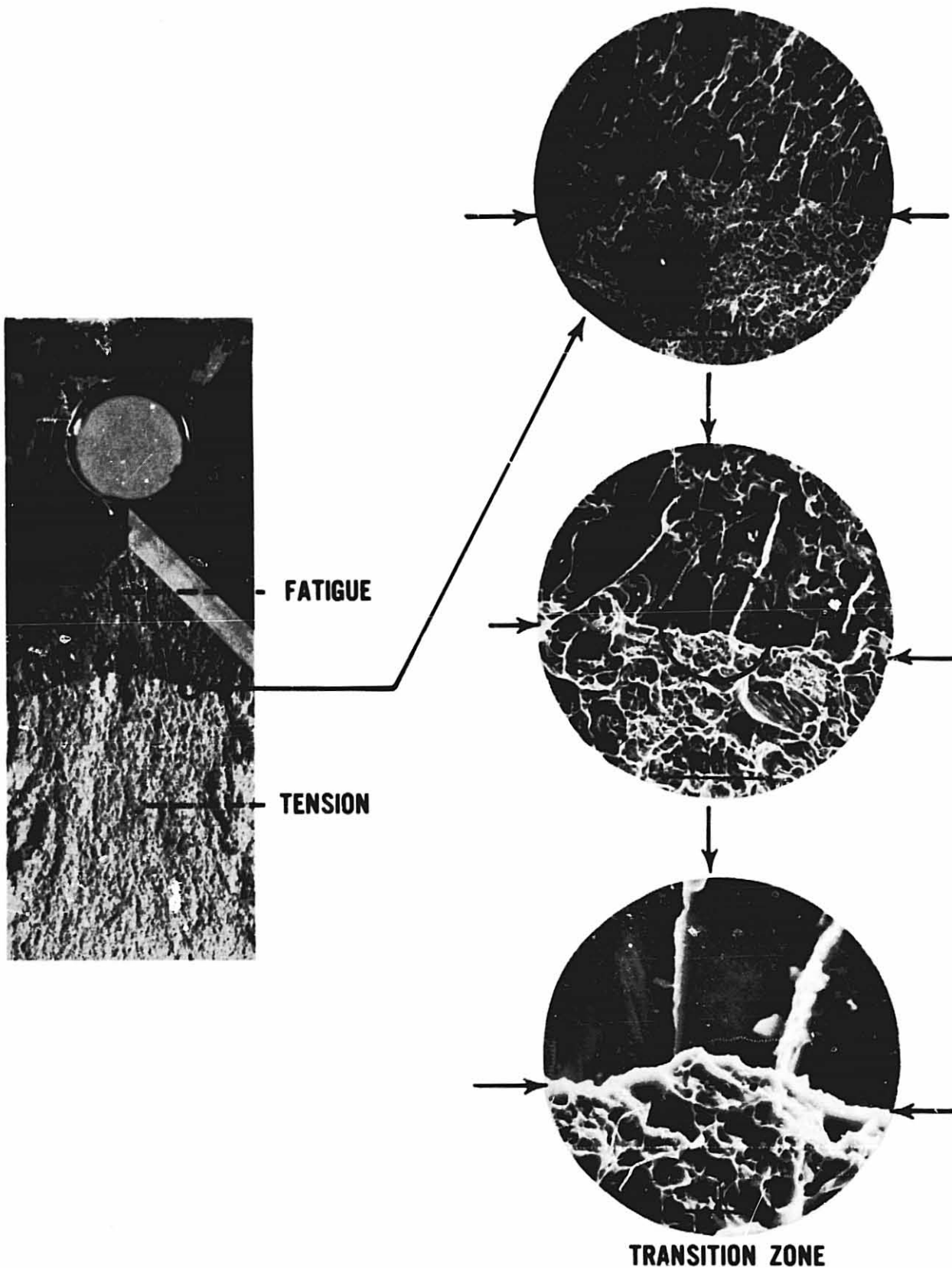
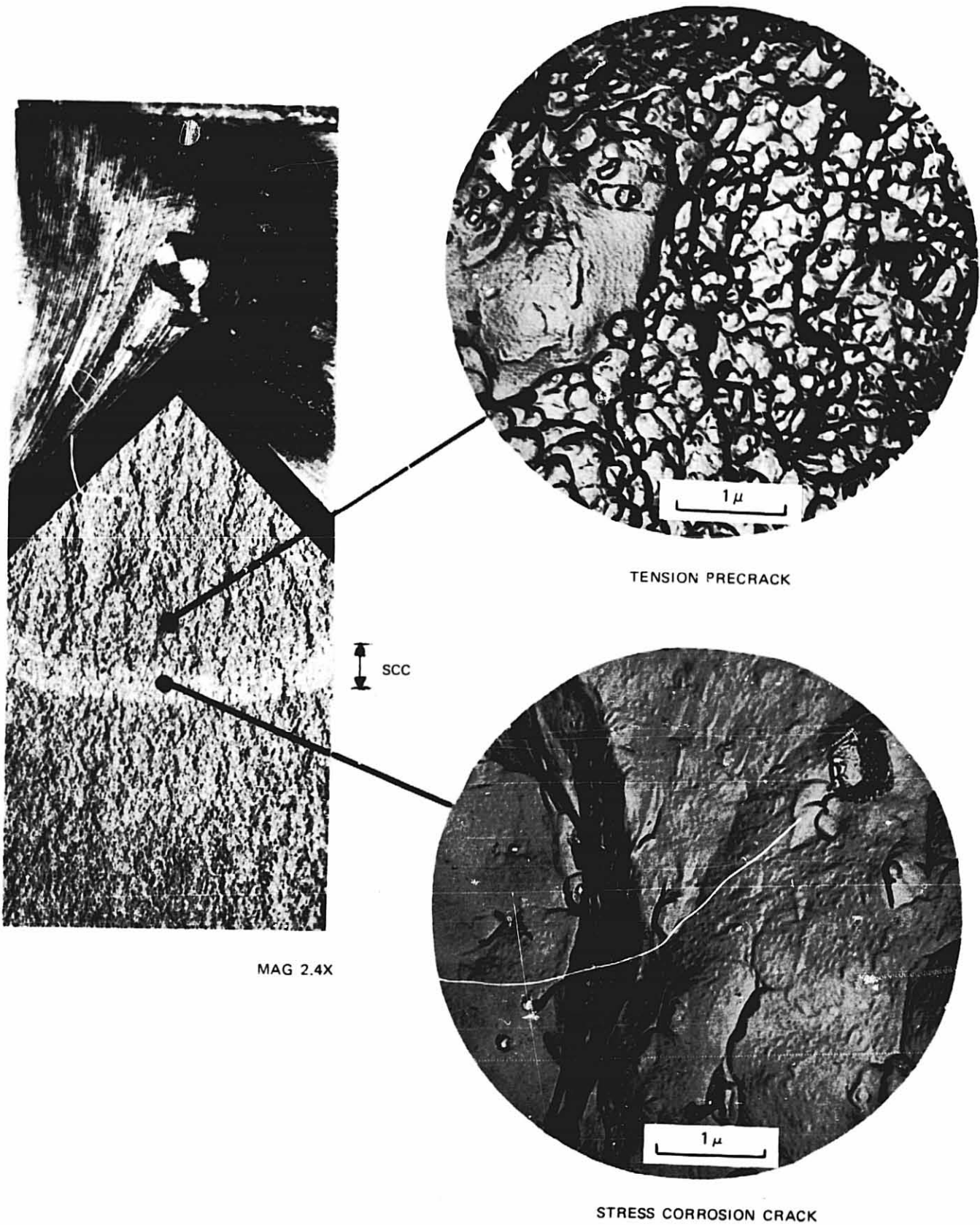


Fig. 71 SEM FRACTOGRAPHS OF S-L COMPACT TENSION SPECIMEN OF 6961-T651 BOLT LOADED TO 75%  $K_{Ic}$ . EXPOSED 2184 hr. TO SALT-DICHROMATE-ACETATE.

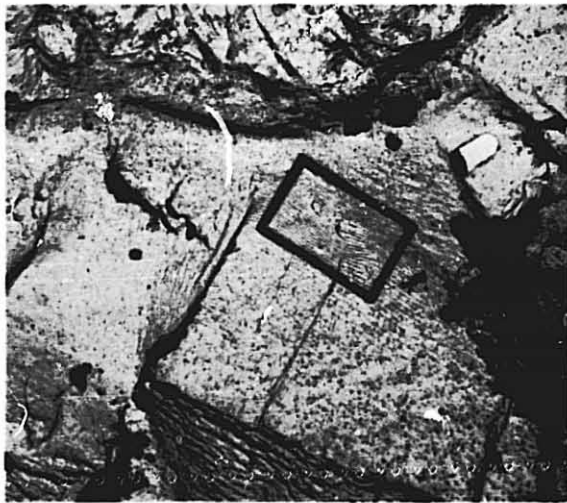


MAG 2.4X

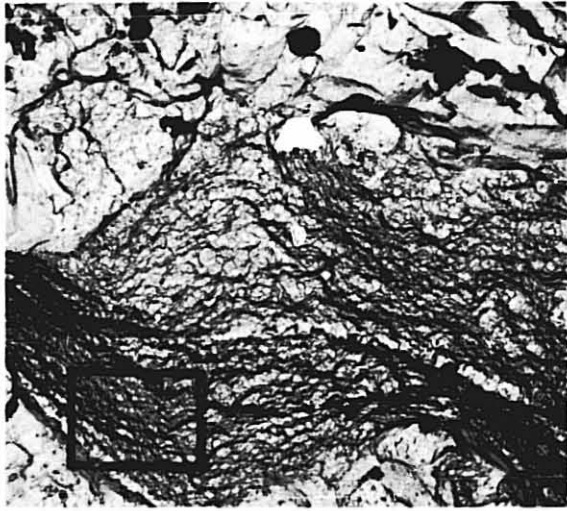
TENSION PRECRACK

STRESS CORROSION CRACK

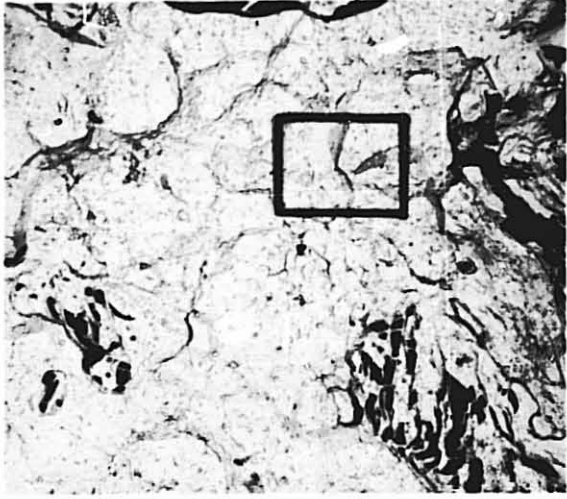
FIG. 72 TEM FRACTOGRAPHS OF TENSION PRECRACK AND STRESS-CORROSION CRACK IN 7075 - T651 ALLOY PLATE



FATIGUE



TENSION



SCC

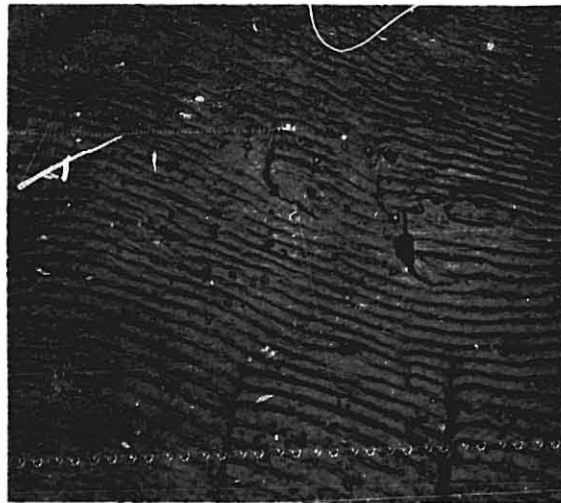
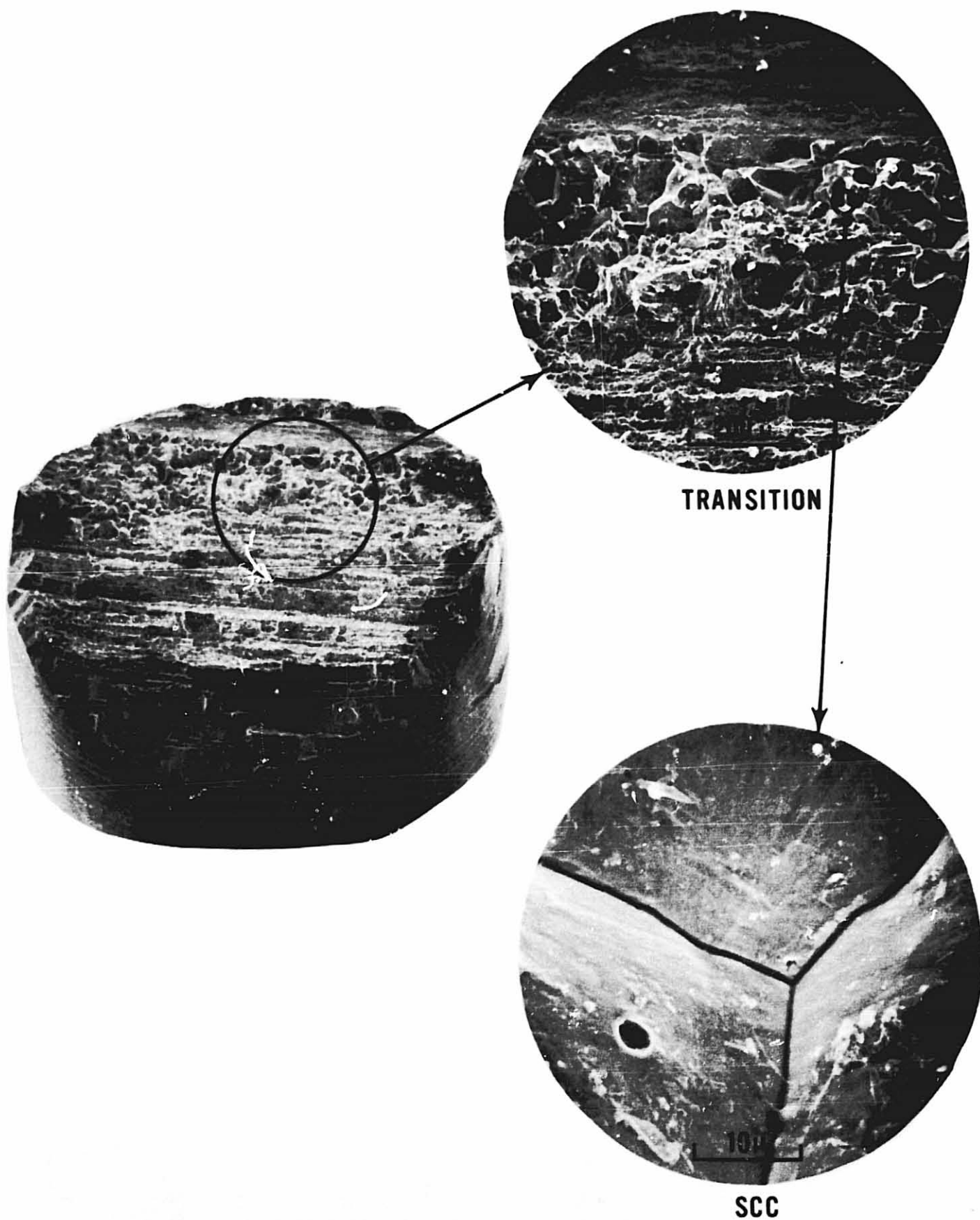
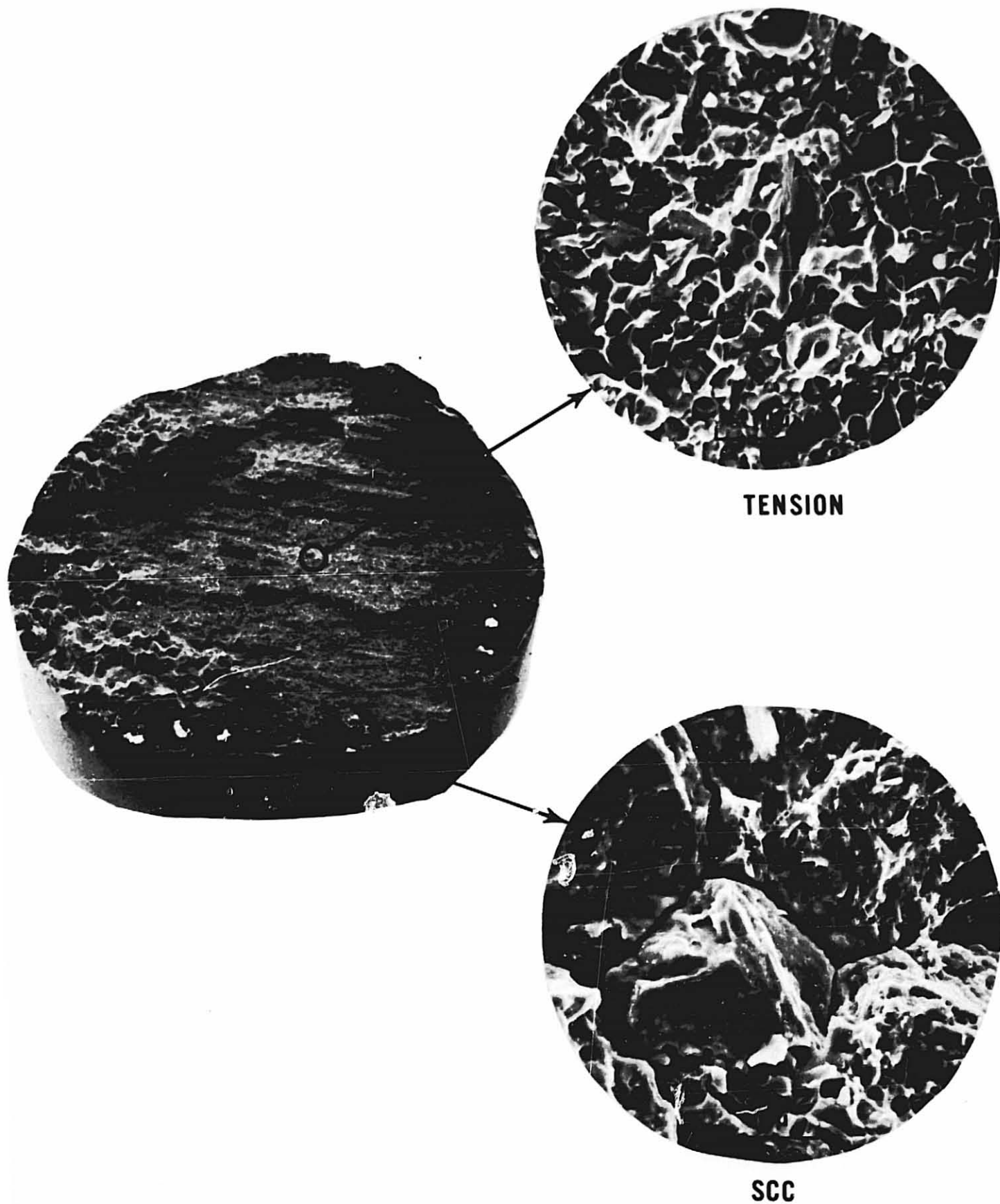


Fig. 73 TEM fractographs of S-L compact tension specimens of 7075-T7351. SCC occurred in 2780 hr exposure to salt-dichromate-acetate.



**Fig. 74 SEM FRACTOGRAPHS OF TENSION AND SCC FRACTURE SURFACES IN (s) SPECIMEN OF 431 HT200 ALLOY EXPOSED 141 DAYS TO SEACOAST ATMOSPHERE.**



**Fig.75 SEM FRACTOGRAPHS OF TENSION AND SCC FRACTURE SURFACES IN (s) SPECIMEN OF AM 355 SCT 850 ALLOY EXPOSED 3 DAYS IN 3.5% NaCl SOLUTION.**

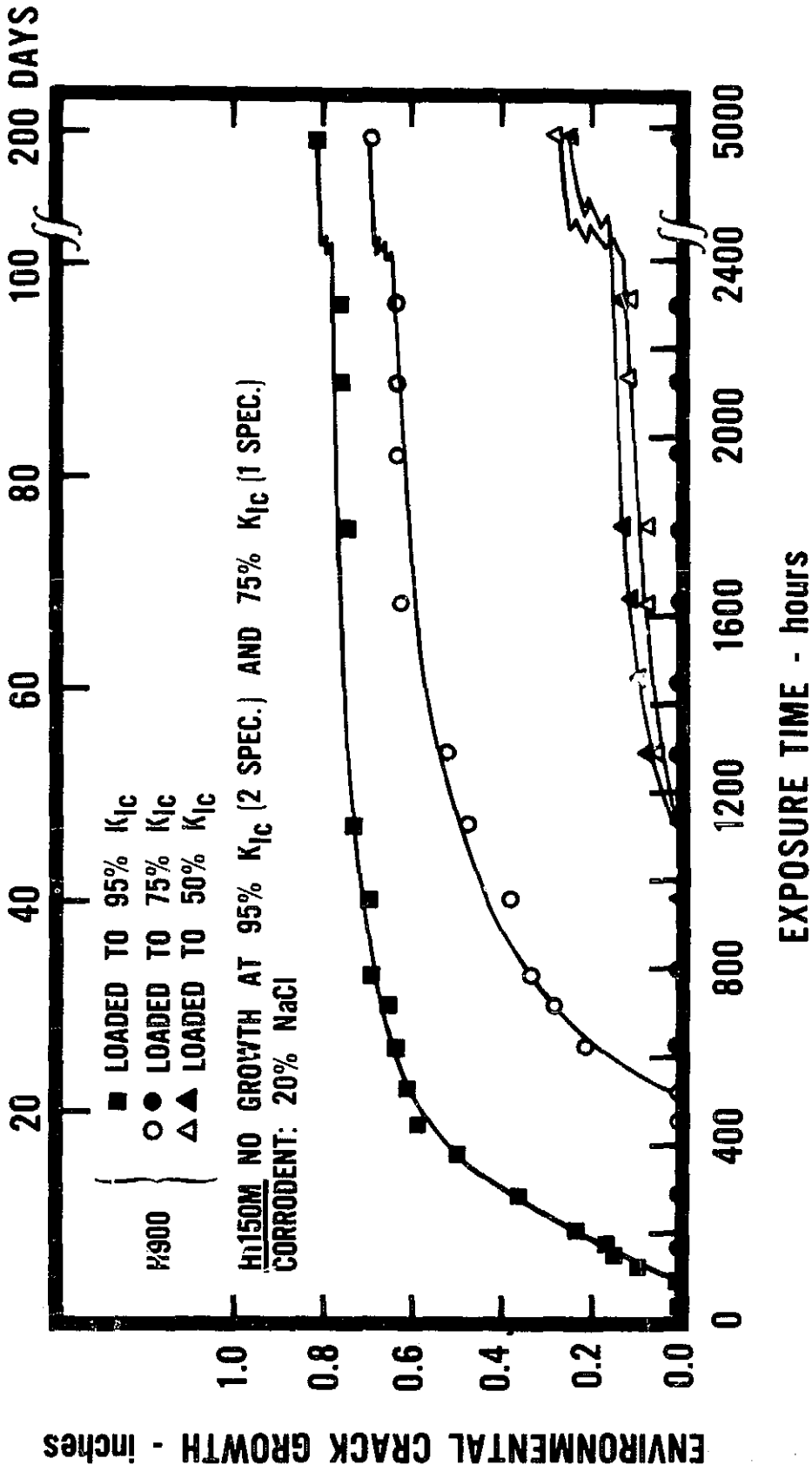
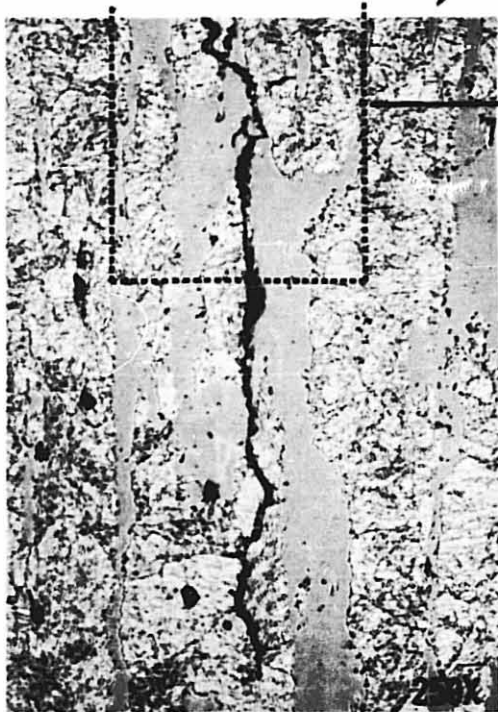
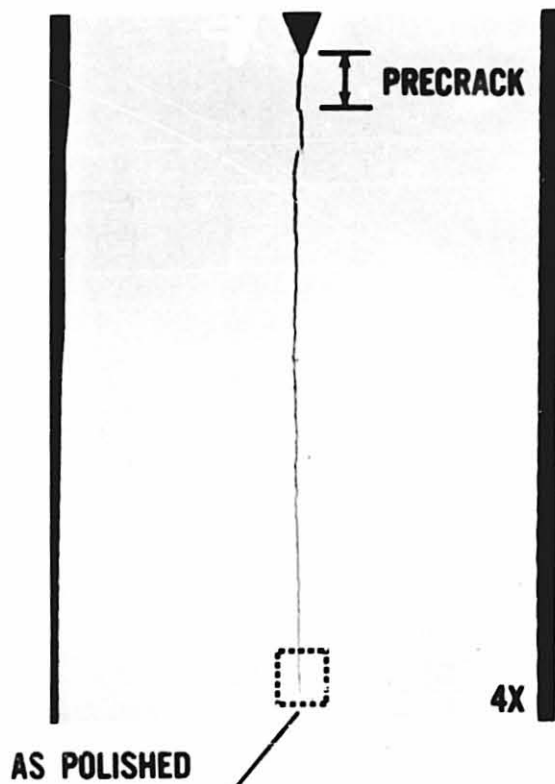


**Fig. 76 EXPLORATORY SCC TEST OF BOLT LOADED PRECRACKED COMPACT TENSION SPECIMENS OF 15-5PH ALLOY STEEL**

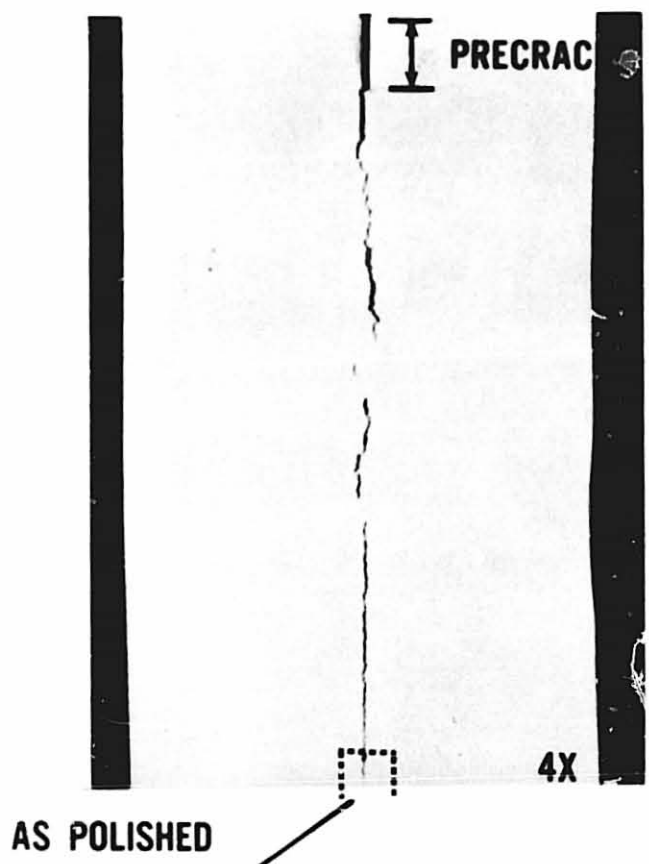


OXALIC ETCH

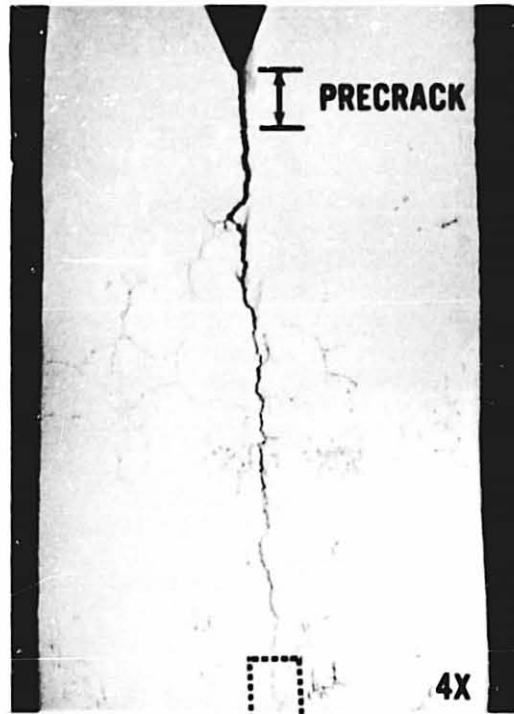


OXALIC ETCH

**Fig. 77 PHOTOMICROGRAPHS OF CROSS SECTION ILLUSTRATING CRACK GROWTH AT MIDPLANE OF T-L SPECIMEN OF 17-7 PH RH1050 ALLOY EXPOSED 41 DAYS TO SEACOAST ATMOSPHERE**

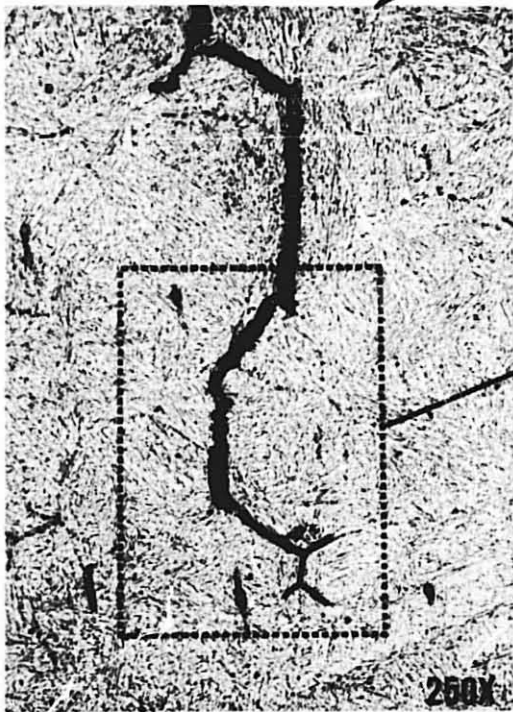


**OXALIC ETCH**  
**Fig. 78** PHOTOMICROGRAPHS OF CROSS SECTION ILLUSTRATING  
CRACK GROWTH AT MIDPLANE OF PH13-8 Mo H1050 ALLOY  
EXPOSED 141 DAYS TO SEACOAST ATMOSPHERE



AS POLISHED

(PRIOR AUSTENITE GRAIN BOUNDARIES  
PARTIALLY SHOWN)



250X

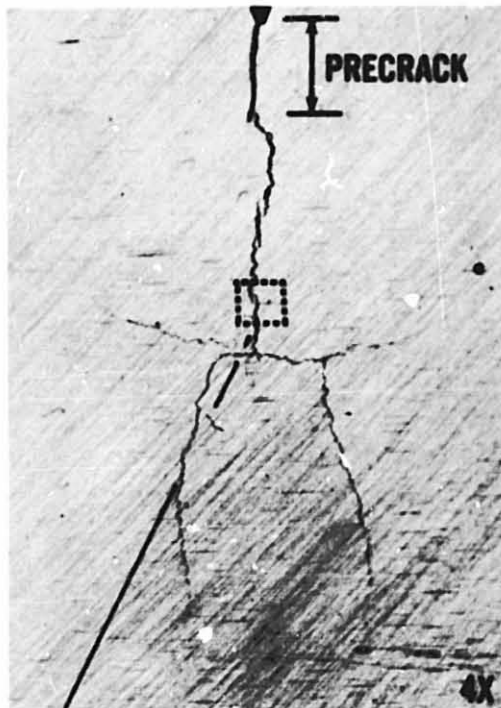


500X

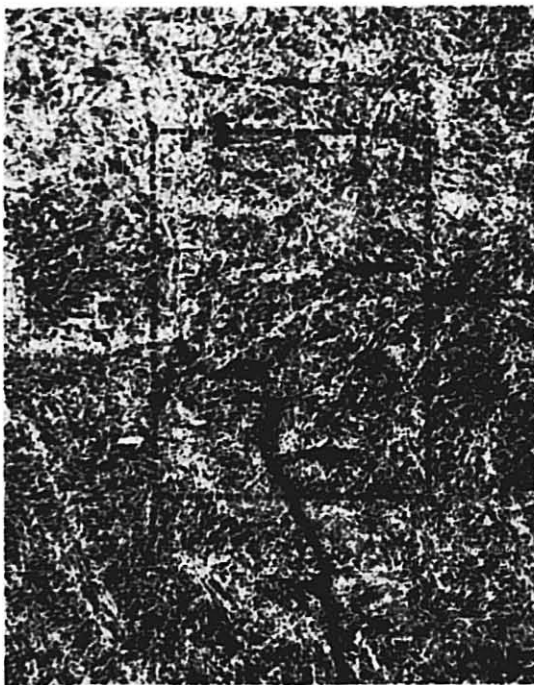
OXALIC ETCH

OXALIC ETCH

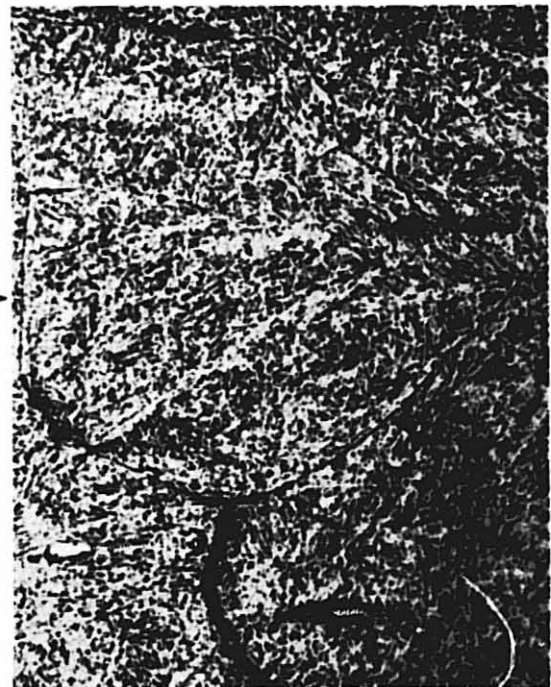
**Fig. 79 PHOTOMICROGRAPHS OF CROSS SECTION ILLUSTRATING  
CRACK GROWTH AT MIDPLANE OF T-L SPECIMEN OF 431 HT200  
ALLOY EXPOSED 141 DAYS TO SEACOAST ATMOSPHERE**



AS POLISHED



OXALIC ETCH



OXALIC ETCH

**Fig. 80 PHOTOMICROGRAPHS OF CROSS SECTION ILLUSTRATING CRACK GROWTH AT MID-PLANE OF L-T SPECIMEN OF AM355 SCT 850 ALLOY BAR EXPOSED 73 DAYS TO SEACOAST ATMOSPHERE**

**TYPICAL**

**ABNORMAL**



**PH15-7Mo RH950**

**AM355 SCT850 (BAR)**

**Fig. 81 FRACTURE FACES OF LONG-TRANSVERSE (T-L)  
COMPACTS EXPOSED UNSTRESSED 205 DAYS  
BY TOTAL IMMERSION IN 20% NaCl SOLUTION**

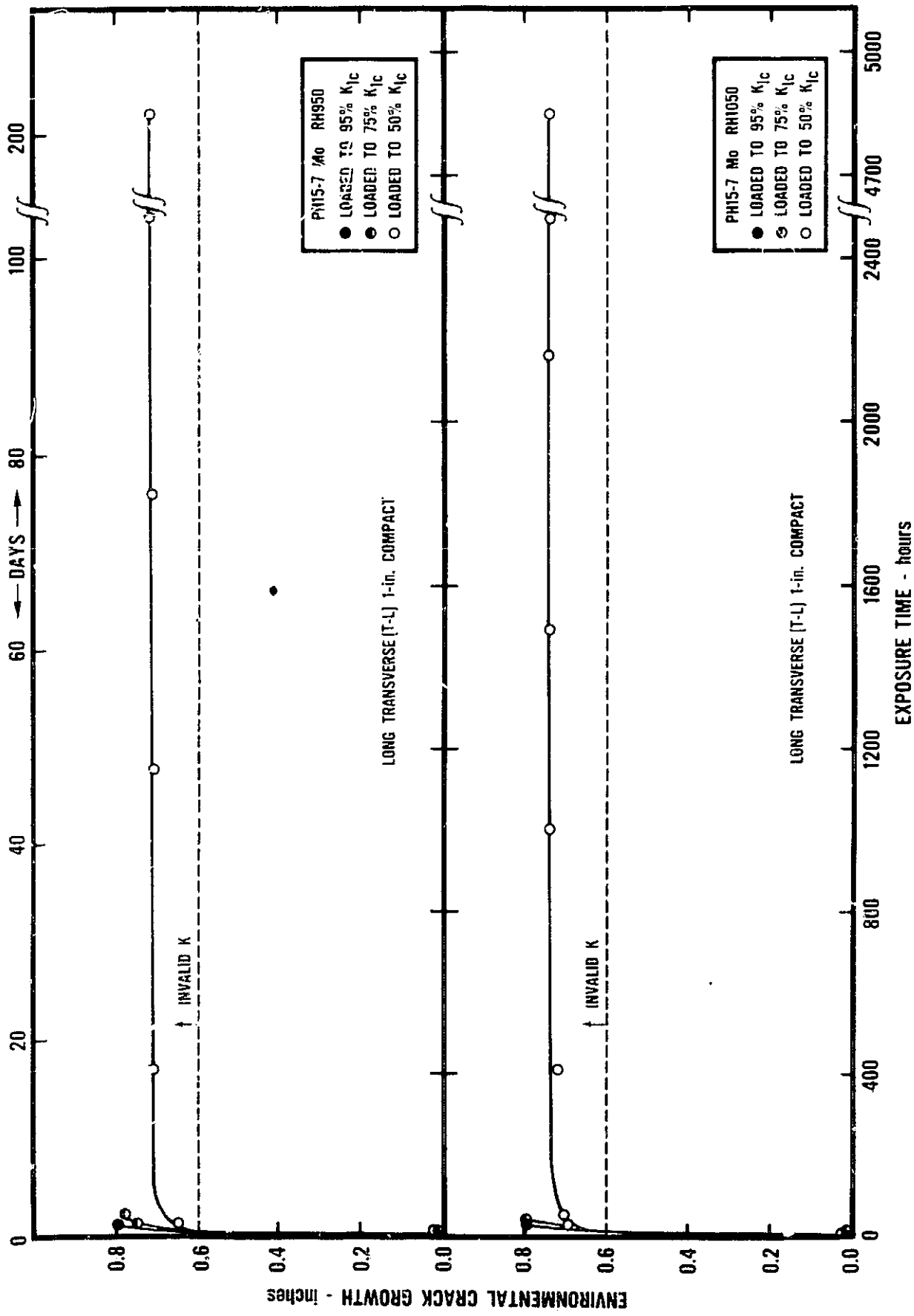


Fig. 82 ENVIRONMENTAL CRACK GROWTH OF VARIOUS STAINLESS STEELS IN 20% NaCl SOLUTION

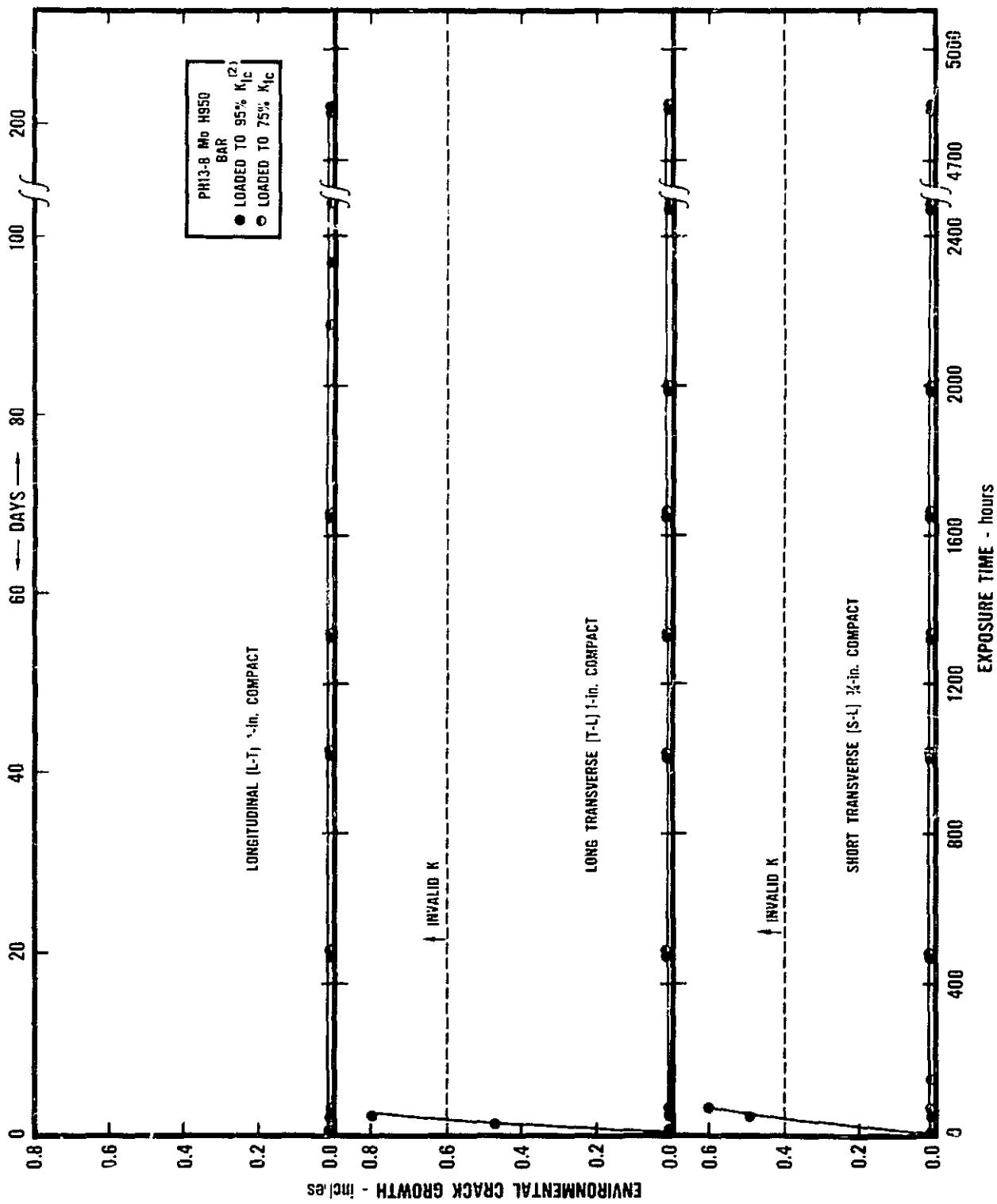


Fig.83 ENVIRONMENTAL CRACK GROWTH OF VARIOUS STAINLESS STEELS IN 20% NaCl SOLUTION

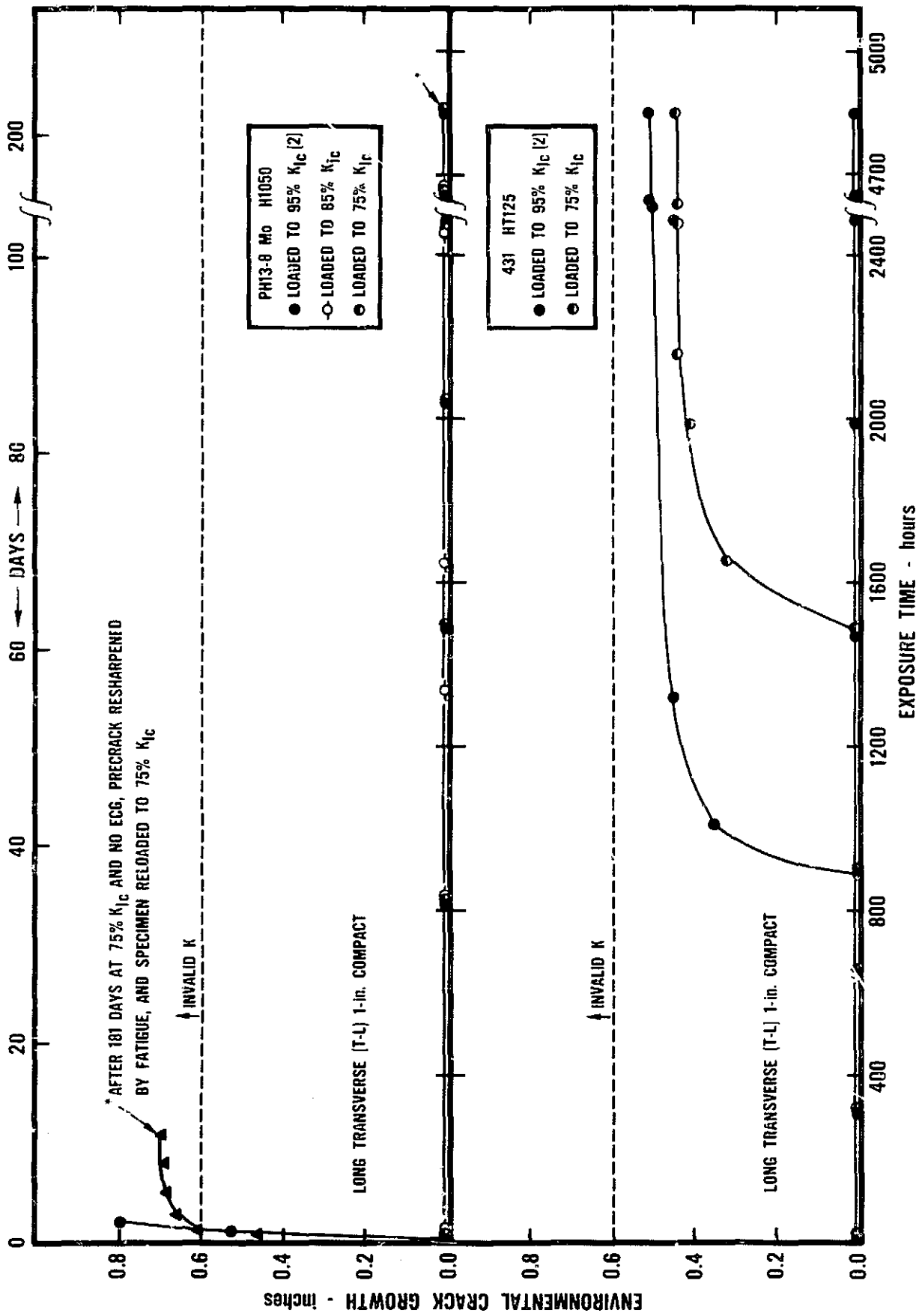


Fig. 84 ENVIRONMENTAL CRACK GROWTH OF VARIOUS STAINLESS STEELS IN 20% NaCl SOLUTION

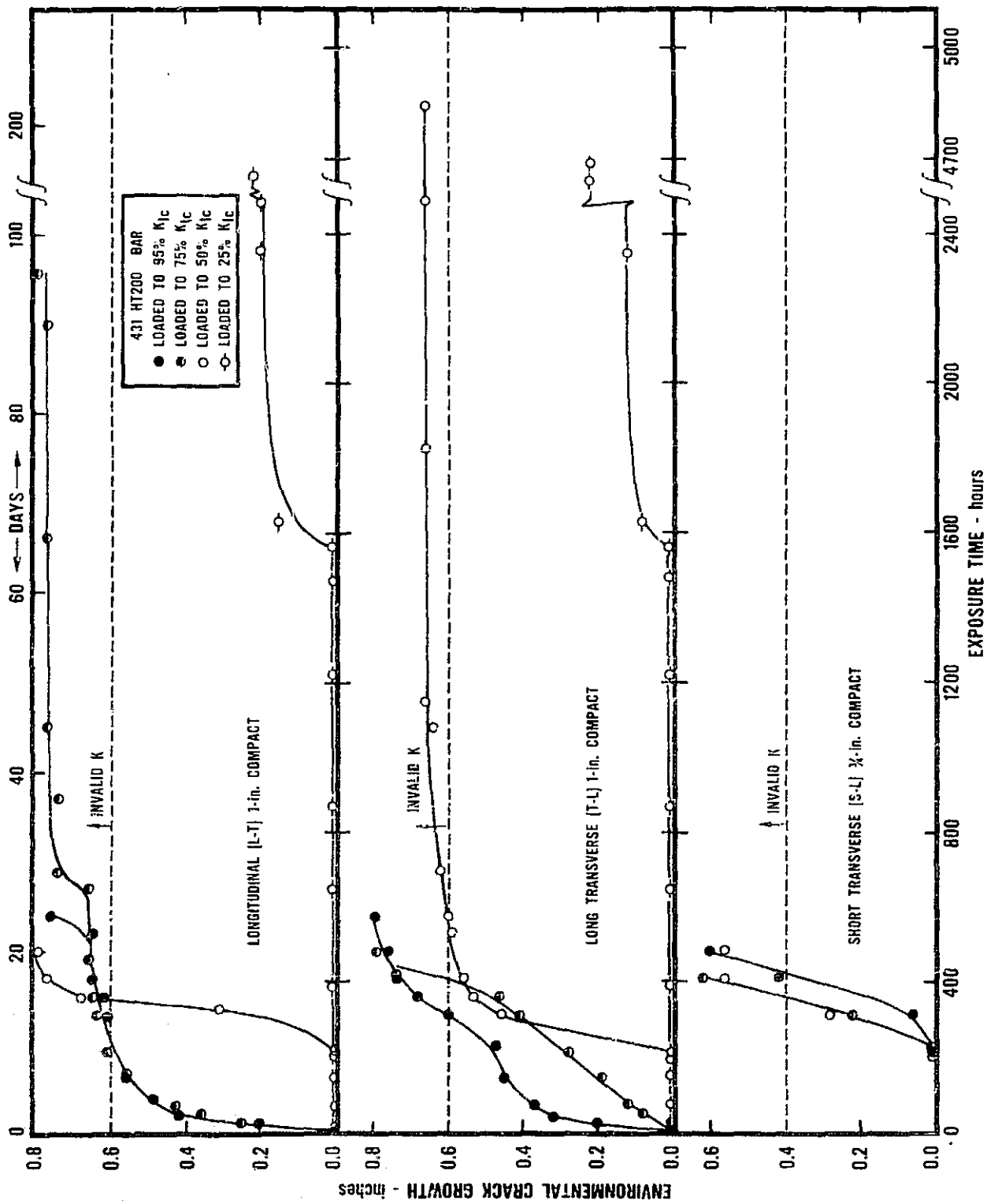


Fig. 85 ENVIRONMENTAL CRACK GROWTH OF VARIOUS STAINLESS STEELS IN 20% NaCl SOLUTION

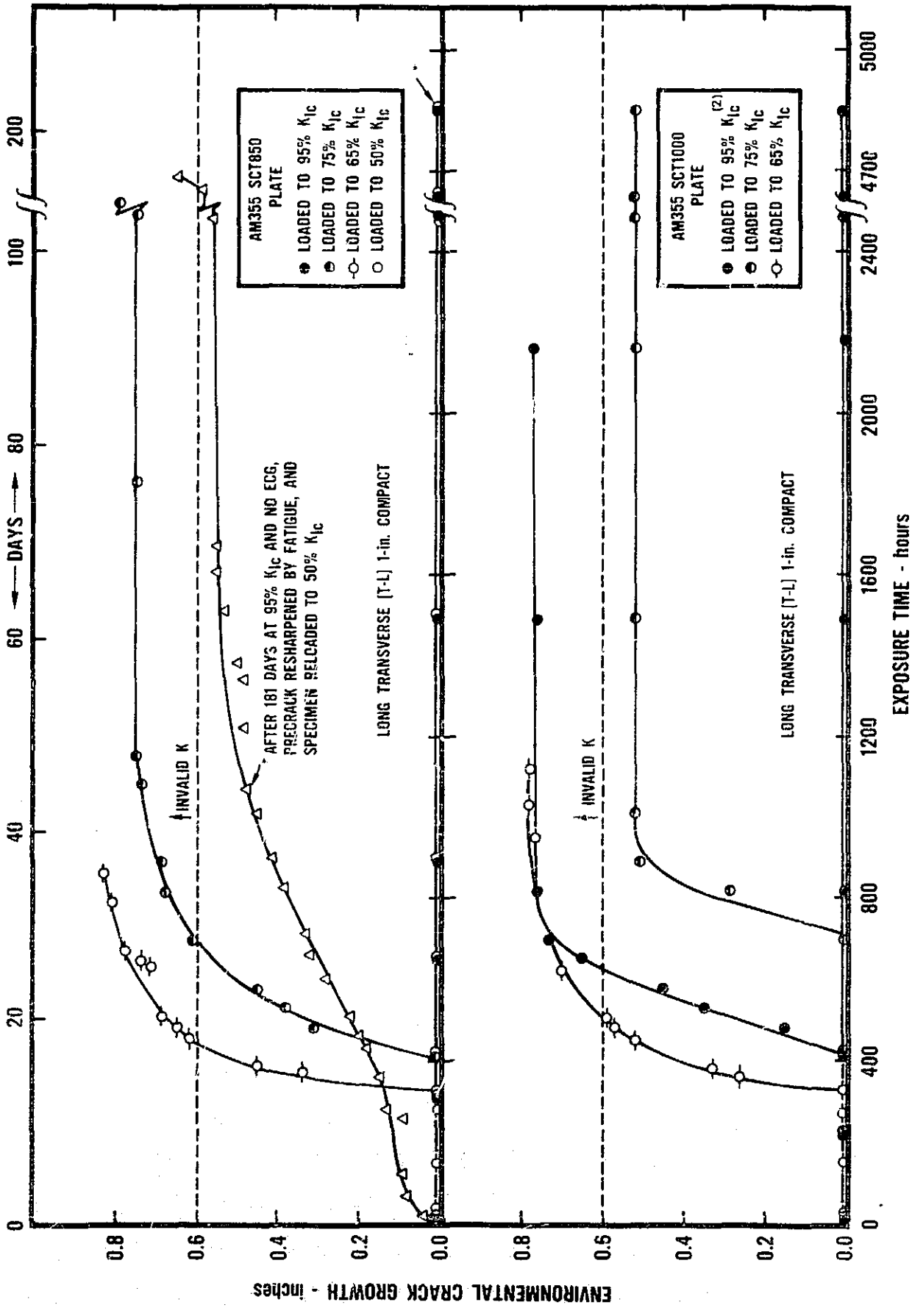


Fig. 86 ENVIRONMENTAL CRACK GROWTH OF VARIOUS STAINLESS STEELS IN 20% NaCl SOLUTION

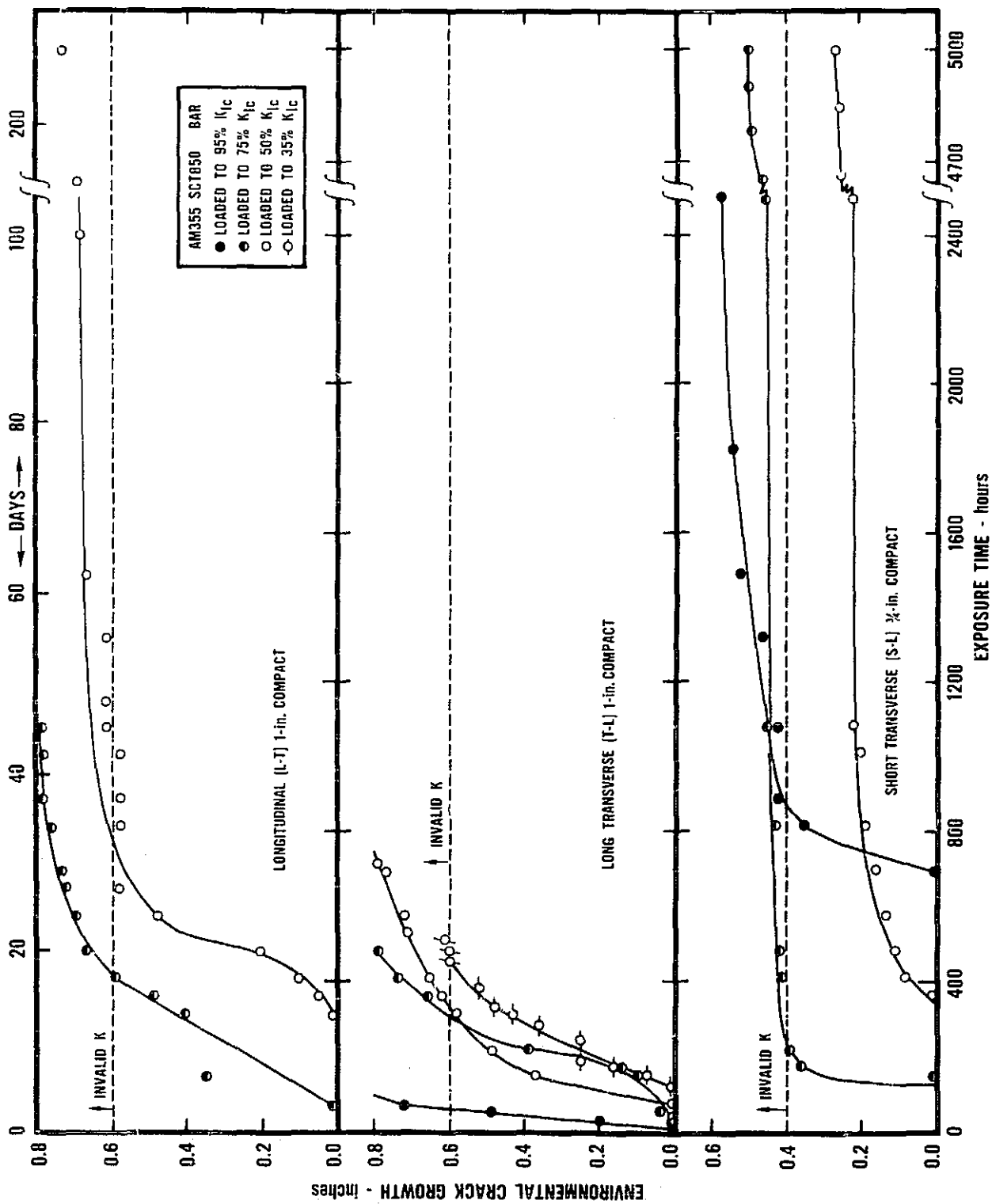


Fig. 87 ENVIRONMENTAL CRACK GROWTH OF VARIOUS STAINLESS STEELS IN 20% NaCl SOLUTION

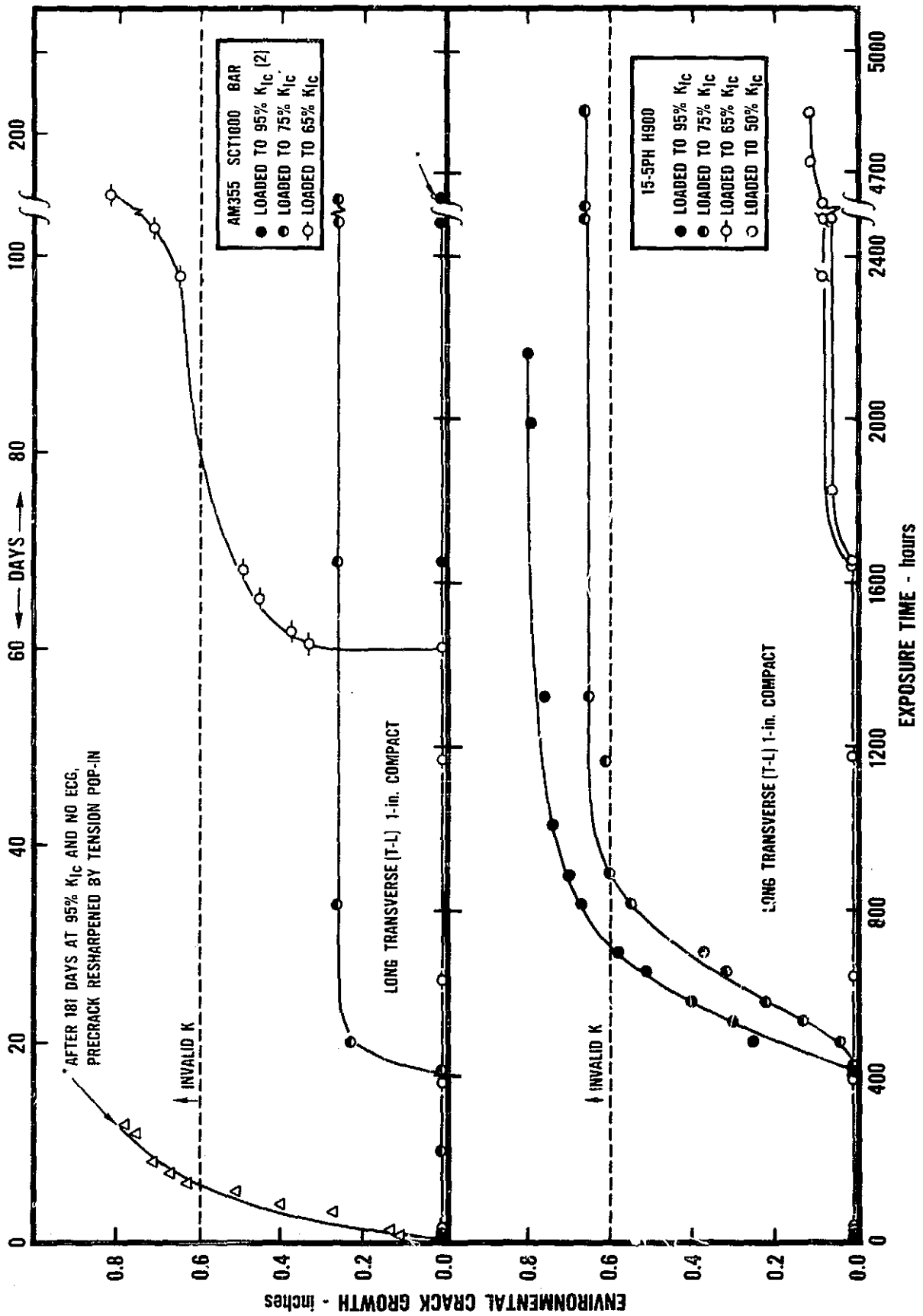


Fig. 88 ENVIRONMENTAL CRACK GROWTH OF VARIOUS STAINLESS STEELS IN 20% NaCl SOLUTION

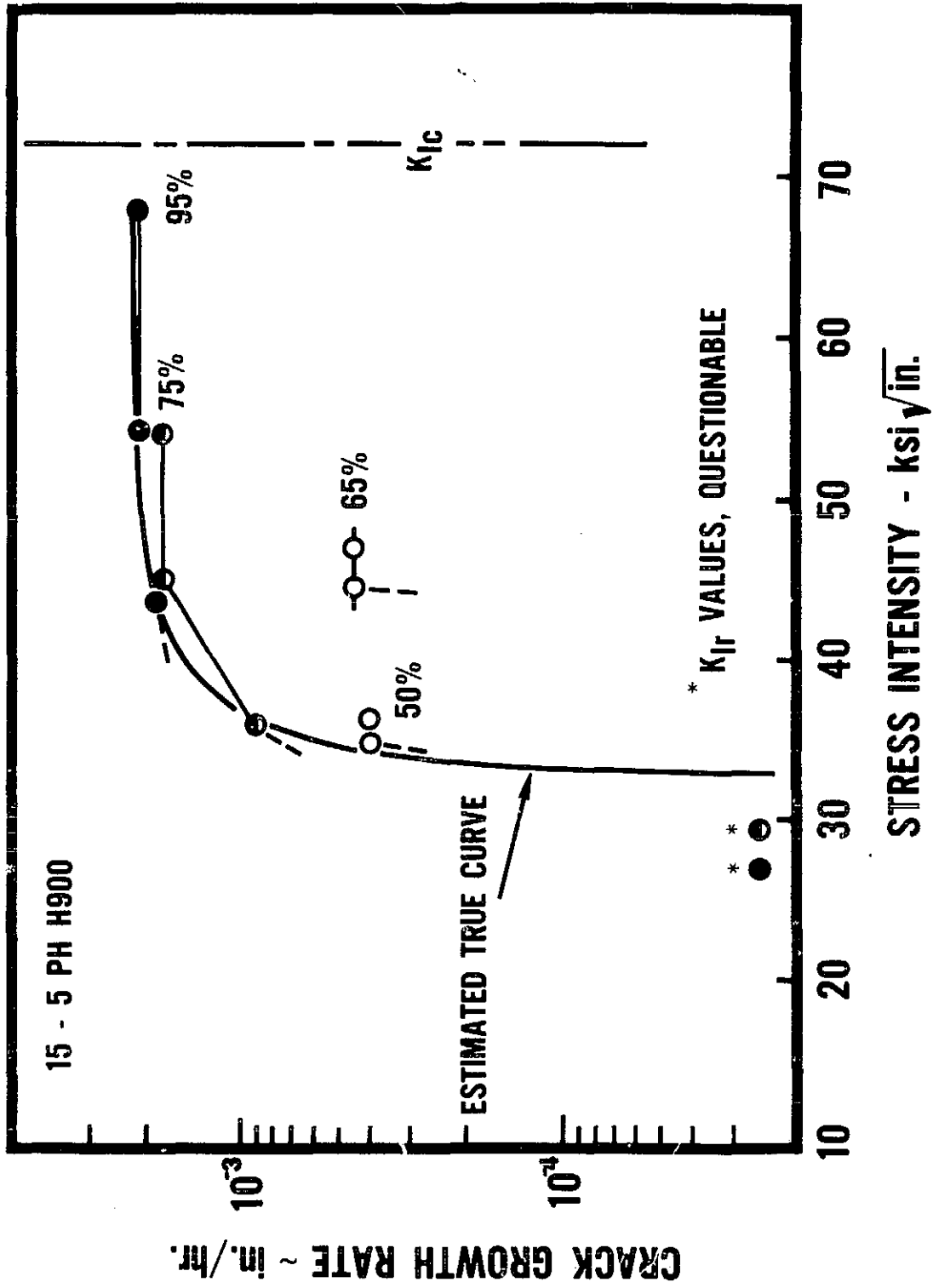
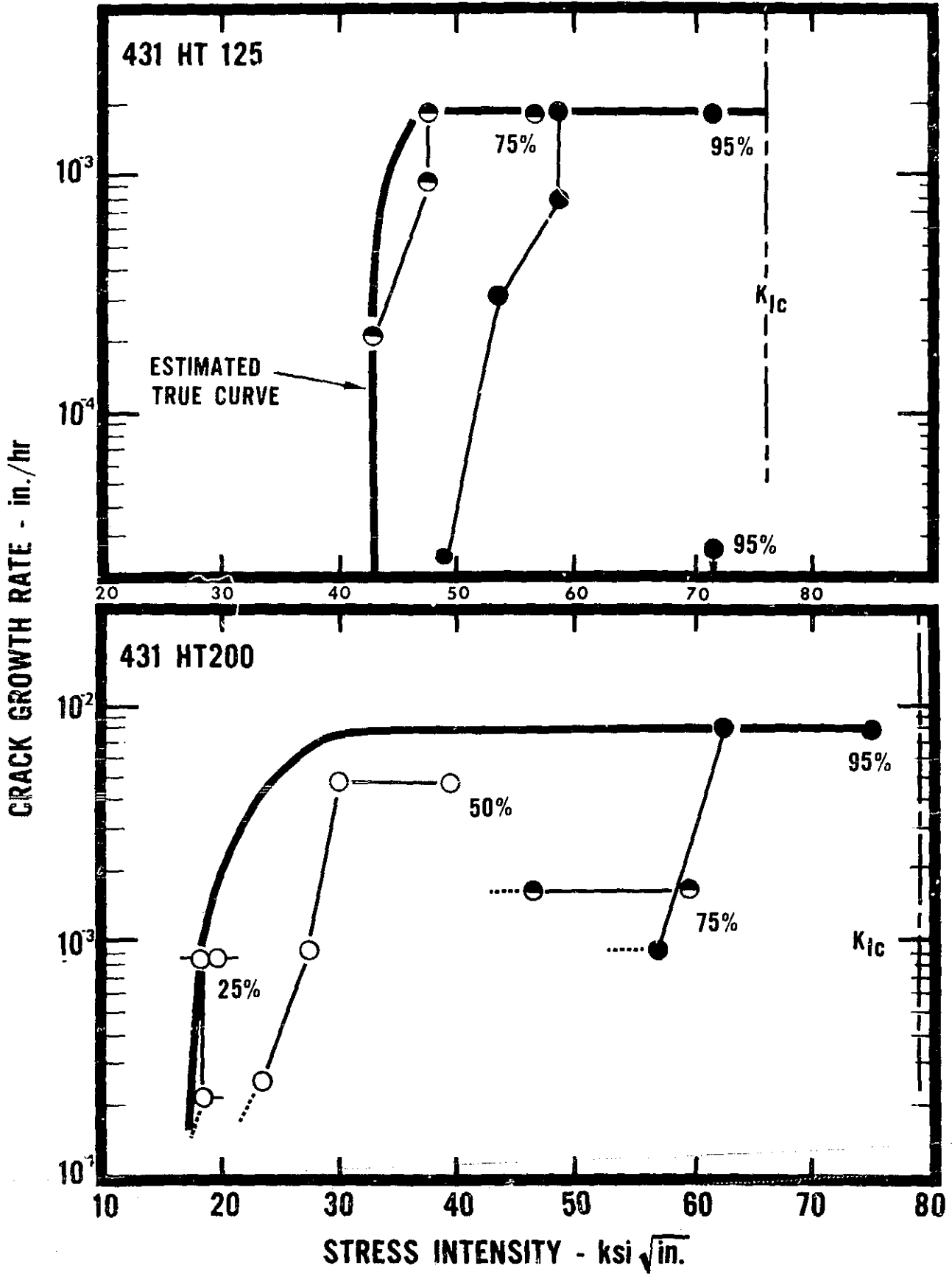
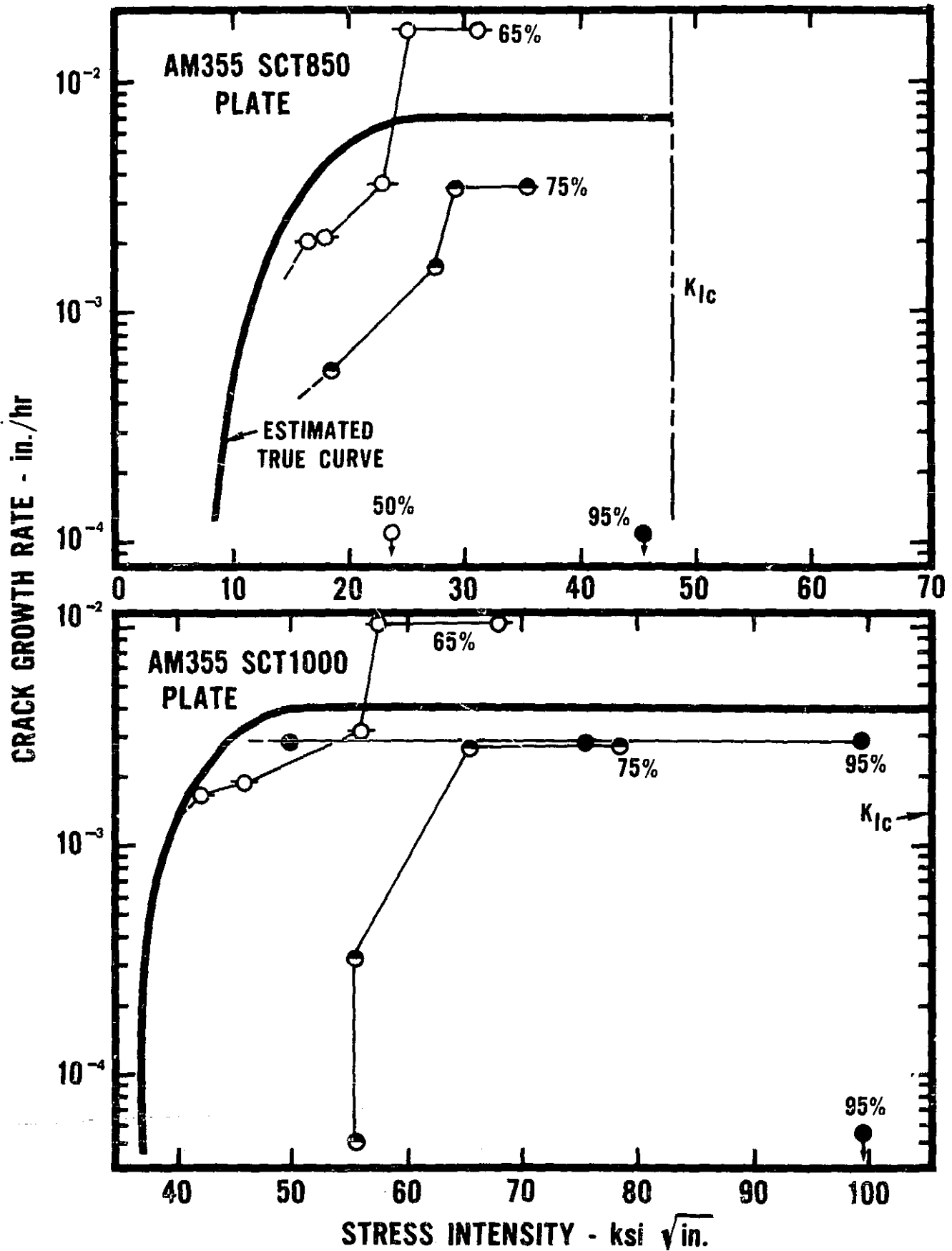


Fig. 89 K-RATE CURVES FOR T-L COMPACTS



**Fig. 90 K-RATE CURVES FOR T-L COMPACTS**



**Fig. 91 K-RATE CURVES FOR T-L COMPACTS**

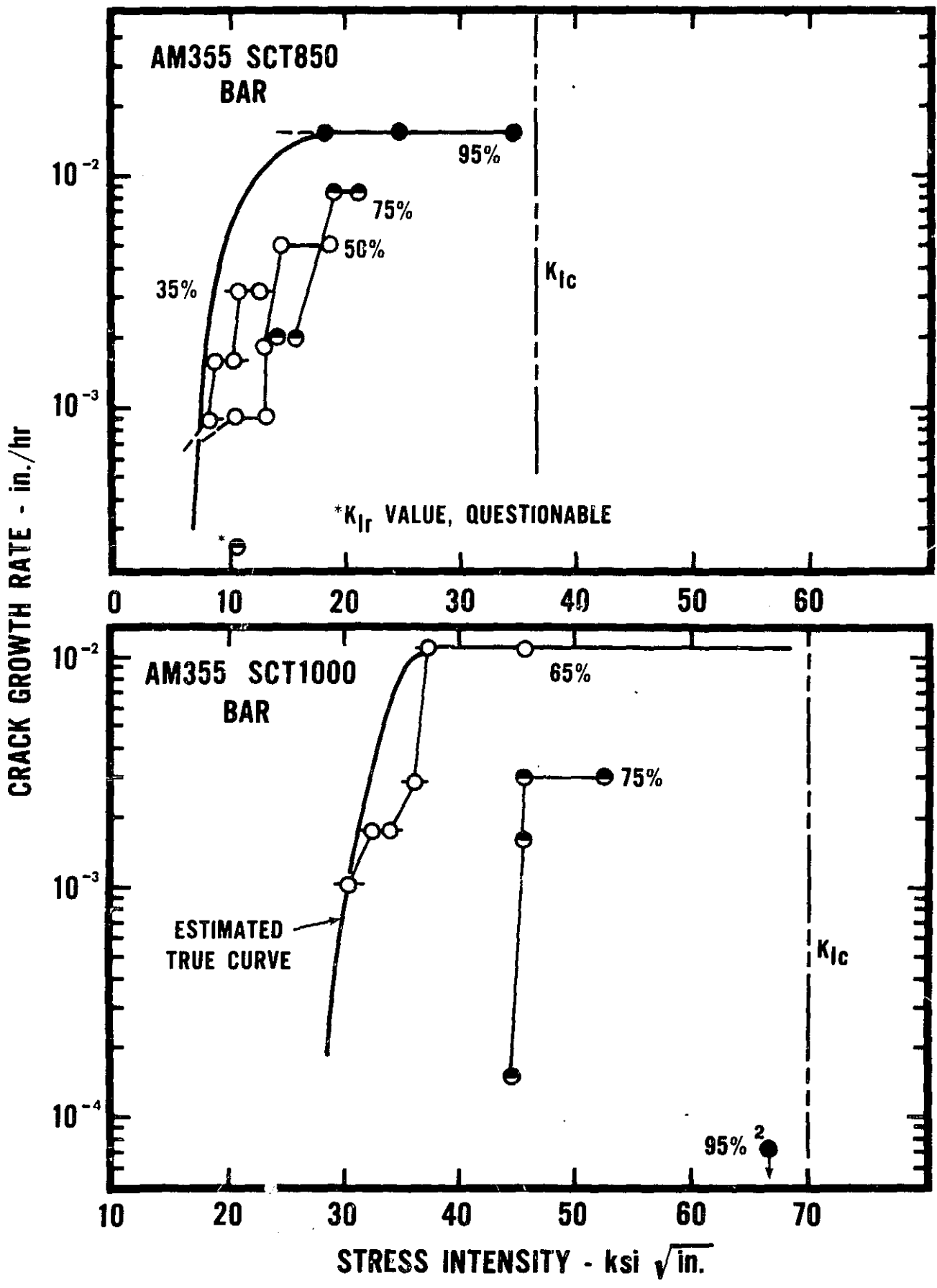


**Fig. 92 K-RATE CURVES FOR T-L COMPACTS**

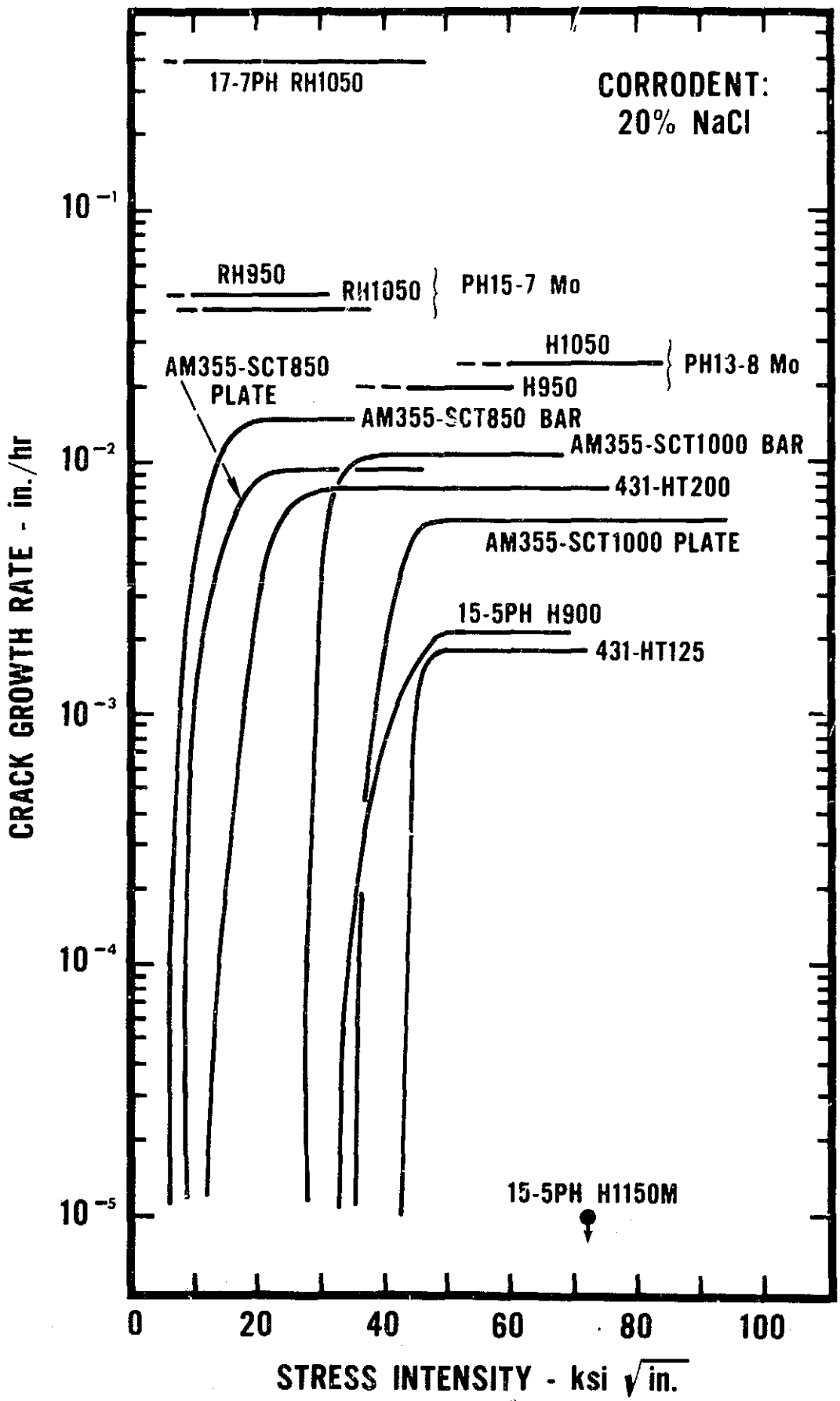


**Fig. 93 K-RATE CURVES FOR T-L COMPACTS OF STAINLESS STEELS (FATIGUE PRECRACKED)**



**Fig. 94 SEM FRACTOGRAPHS OF TENSION AND SCC FRACTURE SURFACES  
T-L SPECIMENS OF 17-7PH RH1050 ALLOY**

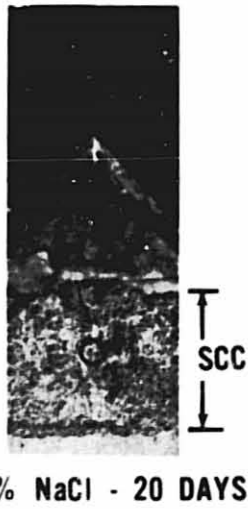
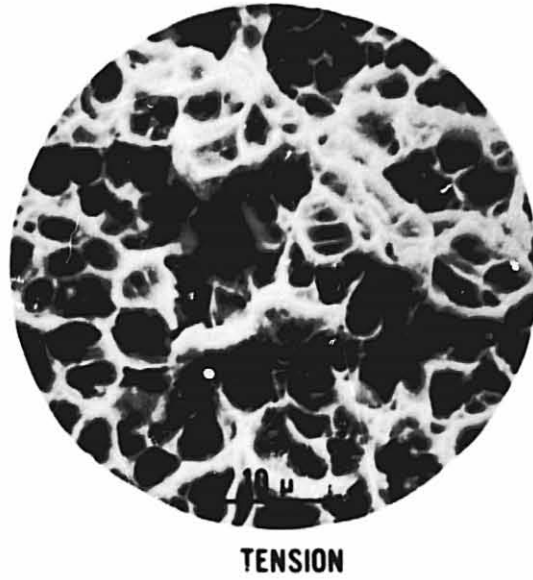
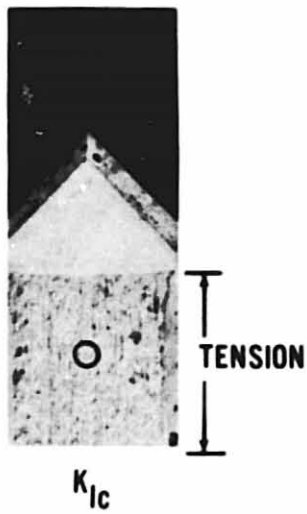


**Fig. 95 SEM FRACTOGRAPHS OF TENSION AND SCC FRACTURE SURFACES IN S-L SPECIMENS OF PH13-8 Mo H1050 ALLOY**

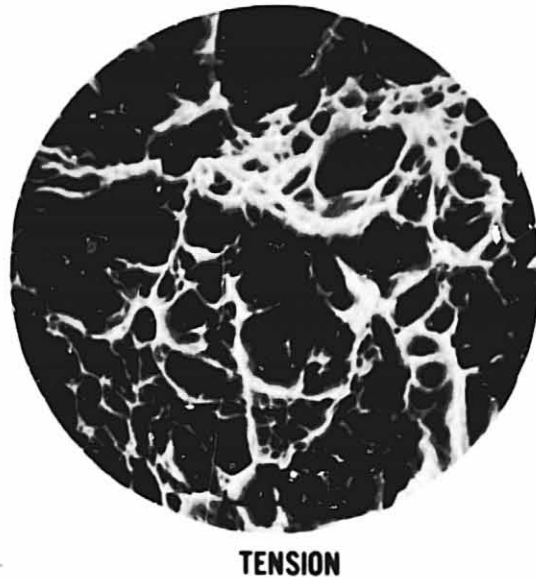
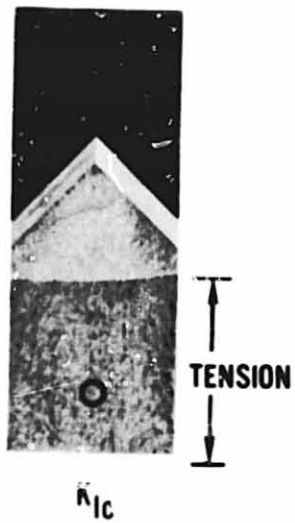


**Fig. 96 SEM FRACTOGRAPHS OF TENSION AND SCC FRACTURE SURFACES IN T-L SPECIMENS OF 431 HT200 ALLOY**



$K_{Ic}$



20% NaCl



**Fig. 97 SEM FRACTOGRAPHS OF TRANSITION BETWEEN FATIGUE PRECRACK AND TENSION FRACTURE SURFACES IN T-L SPECIMENS OF 15-5PH H1150M ALLOY**

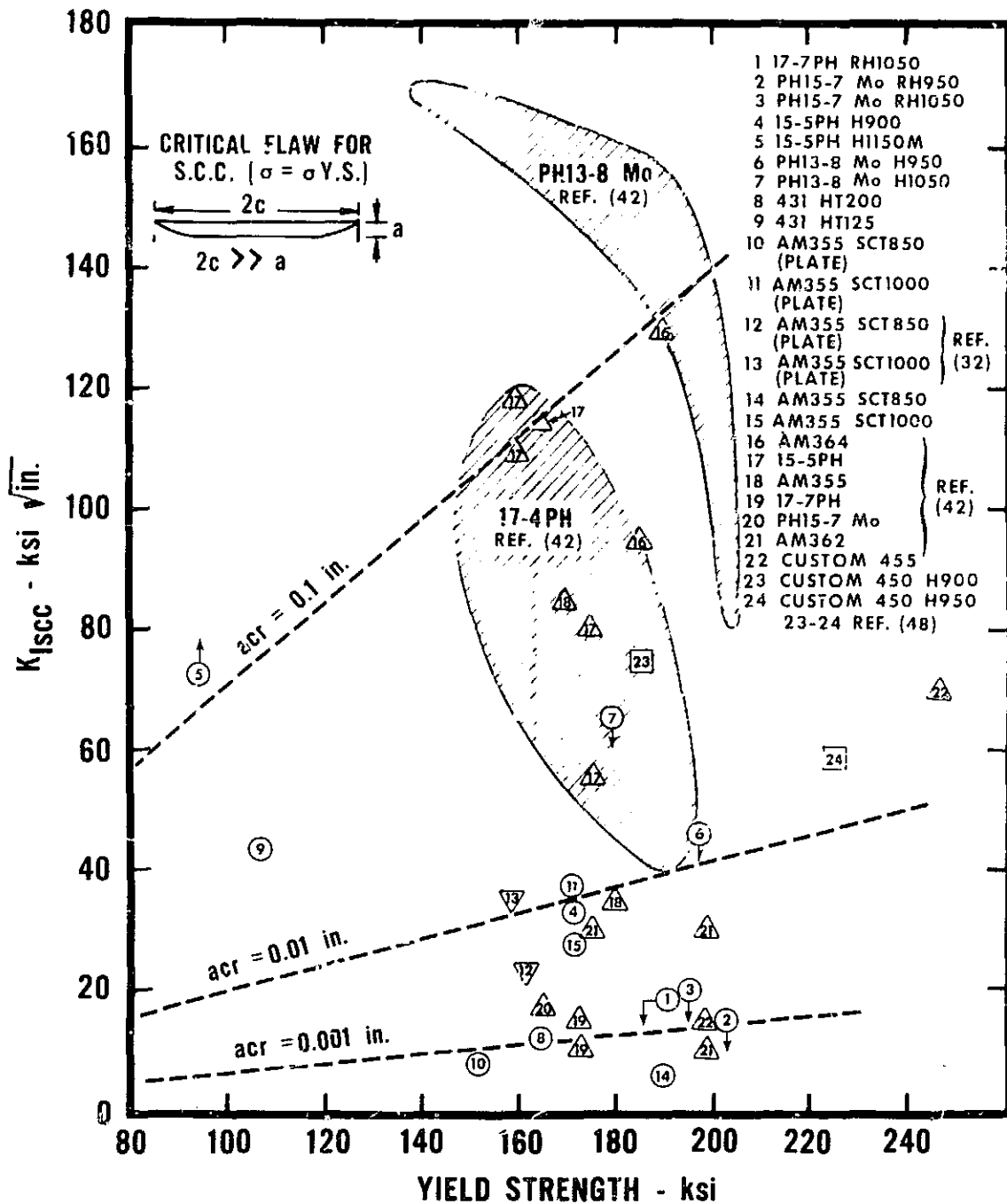
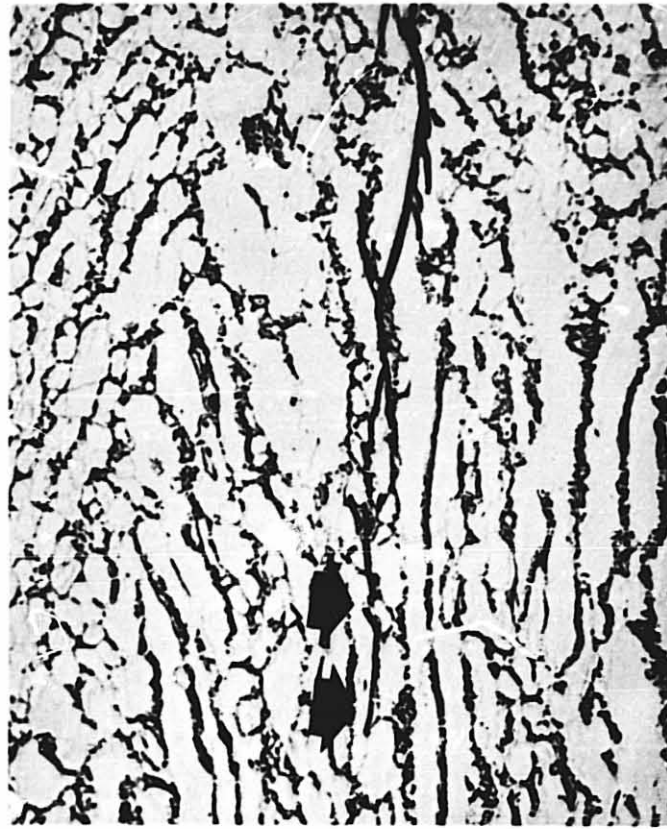


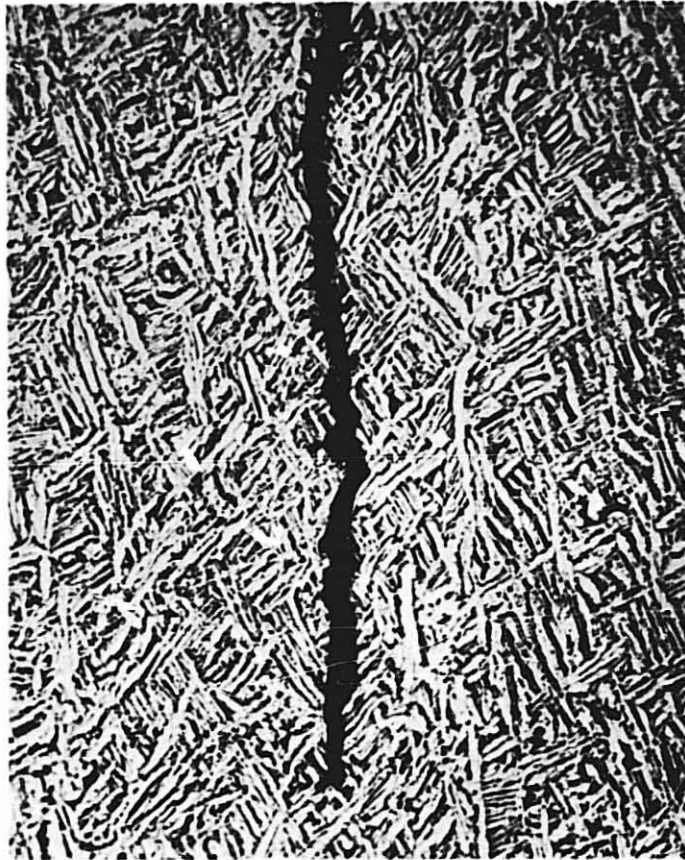
**Fig. 98 RESISTANCE TO SCC IN SALT WATER OF PRECIPITATION HARDENING STAINLESS STEEL ALLOYS**



KELLER'S ETCH

500X

**Fig. 99** SHOWS FINE TIP OF STRESS CORROSION CRACK IN T-L COMPACT TENSION SPECIMEN OF ALPHA-BETA FORGED Ti-6Al-4V ALLOY WHICH SHOWED SIGNIFICANT CRACK GROWTH IN THE SEACOAST ATMOSPHERE WHEN LOADED AT 75%  $K_{Ic}$

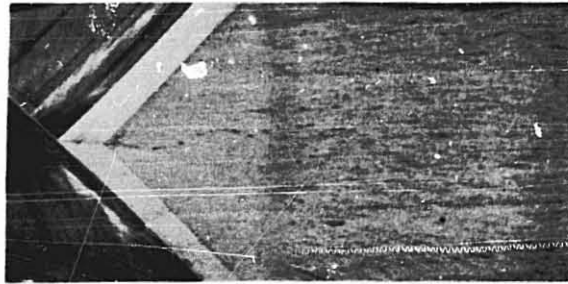


KELLER'S ETCH

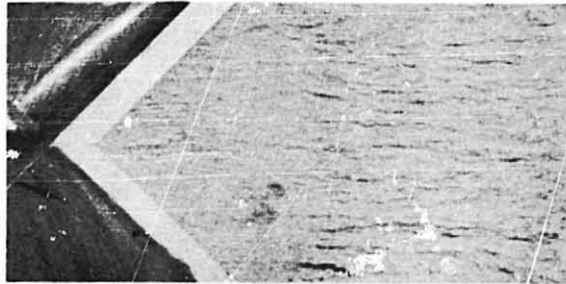
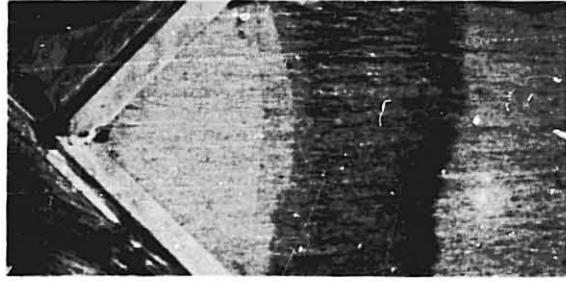
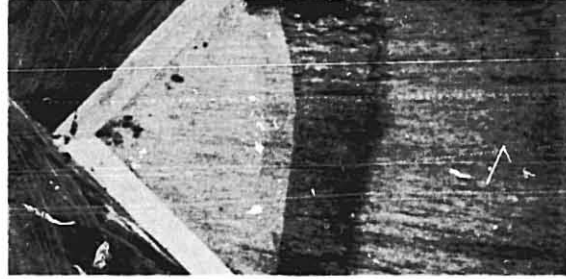
500X

**Fig. 100** SHOWS THE TIP OF THE PRECRACK  
IN T-L COMPACT TENSION SPECIMEN  
OF BETA FORGED Ti-6Al-4V ALLOY  
WHICH SHOWED NO APPRECIABLE CRACK  
GROWTH AFTER 483 DAYS EXPOSURE IN  
THE SEACOAST ATMOSPHERE WHEN  
LOADED AT 75%  $K_{Ic}$

**BETA FORGED**



**ALPHA-BETA FORGED**



**FATIGUE PRECRACK    STRESSED 95%  $K_{Ic}$     STRESSED 75%  $K_{Ic}$     STRESSED 50%  $K_{Ic}$**

**Fig. 101 FRACTURE SURFACES OF T-L COMPACT TENSION SPECIMENS OF 6Al-4V TITANIUM ALLOY SHOWING CRACK GROWTH IN 3.5% NaCl SOLUTION**

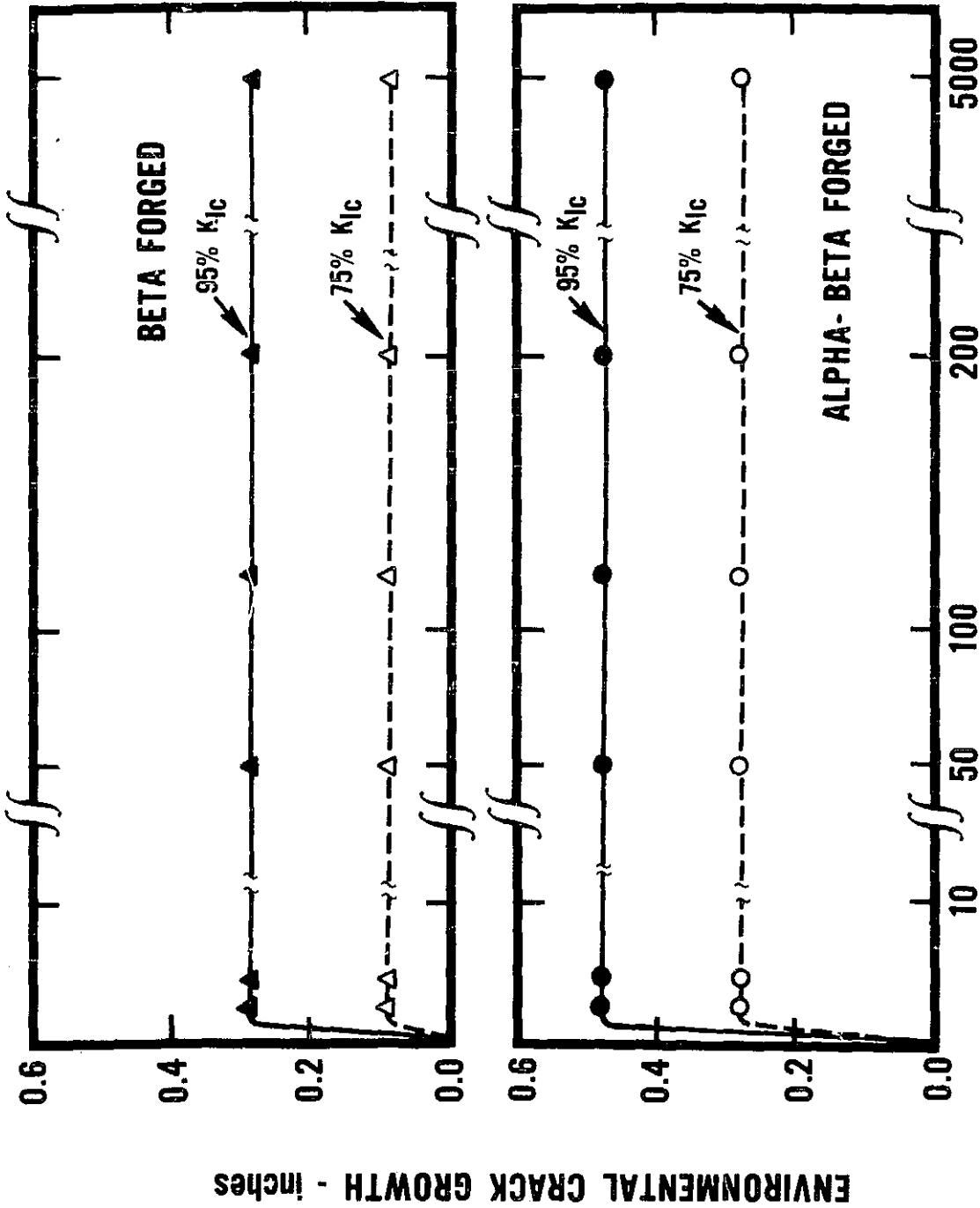


Fig. 102 ENVIRONMENTAL CRACK GROWTH IN Ti-6Al-4V ALLOY FORGINGS IN 3.5% NaCl SOLUTION

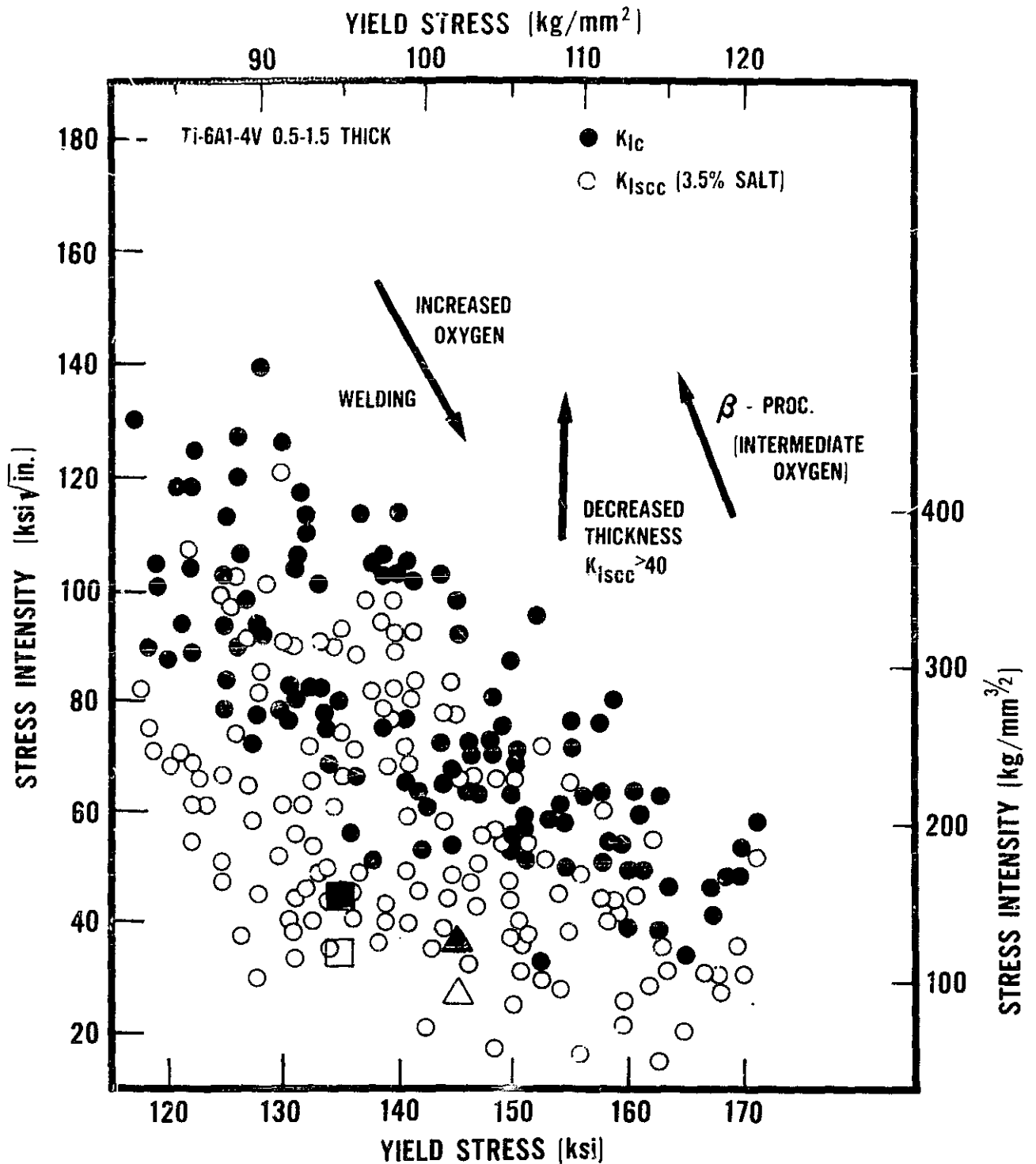
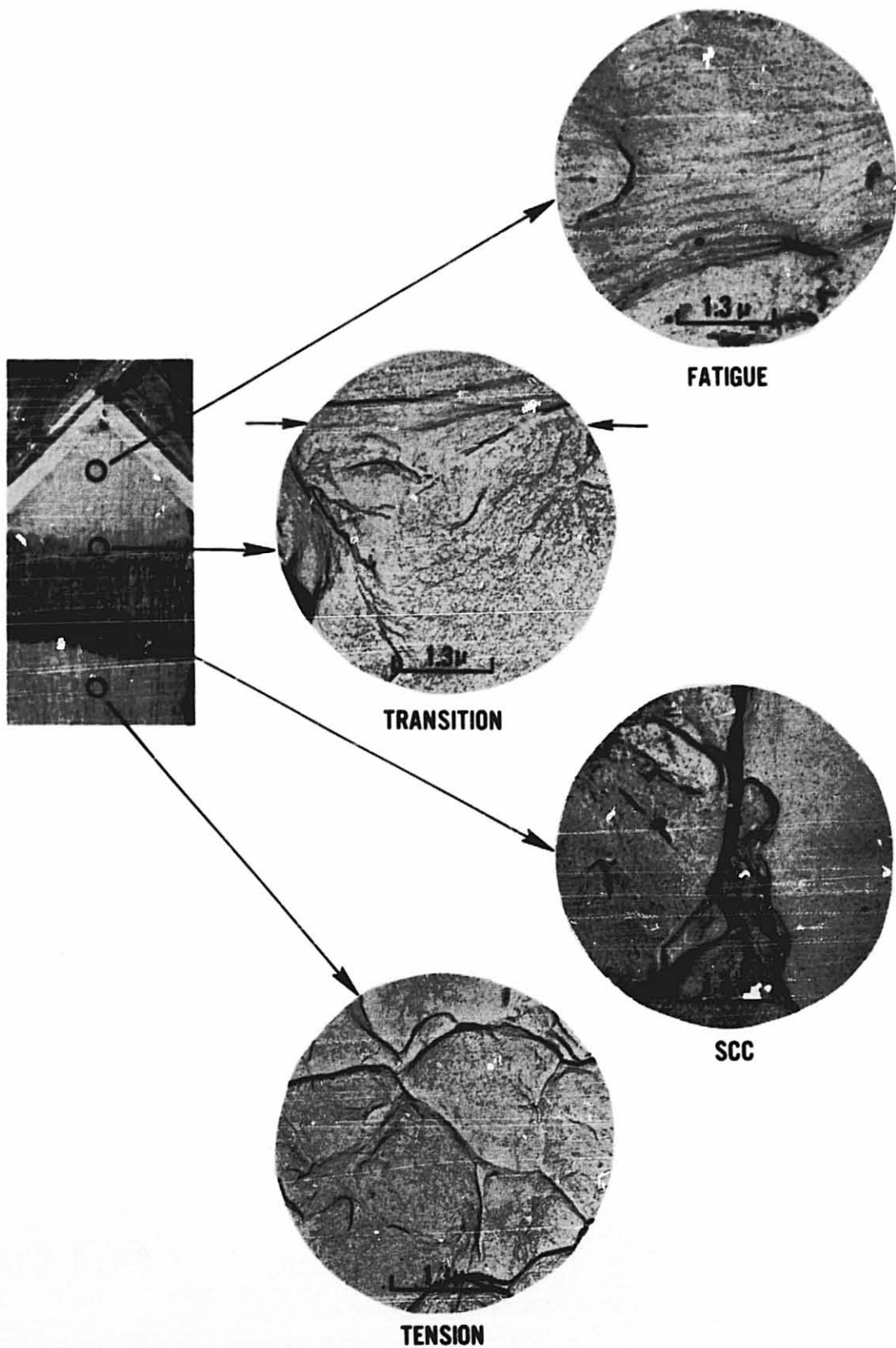


FIG.103 THE VARIATION OF  $K_{Ic}$  AND  $K_{IscC}$  WITH YIELD STRENGTH FOR THE ALLOY Ti-6Al-4V. (REF. 42)

DATA FROM THIS INVESTIGATION

■ □ β- PROC. FORGING

▲ △ α- β PROC. FORGING



**Fig. 104** TEM FRACTOFRAGRAPHS OF T-L COMPACT TENSION SPECIMEN OF ALPHA-BETA FORGED Ti-6Al-4V ALLOY BOLT LOADED TO 95%  $K_{Ic}$ . EXPOSED 209 DAYS TO 3.5% NaCl SOLUTION



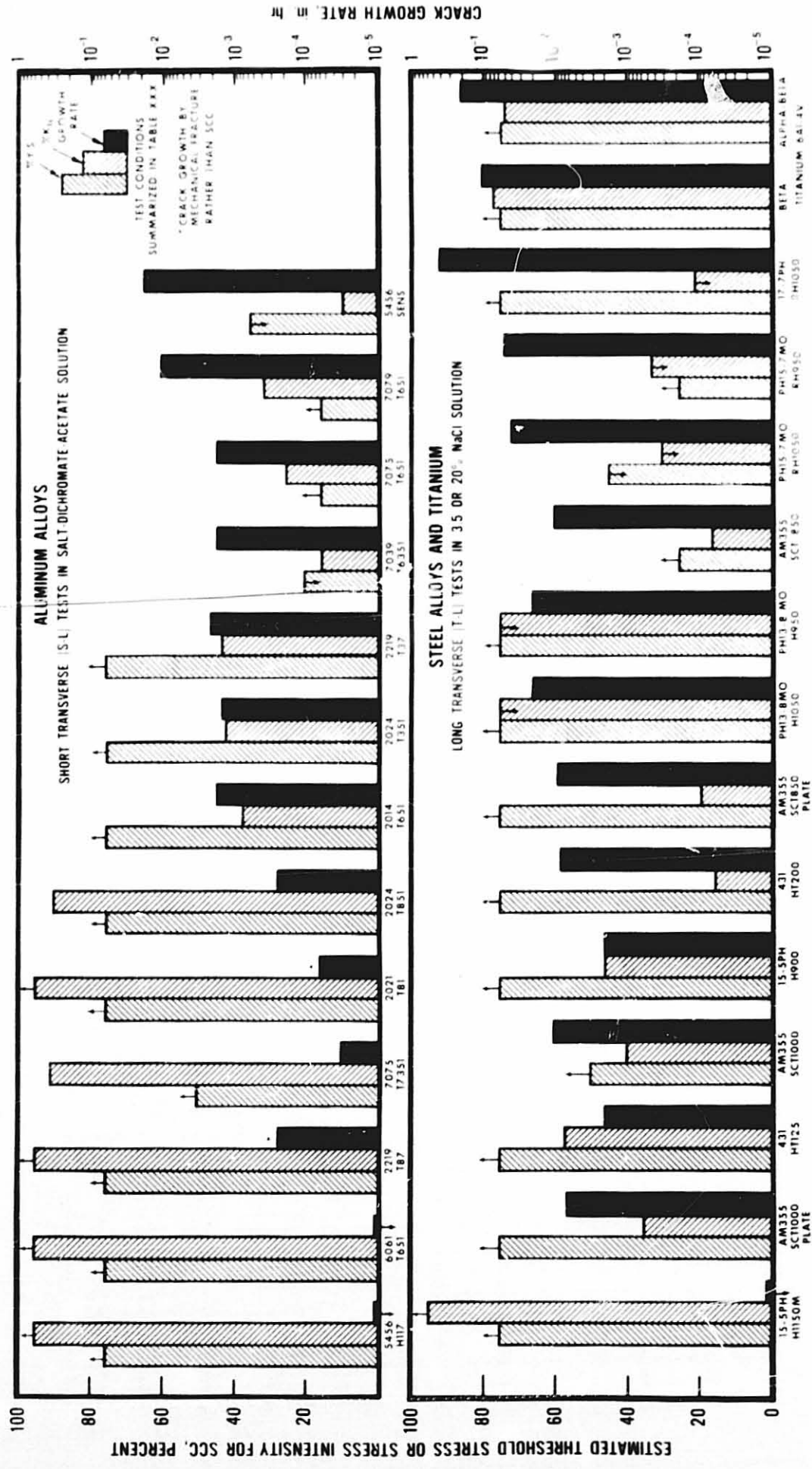
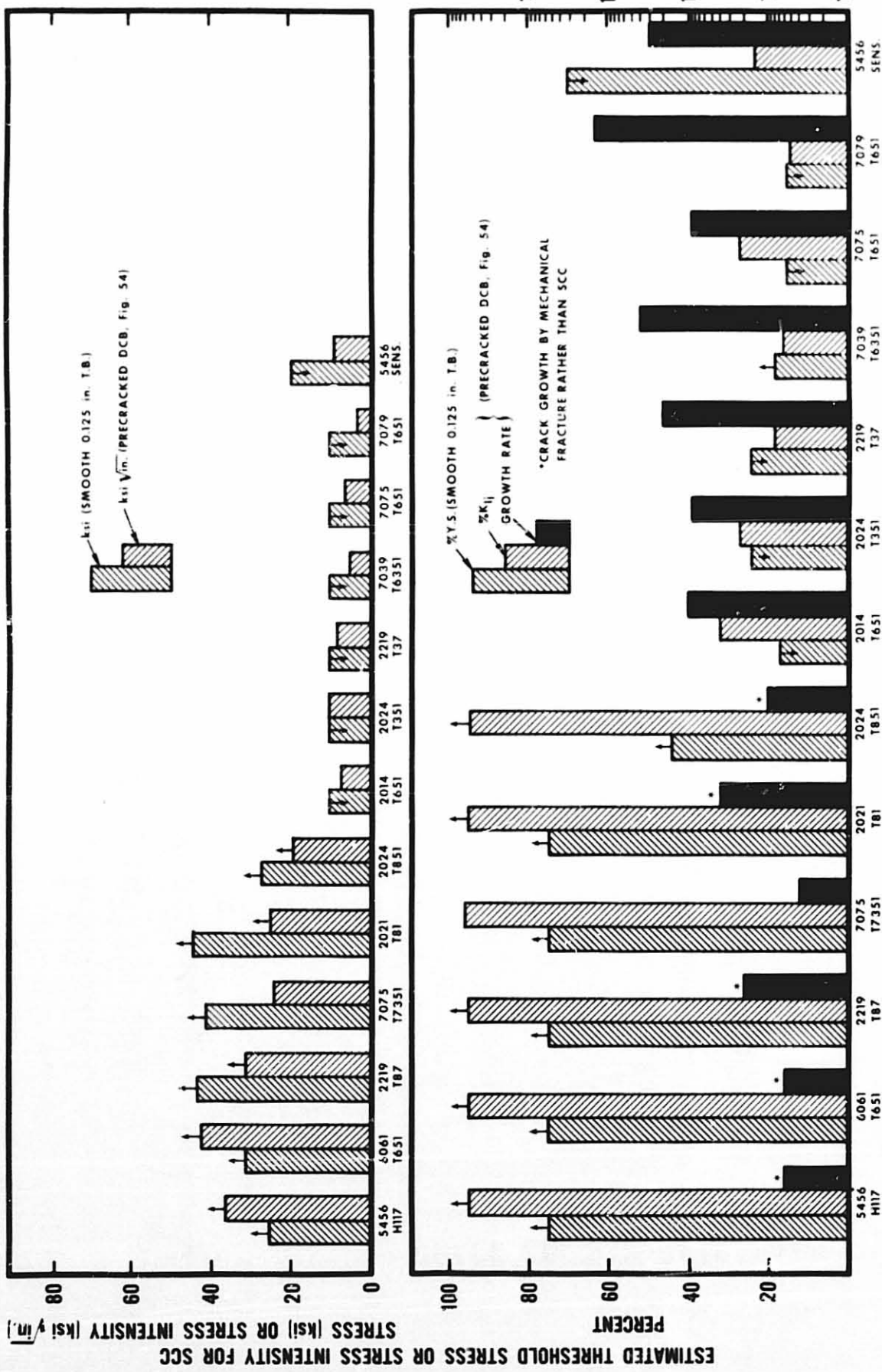
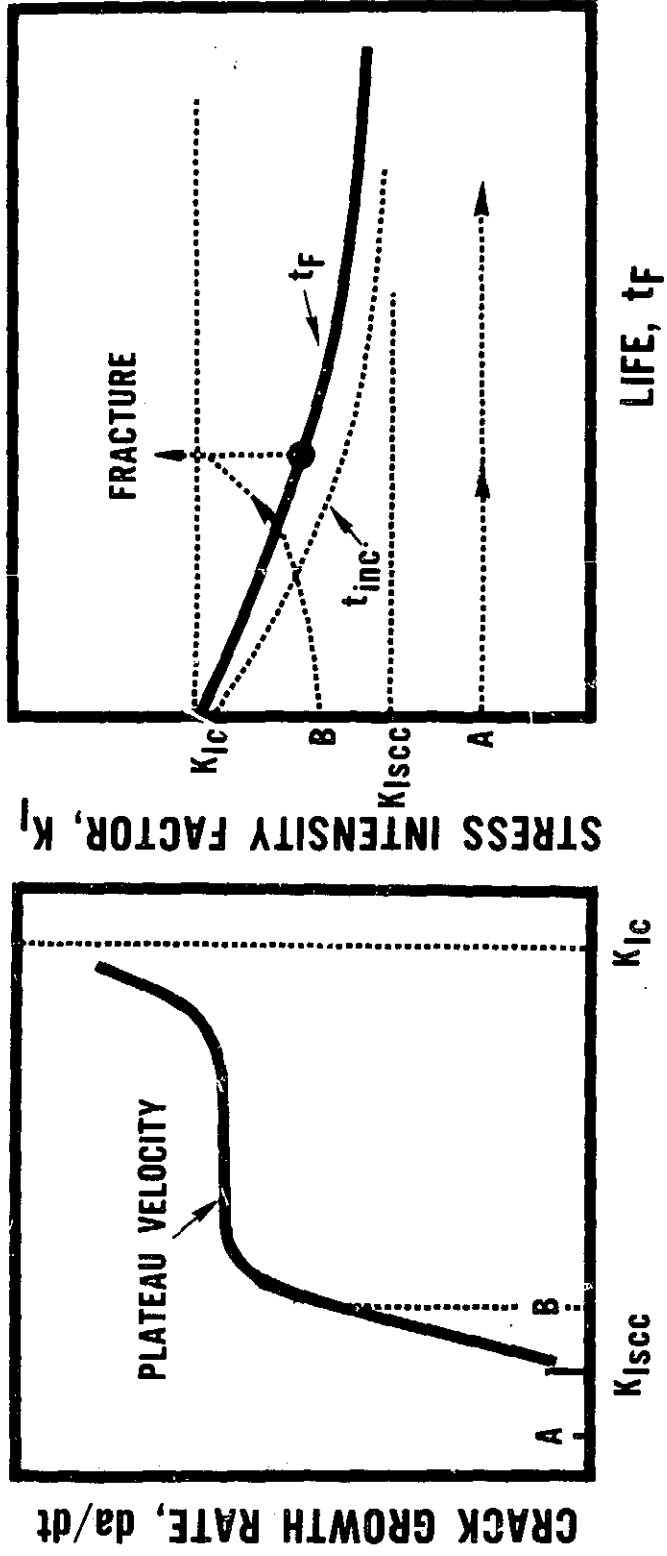


Fig. 106 COMPARISON OF SCC RANKINGS OF ALLOYS TESTED WITH PRECRACKED AND SMOOTH SPECIMENS - ACCELERATED CORROSION TESTS



**Fig. 107 COMPARISON OF SCC RANKINGS OF ALUMINUM ALLOYS TESTED WITH PRECRACKED AND SMOOTH SPECIMENS - SHORT TRANSVERSE (S-L) TESTS IN 3.5% NaCl**



[a]

[b]

**Fig. 108 SCHEMATIC REPRESENTATION OF  $K_{Ic}$ ,  $K_{Isc}$  AND  $da/dt$  FOR MATERIAL X UNDER CONSTANT LOAD IN A SPECIFIED ENVIRONMENT**

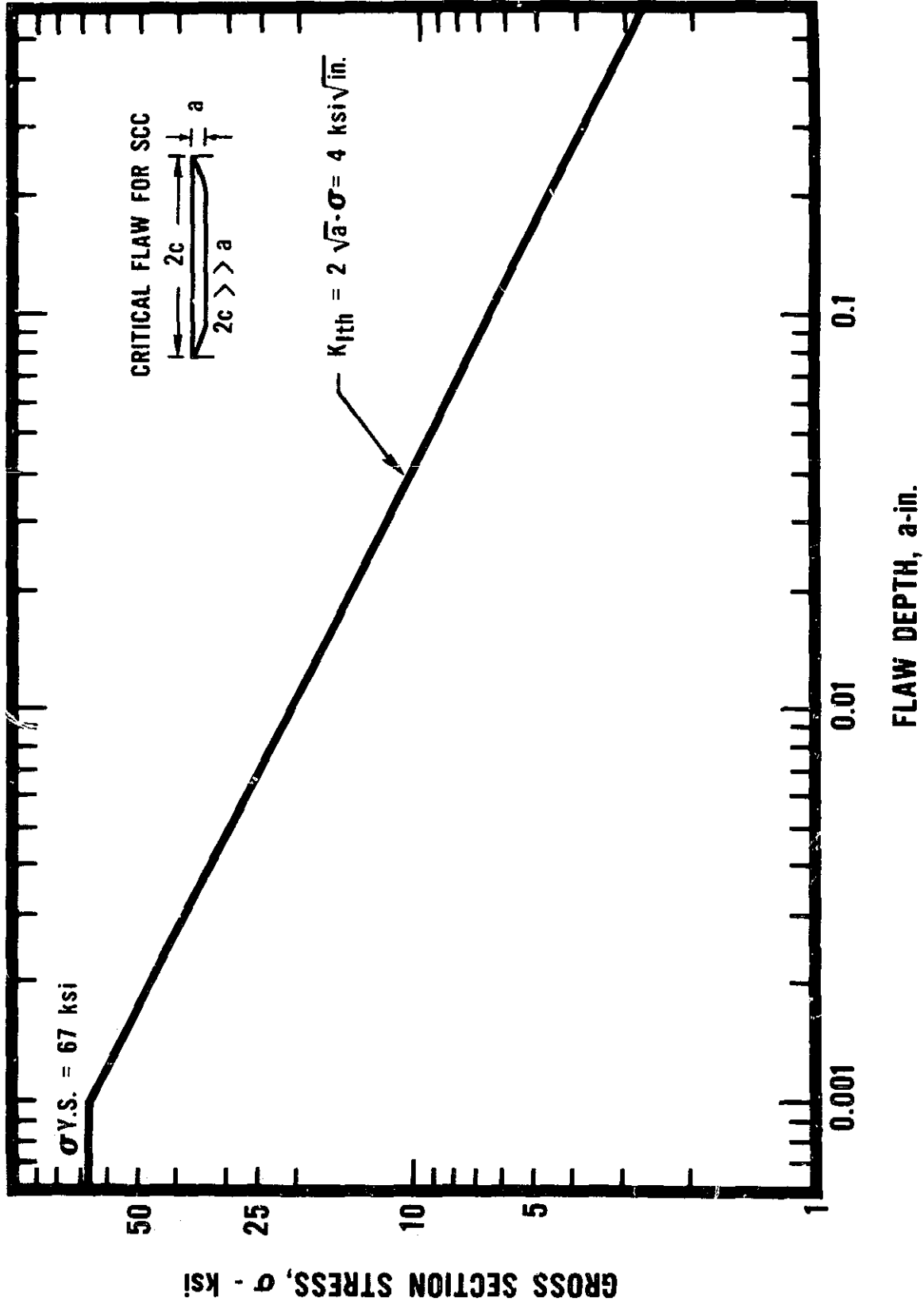


**Fig. 109 STRESS INTENSITY SCC RESISTANCE CHART FOR 7079-T651 PLATE, SHORT TRANSVERSE (S-L) STRESS**

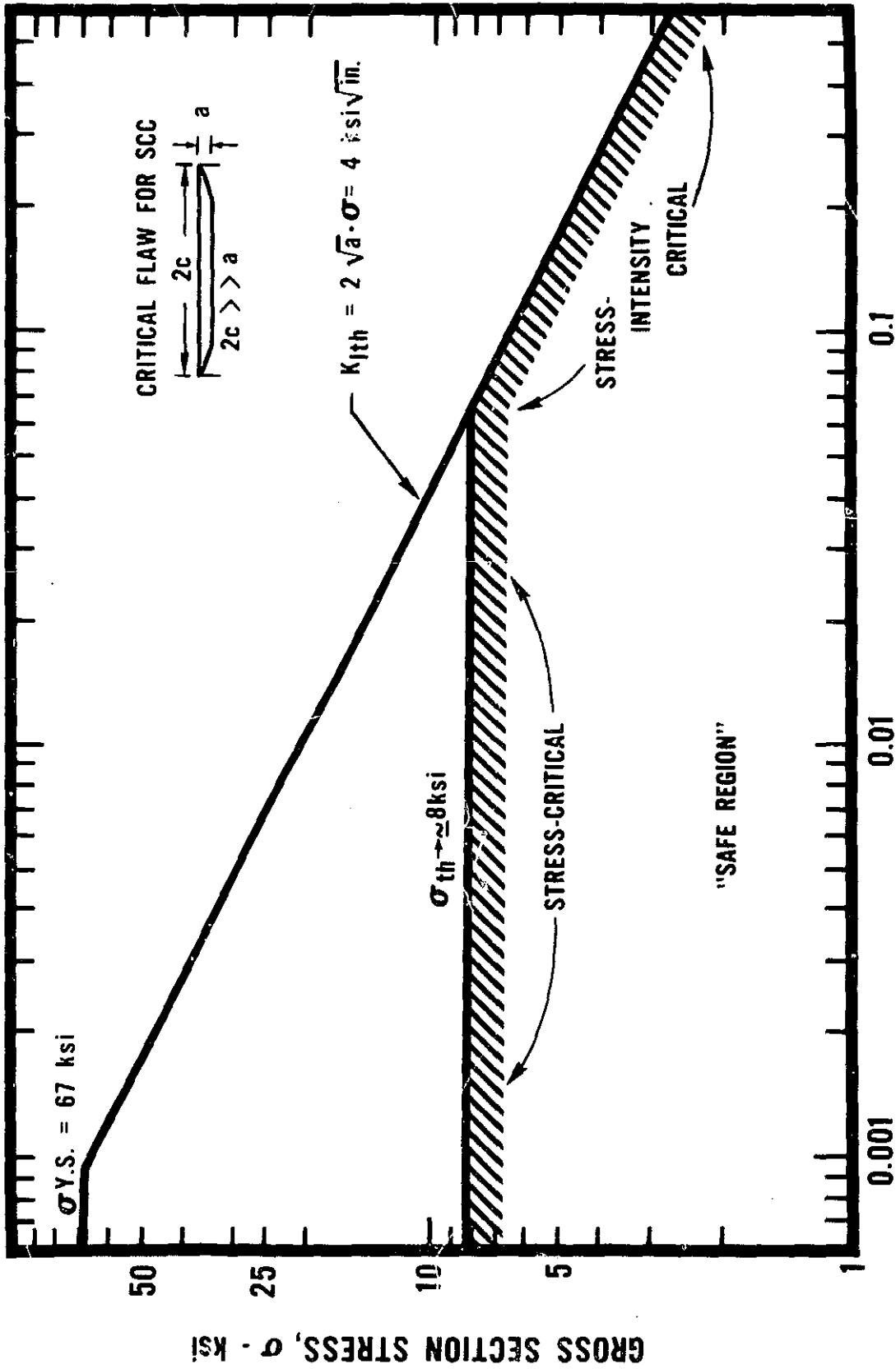
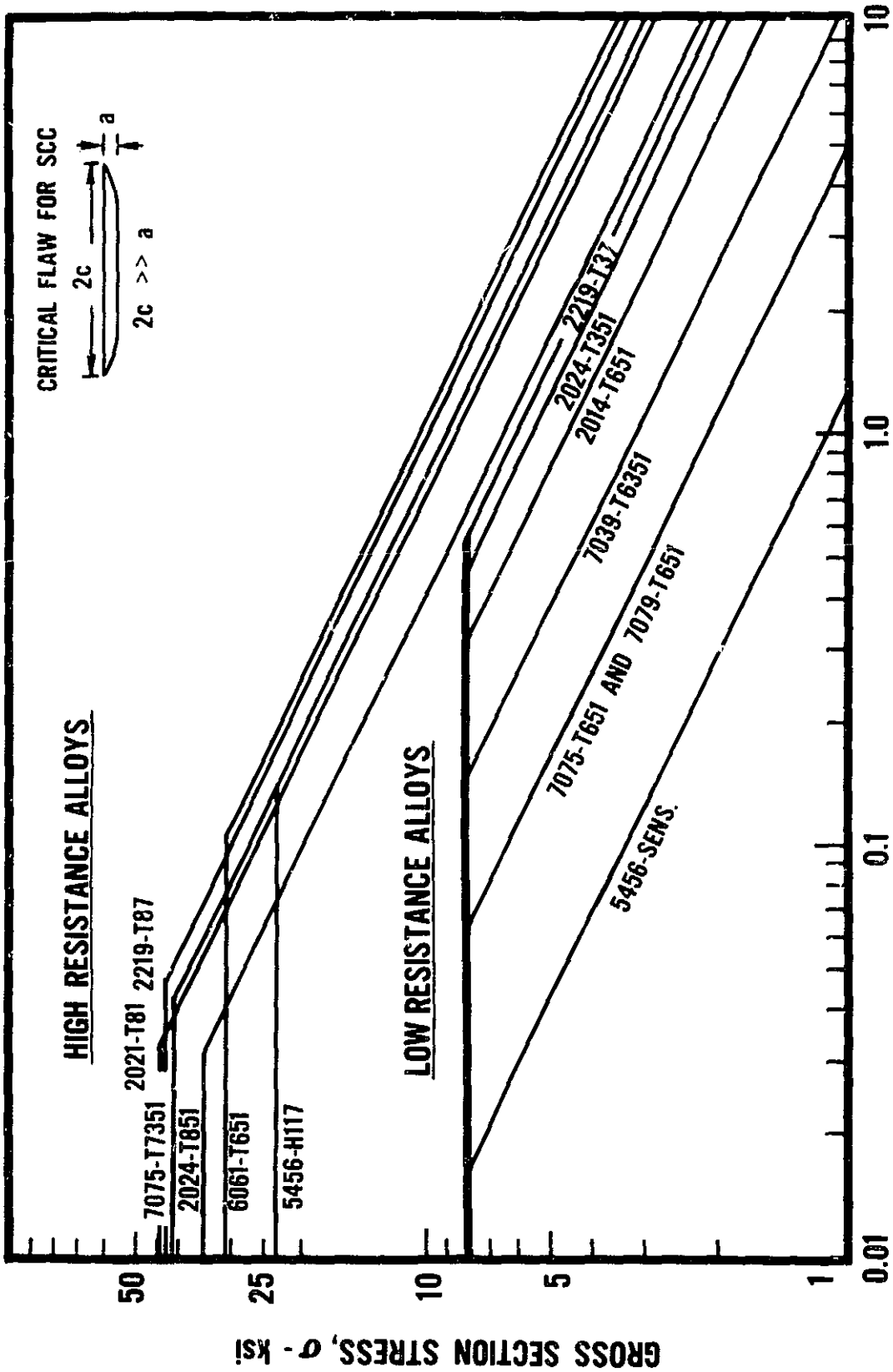
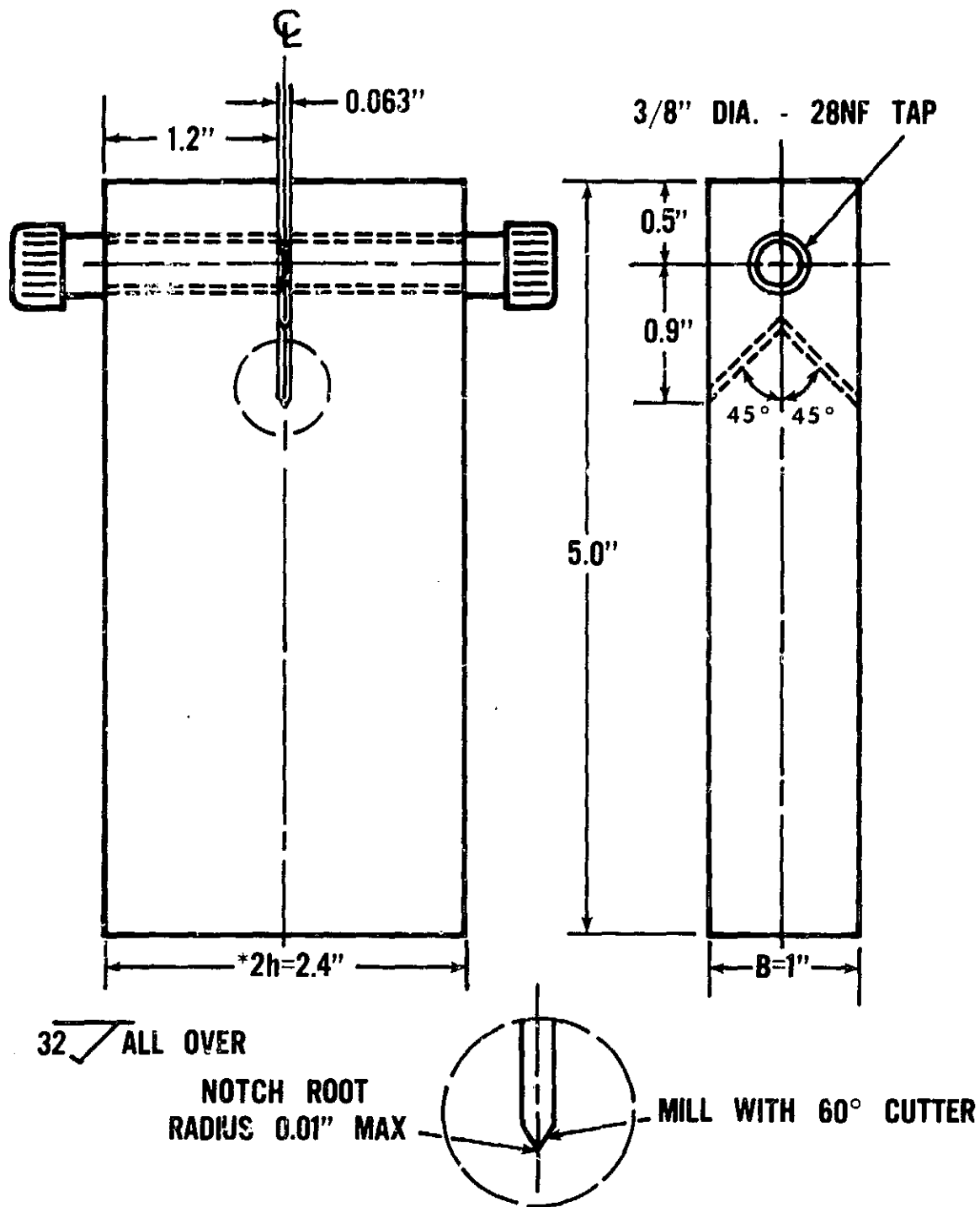


Fig. 110 COMPOSITE  $\sigma$ - $K_I$  SCC THRESHOLD CHART FOR 7079-T651 PLATE, SHORT TRANSVERSE (S-L) STRESS



**Fig. 111 COMPOSITE  $\sigma$ - $K_I$  SCC THRESHOLD CHARACTERIZATION OF ALUMINUM ALLOY PLATE - SHORT TRANSVERSE (S-L) STRESS (SDA SOLUTION)**



\*NOTE: IF STOCK THICKNESS IS INSUFFICIENT FOR 2.4" BEAM HEIGHT, THIS DIMENSION MAY BE REDUCED

**Fig. 112 CONFIGURATION OF DCB SPECIMEN RECOMMENDED FOR SCC TESTING ALUMINUM ALLOYS (S-L ORIENTATION)**

Appendix A

GLOSSARY OF TERMS USED IN THIS REPORT

- SCC - Stress-corrosion cracking
- ECG - Environmental crack growth
- a - Crack length, in.
- $a_i$  - Initial crack length at the beginning of SCC test, in.
- $a_f$  - Final crack length at termination of SCC test, in.
- t - Time, hr.
- da/dt - Rate of environmental crack growth (velocity), in./hr.
- $t_f$  - Total time to failure, hr.
- $t_{inc}$  - Incubation time, hr.
- $K_I$  - Crack-tip stress-intensity factor for the opening mode,  $\text{ksi}\sqrt{\text{in.}}$ . (See ASTM Method E399).
- $K_Q$  - Candidate value for  $K_{Ic}$  (may be invalid according to ASTM Method E399),  $\text{ksi}\sqrt{\text{in.}}$ .
- $K_{Ic}$  - Critical plane-strain stress intensity factor (fracture toughness per ASTM Method E399-70),  $\text{ksi}\sqrt{\text{in.}}$ .
- $K_{Ii}$  - Nominal  $K_I$  applied to specimen at beginning of SCC test,  $\text{ksi}\sqrt{\text{in.}}$ .
- $K_{If}$  -  $K_Q$  value at fracture of SCC specimen while exposed to a corrodent in increasing  $K_I$  test,  $\text{ksi}\sqrt{\text{in.}}$ .
- $K_{Ix}$  -  $K_Q$  value at fracture in air of SCC specimen after exposure to a corrodent,  $\text{ksi}\sqrt{\text{in.}}$ .
- $K_{Ir}$  - Residual  $K_I$  value at termination of SCC test,  $\text{ksi}\sqrt{\text{in.}}$ .
- $K_{Ith}$  - Apparent threshold value of  $K_I$  for environmental crack growth in a specified environment,  $\text{ksi}\sqrt{\text{in.}}$ .
- $K_{Isc}$  - Threshold value of  $K_I$ , and is the minimum  $K_I$  at which SCC initiates in a specified environment,  $\text{ksi}\sqrt{\text{in.}}$ .
- W - Specimen width, in.

Appendix A  
(Continued)

- B - Specimen thickness, in.
- H(h) - One half the specimen height, in.
- $d_0$  - Height of specimen before deflection, measured at center-line of the bolt, in.
- $d_1$  - Height of specimen after deflection, at similar location to  $d_0$ , in.
- $d_2$  - Height of specimen at the end of SCC test, after unloading, at similar location to  $d_0$ , in.
- V - Crack opening displacement (COD), in.
- P - Load, kips
- $\sigma$  - Nominal applied stress or gross-section stress, ksi
- $\sigma_{th}$  - Threshold value of  $\sigma$  for SCC initiating from a smooth surface in a specified environment, ksi
- E - Modulus of elasticity, ksi
- Pop-In - First evidence of mechanical crack growth while tensile precracking

## APPENDIX B

### References

- (1) Tiffany, C. F., "Progress in Measuring Fracture Toughness and Using Fracture Mechanics",--Fifth Report of a Special ASTM Committee, Materials Research & Standards, Vol. 4, No. 3, March, 1964, p. 107.
- (2) Johnson, H. H. and Willner, A. M., "Moisture and Stable Crack Growth in a High Strength Steel", Applied Materials Research, Vol. 4, No. 1, Jan., 1965, p. 34.
- (3) Brown, B. F. and Beachem, C. D., "A Study of the Stress Factor in Corrosion Cracking by the Use of the Precracked Cantilever Beam Specimen", Corrosion Science, Vol. 5, 1965, pp. 745-750.
- (4) Brown, B. F., "A New Stress-Corrosion Cracking Test for High Strength Alloys", Materials Research & Standards, Vol. 6, No. 3, March, 1966, pp. 129-133.
- (5) Johnson, H. H. and Paris, P. C., "Subcritical Flaw Growth", Journal of Engineering Fracture Mechanics, Vol. 1, 1968, pp. 3-45.
- (6) Wei, R. P., "Application of Fracture Mechanics to Stress-Corrosion Cracking Studies", Proceedings of Conference-Fundamental Aspects of Stress-Corrosion Cracking, Ohio State University, 1967, p. 104, published by National Association of Corrosion Engineers, Houston, Texas.
- (7) Smith, H. R., Piper, D. E. and Downey, F. K., "A Study of Stress-Corrosion Cracking by Wedge-Force Loading", Engineering

References  
Page Two

- Fracture Mechanics, Vol. 1, No. 1, June, 1968, pp. 123-128.
- (8) Novak, S. R. and Rolfe, S. T., "Comparisons of Fracture Mechanics and Nominal Stress Analyses in Stress-Corrosion Cracking", Corrosion, Vol. 26, No. 4, April, 1970, pp. 121-130.
- (9) Mulherin, J. H., "Influence of Environment on Crack Propagation Characteristics of High Strength Aluminum Alloys", Stress Corrosion Testing, ASTM STP 425, American Society for Testing Materials, 1967, p. 81.
- (10) NRL Memorandum Report 1864, Fifth Quarterly Report, ARPA Coupling Program on Stress-Corrosion Cracking, Feb., 1968.
- (11) Aluminum Standards and Data - Third Edition 1972-73, published by the Aluminum Association.
- (12) Sprowls, D. O., Lifka, B. W. and Coursen, J. W., "Evaluation of Stress-Corrosion Cracking Susceptibility Using Fracture Mechanics Techniques", Contract No. NAS 8-21487, Summary Report for Period July 1, 1968 to June 30, 1969.
- (13) "Standard Methods of Tension Testing of Metallic Materials, E8-69", 1972 Book of ASTM Standards, Part 31.
- (14) "Standard Recommended Practice for Tension Testing Wrought Aluminum and Magnesium Alloy Products, B557-72", 1972 Book of ASTM Standards, Part 6.
- (15) Beck, W. C., Allegheny Ludlum Steel Corporation, Letter to M. B. Shumaker, Oct. 2, 1969.
- (16) Mackenzie, R. H., Armco Steel Corporation, Letter to D. O. Sprowls, March 31, 1970.

- (17) Sprowls, D. O., Lifka, B. W., Shumaker, M. B., Coursen, J. W., and Walsh, J. D., "Evaluation of Stress-Corrosion Cracking Susceptibility Using Fracture Mechanics Techniques", Contract No. NAS 8-21487, Quarterly Report for Period April 1, 1970 to June 30, 1970.
- (18) "Standard Methods and Definitions for Mechanical Testing of Steel Products, A370-68", 1969 Book of ASTM Standards, Part 31.
- (19) Williams, J. C., "Some Observations on the Stress-Corrosion Cracking of Three Commercial Titanium Alloys", ASM Transactions Quarterly 60:4, Dec. 1967, p. 646.
- (20) "Tentative Method of Test for Plane-Strain Fracture Toughness of Metallic Materials, E399-70T", 1970 Book of ASTM Standards, Part 31.
- (21) Mostovoy, S., Crosley, P. B. and Ripling, E. J., "Use of Crack-line Loaded Specimens for Measuring Plane-Strain Fracture Toughness", Journal of Materials, Vol. 2, No. 3, Sept., 1967, pp. 661-681.
- (22) Sprowls, D. O. and Brown, R. H., "What Every Engineer Should Know About Stress Corrosion of Aluminum", Metal Progress, Vol. 81, No. 4 (1962), pp. 79-85; Vol. 81, No. 5 (1962), pp. 77-83.
- (23) Lifka, B. W., and Sprowls, D. O., "Stress Corrosion Testing of 7079-T6 Aluminum Alloy in Various Environments", Stress Corrosion Testing ASTM STP 425, American Society Testing Materials, 1967, pp. 342-362.

References

Page Four

- (24) Lifka, B. W., Sprowls, D. O. and Kelsey, R.A., "Investigation of Smooth Specimen SCC Test Procedures. Variations in Environment, Specimen Size, Stressing Frame, and Stress State", Final Report of Government Contract NAS 8-21487 - Part II for the period of 7/1/69 to 2/29/72.
- (25) Loginow, A. W., "Stress Corrosion Testing of Alloys", Materials Protection, Vol. 5, No. 5, May, 1966, pp. 33-39.
- (26) Hyatt, M. V., "Use of Precracked Specimens in Stress Corrosion Testing of High Strength Aluminum Alloys", Corrosion, Vol. 26, No. 11 (Nov., 1970), pp. 487-503.
- (27) Smith, H. R. and Piper, D. E., "Stress Corrosion Testing with Precracked Specimens", June, 1970, Part 2 of Monograph Review of the State-of-the-Art of Stress-Corrosion Cracking (SCC) in High-Strength Steels, Titanium Alloys and Aluminum Alloys. Sponsored by ARPA Order No. 878. (Also, Chapter 2 in Ref. 42).
- (28) Dix, E. H., Jr., Anderson, W. A. and Shumaker, M. B., "Development of Wrought Aluminum-Magnesium Alloys", Alcoa Technical Paper No. 14, 1958, Alcoa Research Laboratories, New Kensington, Penna.
- (29) Kaufman, J. G., Schilling, P. E., Nordmark, G. E., Lifka, B. W. and Coursen, J. W., "Fracture Toughness, Fatigue and Corrosion Characteristics of X7080-T7E41 and 7178-T651 Plate and 7075-T6510, 7075-T73510, X7080-T7E42 and 7178-T6510 Extruded Shapes". Technical Report AFML-TR-69-255, Nov., 1969.
- (30) Setterlund, R. B., "Stress-Corrosion Cracking of High Strength Steels", Final Report No. 2684, Sept., 1963, For Contract DA-04-495-ORD-3069.

References  
Page Five

- (31) Leckie, H. P. and Loginow, A. W., "A Comparison of the Stress Corrosion Behavior of Some High Strength Steels", Corrosion, Vol. 24, No. 9 (Sept., 1968), pp. 291-297.
- (32) Freedman, A. H., "Development of an Accelerated Stress Corrosion Test for Ferrous and Nickel Alloys", Final Summary Report of Contract NAS 8-20333, April, 1968.
- (33) "Standard Definitions of Terms Relating to Corrosion and Corrosion Testing, G15-71", 1972 Book of ASTM Standards, Part 31.
- (34) Sprowls, D. O., Lifka, B. W., Vandeburgh, D. G., Horst, R. L. and Shumaker, M. B., "Investigation of the Stress-Corrosion Cracking of High Strength Aluminum Alloys", Final Report of Contract NAS 8-5340 for the period May 6, 1963 to Oct. 6, 1966.
- (35) Nordmark, G. E., Lifka, B. W., Hunter, M. S. and Kaufman, J. G., "Stress-Corrosion and Corrosion-Fatigue Susceptibility of High Strength Aluminum Alloys", Technical Report AFML-TR-70-259, Nov., 1970.
- (36) Pelloux, Regis, M. N., "Corrosion-Fatigue Crack Propagation", Fracture 1969, Proceedings of the Second International Conference on Fracture, Brighton, April, 1969, Chapman and Hall, Ltd., pp. 731-744.
- (37) Feeney, John A., McMillan, J. Corey and Wei, Robert P., "Environmental Fatigue Crack Propagation of Aluminum Alloys at Low Stress Intensities", Metallurgical Transactions, Vol. 1, June, 1971, pp. 1741-1757.
- (38) Helfrich, W. J., "Development of a Rapid Stress Corrosion Test for Aluminum Alloys", Final Summary Report of Contract NAS 8-20285, May 15, 1968.

- (39) Craig, H. L., Jr., Sprowls, D. O. and Piper, D. E., "Stress-Corrosion Cracking", Chapter 10 in Handbook on Corrosion Testing and Evaluation, Edited by W. H. Ailor, published by John Wiley & Sons, Inc., 1971.
- (40) Hyatt, M. V., "Effects of Specimen Geometry and Grain Structure on Stress-Corrosion Cracking Behavior of Aluminum Alloys", Report D6-24470, The Boeing Company, Nov., 1969.
- (41) Wacker, George A. and Chu, Huai-Pu, "Some Observations on the Stress Corrosion Characteristics of High Strength Aluminum Alloys in Marine Environment", Corrosion, Vol. 28, No. 6 (June, 1972), pp. 233-242.
- (42) Brown, B. F., Stress-Corrosion Cracking in High Strength Steels and in Titanium and Aluminum Alloys, Naval Research Laboratory, Washington, D.C., 1972. (Sponsored by the Advanced-Research Projects Agency ARPA Order No. 878).
- (43) Slunder, C. J., "Stress Corrosion Behavior of High Yield Strength Stainless Steels in Atmospheric Environments", DMIC Report 158, September 15, 1961.
- (44) Denhard, Jr., E. E., "Stress-Corrosion Cracking of High Strength Stainless Steels", Paper presented at Twenty-Fourth Meeting of AGARD Structure and Materials Panel at Turin, Italy on 17-20 April, 1967. AGARD Conference Proceedings No. 18.
- (45) Humphries, T. S. and Nelson, E. E., "Stress Corrosion Evaluation of Several Precipitation Hardening Stainless Steels", NASA Technical Memorandum Report No. 53910, September 12, 1969.

References  
Page Seven

- (46) Hyatt, M.V., "Effects of Residual Stresses on Stress Corrosion Crack Growth Rates in Aluminum Alloys", Corrosion, Vol. 26, No. 12 (1970), p. 547.
- (47) Carter, C. S., Farwick, D. G., Ross, A. M. and Uchida, J. M., "Stress Corrosion Properties of High Strength Precipitation Hardening Stainless Steels", Corrosion, Vol. 27, No. 5, May, 1971.
- (48) Sandoz, G., "The Resistance of Some High Strength Steels to Slow Crack Growth In Salt Water", Naval Research Laboratory Memorandum Report 2454, February, 1972.
- (49) Henthorne, Michael, "Stress-Corrosion Cracking of Martensitic Precipitation Hardening Stainless Steels", AGARD Conference Proceedings No. 98, Specialists Meeting on Stress Corrosion Testing Methods, Brussels, Belgium, 5 and 6 October, 1971.
- (50) Technical Documentary Report No. ML-TDR-64-44, Volume I, March 1964, "Chloride Stress Corrosion Susceptibility of High Strength Stainless Steel Titanium Alloy and Superalloy Sheet", prepared under Contract No. AF33(657)-8543 by the Douglas Aircraft Company, Inc.
- (51) Fager, D. N. and Spurr, W. F., "Some Characteristics of Aqueous Stress Corrosion in Titanium Alloys", Document D6-60083, September, 1967, The Boeing Company, Commercial Airplane Division, Renton, Washington (Sponsored by the Advanced-Research Projects Agency ARPA Order No. 878).
- (52) Chu, H. P. and Wacker, G. A., "Fracture Toughness and Stress Corrosion Properties of Aluminum Alloy Hand Forgings", Journal of Materials, Vol. 7, No. 1 (1972); pp. 95-99.

- (53) Bollani, Giovanni, "A Contribution to Stress Corrosion Testing of Aluminum Alloys", AGARD Conference Proceedings No. 98, Specialists Meeting on Stress Corrosion Testing Methods, Brussels, Belgium, 5 and 6 October, 1971.
- (54) Lehmann, W., "Results of Comparative Stress Corrosion Tests on Al-Zn-Mg-Cu Alloys Using Different Types of Specimens", AGARD Conference Proceedings No. 98, Specialists Meeting on Stress Corrosion Testing Methods, Brussels, Belgium, 5 and 6 October, 1971.
- (55) Jacobs, A. J. and Marcus, H. L., "Evaluation of Stress-Corrosion Cracking Test Methods", June, 1972, North American Rockwell Report NRAG-72-1.
- (56) Speidel, Markus O. and Hyatt, Michael, V., "Stress-Corrosion Cracking of High Strength Aluminum Alloys", Advance in Corrosion Science and Technology, Vol. 2, Edited by Mars G. Fontana and Roger W. Staehle (Plenum Press, 1972), p. 158.
- (57) Sprowls, Donald O., "Progress Toward Standardization of Test Techniques by the National Association of Corrosion Engineers and the Aluminum Association", AGARD Conference Proceedings No. 98, Specialists Meeting on Stress Corrosion Testing Methods, Brussels, Belgium, 5 and 6 October, 1971.
- (58) Sprowls, D. O. and Kaufman, J. G., "Discussion on Fracture Toughness and Stress Corrosion Properties of Aluminum Alloy Hand Forgings", Journal of Materials, Vol. 7, No. 1 (1972); pp. 263-265.

References  
Page Nine

- (59) Novak, S. R., "Critical Aspects in the Evaluation of  $K_{I_{sc}}$ "  
(Submitted for publication in Materials Research and Standards).
- (60) Novak, S. R., "Effect of Prior Uniform Plastic Strain on the  $K_{I_{sc}}$  of High Strength Steels in Sea Water", To be published in the Journal of Engineering Fracture Mechanics.
- (61) Wei, R. P., Novak, S. R. and Williams, D. P., "Some Important Considerations in the Development of Stress-Corrosion Cracking Test Methods", AGARD Conference Proceedings No. 98, Specialists Meeting on Stress Corrosion Testing Methods, Brussels, Belgium, 5 and 6 October, 1971.

## APPENDIX C

### Bibliography

- (1) Fracture Toughness Testing and Its Application, ASTM Special Technical Publication No. 381 (1965), Philadelphia, Penna., American Society for Testing and Materials.
- (2) Johnson, H. H. and Paris, P. C., "Subcritical Flaw Growth", Journal of Engineering Fracture Mechanics, Vol. 1, 1968, pp. 3-45.
- (3) Wei, R. P., "Application of Fracture Mechanics to Stress-Corrosion Cracking Studies", Proceedings of Conference-Fundamental Aspects of Stress-Corrosion Cracking, Ohio State University, 1967, p. 104, published by National Association of Corrosion Engineers, Houston, Texas.
- (4) Stress Corrosion Testing, ASTM Special Technical Publication No. 425 (1967), Philadelphia, Penna., American Society for Testing and Materials.
- (5) Brown, B. F., "The Application of Fracture Mechanics to Stress-Corrosion Cracking", Review 129, Metallurgical Reviews, Vol. 13, (Dec., 1968), pp. 171-183.
- (6) Sinclair, G. M. and Rolfe, S. T., "Analytical Procedure for Relating Subcritical Crack Growth to Inspection Requirements", presented at the Metals Engineering Division Conference on Environmental Effects in Failure of Engineering Materials, Washington, D.C., March 31-April 2, 1969.
- (7) AGARD Conference Proceedings No. 53, "Engineering Practice to Avoid Stress-Corrosion Cracking" Istanbul, Turkey, 30 Sept. to 1 Oct., 1969.

- (8) AGARD Conference Proceedings No. 98, "Specialists Meeting on Stress Corrosion Testing Methods", Brussels, Belgium, 5 and 6 October, 1971.
- (9) Piper, D. E., AGARD Advisory Report No. 25, "Standardization of Test Methods for Stress-Corrosion Cracking, December, 1970.
- (10) Brown, B. F., Stress-Corrosion Cracking in High Strength Steels and in Titanium and Aluminum Alloys, Naval Research Laboratory, Washington, D.C., 1972. (Sponsored by the Advanced-Research Projects Agency ARPA Order No. 878).
- (11) Craig, H. L., Jr., Sprowls, D. O. and Piper, D. E., "Stress-Corrosion Cracking", Chapter 10 in Handbook on Corrosion Testing and Evaluation, Edited by W. H. Ailor, published by John Wiley & Sons, Inc., 1971.
- (12) Wei, R. P., Novak, S. R. and Williams, D. P., "Some Important Considerations in the Development of Stress-Corrosion Cracking Test Methods", AGARD Conference Proceedings No. 98, Specialists Meeting on Stress Corrosion Testing Methods, Brussels, Belgium, 5 and 6 October, 1971.
- (13) Stress-Corrosion Cracking of Metals - A State of the Art, ASTM Special Technical Publication No. 518 (1972), Philadelphia, Penna., American Society for Testing and Materials.

TABLE D-1

ALUMINUM ALLOY BOLT LOADED COMPACT TENSION SPECIMENS  
EXPOSED TO SEACOAST ATMOSPHERE

Alloy & Temper	Specimen No.	Specimen Orientation	Initial Crack Length, In.	Initial $K_I$ , (1) $\frac{ksi}{\sqrt{in.}}$	Exposure Date	Months	Initial Crack Growth In./(2)	Exposure, K <sub>I</sub> , No.	Crack Length		Final $K_I$ (3) $\frac{ksi}{\sqrt{in.}}$		
									Surface	Fracture			
2024-T651	366335	S-L	1.000	0	8/3/69	0-8.3	0	8.3	---	0.979	17.7	94.7	
		S-L	0.970	95	8/3/69	0-3	0.25	0.25	8.3	1.250	1.240	15.5	92.9
		S-L	1.010	95	8/3/69	0-3	0.22	0.22	8.3	1.790	---	---	---
		S-L	1.010	95	8/3/69	0-3	0.19	0.19	8.3	1.200	1.160	16.8	90.8
		S-L	0.990	75	8/3/69	0-3	0.15	0.15	8.3	1.840	---	---	---
		S-L	0.975	75	11/9/70	0-5	0.44	0.44	8.3	1.635	---	---	---
		S-L	0.985	50	11/9/70	0-3	0.33	0.33	8.3	1.565	---	---	---
		S-L	0.985	50	11/9/70	0-3	0.405	0.405	8.3	1.625	---	---	---
		S-L	1.020	0	11/9/70	0-5	0.035	0	8.3	1.020	(8)	---	---
		L-T	0.985	95	11/9/70	0-8	0	0	8.3	1.020	(8)	---	---
		L-T	0.980	95	11/9/70	0-13	0	0	13	0.985	(8)	---	---
		L-T	0.990	75	11/9/70	0-5	0.005	0.005	13	0.985	(8)	---	---
		L-T	1.000	75	11/9/70	0-13	0	0	13	0.900	(8)	---	---
		L-T	1.000	75	11/9/70	0-13	0	0	13	1.000	(8)	---	---
		2021-T81	366400	S-L	0.975	0	8/3/69	0-8.3	0	8.3	0.975	(8)	20.7
S-L	1.000			95	8/3/69	3-8.3	0.06	0.06	8.3	1.060	1.005	14.4	73.5
S-L	0.970			95	8/3/69	3-8.3	0.06	0.06	8.3	---	1.088	---	---
S-L	1.050			95	8/3/69	3-8.3	0.04	0.04	24	0.90	---	---	---
S-L	0.990			95	8/3/69	3-8.3	0.04	0.04	15	1.110	---	---	---
L-T	0.980			95	11/9/70	0-13	0	0	13	0.980	(8)	---	---
L-T	0.990			95	11/9/70	0-13	0	0	13	0.990	(8)	---	---
L-T	1.015			0	11/9/70	0-13	0	0	13	1.015	(8)	---	---
S-L	---			0	8/3/69	0-8.3	0	0	8.3	---	0.998	---	---
S-L	0.980			95	8/3/69	0-3	0.26	0.26	8.3	1.870	---	20.5	97.4
S-L	0.990			95	8/3/69	0-3	0.35	0.35	8.3	1.220	(4)	(4)	(4)
S-L	0.980			95	8/3/69	0-3	0.39	0.39	7	1.370	---	19.6	93.1
S-L	0.980			95	8/3/69	0-3	0.21	0.21	8.3	1.870	---	17.7	84.1
S-L	0.965			75	11/9/70	0-3	0.59	0.59	5	1.555	---	(4)	(4)
2024-T351	366206			S-L	0.990	75	11/9/70	0-5	0.66	5	1.640	---	6.5(6)
		S-L	0.990	50	11/9/70	0-5	0.49	8	1.670	---	(4)	(4)	(4)
		S-L	1.000	50	11/9/70	0-5	0.52	0	1.570	---	(4)	(4)	(4)
		L-T	0.985	95	11/9/70	0-8	0	0	8	1.000	(8)	---	---
		L-T	0.975	95	11/9/70	13	0.01	0.01	13(10)	0.995	0.966	21.7	73.3
		L-T	0.980	95	11/9/70	13	0.01	0.01	13(10)	0.985	1.000	21.5	72.6
		L-T	1.000	0	11/9/70	0-13	0	0	13(10)	0.980	1.040	16.1	54.4
		L-T	---	0	11/9/70	0-13	0	0	13(10)	1.000	0.990	---	---
		S-L	1.030	0	8/3/69	0-8.3	0.07	0	8.3	1.023	---	16.8	100.6
		S-L	0.970	95	8/3/69	3-8.3	0.01	0.01	8.3	1.122	---	13.7	82.0
		S-L	0.950	95	8/3/69	3-8.3	0.03	0.03	24	0.920	---	14.1	84.4
		S-L	0.990	95	8/3/69	3-8.3	0.01	0.01	15	1.050	---	(6)	(6)
		L-T	1.005	95	11/9/70	0-13	0	0	13	1.005	---	---	---
		L-T	0.985	95	11/9/70	0-13	0	0	13	0.985	(8)	---	---
		L-T	1.000	95	11/9/70	0-13	0	0	13	1.000	(8)	---	---
2021-T851	366207	S-L	---	0	8/3/69	0-8.3	0	8.3	---	1.023	---	---	
		S-L	1.030	0	8/3/69	3-8.3	0.07	0	8.3	1.122	---	---	
		S-L	0.970	95	8/3/69	3-8.3	0.01	0.01	8.3	1.018	---	---	
		S-L	0.950	95	8/3/69	3-8.3	0.03	0.03	24	0.920	---	---	
		S-L	0.990	95	8/3/69	3-8.3	0.01	0.01	15	1.050	---	---	
		L-T	1.005	95	11/9/70	0-13	0	0	13	1.005	---	---	
		L-T	0.985	95	11/9/70	0-13	0	0	13	0.985	(8)	---	---
		L-T	1.000	95	11/9/70	0-13	0	0	13	1.000	(8)	---	---

Alloy & Temper	Specimen No.	Sp. specimen Orientation	Initial Crack Length, In.	Initial $K_{Ic}$ (1)	Exposure Date	Initial Crack Growth Months	Amt. In. (2)	Exposure Termination No.	Surface	Crack Length	Fracture	Final $K_{Ic}$ (3)		
												ksi	ksi	
2219-T37	344793	S-L	---	0	8/3/69	OK8.3	0	8.3	---	---	0.635	23.7	87.5(11)	
		S-L	0.75	95	8/3/69	0-3	0.48	3	1.230	(4)	---	(4)	(4)	
		S-L	0.76	95	8/3/69	0-3	0.47	3	1.250	(4)	---	(4)	(4)	
		S-L	0.75	95	8/3/69	0-3	0.54	3	1.290	(4)	1.340	---	17.6	64.9
		S-L	0.74	95	8/3/69	0-3	0.49	3	1.230	(4)	1.230	---	8.9	32.8
		TL11	0.752	95	11/9/70	0-5	0.70	5	1.555	(4)	---	---	---	(4)
		TL12	0.765	95	11/9/70	0-5	0.72	5	1.485	(4)	---	---	---	(4)
		TL13	0.765	50	11/9/70	0-5	0.715	5	1.430	(4)	---	---	---	(4)
		TL14	0.770	50	11/9/70	0-5	0.715	5	1.485	(4)	---	---	---	(4)
		TL15	0.765	0	11/9/70	OK5	0	0.765	5	0.765	(8)	---	---	(4)
		LM7	0.740	95	11/9/70	0-5	0.115	5	0.895	(6)	---	---	---	(6)
		LM8	0.735	95	11/9/70	0-5	0.09	5	0.840	(6)	0.752	---	16.0	55.6
		LM9	0.740	75	11/9/70	0-5	0.02	5	0.755	(8)	0.754	---	11.4	39.6
		LM10	0.750	0	11/9/70	OK13	0	0.750	13	0.750	(8)	---	---	(8)
		2219-T97	338148	S-L	---	0	8/3/69	OK18	0	18	0	---	0.57	18.5
S-L	0.750			95	8/3/69	OK8.3	0	8.3	0.750	(8)	0.614	16.0	61.4	
S-L	0.750			95	8/3/69	3-8.3	0.01	8.3	0.760	(8)	0.782	---	11.8	60.1
S-L	0.740			95	8/3/69	OK24	0	0.06	24	0.740	(8)	---	---	(6)
S-L	0.740			95	8/3/69	8.3-15	0	0.06	15	0.80	(8)	---	---	(6)
L-T	1.005			95	11/9/70	OK13	0	0.05	13	1.005	(8)	---	---	(8)
L-T	0.990			95	11/9/70	OK13	0	0.05	13	0.990	(8)	---	---	(8)
L-T	1.000			0	11/9/70	OK13	0	0.05	13	1.000	(8)	---	---	(8)
5156-H117	366656	S-L	---	0	7/20/69	OK16	0	16	---	---	0.992	22.6(9)	103.7(9)	
		S-L	0.980	95	7/20/69	OK8.8	0	8.8	0.980	(8)	0.960	20.2	92.7	
		S-L	0.980	95	7/20/69	OK8.8	0	0.01	8.8	0.980	(8)	0.978	17.8	81.7
		S-L	0.960	95	7/20/69	OK24	0	0.06	24	0.960	(8)	---	---	(6)
		S-L	0.980	95	7/20/69	OK15	0	0.05	15	0.980	(8)	---	---	(6)
		L-T	0.985	95	11/9/70	OK13	0	0.05	13	0.985	(8)	---	---	(8)
		L-T	0.995	95	11/9/70	OK13	0	0.05	13	0.995	(8)	---	---	(8)
		L-T	0.995	0	11/9/70	OK13	0	0.05	13	0.995	(8)	---	---	(8)
5156 Transitized	366657	S-L	---	0	7/20/69	OK8.8	0	8.8	---	---	0.979	22.6(9)	105.6(9)	
		S-L	0.980	95	7/20/69	0-3	0.84	3	1.820	(4)	---	---	(4)	
		S-L	1.020	95	7/20/69	0-3	0.88	3	1.900	(4)	---	---	(4)	
		S-L	0.97	95	7/20/69	0-3	0.88	3	1.850	(4)	---	---	(4)	
		S-L	1.030	95	7/20/69	0-3	0.87	3	1.870	(4)	---	---	(4)	
		TL11	0.970	75	11/9/70	0-5	0.875	5	1.845	(4)	---	---	(4)	
		TL12	0.960	75	11/9/70	0-5	0.895	5	1.895	(4)	---	---	(4)	
		TL13	0.970	50	11/9/70	0-5	0.890	5	1.860	(4)	---	---	(4)	
		TL14	0.955	50	11/9/70	0-5	0.830	5	1.785	(4)	---	---	(4)	
		TL15	1.005	0	11/9/70	OK5	0	0.830	5	1.785	(8)	---	---	(8)
LM7	1.000	95	11/9/70	OK13	0	0.05	13	1.000	(8)	---	---	(8)		
LM8	0.990	95	11/9/70	OK13	0	0.05	13	0.990	(8)	---	---	(8)		
LM9	1.000	75	11/9/70	OK13	0	0.05	13	1.000	(8)	---	---	(8)		
LM10	1.030	0	11/9/70	OK13	0	0.05	13	1.030	(8)	---	---	(8)		

Table D-1 (Continued)

Alloy & Temper	Specimen No.	Specimen Orientation	Initial Crack Length In.	Initial K <sub>I</sub> (1) % F <sub>Yc</sub>	Exposure Date	Initial Crack Growth		Exposure Mo.	Crack Surface	Pressure With Fracture	Exposure Terminated Final K <sub>I</sub> % F <sub>Yc</sub>		
						Months	Am't. In. (2)						
6051-T651	366208	NC3	---	0	3/8/69	OK18	0	13	0.970	23.6	110.0		
		NC4	0.990	95	3/8/69	OK8.3	0	8.3	0.980	19.5	92.5		
		NC5	0.980	95	3/8/69	OK24	0	24	0.990	(8)	90.9		
		NC6	0.990	95	8/3/69	OK15	0	15	0.990	(8)	(6)		
		NC7	0.990	95	11/9/70	OK13	0	13	0.980	(8)	---		
		NC8	0.980	95	11/9/70	OK13	0	13	0.955	(8)	---		
		NC9	0.995	0	8/3/69	OK8.3	0	8.3	0.972	0.972	18.6	91.2(11)	
		NC10	0.990	95	8/3/69	OK2	0.92	2	1.910	---	(4)	(4)	
7079-T651	314758	NC1	1.000	95	8/3/69	OK2	0.90	2	1.900	---	(4)		
		NC2	0.980	95	8/3/69	OK2	0.93	2	1.910	---	(4)		
		NC3	0.980	95	8/3/69	OK2	0.94	2	1.920	---	(4)		
		NC4	0.990	75	11/9/69	OK2	0.58	2	1.570	1.570	3.9(6)	19.1(6)	
		NC5	0.995	75	11/9/69	OK2	0.655	2	1.650	---	(4)	(4)	
		NC6	1.010	50	11/9/70	OK2	0.270	2	1.750	---	(4)	(4)	
		NC7	0.980	50	11/9/70	OK2	0.435	2	1.745	---	(4)	(4)	
		NC8	0.995	0	11/9/70	OK6	0	6	0.995	(8)	---	---	
		NC9	0.990	95	11/9/70	OK13	0	13	0.990	(8)	---	---	
		NC10	0.985	95	11/9/70	OK13	0	13	0.985	(8)	---	---	
		NC11	0.995	75	11/9/70	OK13	0	13	0.995	(8)	---	---	
		NC12	1.000	0	8/3/69	OK8.3	0	8.3	1.000	(8)	---	---	
		NC13	1.010	0	8/3/69	OK2	0.94	2	1.950	---	---	83.9(11)	
		NC14	1.020	95	8/3/69	OK2	0.88	2	1.910	---	---	(4)	
		NC15	1.040	95	8/3/69	OK2	0.92	2	1.940	---	---	(4)	
7079-T651	366259	NC16	1.040	95	8/3/69	OK2	0.86	2	1.900	---	(4)		
		NC17	0.980	75	11/9/70	OK2	0.945	2	1.925	---	(4)		
		NC18	0.995	75	11/9/70	OK2	0.84	2	1.835	---	(4)		
		NC19	0.995	50	11/9/70	OK2	0.925	2	1.925	---	(4)		
		NC20	0.960	50	11/9/70	OK5	0	5	1.905	---	(4)		
		NC21	0.995	0	11/9/70	OK5	0	5	0.995	(8)	---	---	
		NC22	1.005	95	11/9/70	OK5	0.03	5	1.035	1.034	79.6	(Polit Line Crack Irr)	
		NC23	0.995	95	11/9/70	OK13	0	13	0.995	(8)	---	---	
		NC24	0.985	75	11/9/70	OK13	0	13	0.985	(8)	---	---	
		NC25	0.995	0	11/9/70	OK13	0	13	0.995	(8)	---	---	
		7079-T651	366209	NC26	0.990	0	8/3/69	OK8.3	0	8.3	0.995	18.5	94.4(11)
				NC27	0.990	95	8/3/69	OK2	0.81	2	1.800	---	(4)
				NC28	0.970	95	8/3/69	OK2	0.87	2	1.860	---	(4)
				NC29	1.010	95	8/3/69	OK2	0.91	2	1.880	---	(4,6)
				NC30	0.995	75	11/9/70	OK2	0.87	2	1.860	---	(4)
NC31	0.990			75	11/9/70	OK2	0.75	2	1.635	---	(4)		
NC32	0.975			50	11/9/70	OK2	0.50	2	1.740	---	(4)		
NC33	0.985			50	11/9/70	OK2	0.495	2	1.610	---	(4)		
NC34	0.995			0	11/9/70	OK6	0	6	1.500	---	(4)		
NC35	0.995			0	11/9/70	OK6	0	6	0.995	(8)	---		

Table D-1 (Continued)

Alloy & Timber	Specimen No.	Specimen Orientation	Initial Crack Length in.	Initial $K_I$ (1) % K <sub>IC</sub>	Exposure Rate	Months	Initial Crack Growth		Exposure No.	Exposure Terminated		Final $K_I$ (1) % K <sub>IC</sub>
							Amt. in. (2)	Months		Crack Length Surface	Fracture	
7075-T651	366209	L-T	1.000	95	11/9/70	OK13	0	0	13	1.000	(2)	---
		L-T	0.995	95	11/9/70	13	0.02	0	13	1.015	(8)	---
		L-T	0.995	75	11/9/70	13	0.015	0	13	1.010	(8)	---
		L-T	1.015	0	11/9/70	OK13	0	0	13	1.015	(8)	---
7075-T7351	366210	S-L	---	0	8/3/69	OK18	0	0	18	---	.998	20.5
		S-L	1.010	95	8/3/69	OK8.3	0	0	8.3	1.010	1.022	15.1
		S-L	0.980	95	8/3/69	OK8.3	0	0	8.3	0.980	1.034	15.7
		S-L	1.010	95	8/3/69	21-24	0.07	0	24	1.080	(8)	---
		S-L	0.990	95	8/3/69	8.3-15	0.03	0	15	1.020	---	(6)
		L-T	0.990	95	11/9/70	OK13	0	0	13	0.990	(8)	---
		L-T	0.975	95	11/9/70	OK3	0	0	13	0.975	(8)	---
		L-T	0.990	0	11/9/70	OK13	0	0	13	0.990	(8)	---

- Notes:
- (1) Calculated from applied load and average crack length measured on exterior of specimens.
  - (2) Calculated from average crack lengths measured on exterior of specimens.
  - (3) Calculated from crack lengths measured on the fracture surface and the measured load.
  - (4) Reliable residual stress intensity could not be calculated because of excessive crack growth.
  - (5) Reliable residual stress intensity could not be calculated because of occurrence of branching or multiple cracks.
  - (6) Used for metallographic examinations.
  - (7) Based on surface crack.
  - (8) Specimen still in test, numbers indicates the crack length at the time of the last measurements
  - (9) Not valid per E399 criteria for  $K_{Ic}$ .
  - (10) Removed from test due to severe exfoliation.
  - (11) Small SCC at tip of precrack as in Figure 30.

TABLE D-2

ALUMINUM ALLOYS BOLT LOADED COMPACT TENSION SPECIMENS (FATIGUE PRECRACK) EXPOSED TO INDUSTRIAL ATMOSPHERE

Alloy & Temper	Specimen No.	Specimen Orientation	Initial Crack Length In.	Initial $K_I$ (1) % K <sub>IC</sub>	Exposure Date	Initial Crack Growth Months	Initial Crack Amt. In. (2)	Exposure No.	Crack Length		Exposure Terminated Residual $K_I$ (75)		
									Surface	Fracture			
2024-T651	36335	S-L	---	0	5/29/69	OK12	0	12	---	991	18.1		
		S-L	1.000	95	5/29/69	12-18	0.01	18	1.010	1.066	16.1		
		S-L	1.010	95	5/29/69	12-18	0.04	18	1.040	---	87.7		
		S-L	1.000	95	5/29/69	12-18	0.035	33	1.090	---	(6)		
		TL16	1.015	95	2/11/70	1-2	0.01	18	1.390	---	---		
		S-L	0.990	75	2/11/70	OK18	0	18	1.390	---	---		
		TL18	1.035	50	2/11/70	OK18	0	18	1.035	---	---		
		TL19	0.990	50	2/11/70	5-6	0.01	18	1.050	---	---		
		TL20	0.990	50	2/11/70	OK18	0	18	0.990	---	---		
		LM11	1.005	95	2/11/70	OK18	0	18	1.065	---	---		
		LM12	1.000	95	2/11/70	OK18	0	18	1.000	---	---		
		LM13	0.985	75	2/11/70	OK18	0	18	0.985	---	---		
		LM14	0.985	0	2/11/70	OK18	0	18	0.985	---	---		
		2021-T81	36400	S-L	---	0	5/29/69	OK28	0	28	---	1.003	20.7
S-L	0.990			95	5/29/69	OK12	0	12	0.990	1.034	16.9		
S-L	0.990			95	5/29/69	OK12	0	12	0.990	---	86.2		
S-L	1.000			95	5/29/69	OK18	0	18	1.000	---	14.9		
S-L	1.030			95	5/29/69	OK18	0	18	1.01	---	(6)		
S-L	1.010			95	5/29/69	OK16	0	16	0.980	---	---		
LM9	0.980			95	2/11/70	OK16	0	16	0.985	---	---		
LM10	0.985			95	2/11/70	OK16	0	16	0.985	---	---		
LM11	0.985			0	2/11/70	OK16	0	16	0.985	---	---		
2024-T351	365206			S-L	---	0	5/29/69	OK12	0	12	---	0.996	21.6
				S-L	1.000	95	5/29/69	12-18	0.07	18	1.07	1.028	19.0
				S-L	1.000	95	5/29/69	12-18	0.06	18	1.06	1.01	19.4
				S-L	1.000	95	5/29/69	12-18	0.05	18	1.05	---	(6)
				S-L	1.030	95	5/29/69	12-18	0.015	33	1.045	---	---
		TL16	0.985	75	2/11/70	1-2	0.03	18	1.490	---	---		
		TL17	0.990	75	2/11/70	6-7	0.02	18	1.260	---	---		
		TL18	0.985	50	2/11/70	6-7	0.01	18	1.010	---	---		
		TL19	0.975	50	2/11/70	1-2	0.01	18	1.065	---	---		
		TL20	1.020	0	2/11/70	OK18	0	18	1.020	---	---		
		LM11	0.990	95	2/11/70	OK18	0	18	0.990	---	---		
		LM12	0.975	95	2/11/70	OK18	0	18	0.975	---	---		
		LM13	0.985	75	2/11/70	OK18	0	18	0.985	---	---		
		LM14	0.990	0	2/11/70	OK18	0	18	0.990	---	---		
2024-T851	366207	S-L	---	0	5/29/69	OK28	0	28	---	1.019	16.7		
		S-L	0.990	95	5/29/69	OK12	0	12	0.99	0.996	15.1		
		S-L	0.990	95	5/29/69	OK12	0	12	0.99	0.994	15.0		
		S-L	0.990	95	5/29/69	OK18	0	18	0.99	---	(6)		
		S-L	1.020	95	5/29/69	OK16	0	16	1.02	---	---		
		LM9	0.995	95	2/11/70	OK16	0	16	1.000	---	---		
		LM10	1.000	95	2/11/70	OK16	0	16	1.000	---	---		
		LM11	0.995	0	2/11/70	OK16	0	16	0.995	---	---		

Table D-2 (Continued)

Alloy & Temper	Specimen No.	Specimen Orientation	Initial Crack Length		Initial $K_I$ (1) % $K_{Ic}$	Exposure Date	Initial Crack Growth Amt. In. (2)	Exposure Mo.	Exposure Terminated		Residual $K_I$ (3) % $K_{Ic}$
			In.	In.					Surface	Fracture	
2219-T37	344793	S-L	---	0.780	0	5/29/69	0.012	12	---	0.807	22.6
		S-L	0.730	0.730	95	5/29/69	0.02	18	1.05	1.032	83.4
		S-L	0.750	0.750	95	5/29/69	0.13	18	1.03	1.05	83.4
		S-L	0.740	0.740	95	5/29/69	0.10	18	1.02	---	81.5
		S-L	0.755	0.755	95	5/29/69	0.02	24	1.25	---	(6)
		S-L	0.740	0.740	75	2/11/70	0.025	18	0.880	---	(4)
		S-L	0.740	0.740	75	2/11/70	0.020	18	0.945	---	---
		S-L	0.730	0.730	50	2/11/70	0.035	18	0.880	---	---
		S-L	0.800	0.800	50	2/11/70	0.01	18	0.980	---	---
		S-L	0.755	0.755	0	2/11/70	0	18	0.775	---	---
		L-T	0.740	0.740	95	2/11/70	0	18	0.740	---	---
		L-T	0.740	0.740	95	2/11/70	0	18	0.740	---	---
		L-T	0.735	0.735	75	2/11/70	0	18	0.735	---	---
		L-T	0.750	0.750	0	2/11/70	0	18	0.750	---	---
2219-T37	338148	S-L	---	0.760	0	5/29/69	0.028	28	---	0.734	17.8
		S-L	0.740	0.740	95	5/29/69	0.012	12	0.760	0.793	76.8
		S-L	0.760	0.760	95	5/29/69	0.018	12	0.760	0.786	76.8
		S-L	0.760	0.760	95	5/29/69	0.033	33	0.760	---	16.3
		L-T	0.985	0.985	95	2/11/70	0.016	16	0.985	---	(6)
		L-T	0.990	0.990	95	2/11/70	0.016	16	0.990	---	---
		L-T	0.985	0.985	0	2/11/70	0.016	16	0.985	---	---
		S-L	---	0.980	0	8/25/69	0.015	15	---	0.918	22.4(9)
		S-L	0.990	0.990	95	8/25/69	0.012	12	0.980	0.960	76.1
		S-L	0.980	0.980	95	8/25/69	0.012	12	0.990	0.962	83.0
		S-L	0.990	0.990	95	8/25/69	0.016	16	0.980	---	(6)
S-L	0.980	0.980	95	8/25/69	0.026	26	0.980	---	---		
L-T	1.015	1.015	95	2/11/70	0.016	16	1.015	---	---		
L-T	0.990	0.990	95	2/11/70	0.016	16	1.010	---	---		
L-T	0.990	0.990	0	2/11/70	0.016	16	0.990	---	---		
3456-H117	366656	S-L	---	0.990	0	8/25/69	0.015	15	---	0.972	21.7(9)
		S-L	0.980	0.980	95	8/25/69	0.015	15	0.980	1.390	101.4(9)
		S-L	0.980	0.980	95	8/25/69	0.014	16	0.990	1.360	109.8(7)
		S-L	0.990	0.990	95	8/25/69	0.014	16	0.980	1.400	87.9
		S-L	0.990	0.990	95	8/25/69	0.015	26	0.980	1.465	(6)
		S-L	0.975	0.975	75	2/11/70	0.01	18	1.190	1.240	---
		S-L	0.995	0.995	75	2/11/70	0.01	18	1.140	1.140	---
		S-L	0.975	0.975	50	2/11/70	0.01	18	1.105	1.105	---
		S-L	0.990	0.990	0	2/11/70	0.018	18	0.990	---	---
		L-T	1.005	1.005	95	2/11/70	0.018	18	1.005	---	---
		L-T	0.990	0.990	75	2/11/70	0.018	18	1.005	---	---
		L-T	0.990	0.990	75	2/11/70	0.018	18	0.990	---	---
		L-T	1.000	1.000	0	2/11/70	0.018	18	1.000	---	---
		3456 Sensitized	366657	S-L	---	0.990	0	8/25/69	0.015	15	---
S-L	0.980			0.980	95	8/25/69	0.014	16	0.980	1.268	101.4(9)
S-L	0.980			0.980	95	8/25/69	0.014	16	0.980	1.188	109.8(7)
S-L	0.990			0.990	95	8/25/69	0.014	16	0.980	---	87.9
S-L	0.990			0.990	95	8/25/69	0.015	26	0.980	---	(6)
S-L	0.975			0.975	75	2/11/70	0.01	18	1.190	1.240	---
S-L	0.995			0.995	75	2/11/70	0.01	18	1.140	1.140	---
S-L	0.975			0.975	50	2/11/70	0.01	18	1.105	1.105	---
S-L	0.990			0.990	0	2/11/70	0.018	18	0.990	---	---
L-T	1.005			1.005	95	2/11/70	0.018	18	1.005	---	---
L-T	0.990			0.990	75	2/11/70	0.018	18	0.990	---	---
L-T	0.990	0.990	75	2/11/70	0.018	18	0.990	---	---		
L-T	1.000	1.000	0	2/11/70	0.018	18	1.000	---	---		
061-T651	366208	S-L	---	0.990	0	5/29/69	0.028	23	---	0.949	21.2
		S-L	0.980	0.980	95	5/29/69	0.012	12	0.980	0.976	98.8
		S-L	0.980	0.980	95	5/29/69	0.012	12	0.980	0.964	88.6
		S-L	0.960	0.960	95	5/29/69	0.018	18	0.980	---	92.3
		S-L	0.975	0.975	95	5/29/69	0.033	33	0.960	---	(6)
		L-T	0.975	0.975	95	2/11/70	0.016	16	0.975	---	---
		L-T	0.970	0.970	95	2/11/70	0.016	16	0.975	---	---
		L-T	0.985	0.985	0	2/11/70	0.016	16	0.985	---	---
		S-L	---	0.990	0	8/25/69	0.012	12	---	0.949	21.2
		S-L	0.980	0.980	95	8/25/69	0.012	12	0.980	0.976	98.8
		S-L	0.980	0.980	95	8/25/69	0.012	12	0.980	0.964	88.6
S-L	0.960	0.960	95	8/25/69	0.018	18	0.980	---	92.3		
S-L	0.975	0.975	95	8/25/69	0.033	33	0.960	---	(6)		
L-T	0.975	0.975	95	2/11/70	0.016	16	0.975	---	---		
L-T	0.970	0.970	95	2/11/70	0.016	16	0.975	---	---		
L-T	0.985	0.985	0	2/11/70	0.016	16	0.985	---	---		

Alloy & Temper	Specimen No.	Specimen Orientation	Initial Crack Length (in.)	Initial $K_I$ (ksi)	Exposure Date	Crack Growth Mechanism	Initial Amt. In. (2)	Exposure No.	Exposure Surface	Crack Length	Exposure Terminated Fracture	Residual $K_I$ (ksi)	Residual $K_I$ (ksi)				
7039-T6351	314758	S-L	1.010	0	5/29/69	OK12	0	12	1.90	0.991	19.7	96.5(10)	96.5(10)				
			0.980	95	5/29/69	0-3 wk.	0.24	1.91	---	---	---	---	---	---			
			0.990	95	5/29/69	0-3 wk.	0.23	1.92	---	---	---	---	---	---			
			1.020	95	5/29/69	0-3 wk.	0.21	1.880	---	---	---	---	---	---			
			0.985	75	2/11/70	0-1	0.06	1.870	---	---	---	---	---	---			
			0.990	75	2/11/70	0-1	0.065	1.870	---	---	---	---	---	---			
			0.995	50	2/11/70	0-1	0.02	1.870	---	---	---	---	---	---			
			0.990	50	2/11/70	0-1	0.015	1.715	---	---	---	---	---	---			
			0.990	0	OK5	0	0	0.990	---	---	---	---	---	---			
			1.045	95	2/11/70	7-8	0.01	0.985	---	---	---	---	---	---			
			0.985	95	2/11/70	OK16	0	0.985	---	---	---	---	---	---			
			0.995	75	2/11/70	OK16	0	0.995	---	---	---	---	---	---			
			0.990	0	OK16	0	0	0.990	---	---	---	---	---	---			
			7070-T651	366259	S-L	0.990	0	5/29/69	OK12	0	12	1.880	1.044	17.1	80.1(10)	80.1(10)	
						0.980	95	5/29/69	0-3 wk.	0.23	1.870	---	---	---	---	---	---
						1.000	95	5/29/69	0-3 wk.	0.22	1.880	---	---	---	---	---	---
1.010	95	5/29/69				0-3 wk.	0.24	1.880	---	---	---	---	---	---			
1.005	75	2/11/70				0-1	0.16	1.715	---	---	---	---	---	---			
1.010	75	2/11/70				0-1	0.19	1.715	---	---	---	---	---	---			
1.005	50	2/11/70				1-2	0.045	1.555	---	---	---	---	---	---			
1.010	50	2/11/70				0-6	0.015	1.015	---	---	---	---	---	---			
1.055	95	2/11/70				7-8	0.015	0.995	---	---	---	---	---	---			
0.990	95	2/11/70				OK16	0	0.990	---	---	---	---	---	---			
0.995	75	2/11/70				OK16	0	0.995	---	---	---	---	---	---			
0.995	0	OK16				0	0	0.995	---	---	---	---	---	---			
7075-T651	366200	S-L				0.970	0	5/29/69	OK12	0	12	1.680	1.020	18.0	86.4	86.4	
						0.990	95	5/29/69	0-3 wk.	0.12	1.870	---	---	---	---	---	---
						0.980	95	5/29/69	0-3 wk.	0.11	1.870	---	---	---	---	---	---
						0.970	95	5/29/69	0-3 wk.	0.09	1.870	---	---	---	---	---	---
			0.985	75	2/11/70	0-3 wk.	0.04	1.450	---	---	---	---	---	---			
			1.000	75	2/11/70	1-2	0.01	1.605	---	---	---	---	---	---			
			0.990	50	2/11/70	4-5	0.02	1.250	---	---	---	---	---	---			
			0.995	50	2/11/70	OK18	0	0.995	---	---	---	---	---	---			
			1.030	95	2/11/70	OK16	0	1.000	---	---	---	---	---	---			
			0.995	95	2/11/70	OK16	0	0.995	---	---	---	---	---	---			
			1.000	75	2/11/70	OK16	0	1.000	---	---	---	---	---	---			
			1.000	0	OK16	0	0	1.000	---	---	---	---	---	---			
			7075-T7351	366210	S-L	1.000	0	5/29/69	OK28	0	28	1.000	0.997	20.0	95.0	95.0	
						0.990	95	5/29/69	OK12	0	1.000	---	---	---	---	---	---
						1.000	95	5/29/69	OK12	0	0.990	---	---	---	---	---	---
						1.010	95	5/29/69	OK18	0	1.000	---	---	---	---	---	---
0.990	95	5/29/69				OK16	0	0.990	---	---	---	---	---	---			
0.990	95	2/11/70				OK16	0	0.990	---	---	---	---	---	---			
0.995	95	2/11/70				OK16	0	0.995	---	---	---	---	---	---			
1.000	0	OK16				0	0	0.990	---	---	---	---	---	---			

- Notes:
- (1) Calculated from applied load and average crack length measured on exterior of specimens.
  - (2) Calculated from average crack lengths measured on exterior of specimens.
  - (3) Calculated from crack lengths measured on the fracture surface and the measured load.
  - (4) Reliable residual stress intensity could not be calculated because of excessive crack growth.
  - (5) Reliable residual stress intensity could not be calculated because of occurrence of branching or multiple cracks.
  - (6) Used for metallographic examinations.
  - (7) Calculation of residual  $K_I$  unreliable because of irregular shape of the crack front.
  - (8) Specimen still in test, number indicates the crack length at the time of the last measurement.
  - (9) Not valid per E399 criteria for  $K_{Ic}$ .
  - (10) Small SCR at tip of precrack as in Figure 30.

Table D-2 (Continued)

Alloy & Temper	Specimen No.	Specimen Orientation	Initial Crack Length in.	Initial $K_I$ (1)	Exposure Date	Crack Growth Months	Crack Growth Amt. In. (2)	Exposure No.	Exposure Terminated Crack Length Surface	Residual $K_I$ (3)	Residual $K_I$ (4)		
7039-T6351	314758	S-L	---	0	5/29/69	0K12	0	12	---	19.7	95.6(10)		
		S-L	1.010	95	5/29/69	0-3 wk.	0.24	1	1.90	(4)	(4)		
		S-L	0.980	95	5/29/69	0-3 wk.	0.23	2	1.91	(4)	(4)		
		S-L	0.990	95	5/29/69	0-3 wk.	0.21	3	1.92	(4)	(4)		
		S-L	1.030	95	5/29/69	0-3 wk.	0.30	4	1.900	(4)	(4)		
		S-L	0.985	95	2/11/70	0-1	0.06	5	1.880	(4)	(4)		
		S-L	0.990	75	2/11/70	0-1	0.065	6	1.560	(4)	(4)		
		S-L	0.990	50	2/11/70	0-1	0.02	7	1.670	(4)	(4)		
		S-L	0.995	50	2/11/70	0-1	0.015	8	1.715	(4)	(4)		
		S-L	0.990	0	2/11/70	0-5	0.01	9	0.690	(8)	(8)		
		L-T	1.045	95	2/11/70	7-8	0.01	10	1.045	(8)	(8)		
		L-T	0.985	95	2/11/70	0K16	0	0.985	(8)	(8)	(8)		
		L-T	0.990	0	2/11/70	0K16	0	0.990	(8)	(8)	(8)		
		7070-T651	366259	S-L	---	0	5/29/69	0K12	0	12	---	17.1	90.1(10)
S-L	0.980			95	5/29/69	0-3 wk.	0.25	1	1.890	(4)	(4)		
S-L	1.000			95	5/29/69	0-3 wk.	0.35	2	1.860	(4)	(4)		
S-L	1.010			95	5/29/69	0-3 wk.	0.34	3	1.880	(4)	(4)		
S-L	1.005			75	2/11/70	0-1	0.16	4	1.745	(4)	(4)		
S-L	1.010			50	2/11/70	1-2	0.19	5	1.700	(4)	(4)		
S-L	1.005			50	2/11/70	0-1	0.045	6	1.555	(4)	(4)		
S-L	1.010			0	2/11/70	0-1	0.015	7	1.010	(8)	(8)		
L-T	1.055			95	2/11/70	7-8	0.015	8	1.075	(8)	(8)		
L-T	0.990			95	2/11/70	0K16	0	0.990	(8)	(8)	(8)		
L-T	0.995			75	2/11/70	0K16	0	0.995	(8)	(8)	(8)		
L-T	0.995			0	2/11/70	0K16	0	0.995	(8)	(8)	(8)		
7075-T651	366200			S-L	---	0	5/29/69	0K12	0	12	---	18.0	95.4
				S-L	0.990	95	5/29/69	0-3 wk.	0.12	1	1.690	(4)	(4)
		S-L	0.990	95	5/29/69	0-3 wk.	0.11	2	1.890	(4)	(4)		
		S-L	0.970	95	5/29/69	0-3 wk.	0.09	3	1.870	(4)	(4)		
		S-L	0.985	95	5/29/69	0-3 wk.	0.04	4	1.450	(4)	(4)		
		S-L	1.060	75	2/11/70	0-1	0.01	5	1.645	(4)	(4)		
		S-L	0.990	50	2/11/70	1-2	0.015	6	1.695	(8)	(8)		
		S-L	0.990	50	2/11/70	4-5	0.03	7	1.950	(8)	(8)		
		S-L	0.995	0	2/11/70	0K18	0	0.995	(8)	(8)	(8)		
		L-T	1.030	95	2/11/70	0K16	0	1.030	(8)	(8)	(8)		
		L-T	1.000	95	2/11/70	0K16	0	1.000	(8)	(8)	(8)		
		L-T	0.995	75	2/11/70	0K16	0	0.995	(8)	(8)	(8)		
		L-T	1.000	0	2/11/70	0K16	0	1.000	(8)	(8)	(8)		
		7075-T7351	366210	S-L	---	0	5/29/69	0K12	0	22	---	20.0	95.0
S-L	1.000			95	5/29/69	0K12	0	1	1.000	(4)	(4)		
S-L	0.990			95	5/29/69	0K12	0	2	0.990	(4)	(4)		
S-L	1.000			95	5/29/69	0K18	0	3	1.000	(4)	(4)		
S-L	1.010			95	5/29/69	0K33	0	4	1.010	(4)	(4)		
L-T	0.990			95	2/11/70	0K16	0	5	0.990	(8)	(8)		
L-T	0.995			95	2/11/70	0K16	0	6	0.995	(8)	(8)		
L-T	0.990			0	2/11/70	0K16	0	7	0.990	(8)	(8)		
L-T	1.000			0	2/11/70	0K16	0	8	0.990	(8)	(8)		
L-T	1.000			0	2/11/70	0K16	0	9	1.000	(8)	(8)		
L-T	1.000			0	2/11/70	0K16	0	10	1.000	(8)	(8)		
L-T	1.000			0	2/11/70	0K12	0	11	1.000	(8)	(8)		
L-T	0.990			95	5/29/69	0K12	0	12	0.990	(8)	(8)		
L-T	1.000			95	5/29/69	0K12	0	13	1.000	(8)	(8)		

Notes: (1) Calculated from applied load and average crack length measured on exterior of specimens.  
 (2) Calculated from average crack lengths measured on exterior of specimens.  
 (3) Calculated from crack lengths measured on the fracture surface and the measured load.  
 (4) Reliable residual stress intensity could not be calculated because of excessive crack growth.  
 (5) Reliable residual stress intensity could not be calculated because of occurrence of branching or multiple cracks.  
 (6) Used for metallographic examinations.  
 (7) Calculation of residual  $K_I$  unreliable because of irregular shape of the crack front.  
 (8) Specimen still in test, number indicates the crack length at the time of the last measurement.  
 (9) Not valid per E399 criteria for  $K_{Ic}$ .  
 (10) Small  $S_{OC}$  at tip of precrack as in Figure 30.

TABLE D-3

ALUMINUM ALLOY BOLT LOADED COMPACT TENSION SPECIMENS EXPOSED TO SALT-DICHROMATE-ACETATE SOLUTION

Alloy & Temper.	Specimen No.	Specimen Orientation	Initial Crack Length in.	Initial KI (1) % K <sub>1c</sub>	Exposure Date	Initial Crack Growth Hours	Initial Amt. In. (2)	Exp. Frs.	Exposure Terminated		Residual K <sub>1</sub> (3)	Residual K <sub>1</sub> % K <sub>1c</sub>		
									Surface	Fracture				
2014-T651	366335	TL5	0.985	75	1/5/71	24-48	0.010	840	1.620	1.592	(4)	(4)		
		TL6	0.985	50	1/5/71	0-24	0.005	1152	1.535	1.530	65	34.8		
		TL7	0.975	50	1/5/71	48-144	0.005	1152	1.500	(6)	6.1	32.6(2)		
		TL8	0.985	25	1/5/71	144-216	0.005	1152	1.005	0.945	4.8	25.7		
		TL9	1.000	25	1/5/71	144-216	0.010	1152	1.020	0.994	5.0	26.7		
		TL10	0.980	0	1/5/71	0K1152	0	1152	0.980	---	---	---	---	
		LM3	0.975	95	1/5/71	24-48	0.005	2328	1.015	0.986	20.3	86.8		
		LM4	0.985	75	1/5/71	144-216	0.015	2328	1.030	0.974	19.5	83.3		
		LM5	0.990	75	1/5/71	144-216	0.005	2328	1.010	0.984	16.4	70.1		
		LM6	0.985	0	1/5/71	0K2328	0	2328	0.985	---	---	---	---	
		2024-T351	366400	TL3	1.100	100	12/15/70	168-504	0.06	1656	1.340	(6)	1.5	7.7(2)
				TL4	0.975	95	12/15/70	0K2184	0	2184	1.070	1.090	16.2	82.7
				TL5	0.995	95	12/15/70	1368-1536	0.01	2184	1.045	1.012	13.6	69.4
				TL6	0.995	75	12/15/70	0K2184	0	2184	0.995	0.944	10.5	53.6
				TL7	0.990	0	12/15/70	0K2184	0	2184	0.990	0.966	20.3	103.6
				LM3	0.960	95	12/15/70	0K2184	0	2184	0.960	0.968	28.7	72.3
LM4	0.995			95	12/15/70	0K2184	0	2184	0.995	0.975	28.7	72.3		
LM5	0.960			0	12/15/70	0K2184	0	2184	0.960	0.861	27.3(2)	87.8(2)		
2024-T351	366206			TL5	0.985	75	1/5/71	24-48	0.005	1152	1.500	1.505	11.6	35.0
				TL6	0.985	50	1/5/71	24-48	0.010	1152	1.375	(6)	(4)	(4)
				TL7	0.990	50	1/5/71	144-216	0.010	1152	1.340	(6)	(4)	(4)
				TL8	0.990	25	1/5/71	24-48	0.005	1152	0.995	0.995	5.8	29.9(2)
				TL9	0.990	25	1/5/71	840-984	0.005	1152	0.995	1.008	3.3	15.7
				TL10	1.000	0	1/5/71	0K1152	0	1152	1.000	---	---	---
				LM3	0.990	95	1/5/71	72-144	0.01	2328	1.020	1.050	23.6	79.7
				LM4	0.990	95	1/5/71	480-720	0.055	2328	1.030	0.998	24.0	81.1
		LM5	0.990	75	1/5/71	48-144	0.005	2328	1.000	0.998	19.8	66.9		
		LM6	0.990	0	1/5/71	0K2328	0.00	2328	0.990	---	---	---		
		2024-T351	366207	TL3	0.965	100	12/15/70	168-504	0.005	1656	1.485	(6)	17.7	106.0(2)
				TL4	0.995	95	12/15/70	696-864	0.005	2184	1.160	1.134	15.7	54.0
				TL5	0.995	95	12/15/70	864-1032	0.045	2184	1.115	1.056	16.2	57.0
				TL6	0.990	75	12/15/70	1032-1175	0.030	2184	1.055	1.026	6.5	38.9
				TL7	0.990	0	12/15/70	0K2184	0	2184	0.990	0.990	16.0	55.8
				LM3	0.995	95	12/15/70	168-504	0.005	2184	1.000	1.048	20.6	88.4
LM4	0.995			95	12/15/70	168-504	0.005	2184	1.005	1.092	17.6	75.3		
LM5	0.990			0	12/15/70	0K2184	0	2184	0.990	0.962	22.7	97.4		
2019-T37	344793			TL5	0.750	75	1/6/71	0-24	0.005	1152	1.185	1.345	(4)	(4)
				TL6	0.755	50	1/6/71	24-48	0.005	1152	1.215	(6)	(4)	(4)
				TL7	0.745	50	1/6/71	24-48	0.050	1152	1.060	1.056	4.8	17.7(2)
				TL8	0.765	25	1/6/71	48-120	0.005	1152	0.910	0.978	5.8	21.4
				TL9	0.780	25	1/6/71	120-144	0.010	1152	0.830	0.894	5.4	19.9
				TL10	0.740	0	1/6/71	0K1152	0	1152	0.740	0.802	25.5(2)	94.1(2)
				LM3	0.735	95	1/6/71	48-120	0.015	528	0.860	---	---	---
				LM4	0.750	95	1/6/71	24-48	0.005	528	0.890	(6)	21.8	75.7(2)
		LM5	0.750	75	1/6/71	24-120	0.040	528	0.895	0.802	15.7	54.5		
		LM6	0.730	0	1/6/71	0K528	0	528	0.730	0.777	27.4(2)	95.1(2)		

Table D-3 (Continued)

Alloy & Temper	Specimen No.	Specimen Orientation	Initial Crack Length In.	Initial KI(1) 1/2 K <sub>IC</sub>	Exp. Date	Initial Crack Growth		Exp. Hrs.	Exposure Terminated Surface Fracture	Residual Stress, Psi		
						Hours	Amt. In. (2)			Initial	Final	
2210-m97	358148	S-I	0.750	100	12/15/70	0-168	0.005	1656	1.140	10.5	53.4(2)	
		S-I	0.750	95	12/15/70	168-504	0.015	2184	0.796	15.7	70.9	
		S-I	0.770	95	12/15/70	0-168	0.005	2184	0.900	17.2	87.5	
		S-I	0.750	75	12/15/70	168-504	0.010	2184	0.760	13.3	67.7	
		S-I	0.770	0	12/15/70	0K2184	0.005	2184	0.768	19.8	107.8	
		I-T	0.985	95	12/15/70	0-168	0.005	2184	0.998	21.4	82.8	
		I-T	0.985	95	12/15/70	168-504	0.005	2184	1.010	21.3	82.4	
		I-T	0.985	0	12/15/70	0K2184	0	2184	0.955	25.8	99.0	
		S-I	0.955	100	12/15/70	504-696	0.005	2184	1.242	30.7	138.5	
		S-I	0.980	95	12/15/70	0K2184	0	2184	0.962	18.7	85.8	
		S-I	0.970	95	12/15/70	0K2184	0	2184	0.915	18.6	85.3	
		S-I	0.975	75	12/15/70	0K2184	0	2184	0.938	15.9	72.9	
		S-I	0.950	0	12/15/70	0K2184	0	2184	0.882	21.7(R)	99.5(R)	
		I-T	1.020	95	12/15/70	0K2184	0	2184	1.042	17.2	73.2	
		I-T	0.975	95	12/15/70	0K2184	0	2184	0.970	18.7	79.6	
I-T	0.975	0	12/15/70	0K2184	0	2184	1.003	26.4(P)	112.3(R)			
456 Sensitized	366657	S-I	0.970	75	1/6/71	0-24	0.825	216	1.015	(4)	(4)	
		S-I	0.995	50	1/6/71	0-24	0.555	216	1.865	(4)	(4)	
		S-I	0.975	50	1/6/71	0-24	0.610	456	1.940	(4)	(4)	
		S-I	0.965	25	1/6/71	0-24	0.04	456	1.750	(4)	(4)	
		S-I	0.950	25	1/6/71	0-24	0.165	456	1.740	(4)	(4)	
		S-I	0.985	0	1/6/71	0K456	0	1008	0.985	0.988	15.5	71.8(7)
		I-T	0.980	95	1/6/71	456-824	0.01	1008	0.900	(6)	15.4	71.7(7)
		I-T	0.965	95	1/6/71	0K1008	0	1008	0.965	1.010	12.4	57.4(7)
		I-T	0.990	75	1/6/71	0K1008	0	1008	0.990	1.010	12.4	57.4(7)
		I-T	0.980	0	1/6/71	0K1008	0	1008	0.980	1.011	24.5(R)	113.4(R)
		S-I	0.985	100	12/15/70	0K2184	0	2184	0.985	1.280	25.5	137.0
		S-I	0.995	95	12/15/70	0K2184	0	2184	0.995	0.998	19.2	90.0
		S-I	0.980	95	12/15/70	0K2184	0	2184	0.980	0.998	19.0	91.4
		S-I	0.985	75	12/15/70	1032-1176	0.005	2184	0.940	0.940	16.0	74.6
		S-I	1.015	0	12/15/70	0K2184	0.010	2184	1.015	0.972	20.4	95.7
I-T	0.975	95	12/15/70	1176-1368	0	2184	0.985	0.985	26.8	79.6		
I-T	0.985	95	12/15/70	0K2184	0	2184	0.956	0.956	27.6	82.0		
I-T	0.980	0	12/15/70	0K2184	0	2184	0.980	0.868	27.3(R)	81.1 (R)		
039-m651	314758	S-I	0.985	75	1/6/71	0-24	0.020	1128	1.615	(4)	(4)	
		S-I	0.980	50	1/6/71	24-43	0.005	1128	1.690	6.9	33.8	
		S-I	1.000	50	1/6/71	24-120	0.045	1128	1.605	5.9	28.9(2)	
		S-I	0.985	25	1/6/71	168-312	0.005	10,560	1.275	1.445	27.0	
		S-I	0.970	25	1/6/71	0-24	0.005	10,560	1.145	1.194	24.0	
		S-I	0.980	0	1/6/71	0K10,560	0	2304	0.980	0.878	21.7	79.8
		I-T	1.000	95	1/6/71	48-120	0.015	2304	1.015	1.044	22.8	83.8
		I-T	0.985	95	1/6/71	0K2304	0	2304	0.985	0.995	17.2	63.2
		I-T	1.000	75	1/6/71	0K2304	0	2304	1.000	1.048	17.2	63.2
		I-T	0.980	0	1/6/71	0K2304	0	2304	0.959	0.959	26.7	96.2

Table D-3 (Continued)

Alloy & Temper	Specimen No.	Specimen Orientation	Initial Crack Length In.	Initial KI(1) % K <sub>IC</sub>	Exp. Date	Initial Crack Growth		Exp. Hrs.	Exposure Terminated		Residual KI(3) % K <sub>IC</sub>			
						Hours	Amt. In.(2)		Surface	Crack Length Fracture				
7079-T651	366259	TL5 S-L	0.980	75	1/6/71	0-24	0.13	216	1.730	1.784	(4) 44.4			
		TL6 S-L	0.980	50	1/6/71	24-48	0.035	1128	1.485	1.556	8.5			
		TL7 S-L	0.985	50	1/6/71	24-48	0.025	1128	(6) 1.085	1.405	7.8			
		TL8 S-L	0.975	25	1/6/71	48-120	0.010	1128	1.080	1.372	4.1			
		TL9 S-L	0.985	25	1/6/71	624-816	0.005	1128	0.990	1.058	27.2			
		TL10 S-L	0.990	0	OK1128	0-120	0.01	2304	0.985	1.062	21.4			
		LM3 L-T	0.990	95	OK2304	0	0	2304	0.985	1.055	79.2			
		LM4 L-T	0.985	95	OK2304	0	0	2304	0.980	1.062	58.7			
		LM5 L-T	0.980	75	OK2304	0	0	2304	0.970	---	---			
		LM6 L-T	0.970	0	OK2304	0	0	2304	0.970	---	---			
		7075-T451	366209	TL5 S-L	1.005	75	1/6/71	24-48	0.025	1128	1.660	1.80	(4) 44.4	
				TL6 S-L	0.980	50	1/6/71	0-24	0.010	1128	1.390	1.47	7.4	
				TL7 S-L	0.975	50	1/6/71	0-24	0.005	1128	1.560	(6) 3.8	37.0	
				TL8 S-L	0.970	25	1/6/71	24-120	0.010	1128	0.990	0.976	28.6(2)	
				TL9 S-L	0.975	25	1/6/71	24-120	0.005	1128	1.300	1.386	9.4	
				TL10 S-L	0.985	0	OK1128	0	0	1008	0.995	---	27.1	
LM3 L-T	0.975			95	OK1008	0-24	0.010	1008	0.995	(6) 22.2	79.9(7)			
LM4 L-T	0.995			95	OK1008	24-120	0	1008	0.995	17.2	73.4(7,2)			
LM5 L-T	0.985			75	OK1008	0	0	1008	0.985	---	61.9(7)			
LM6 L-T	0.985			0	OK1008	0	0	1008	0.985	---	---			
7075-T7351	366210			TL3 S-L	0.975	95-100	12/15/70	0-168	0.005	2304	0.995	1.132	22.0	
				TL4 S-L	0.995	95	12/15/70	1176-1368	0.005	2304	1.015	0.996	86.5	
				TL5 S-L	1.020	95	12/15/70	OK2304	0	2304	1.020	1.012	79.8	
				TL6 Specimen Lost										
				TL7 S-L	0.985	0	OK2304	0	0	2304	0.985	0.955	20.1	
				LM3 L-T	0.990	95	864-1032	0.010	2304	1.000	0.978	25.2		
		LM4 L-T	0.995	95	1032-1176	0.025	2304	1.030	1.010	67.6				
		LM5 L-T	0.980	0	OK2304	0	0	2304	0.980	0.953	91.1			

- Notes:
- (1) Calculated from applied load and average crack length measured on exterior of specimens; 95-100 denotes pop-in load.
  - (2) Calculated from average crack lengths measured on exterior of specimens.
  - (3) Calculated from crack lengths measured on the fracture surface and the measured load.
  - (4) Reliable residual stress intensity could not be calculated because of excessive crack growth.
  - (5) Reliable residual stress intensity could not be calculated because of occurrence of branching or multiple cracks.
  - (6) Used for metallographic examinations.
  - (7) Removed from test because of severe surface exfoliation.
  - (8) Not valid per E399 criteria for K<sub>IC</sub>.

Table D-4

STRESS INTENSITY DETERMINATION FOR S-L BOEING DCB SPECIMENS  
EXPOSED TO SEACOAST ATMOSPHERE

Alloy	Specimen Number	E psi ( $\times 10^6$ )	H, In.	Elastic V(2)	Initial Crack Length So, In.	$K_{I1}$ -ksi $\sqrt{\text{in.}}$	8 Months Crack Length, In.	$K_{I1}$ ksi $\sqrt{\text{in.}}$
2014-T651	366335-TL3B -TL4B	10.5	0.5	0.016	0.750	20.5	1.74	5.9
2021-T81	326400-TL3B -TL4B	10.5	0.5010	0.021	0.740	27.4	1.06	16.7
2024-T351	366206-TL3B -TL4B	10.5	0.5015	0.0258	0.750	33.1	1.750	9.5
2024-T851	366207-TL3B -TL4B	10.5	0.5005	0.0158	0.805	18.4	0.925	15.3
2219-T37(1)	344793-TL3B -TL4B	10.5	0.5 Est.	0.0363	0.690	51.6	2.53	7.1
2219-T87	338148-TL3B -TL4B	10.5	0.5	0.0238	0.755	30.2	0.965	21.6
5456-Sens.	366657-TL3B -TL4B	10.3	0.5005	0.0285	0.725	37.4	2.485	5.7
5456-H117	366656-TL3B -TL4B	10.3	0.5005	0.0295	0.740	37.7	0.740	37.7
6061-T651	366208-TL3B -TL4B	10.0	0.5	0.037	0.725	47.1	0.725	47.1
7039-T6351	314758-TL3B -TL4B	10.3	0.5010	0.024	0.740	30.7	2.38	5.1
7075-T651	366209-TL3B -TL4B	10.3	0.5005	0.015	0.735	19.3	2.095	4.0
7075-T7351	366210-TL3B -TL4B	10.3	0.5005	0.0195	0.730	25.3	0.78	23.3
7079-T651	366259-TL3B -TL4B	10.3	0.5005	0.0155	0.680	22.0	2.37	3.3

Notes: (1) Exfoliation noted on sides of specimen.

(2) V(elastic) were taken from Table 21 and were used for all calculations of K for this Table.

Table D-5

STRESS INTENSITY DETERMINATION FOR S-L BOEING DCB SPECIMENS  
EXPOSED TO INDUSTRIAL ATMOSPHERE

Alloy	Specimen Number	E psi ( $\times 10^6$ )	H, In.	Elastic V(l)	Initial Crack Length $s_0$ , In.	$K_{Ii}$ -ksi $\sqrt{\text{in.}}$	13 Months	
							Crack Length, In.	$K_{Ir}$ ksi $\sqrt{\text{in.}}$
2014-T651	366335-TL6B	10.5	0.495	0.016	0.700	22.2	1.250	9.9
2021-T81	326400-TL6B	10.5	0.50	0.021	0.715	28.5	0.840	23.1
2024-T351	366206-TL6B	10.5	0.5005	0.0258	0.725	34.5	1.350	14.3
2024-T851	366207-TL6B	10.5	0.501	0.0158	0.695	22.3	0.730	20.9
2219-T37	344793-TL6B	10.5	0.50	0.363	0.705	50.2	1.765	13.1
2219-T87	338148-TL6B	10.5	0.5005	0.0238	0.735	31.3	0.785	28.7
5456-Sens.	366657-TL6B	10.3	0.50	0.0285	0.720	37.7	1.160	19.5
5456-H117	366656-TL6B	10.3	0.501	0.0295	0.705	40.1	0.705	40.1
6061-T651	366208-TL6B	10.0	0.5005	0.037	0.705	48.8	0.705	48.8
7039-T6351	334758-TL6B	10.3	0.5005	0.024	0.725	31.5	2.110	6.3
7075-T651	366209-TL6B	10.3	0.5	0.015	0.690	20.9	1.35	8.1
7075-T7351	366210-TL6B	10.3	0.5005	0.0195	0.735	25.1	0.765	23.9
7079-T651	366259-TL6B	10.3	0.5005	0.0155	0.695	21.4	1.875	5.0

Note: (1) V(elastic) were taken from Table 21 and were used for all calculations of K for this Table.

Table D-6

## STRESS INTENSITY DETERMINATIONS FOR S-L FROING PCB SPECIMENS USED IN ACCELERATED SCC TESTS

Alloy	Specimen Number	Corrosion (1)	E psi (x10 <sup>6</sup> )	H, In.	V(Elastic) In. (2)	Initial Crack Length a <sub>i</sub> , In.	K <sub>I1</sub> ksi √in.	Exposure Time Hours	Crack Length, a <sub>c</sub> , In.		K <sub>Ic</sub> , ksi √in.	
									Surface	Fracture	Surface	Fracture
2014-T651	366335-TL5B	3.5% NaCl SDA	10.5	0.5	0.016	0.70	22.3	2184	1.605	1.63	6.7	6.6
2014-T651	-TL1B	SDA	10.5	0.5	0.016	0.71	22.9	4080	2.045	---	4.5	---
2014-T651	-TL2B	SDA	10.5	0.5	0.016	0.695	22.5	1392	1.605	1.695	6.7	6.2
2021-T81	326400-TL5B	3.5% NaCl SDA	10.5	0.5001	0.021	0.765	26.2	2208	1.125	1.385	15.3	11.2
2021-T81	-TL1B	SDA	10.5	0.5	0.021	0.735	27.6	4056	1.16	---	14.6	---
2021-T81	-TL2B	SDA	10.5	0.5	0.021	0.70	29.3	2352	1.045	1.120	17.0	15.2
2024-T351	366206-TL5B	3.5% NaCl SDA	10.5	0.5007	0.0258	0.685	37.1	2184	1.73	1.72	8.1	9.7
2024-T351	-TL1B	SDA	10.5	0.5005	0.0238	0.705	35.7	1576	1.795	---	9.1	---
2024-T351	-TL2B	SDA	10.5	0.5005	0.0258	0.630	37.4	1848	1.795	2.005	9.1	7.5
2024-T851	366207-TL5B	3.5% NaCl SDA	10.5	0.5008	0.0158	0.735	20.0	2208	0.87	1.031	16.0	13.1
2024-T851	-TL1B	SDA	10.5	0.5005	0.0158	0.76	19.9	4056	1.18	---	10.7	---
2024-T851	-TL2B	SDA	10.5	0.5005	0.0158	0.72	21.3	2352	1.07	1.104	12.4	11.4
2219-T37	344793-TL5B	3.5% NaCl SDA	10.5	0.5002	0.0363	0.77	44.9	2184	2.595	---	6.8	---
2219-T37	-TL1B	SDA	10.5	0.5005	0.0363	0.685	52.1	1800	1.99	---	10.7	---
2219-T37	-TL2B	SDA	10.5	0.5005	0.0363	0.675	53.1	1800	1.895	2.08	11.7	10.0
2219-T87	338148-TL5B	3.5% NaCl SDA	10.5	0.5	0.0238	0.70	33.2	2208	0.92	1.255	23.1	14.7
2219-T87	-TL1B	SDA	10.5	0.5005	0.0238	0.725	31.8	4056	1.085	---	18.3	---
2219-T87	-TL2B	SDA	10.5	0.5005	0.0238	0.745	30.7	2352	1.05	1.076	19.2	18.5
5456-Sens.	366657-TL5B	3.5% NaCl SDA	10.3	0.5005	0.0285	0.695	39.4	7560	2.260	2.405	6.0	5.4
5456-Sens.	-TL1B	SDA	10.3	0.5010	0.0285	0.650	42.9	1536	3.725	---	---	---
5456-Sens.	-TL2B	SDA	10.3	0.5005	0.0285	0.660	42.0	1848	3.71	3.91	2.8	2.5
5456-TL17	366656-TL5B	3.5% NaCl SDA	10.3	0.5015	0.0295	0.73	38.4	2184	0.745	0.963	37.4	36.5
5456-TL17	-TL1B	SDA	10.3	0.5010	0.0295	0.665	43.2	4056	0.69	---	41.2	---
5456-TL17	-TL2B	SDA	10.3	0.5015	0.0295	0.655	44.0	2352	0.695	0.888	40.3	39.6
6061-T651	366208-TL5B	3.5% NaCl SDA	10.0	0.5013	0.037	0.76	44.4	2184	0.77	1.046	43.6	28.0
6061-T651	-TL1B	SDA	10.0	0.5005	0.037	0.675	51.5	4080	0.665	---	50.6	---
6061-T651	-TL2B	SDA	10.0	0.490	0.037	0.70	48.4	1800	0.705	0.955	8.7	31.4
7075-T651	314758-TL5B	3.5% NaCl SDA	10.3	0.5008	0.024	0.725	31.5	2184	2.405	2.645	5.0	4.3
7075-T651	-TL1B	SDA	10.3	0.5	0.024	0.660	34.1	4080	1.820	---	8.1	---
7075-T651	-TL2B	SDA	10.3	0.5005	0.024	0.695	33.2	1536	1.735	1.735	8.7	3.7
7075-T651	366209-TL5B	3.5% NaCl SDA	10.3	0.5003	0.015	0.665	21.9	2184	1.650	1.775	5.7	5.1
7075-T651	-TL1B	SDA	10.3	0.5005	0.015	0.68	21.3	1576	1.60	---	6.2	---
7075-T651	-TL2B	SDA	10.3	0.5005	0.015	0.72	19.8	1848	1.815	2.003	5.1	4.3
7075-T7351	366210-TL5B	3.5% NaCl SDA	10.3	0.5011	0.0195	0.73	25.4	2184	0.75	1.095	24.5	14.5
7075-T7351	-TL1B	SDA	10.3	0.5010	0.0195	0.725	25.6	4032	0.74	---	24.9	---
7075-T7351	-TL2B	SDA	10.3	0.5010	0.0195	0.71	26.3	1800	0.715	0.873	26.0	20.0
7079-T651	366259-TL5B	3.5% NaCl SDA	10.3	0.5005	0.0155	0.705	21.1	7560	2.52	2.655	3.0	2.7
7079-T651	-TL1B	SDA	10.3	0.5005	0.0155	0.635	24.0	4032	1.310	---	8.8	---
7079-T651	-TL2B	SDA	10.3	0.5	0.0155	0.695	21.4	1800	1.395	1.47	8.0	7.4

Notes: (1) Corrosion

3.5% NaCl - Added dropwise three times per day.

SDA - Total immersion in salt-dichromate-acetate solution at pH 4.0.

(2)  $\nu$ (elastic) were taken from Table 21 and were used for all calculations of K for this Table.

Table D-7  
STEEL ALLOY, BOLT LOADED COMPACT TENSION SPECIMENS EXPOSED TO SEACOAST ATMOSPHERE

Alloy	Temper	Specimen No.	Specimen Orientation	Initial Crack Length, In.	Initial K <sub>I</sub> (1) #K <sub>I</sub> C	Exposure Date	Initial Crack Growth		Exposure Month	Exposure Terminated		Final K <sub>I</sub> (2) #K <sub>I</sub> C
							Months	Amt. In. (2)		Surface (2)	Crack Length Fracture	
17-7 PF	RH1050	366665-T013	T-L	0.98	95	5/3/70	(8)	0.81	---	---	---	---
		366665-T014	T-L	0.98	95	5/3/70	(9)	0.84	---	---	---	---
		366665-T015	T-L	0.99	75	5/3/70	(9)	0.63	1.3	1.77	(10)	(10)
		366665-T016	T-L	0.99	50	5/3/70	0-1.3	0.83	1.4	1.82	(6)	(6)
		366665-T025	T-L	0.96	35	4/2/71	2.4-4.7	0.57	2.4	1.53	1.576	30
PH15-7MO	RH950	366666-T013	T-L	1.02	25	4/2/71	2.4-4.7	0.50	29.0	1.32	(7)	---
		366666-T012	T-L	0.98	0	5/3/70	OK 29	---	24.0	0.98	(7)	---
		366666-T013	T-L	0.99	95	5/3/70	0-1.3	0.46	1.3	1.45	1.914	(4)
		366666-T014	T-L	0.98	95	5/3/70	0-1.3	0.88	1.3	1.90	(10)	(10)
		366666-T015	T-L	0.99	75	5/3/70	0-1.3	0.83	1.3	1.84	(10)	(10)
PH15-7MO	RH1050	366666-T016	T-L	0.98	50	5/3/70	2.4-4.7	0.25	11.0	1.77	(10)	(10)
		366666-T012	T-L	0.98	0	5/3/70	OK 29	---	29.0	0.98	(7)	---
		366666-T034	T-L	0.98	95	5/3/70	0-1.3	0.59	1.3	1.57	1.902	(4)
		366666-T035	T-L	0.99	95	5/3/70	0-1.3	0.42	1.3	1.41	(10)	(10)
		366666-T036	T-L	0.99	75	5/3/70	0-1.3	0.91	1.3	1.92	(10)	(10)
15-5 PH	H900	366667-T037	T-L	0.99	50	5/3/70	1.3-4.7	0.76	4.7	1.77	(10)	(10)
		366667-T033	T-L	0.99	0	5/3/70	OK 29	---	29.0	0.99	(7)	---
		366668-T013	T-L	0.99	95	5/3/70	OK 29	---	29.0	0.99	(7)	---
		366668-T014	T-L	0.98	75	5/3/70	13.7-16.7	0.25	29.0	1.55	(7)	---
		366668-T015	T-L	0.98	75	5/3/70	23.6-26.2	0.35	29.0	1.32	(7)	---
15-5 PH	H150M	366667-T016	T-L	0.98	50	5/3/70	13.7-16.7	0.31	29.0	1.36	(7)	---
		366667-T012	T-L	0.98	0	5/3/70	OK 29	---	29.0	0.98	(7)	---
		366667-T013	T-L	0.98	95	5/3/70	OK 29	---	29.0	0.98	(7)	---
		366667-T014	T-L	0.99	95	5/3/70	OK 29	---	29.0	0.99	(7)	---
		366667-T015	T-L	1.00	50	5/3/70	OK 29	---	29.0	1.00	(7)	---
PH13-8MO	H950	366669-T016	T-L	0.98	50	5/3/70	OK 29	---	29.0	0.98	(7)	---
		366669-T013	L-T	0.99	95	5/3/70	2.4-4.7	0.82	4.7	1.81	1.538	69
		366669-T014	L-T	0.98	95	5/3/70	2.4-4.7	0.87	4.7	1.85	(10)	(10)
		366669-T015	L-T	1.00	75	5/3/70	13.7-16.7	0.73	16.7	1.73	(10)	(10)
		366669-T012	L-T	1.00	50	5/3/70	13.7-16.7	0.66	16.7	1.68	(10)	(10)
PH13-8MO	H950	366669-T013	L-T	0.98	95	5/3/70	OK 29	---	29.0	0.98	(7)	---
		366669-T014	T-L	0.98	95	5/3/70	2.4-4.7	0.75	4.7	1.73	1.822	(4)
		366669-T015	T-L	1.00	75	5/3/70	OK 29	0.79	4.7	1.78	(10)	(10)
		366669-T016	T-L	1.00	50	5/3/70	OK 29	0.68	29.0	1.00	(7)	(7)
		366669-T012	T-L	0.99	0	5/3/70	OK 29	---	29.0	0.99	(7)	(10)

-Continued-

Table I-7  
(Continued)

Alloy	Temper	Specimen No.	Specimen Orientation	Initial Crack Length, in.	K <sub>IC</sub> (1) K <sub>IC</sub> (2)	Exposure Date	Initial Crack Growth		Exposure Months	Exposure Terminated		Final K <sub>IC</sub>	
							Months	Amt. in. (2)		Surface(2)	Crack Length Fracture	psi	sqrt. K <sub>IC</sub>
PH13-8Mo	H950	366669-NCL3 -NCL4 -NCL5 -NCL6 -NCL2	S-L	0.74	95	5/3/70	OK 29	---	29.0	0.74	(7)	---	---
			S-L	0.75	95	5/3/70	OK 29	---	29.0	0.75	(7)	---	---
			S-L	0.75	75	5/3/70	OK 29	---	29.0	0.75	(7)	---	---
			S-L	0.74	50	5/3/70	OK 29	---	29.0	0.74	(7)	---	---
PH13-8Mo	H1050	366669-TC34 -TC35 -TC36 -TC37 -TC33	T-L	0.99	95	5/3/70	2.4-4.7	0.61	4.7	1.60	(10)	(10)	(10)
			T-L	1.00	95	5/3/70	2.4-4.7	0.90	4.7	1.90	(10)	(6)	(6)
			T-L	1.00	75	5/3/70	13.7-16.7	0.81	16.7	1.81	(10)	(16)	(10)
			T-L	1.00	50	5/3/70	OK 29	---	29.0	1.00	(7)	---	---
431	H1125	366670-TC34 -TC35 -TC36 -TC37 -TC33	T-L	1.00	95	5/3/70	4.7-6.3	0.34	11.0	1.70	1.716	(4)	(4)
			T-L	1.00	75	5/3/70	13.7-16.7	0.37	18.7	1.48	(10)	(10)	(10)
			T-L	1.00	75	5/3/70	6.3-11.0	0.68	29.0	1.08	(7)	---	---
			T-L	1.00	50	5/3/70	6.3-11.0	0.19	29.0	1.20	(7)	---	---
431	H1200	366670-LCL3 -LCL4 -LCL5 -LCL6 -LCL2	L-T	1.00	95	5/3/70	2.4-4.7	0.46	4.7	1.95	1.888	(4)	(4)
			L-T	0.98	75	5/3/70	1.3-2.4	0.46	4.7	1.95	(10)	(10)	(10)
			L-T	1.00	75	5/3/70	1.3-2.4	0.57	4.7	1.86	(10)	(10)	(10)
			L-T	1.00	50	5/3/70	2.4-4.7	0.21	1.0	1.90	(10)	(10)	(10)
431	H1200	366670-TC13 -TC14 -TC15 -TC16 -TC12	T-L	1.00	95	5/3/70	1.3-2.4	0.46	4.7	1.88	(10)	(10)	(10)
			T-L	1.00	75	5/3/70	1.3-2.4	0.68	4.7	1.81	(10)	(6)	(6)
			T-L	1.00	75	5/3/70	1.3-2.4	0.50	4.7	1.77	(4)	(4)	(4)
			T-L	0.98	50	5/3/70	2.4-4.7	0.28	11.0	1.66	1.750	(10)	(10)
431	H1200	366670-NC13 -NC14 -NC15 -NC16 -NC12	S-L	0.75	95	5/3/70	2.4-4.7	0.33	4.7	1.08	1.180	90.1	(11)
			S-L	0.75	75	5/3/70	2.4-4.7	0.04	11.0	1.09	(10)	(10)	(10)
			S-L	0.75	75	5/3/70	1.3-2.4	0.08	13.7	1.32	(10)	(10)	(10)
			S-L	0.75	50	5/3/70	6.3-11.0	0.25	29.0	1.06	(7)	---	---
AN355	SOT850	366671-TC13 -TC14 -TC15 -TC16 -TC12	T-L	1.00	95	5/3/70	1.3-2.4	0.51	4.7	1.80	1.754	(4)	(4)
			T-L	1.00	75	5/3/70	1.3-2.4	0.26	4.7	1.75	(10)	(10)	(10)
			T-L	1.00	75	5/3/70	1.3-2.4	0.46	4.7	1.82	(10)	(10)	(10)
			T-L	1.00	50	5/3/70	2.4-4.7	0.60	6.3	1.59	(10)	(10)	(10)

-Continued-

C4

Table D-7  
(Continued)

Alloy	Temper	Specimen No.	Specimen Orientation	Initial Crack Length, In.	Initial $K_I$ (1) % $K_{Ic}$	Exposure Date	Initial Crack Growth		Exposure Months	Exposure Months	Exposure Terminated		Final $K_I$ (1) % $K_{Ic}$
							Months	Amt. In. (2)			Surface (2)	Crack Length Fracture	
AM355	SCT1000	366671-TC34	T-L	1.00	95	5/3/70	13.7-16.7	0.13	29.0	1.60	(7)	---	---
		-TC35	T-L	0.98	95	5/3/70	6.3-11.0	0.67	11.0	1.69	1.602	(4)	(4)
		-TC36	T-L	0.99	75	5/3/70	13.7-16.7	0.48	16.7	1.49	(10)	(10)	(10)
		-TC37	T-L	0.98	50	5/3/70	16.7-18.7	0.29	23.0	1.64	(10)	(10)	(10)
AM355	SCT850	366673-LC13	T-L	0.98	0	5/3/70	OK 29	----	29.0	0.98	(7)	---	---
		-LC14	L-T	0.99	95	5/3/70	0-1.3	0.73	1.3	1.72	1.800	(4)	(4)
		-LC15	L-T	1.00	75	5/3/70	0-1.3	0.67	1.3	1.67	(5)	(5)	(5)
		-LC16	L-T	0.99	75	5/3/70	1.3-2.4	0.79	2.4	1.81	(8)	(8)	(8)
AM355	SCT850	366673-TC13	T-L	1.00	50	5/3/70	1.3-2.4	0.52	29.0	1.69	(5)	---	---
		-TC14	L-T	1.00	0	5/3/70	6.3-11.0	0.09	29.0	1.00	(7)	---	---
		-TC15	T-L	1.00	95	5/3/70	1.3-2.4	0.71	2.4	1.71	1.662	(4)	(4)
		-TC16	T-L	1.00	75	5/3/70	0-1.3	0.68	1.3	1.68	(5)	(5)	(5)
AM355	SCT850	366673-NC13	S-L	0.75	95	5/3/70	1.3-2.4	0.51	2.4	1.26	1.234	(4)	(4)
		-NC14	S-L	0.72	75	5/3/70	1.3-2.4	0.34	4.7	1.27	(5)	(5)	(5)
		-NC15	S-L	0.75	75	5/3/70	2.4-4.7	0.04	11.0	1.18	(5)	(5)	(5)
		-NC16	S-L	0.75	50	5/3/70	1.3-2.4	0.15	11.0	1.08	(5)	(5)	(5)
AM355	SCT1000	366673-TC34	T-L	1.00	95	5/3/70	2.4-4.7	0.92	4.7	1.92	1.830	(4)	(4)
		-TC35	T-L	1.00	95	5/3/70	1.3-2.4	0.18	4.7	1.99	(10)	(10)	(10)
		-TC36	T-L	1.00	75	5/3/70	13.7-16.7	0.48	16.7	1.48	(10)	(10)	(10)
		-TC37	T-L	1.00	50	5/3/70	1.3-2.4	0.09	4.7	1.64	(10)	(10)	(10)
AM355	SCT850	366673-TC34	T-L	1.00	0	5/3/70	OK 29	----	29.0	1.00	(7)	---	---

- Notes:
- {1} Calculated from applied load and average crack length measured on exterior of specimens.
  - {2} Calculated from average crack lengths measured on exterior of specimens.
  - {3} Calculated from crack lengths measured on fractured surface and time measured load.
  - {4} Reliable residual stress intensity could not be calculated because of excessive crack growth.
  - {5} Reliable residual stress intensity could not be calculated because of occurrence of excessive branching or multiple cracks.
  - {6} Used for metallographic examination.
  - {7} Specimen still in test, number indicates the crack length at the time of last measurement.
  - {8} Measurement taken 4 days after stressing - not exposed.
  - {9} Measurement taken 4 days after stressing - exposed.
  - {10} Specimen not submitted for residual measurements because crack growth judged excessive.
  - {11} Not determined because original  $K_I$  was not valid.
  - {12} Value not valid because it did not meet crack curvature validity check (Figure 81).

Table D-8

STEEL ALLOY, POINT LOADED COMPACT TENSION SPECIMENS EXPOSED TO INDUSTRIAL ATMOSPHERE

Alloy	Temper.	Specimen No.	Specimen Orientation	Initial Crack Length, In.	Initial $K_I$ (1) $\sqrt{K_{Ic}}$	Exposure Date	Initial Crack Growth		Exposure Months	Exposure Terminated		Final $K_I$ (1) $\sqrt{K_{Ic}}$	
							Months	Amt. In. (2)		Surface (2)	Fracture		
17-7 PH	RH1050	366665-TC18	T-L	0.99	95	4/13/70	0-0.1	0.89	0.1	1.88	(4)	(4)	
		-TC19	T-L	0.98	95	4/13/70	0-0.1	0.89	0.1	1.87	(4)	(4)	
		-TC20	T-L	0.99	75	4/13/70	0-0.1	0.79	0.1	1.78	(4)	(4)	
		-TC21	T-L	0.92	50	2/19/71	OK 29	---	29.0	0.99	---	---	(4)
		-TC17	T-L	0.99	0	4/13/70	OK 29	---	29.0	0.99	---	---	(4)
PH15-7Mo	RH950	366666-TC18	T-L	0.98	95	4/13/70	0-0.1	0.83	0.1	1.81	(4)	(4)	
		-TC19	T-L	0.99	75	4/13/70	OK 29	---	29.0	0.98	---	---	---
		-TC20	T-L	0.98	50	4/13/70	OK 29	---	29.0	0.98	---	---	---
		-TC21	T-L	0.99	0	4/13/70	OK 29	---	29.0	0.99	---	---	---
		-TC17	T-L	0.98	0	4/13/70	OK 29	---	29.0	0.98	---	---	---
PH15-7Mo	RH1050	366666-TC39	T-L	0.99	95	4/13/70	6.0-9.0	0.07	29.0	1.24	(7)	(4)	
		-TC40	T-L	0.99	95	4/13/70	0-0.2	0.74	0.3	1.73	(4)	(4)	
		-TC41	T-L	0.99	75	4/13/70	OK 29	---	29.0	0.99	---	---	---
		-TC42	T-L	0.98	50	4/13/70	OK 29	---	29.0	0.98	---	---	---
		-TC38	T-L	1.00	0	4/13/70	OK 29	---	29.0	1.00	---	---	---
15-5 PH	H900	366668-TC18	T-L	0.98	95	4/13/70	OK 29	---	29.0	0.98	(7)	---	
		-TC19	T-L	0.99	75	4/13/70	OK 29	---	29.0	0.99	(7)	---	
		-TC20	T-L	0.98	50	4/13/70	OK 29	---	29.0	0.98	(7)	---	
		-TC21	T-L	0.95	0	4/13/70	OK 29	---	29.0	0.99	(7)	---	
		-TC17	T-L	0.98	0	4/13/70	OK 29	---	29.0	0.98	(7)	---	
15-5 PH	H1150M	366667-TC18	T-L	0.97	95	4/13/70	3.0-6.0	0.08	29.0	1.05	(7)	---	
		-TC19	T-L	0.97	95	4/13/70	OK 29	---	29.0	0.97	(7)	---	
		-TC20	T-L	0.97	75	4/13/70	OK 29	---	29.0	0.97	(7)	---	
		-TC21	T-L	0.97	50	4/13/70	OK 29	---	29.0	0.97	(7)	---	
		-TC17	T-L	0.97	0	4/13/70	OK 29	---	29.0	0.97	(7)	---	
PH13-8Mo	H950	366669-LC18	L-T	0.98	95	4/13/70	OK 29	---	29.0	0.98	(7)	---	
		-LC19	L-T	0.99	95	4/13/70	OK 29	---	29.0	0.99	(7)	---	
		-LC20	L-T	0.99	75	4/13/70	OK 29	---	29.0	0.99	(7)	---	
		-LC21	L-T	0.98	50	4/13/70	OK 29	---	29.0	0.98	(7)	---	
		-LC17	L-T	0.97	0	4/13/70	OK 29	---	29.0	0.97	(7)	---	
PH13-8Mo	H950	366669-TC18	T-L	0.98	95	4/13/70	OK 29	---	29.0	0.98	(7)	---	
		-TC19	T-L	0.99	95	4/13/70	OK 29	---	29.0	0.99	(7)	---	
		-TC20	T-L	0.99	75	4/13/70	OK 29	---	29.0	0.99	(7)	---	
		-TC21	T-L	0.99	50	4/13/70	OK 29	---	29.0	0.99	(7)	---	
		-TC17	T-L	0.99	0	4/13/70	OK 29	---	29.0	0.99	(7)	---	

-Continued-

Table D-8  
(Continued)

Alloy	Temper	Specimen No.	Specimen Orientation	Initial Crack Length, in.	Initial $K_{Ic}$ (1) $\sqrt{ksi}$	Exposure Date	Initial Crack Growth		Exposure Months	Exposure Terminated		Final $K_{Ic}$ (2) $\sqrt{ksi}$
							Months	Amt. in. (2)		Surface(2)	Fracture	
PH13-8Mo	HT250	366669-NC18	S-L	0.72	95	4/13/70	OK 29	---	29.0	0.72	(7)	---
		-TC19	S-L	0.72	95	4/13/70	OK 29	---	29.0	0.72	(7)	---
		-NC20	S-L	0.74	75	4/13/70	OK 29	---	29.0	0.74	(7)	---
		-NC21	S-L	0.73	50	4/13/70	OK 29	---	29.0	0.73	(7)	---
		-NC17	S-L	0.73	0	4/13/70	OK 29	---	29.0	0.73	(7)	---
PH13-8Mo	HT050	366669-TC39	T-L	1.00	95	4/13/70	OK 29	---	29.0	1.00	(7)	---
		-TC40	T-L	0.99	95	4/13/70	OK 29	---	29.0	0.99	(7)	---
		-TC41	T-L	1.00	75	4/13/70	OK 29	---	29.0	1.00	(7)	---
		-TC42	T-L	1.00	50	4/13/70	OK 29	---	29.0	1.00	(7)	---
		-TC38	T-L	0.99	0	4/13/70	OK 29	---	29.0	0.99	(7)	---
431	HT125	366670-TC39	T-L	1.00	95	4/13/70	OK 29	---	29.0	1.00	(7)	---
		-TC40	T-L	0.98	95	4/13/70	OK 29	---	29.0	0.98	(7)	---
		-TC41	T-L	0.98	75	4/13/70	OK 29	---	29.0	0.98	(7)	---
		-TC42	T-L	0.99	50	4/13/70	OK 29	---	29.0	0.99	(7)	---
		-TC38	T-L	0.98	0	4/13/70	OK 29	---	29.0	0.98	(7)	---
431	HT200	366670-LC18	L-T	1.00	95	4/13/70	OK 29	---	29.0	1.00	(7)	---
		-LC19	L-T	1.00	75	4/13/70	OK 29	---	29.0	1.00	(7)	---
		-LC20	L-T	1.00	50	4/13/70	3.0-6.0	0.30	29.0	1.30	(7)	---
		-LC21	L-T	1.00	50	4/13/70	3.0-6.0	0.07	29.0	1.07	(7)	---
		-LC17	L-T	0.97	0	4/13/70	OK 29	---	29.0	0.97	(7)	---
431	HT200	366670-TC18	T-L	0.99	95	4/13/70	OK 29	---	29.0	0.99	(7)	---
		-TC19	T-L	0.98	75	4/13/70	6.0-9.0	(5)	---	---	---	---
		-TC20	T-L	0.98	75	4/13/70	6.0-9.0	0.03	29.0	1.01	(7)	---
		-TC21	T-L	0.99	50	4/13/70	OK 29	---	29.0	0.99	(7)	---
		-TC17	T-L	1.00	0	4/13/70	9.0-12.0	0.22	29.0	1.22	(7)	---
431	HT200	366670-NC18	S-L	0.73	95	4/13/70	9.0-12.0	0.03	29.0	0.76	(7)	---
		-NC19	S-L	0.74	75	4/13/70	9.0-12.0	---	---	---	---	---
		-NC20	S-L	0.76	75	4/13/70	9.0-12.0	---	---	---	---	---
		-NC21	S-L	0.75	50	4/13/70	2.0-3.0	0.02	29.0	0.77	(7)	---
		-NC17	S-L	0.75	0	4/13/70	OK 29	---	29.0	0.75	(7)	---
AISI55	SCT850	366671-TC18	T-L	1.00	95	4/13/70	OK 29	---	29.0	1.00	(7)	---
		-TC19	T-L	0.98	75	4/13/70	OK 29	---	29.0	0.98	(7)	---
		-TC20	T-L	1.00	75	4/13/70	OK 29	---	29.0	1.00	(7)	---
		-TC21	T-L	0.99	50	4/13/70	OK 29	---	29.0	0.99	(7)	---
		-TC17	T-L	0.99	0	4/13/70	OK 29	---	29.0	0.99	(7)	---

-Continued-

Table D-8  
(Continued)

Alloy	Temper	Specimen No.	Specimen Orientation	Initial Crack Length, In.	Initial $K_I$ (1)	Exposure Date	Initial Crack Growth		Exposure Months	Exposure Terminated		Final $K_I$ (2)
							Months	Amt. In. (2)		Surface (2)	Crack Length Fracture	
AM355	SCT1000	366671-TC39 -TC40 -TC41 -TC42 -TC38	T-L	0.99	95	4/13/70	OK 29	---	29.0	0.99	(7)	---
			T-L	0.98	95	4/13/70	OK 29	---	29.0	0.98	(7)	---
			T-L	0.99	75	4/13/70	OK 29	---	29.0	0.99	(7)	---
			T-L	0.99	50	4/13/70	OK 29	---	29.0	0.99	(7)	---
AM355	SCT850	366673-LC18 -LC19 -LC20 -LC21 -LC17	L-T	1.04	95	4/13/70	6.0-9.0	0.03	29.0	1.07	(7)	---
			L-T	---	(6)	---	---	---	---	---	---	---
			L-T	1.00	75	4/13/70	3.0-5.0	0.05	29.0	1.05	(7)	---
			L-T	1.01	50	4/13/70	OK 29	---	29.0	1.01	(7)	---
			L-T	0.99	0	4/13/70	OK 29	---	29.0	0.98	(7)	---
AM355	SCT850	366673-TC18 -TC19 -TC20 -TC21 -TC17	T-L	1.00	95	4/13/70	2.0-3.0	0.05	29.0	1.36	(7)	---
			T-L	1.00	75	4/13/70	2.0-3.0	0.03	29.0	1.08	(7)	---
			T-L	0.99	75	4/13/70	2.0-3.0	0.02	29.0	1.02	(7)	---
			T-L	0.99	50	4/13/70	OK 29	---	29.0	0.99	(7)	---
			T-L	1.00	0	4/13/70	OK 29	---	29.0	1.00	(7)	---
AM355	SCT850	366673-NC18 -NC19 -NC20 -NC21 -NC17	S-L	0.78	95	4/13/70	OK 29	---	29.0	0.78	(7)	---
			S-L	0.86	75	4/13/70	OK 29	---	29.0	0.86	(7)	---
			S-L	0.75	75	4/13/70	OK 29	---	29.0	0.75	(7)	---
			S-L	---	(6)	---	---	---	---	---	---	---
AM355	SCT1000	366673-TC39 -TC40 -TC41 -TC42 -TC38	S-L	0.87	0	4/13/70	9.0-12.0	0.02	29.0	0.89	(7)	---
			T-L	1.00	95	4/13/70	OK 29	---	29.0	1.00	(7)	---
			T-L	1.00	75	4/13/70	OK 29	---	29.0	1.00	(7)	---
			T-L	1.00	50	4/13/70	OK 29	---	29.0	1.00	(7)	---
			T-L	0.99	0	4/13/70	OK 29	---	29.0	0.99	(7)	---

Notes: (1) Calculated from applied load and average crack length measured on exterior of specimens.  
 (2) Calculated from average crack lengths measured on exterior of specimens.  
 (3) Calculated from crack lengths measured on fractured surface and the measured load.  
 (4) Reliable residual stress intensity could not be calculated because of excessive crack growth.  
 (5) Branching or multiple cracks occurred and accurate crack growth could not be measured.  
 (6) Specimen damaged during final machining - not submitted for testing.  
 (7) Specimen still in test, number indicates the crack length at the time of last measurement.

Table D-9

STEEL ALLOY, BOLT LOADED COMPACT TENSION SPECIMENS EXPOSED TO 20% NaCl TOTAL DIMENSION

Alloy	Temper	Specimen No.	Specimen Orientation	Initial Crack Length, In.	Initial KI (1) $\frac{K}{\sqrt{K_{IC}}}$	Exposure Date	Initial Crack Growth		Exposure Days	Exposure Days	Exposure Surfaces(2)	Exposure Terminated		Final KI (1) $\frac{K}{\sqrt{K_{IC}}}$	
							Days	In. (2)				Crack Length	Practure		
17-7 FH	RH1050	366665-TC8	T-L	0.99	95	7/28/70	---	---	---	---	---	1.902	(4)	(4)	
		-TC9	T-L	0.99	95	7/28/70	0.12	0.90	0.12	181	1.89	1.856	(4)	(4)	
		-TC10	T-L	---	(8)	---	---	---	---	---	---	---	---	---	---
		-TC11	T-L	1.00	38	8/6/70	0.12	0.12	0.12	193	1.13	1.148	(4)	(4)	
		-TC22	T-L	1.01	35	2/18/71	0.12	0.24	0.12	185	1.74	(10)	(10)	(10)	
		-TC23	T-L	0.98	25	2/18/71	32.0	0.03	---	185	1.02	(10)	(10)	(10)	
		-TC7	T-L	0.94	0	7/28/70	OK 2	---	---	2	---	1.07	(7)	(7)	
PH15-7Mo	RH950	366666-TC8	T-L	1.00	95	7/28/70	1	0.81	2	1.82	1.868	(4)	(4)		
		-TC9	T-L	1.00	75	7/28/70	1	0.74	2	1.77	1.818	(4)	(4)		
		-TC11	T-L	1.01	50	7/28/70	1	0.64	181	1.71	1.736	(4)	(4)		
		-TC7	T-L	1.02	0	7/28/70	OK 181	---	---	181	0.994	(7)	(7)		
PH15-7Mo	RH1050	366666-TC29	T-L	1.00	95	7/28/70	0.12	0.86	2	1.87	1.886	(4)	(4)		
		-TC31	T-L	1.02	75	7/28/70	0.12	0.80	2	1.82	1.832	(4)	(4)		
		-TC32	T-L	1.01	50	7/28/70	0.12	0.67	181	1.76	1.700	(4)	(4)		
		-TC28	T-L	1.02	0	7/28/70	OK 181	---	---	181	0.988	(7)	(7)		
15-5 PH	H900	366668-TC8	T-L	1.01	95	7/28/70	22.0	0.69	90	1.80	1.798	(4)	(4)		
		-TC9	T-L	1.01	75	7/28/70	22.0	0.11	181	1.67	1.66	23.5	(3)	(3)	
		-TC10	T-L	1.03	65	2/24/71	98.0	0.12	181	1.15	(10)	(10)	(10)		
		-TC11	T-L	1.02	50	7/28/70	76.0	0.02	181	1.18	1.10	26.2	(3)	(3)	
		-TC7	T-L	1.02	0	7/28/70	OK 181	---	---	181	---	1.01	(7)	(7)	
15-5 PH	HL150M	366667-TC8	T-L	1.02	95	7/28/70	OK 181	---	181	---	---	0.980	70	(6)	
		-TC9	T-L	1.02	95	7/28/70	OK 181	---	181	---	---	0.975	58	(5)	
		-TC10	T-L	1.01	75	7/28/70	OK 181	---	181	---	---	0.990	60	(6)	
		-TC7	T-L	1.01	0	7/28/70	OK 181	---	181	---	---	0.980	(7)	(7)	
PH13-8Mo	H950	366669-TC8	L-T	1.01	95	7/28/70	OK 181	---	181	---	---	1.000	76	(6)	
		-LC9	L-T	1.01	95	7/28/70	OK 181	---	181	---	---	0.998	80	(6)	
		-LC10	L-T	1.00	75	7/28/70	OK 181	---	181	---	---	1.006	61	(6)	
		-LC7	L-T	1.02	0	7/28/70	OK 181	---	181	---	---	1.008	(7)	(7)	
PH13-8Mo	H950	366669-TC8	T-L	0.99	95	7/28/70	1	0.48	2	1.85	(6)	1.002	48.5	(5)	
		-TC9	T-L	1.00	85	2/24/71	OK 181	---	181	---	---	1.35	(5)	(5)	
		-TC11	T-L	0.99	85	7/28/70	OK 181	---	181	---	---	---	(10)	(10)	
		-TC7	T-L	1.00	75	7/28/70	OK 181	---	181	---	---	1.008	(7)	(7)	

-Continued-

Table D-9  
(Continued)

Alloy	Temper	Specimen No.	Specimen Orientation	Initial Crack Length, In.	Initial $K_{Ic}$ (1) $\frac{ksi}{\sqrt{in}}$	Exposure Date	Initial Crack Growth		Exposure Days	Exposure Days	Exposure Terminated		Final $K_{Ic}$ (2) $\frac{ksi}{\sqrt{in}}$	
							Days	Am. In. (2)			Crack Length Surface (2)	Crack Length Fracture		
PH13-8Mo	H950	366669-NC8 -NC9 -NC10 -NC7	S-L	0.76	95	7/28/70	2	0.48	OK 181	3	1.42	(6)	61.4 (8)	
			S-L	0.76	95	7/28/70	OK 181	---	---	181	---	---	(11)	181 (11)
			S-L	0.76	0	7/28/70	OK 181	---	---	181	---	---	(7)	181 (7)
PH13-8Mo	H1050	366669-TC29 -TC30 -TC32 -TC31 -TC28	T-L	1.01	95	7/28/70	1	0.51	OK 181	2	1.85	(6)	65.5 (6)	
			T-L	1.00	95	2/24/71	OK 181	---	---	181	---	---	(10)	181 (10)
			T-L	1.00	85	7/28/70	OK 181	---	---	181	---	---	(11)	181 (11)
			T-L	1.00	75	7/28/70	OK 181	---	---	181	---	---	(7)	181 (7)
431	HT125	366670-TC29 -TC30 -TC31 -TC28	T-L	1.01	95	7/28/70	OK 181	---	---	181	---	(6)	28.6 (6)	
			T-L	1.00	95	7/28/70	49	0.35	OK 181	181	1.47	1.668	38 (4)	181 (4)
			T-L	0.99	75	7/28/70	69	0.34	OK 181	181	1.34	1.518	45 (4)	181 (4)
			T-L	0.99	0	7/28/70	OK 181	---	---	181	---	---	(7)	181 (7)
431	HT200	366670-IC8 -IC9 -IC11 -IC10 -IC7	L-T	1.01	95	7/28/70	1	0.18	OK 181	24	1.75	(4)	1.856 (4)	
			L-T	0.98	75	7/28/70	1	0.25	OK 181	111	1.62	(4)	1.810 (4)	
			L-T	0.99	50	7/28/70	13	0.32	OK 181	20	1.81	(4)	1.800 (4)	
			L-T	1.00	25	2/24/71	68	0.16	OK 181	181	1.30	(10)	1.90 (10)	
			L-T	0.99	0	7/28/70	OK 181	---	---	181	---	---	(7)	1.01 (7)
431	HT200	366670-TC8 -TC9 -TC11 -TC10 -TC7	T-L	1.00	95	7/28/70	1	0.20	OK 181	24	1.82	(4)	1.820 (4)	
			T-L	1.00	75	7/28/70	2	0.08	OK 181	20	1.79	(4)	18.7 (4)	
			T-L	1.02	50	7/28/70	13	0.54	OK 181	181	1.70	(10)	1.588 (10)	
			T-L	1.01	25	2/24/71	68	0.08	OK 181	181	1.23	(10)	1.93 (10)	
			T-L	1.02	0	7/28/70	OK 181	---	---	181	---	---	(7)	1.01 (7)
431	HT200	366670-NC8 -NC9 -NC10 -NC11 -NC7	S-L	0.76	95	7/28/70	13	0.16	OK 181	20	1.34	(4)	1.340 (4)	
			S-L	0.75	75	7/28/70	13	0.22	OK 181	17	1.37	(4)	1.356 (4)	
			S-L	0.76	50	7/28/70	13	0.28	OK 181	20	1.30	(7)	27.3 (7)	
			S-L	0.75	0	7/28/70	OK 181	---	---	181	---	---	(7)	0.735 (7)
AM55	SCT850	366671-TC8 -TC9 -TC10 -TC11 -TC7	T-L	1.01	95	7/28/70	OK 181	---	---	181	---	(6)	1.746 (6)	
			T-L	1.01	75	2/24/71	20	0.29	OK 181	111	1.82	(10)	1.746 (10)	
			T-L	1.00	65	7/28/70	15	0.34	OK 181	36	1.85	(10)	1.85 (10)	
			T-L	1.00	50	7/28/70	OK 181	---	---	181	---	---	(7)	0.992 (7)
AM55	SCT1000	366671-TC29 -TC30 -TC31 -TC32 -TC28	T-L	1.01	95	7/28/70	20	0.13	OK 181	90	1.79	(4)	1.812 (4)	
			T-L	1.02	95	7/28/70	OK 181	---	---	181	---	---	(11)	1.812 (11)
			T-L	1.02	75	2/24/71	34	0.33	OK 181	181	1.55	(10)	47.7 (10)	
			T-L	1.00	65	7/28/70	15	0.28	OK 181	47	1.75	(10)	1.75 (10)	

-Continued-

Table D-9  
(Continued)

Alloy	Temper	Specimen No.	Specimen Orientation	Initial Crack Length, In.	Initial $K_{Ic}$ (1)	Exposure Date	Initial Crack Growth		Exposure Days	Surface(2)	Exposure Terminated Crack Length		Final $K_{Ic}$ (1)				
							Days	Amt. In.(2)			Fracture	ksi.y.in.					
AM355	SCT850	366673-LC8 -LC9 -LC10 -LC11 -LC7	L-T L-T L-T L-T	---	(8)	7/28/70	---	0.37	48	1.82	1.774	---	(4)				
														6	0.07	1.76	1.676
														15	---	---	16.9
														OK 181	---	0.994	(7)
AM355	SCT850	366673-TC8 -TC9 -TC11 -TC10 -TC7	T-L T-L T-L T-L T-L	95	75	7/28/70	1	0.21	6	1.87	1.796	---	(4)				
														2	---	1.82	1.596
														34	0.37	1.80	17.4
														OK 181	0.09	1.63	(10)
AM355	SCT850	366673-TC8 -TC9 -NC10 -NC11 -NC7	S-L S-L S-L S-L	(8)	75	7/28/70	34	0.37	139	1.32	1.308	---	(4)				
														7	0.48	1.26	16.1
														OK 181	---	1.00	35
														OK 181	---	0.740	(7)
AM355	SCT1000	366673-TC29 -TC30 -TC31 -TC32 -TC38	T-L T-L T-L T-L	95	75	7/28/70	OK 181	---	181	---	1.005	---	(11)				
														OK 181	---	---	49.8
														20	0.23	1.27	17.8
														61	0.32	1.85	(10)
PH13-8Mo	H950	366669-TC10 -NC10	T-L S-L	75	75	2/18/71	5	(5)	5	(5)	1.312	(5)					
													0.12	0.06	(5)	(5)	
PH13-8Mo	H1050	366669-TC31	T-L	75	75	2/18/71	1	0.46	11	1.61	1.776	(4)					
													1	0.04	1.56	(10)	
AM355	SCT850	366671-TC11	T-L	50	95	2/18/71	1	0.16	185	(5)	1.848	(4)					
													3	0.11	1.79	(5)	
AM355	SCT1000	366671-TC30	T-L	95	95	2/18/71	1	0.11	13	(5)	1.848	(4)					
													1	0.11	1.79	(5)	

Notes: (1) Calculated from air load and average crack length measured on exterior of specimens.  
 (2) Calculated from air load and average crack length measured on exterior of specimens.  
 (3) Calculated from air load and average crack length measured on exterior of specimens.  
 (4) Reliable residual stress intensity could not be calculated because of occurrence of branching or multiple cracks.  
 (5) Used for metallographic examination.  
 (6) Unstr. specimen measured but load not determined.  
 (7) Specimen damaged during machining or stressing and not exposed.  
 (8) Specimen failed approx. 2 hrs. after stressing not exposed.  
 (9) Specimen not submitted for residual measurements.  
 (10) Pre-crack resharpened and specimen re-exposed as noted above.

Table D-10

## T1-6Al-4V BOLT LOADED COMPACT TENSION SPECIMENS EXPOSED TO ATMOSPHERES AND ACCELERATED TESTS

Temper	Specimen No.	Specimen Orientation	Initial Crack Length, in.	Initial $K_{Ic}$ (1) % $K_{Ic}$	Exposure Date	Crack Growth		Exposure Days	Exposure Terminated		Final $K_{Ic}$ (2) % $K_{Ic}$
						Seacoast Atmosphere	Am. In. (2)		Surface	Crack Length Fracture	
Beta Forged	366965-TC12 -TC13 -TC14 -TC15 -TC16	T-L T-L T-L T-L	1.000	0	5/3/70	OK 812	0	812	---	---	---
			1.015	95	5/3/70	OK 812	0	812	1.015	{4}	---
			1.005	75	5/3/70	OK 812	0	483	1.005	{4}	---
			1.000	50	5/3/70	OK 812	0	812	1.000(5)	{4}	31.1(6)
Alpha-Beta Forged	366966-TC12 -TC13 -TC14 -TC15 -TC16	T-L T-L T-L T-L	0.985	0	5/3/70	OK 812	0	812	---	{4}	---
			0.995	95	5/3/70	P.E. (7)	---	141	1.680	1.614	23.6(9)
			0.995	75	5/3/70	410-483	0.11	812	1.105	{4}	---
			0.995	75	5/3/70	353-410	0.24	410	1.230	{4}	24.2(6)
			0.995	50	5/3/70	410-483	0.03	812	1.030	{4}	---
			1.030	---	---	---	---	---	---	---	---
Beta Forged	366965-TC17 -TC18 -TC19 -TC20 -TC21	T-L T-L T-L T-L	1.010	0	4/13/70	OK 861	0	861	---	{4}	---
			0.995	95	4/13/70	OK 861	0	861	0.995	{4}	---
			1.005	75	4/13/70	OK 486	0	486	1.015(5)	{4}	31.6(6)
			1.000	75	4/13/70	OK 861	0	861	1.000	{4}	---
			1.000	50	4/13/70	OK 861	0	861	1.000	{4}	---
			1.000	0	4/13/70	OK 861	0	861	---	{4}	---
Alpha-Beta Forged	366966-TC17 -TC18 -TC19 -TC20 -TC21	T-L T-L T-L T-L	1.000	0	4/13/70	OK 861	0	861	---	{4}	---
			0.995	95	4/13/70	OK 861	0.34	486	1.335	1.380	31.0
			0.995	75	4/13/70	OK 486	0	486	1.000(5)	{4}	25.6(6)
			0.995	75	4/13/70	OK 861	0	861	0.995	{4}	---
			0.995	50	4/13/70	OK 861	0	861	1.000	{4}	---
			1.000	---	---	---	---	---	---	---	---
Beta Forged	366965-TC7 -TC8 -TC9 -TC10	T-L T-L T-L	0.995	0	7/29/70	OK 209	0	209	0.995	1.035	45.2(8)
			0.995	95	7/29/70	<1	0.29	209	1.285	1.290	39.0
			1.000	75	7/29/70	<1	0.09	209	1.090	1.110	34.4
			1.000	50	7/29/70	OK 209	0	209	1.000	1.006	21.7
Alpha-Beta Forged	366966-TC7 -TC8 -TC9 -TC10	T-L T-L T-L	0.990	0	7/29/70	OK 209	0	209	0.990	1.044	37.1(8)
			0.995	95	7/29/70	<1	0.58	209	1.375	1.392	29.3(9)
			0.995	75	7/29/70	<1	0.29	209	1.285	1.324	27.5
			0.995	50	7/29/70	OK 209	0	209	0.995	1.020	17.7

- Notes:
- (1) Calculated from applied load and average crack length measured on exterior of specimens.
  - (2) Calculated from average crack lengths measured on exterior of specimens.
  - (3) Calculated from crack lengths measured on the fracture surface and the measured load, unless otherwise noted.
  - (4) Specimen still in test, numbers indicate the crack length at the time of the last measurement.
  - (5) Small amount of crack growth indicated by this measurement not observed during exposure, but was measured when determining final  $K_{Ic}$  value.
  - (6) Calculated from average crack lengths measured on exterior of specimens and the measured load; specimen sectioned for metallographic examination.
  - (7) P.E. denotes prior to exposure (crack growth began during shipment to the exposure site).
  - (8) Value for fracture toughness test conducted at termination of exposure.
  - (9) Calculated stress intensity may not be reliable due to excessive crack length.